From elements to landscapes: the role of terrestrial consumers in ecosystem functioning

by

© Matteo Rizzuto

A thesis submitted to the
School of Graduate Studies
in partial fulfilment of the requirements for the degree of
Doctor of Philosophy

Department of Biology, Faculty of Science
Memorial University of Newfoundland and Labrador

November 2021

St. John's Newfoundland and Labrador

Abstract

Consumers are key actors in ecosystems, shaping processes and functions at multiple spatio-temporal scales via their interactions with biotic and abiotic ecosystem features. Yet, research on the dynamics of local and meta-ecosystems rarely accounts for the effects of consumers—particularly terrestrial mammals. Two hurdles hamper progress in this field: the lack of common units of measurement for biotic and abiotic ecosystem components, and the need for flexible, system-agnostic ways to investigate how consumers interact with and influence ecosystem functioning. In this dissertation, I offer a concerted approach to address these issues, integrating wildlife, landscape, and ecosystem ecology within an ecological stoichiometry framework. I begin by showing that terrestrial mammals are variable in their ecological stoichiometry, using data from the snowshoe hare (*Lepus americanus*), a keystone boreal herbivore. Importantly, unlike invertebrates, organismal stoichiometry in vertebrates appears unrelated to age, sex, body size, and body condition. Building on these results, I investigate the responses of terrestrial herbivores to biotic variability in their environment, finding that snowshoe hares vary their space use when facing intraspecific variability in the stoichiometry of their foraging resources. Hares had larger home ranges in areas of poor or highly variable forage stoichiometry compared to areas of high and consistent forage stoichiometry. This differential space use by consumers may elicit changes in both their ecology and ecosystem dynamics. Thus, I develop a novel mathematical model of a meta-ecosystem to investigate how multiple types of consumer movement over the landscape influence ecosystem processes and functions. Expanding a classic, two-patch meta-ecosystem model to include the surrounding matrix, I demonstrate that active, non-diffusive movement of consumers can reduce or enhance ecosystem functions at local and regional spatial scales. Throughout my thesis, ecological stoichiometry ties together the diverse themes of each chapter, further demonstrating how elemental currencies can work as shared units of measurement across levels of biological organization. Overall, my thesis combines a laboratory study, spatial statistical models fit to a field-based case study, and a novel mathematical model to provide testable predictions to guide future research into the role of consumers within meta-ecology.

General Summary

Animal activities can change how ecosystems work, including plant growth, organism interactions, and the cycling of essential nutrients between organisms and the environment. Yet, the details of how this occurs remain largely unknown because existing conceptual and mathematical approaches make it difficult to identify important patterns across more than one ecosystem at a time. Identifying these patterns is an important step towards understanding the links between animals activities and how ecosystems work. A detailed understanding of these links is also important in preserving the integrity of natural environments and the services they provide us: clean air, water, and recreational spaces. Here, I present new insights into animal-environment links, using an approach that allows for comparisons across different ecosystems. I use chemical elements, the building blocks of life, and mathematical tools to explore the links between animals, plants, and their environment. I focus on an important herbivore in the boreal forest of Canada, the snowshoe hare (*Lepus americanus*). First, I study how chemically similar hares are among themselves. I find that hares can be quite different in their body chemistry, but not what drives these differences. Differences in body chemistry may change how hares use their environment, as the same chemical elements are found in their food. So, second, I investigate how food chemical qualities influence hare space use. I find that hares eating good quality food use less space, whereas where food quality is poor they use more space. As animals move to forage, these results suggest that hares may change how their ecosystem works by transporting elements as they move in their habitats. Lastly, I develop a mathematical model to explore how the movement of chemical elements by animals among ecosystems can change how ecosystems work. I find that animal movement of chemical elements can strongly change how ecosystems work by, for instance, increasing plant growth. My results show that new insights can be gained by linking animals and ecosystems through chemical elements, and that we need to consider animals' activities in our plans to protect the environment.

Land Acknowledgement

I acknowledge that the lands that I lived and worked on to complete this thesis are the traditional homelands of the Beothuk people and their ancestors. I acknowledge with respect the diverse histories and cultures of the Beothuk, Mi’Kmaq, Innu, and Inuit of this province. I offer this land acknowledgement to recognize that when occupying these territories I am hosted by diverse Indigenous groups who have known and cared for these lands since time immemorial.

Acknowledgements

"Science is a collaborative enterprise, spanning the generations. When it permits us to see the far side of some new horizon, we remember those who prepared the way—seeing for them also."

~ Carl Sagan

I would like thank my supervisor Dr. Shawn Leroux for his advice, support, and patience. Shawn's calm resolve, gentle guidance, and dedication to helping me achieve my goals were key to the development and completion of this thesis. Under Shawn's tutelage, I grew as a scientist and as a person: I could not have hoped for a better mentor. I would also like to extend my gratitude to my thesis committee, Dr. Yolanda Wiersma and Dr. Eric Vander Wal, who helped, advised, and challenged me to expand my research and teaching horizons. I am thankful to my fellow graduate students in the Terrestrial Ecology Research Group, Travis Heckford, Juliana Balluffi-Fry, Isabella Richmond, and Joanie Kennah: I learned a lot from them and I hope I gave something in return. I thank Dr. Oswald Schmitz for hosting me in his lab and for helping me see the links between mathematical models and the real world. I am grateful to the staff of Terra Nova National Park, particularly Janet Feltham and Collier Ross, for their invaluable help with the logistics of three long field seasons. My deep gratitude goes the many Research Assistants who helped me collect data in the lab and field: they made this thesis possible. I thank my previous mentors and teachers, particularly Dr. Samraat Pawar, Dr. Chris Carbone, and Dr. Francesca Marucco, whose lasting influence surfaces throughout this thesis.

I was lucky to find a friendly, welcoming, and supportive group of colleagues in the Ecosystem Ecology Lab at Memorial University. To all past and present members of EEL, thank you for the laughs, games, discussions, warm beverages, and comfort foods that we shared. Likewise, I thank all members of the Greeley Lab at Yale University for welcoming me and sharing ideas, insights, and advice with me.

No thesis is a straight path, and many friends helped me navigate twists and turns along the road. My heartfelt thanks go to Costanza Frola, my “second” sister, with whom I shared my first microscope and is always there for me; to Samantha Andrews, who patiently answered all my English-related questions and always had a joke ready; to Anne McLeod, for countless draft reviews, math advice, and book recommendations; to Chelsea Little, for taking me along to explore exciting new areas of meta-ecology; to Robert Buchkowski, Julia Monk, Kristy Ferraro, and Diego Ellis-Soto, for inspiring conversations about animals, elements, and ecosystems. I am grateful for Marie Isabelle Rochon, Adam Meyer, Elaine Xie, J. Drew Hancock-Teed, Róisín Renouf Thompson, Peter Marcouillier, Ana Fanton-Borges, Taylor Gorham, Sara Meneghetti, Cecilia Giolo, and Giulia Copersito: their friendship helped me navigate the challenges of this PhD with a light heart and a smile on my face. I owe much and am grateful to yoga teacher Hope Jamieson and the Yoga for Guys crew for helping me keep my sanity over the years. And to all the friends I shared a Dungeons & Dragons game with: thank you, our imaginary adventures brought much happiness and relief.

My parents Anna and Cosimo, my sister Marta and her partner Roberto, and my family supported me in all my scientific endeavours and are the rock upon which this Ph.D. is built. They listened, dabbed my tears, kept my impostor syndrome at bay, and cheered me every step of the way. More than anyone else, they know what went into writing this thesis. Grazie.

Finally, I thank my partner Dorota for her love, support, and the small everyday acts of kindness and care with which she helped, comforted, and encouraged me as I wrote this dissertation. I could not have done this without her.

This research was supported by a Government of Newfoundland and Labrador Centre for Forest Science and Innovation grant to SJL, YW, and EVW, a Government of Newfoundland and Labrador Innovate NL Leverage R&D program grant to EVW and SJL and an Ignite R&D program grant to SJL, a Mitacs Accelerate Graduate Research Internship program grant to YW, EVW, and SJL, a Canada Foundation for Innovation John R. Evans Leaders Fund grant to EVW and SJL, a Natural Science and Engineering Research Council Discovery grant to SJL, and a Mitacs Globalink Research Award and a Mitacs Research Training Award to MR. Thank you.

Table of Contents

List of Tables

List of Figures

List of Appendices

Chapter 1

Introduction and overview

"All have their worth, and each contributes to the worth of the others." ~ J. R. R. Tolkien

Ecosystems are shaped by interactions and exchanges among their organic and inorganic components (Currie 2011). Energy, nutrients, and information (Loreau, Mouquet, and Holt 2003; Marleau, Peller, et al. 2020) flow from inorganic environmental pools—e.g., the sun, soil, and atmosphere—to primary producers and then consumers, before being broken down by decomposers and detritivores, thus reentering the cycle. These flows mediate and modulate ecosystem functions (Loreau, Mouquet, and Holt 2003; Díaz et al. 2015), which in turn determine the ecosystem services enjoyed and exploited by humankind (Garland et al. 2021). Furthermore, ecosystems exist in continuity with one another, forming meta-ecosystems connected by biotic and abiotic pathways (Loreau, Mouquet, and Holt 2003; Gounand, Harvey, et al. 2018). This complex network of ecosystems spans spatio-temporal scales and can further shape the services local and meta-ecosystems mediate (Schiesari et al. 2019)—for instance, by enhancing nutrient cycling through spatial flows across adjacent ecosystems (e.g., Yang and Chen 2018). As the Anthropocene progresses, protecting and maintaining ecosystem functions and services have come to the forefront as key actions necessary to ensure the continued survival of humanity on Earth (Schiesari et al. 2019). Yet, our knowledge of the components of these complex systems, and thus our ability to disentangle their individual effects and devise strategies to mitigate humankind's impact on them, is patchy at best. This is particularly true for vertebrate consumers and the role they play in ecosystem functions and services (Schmitz, Raymond, et al. 2014; Sitters, Atkinson, et al. 2015; Sitters and Olde Venterink 2015; Gounand, Harvey, et al. 2018).

The ways in which vertebrate consumers shape ecosystem processes, functions, and services are myriad—from changing the distribution of key inorganic resources in the landscape to modulating microbial decomposers activity through soil compaction (Schmitz, Wilmers, et al. 2018; Enquist et al. 2020; Schmitz and Leroux 2020). Part of the effects of vertebrate consumers on ecosystem dynamics stems directly from the way they forage in and otherwise use their space. For instance, through consumptive effects, the million-strong migration of wildebeest (*Connochaetes taurinus*) increases the rates of nutrient cycling in the savannah ecosystems they traverse during their seasonal migration in the Serengeti (Tanzania; Holdo, Holt, Sinclair, et al. 2011). Marine central-place foragers, such as the humpback whale (*Megaptera novaeangliae*), mediate similar nutrient cycling and primary productivity enhancing effects in the photic zone of the Gulf of Maine (Roman and McCarthy 2010; Roman, Estes, et al. 2014). Conversely, consumers' consumptive effects can also dampen ecosystem functions, as moose (*Alces alces*) do in the boreal forests of North America (Pastor, Cohen, and Hobbs 2006). Moose selectively forage on the most nutritious plant matter available leading to sequestration of limiting nutrients in their own biomass (Pastor, Cohen, and Hobbs 2006, but see Balluffi-Fry, Leroux, Wiersma, Heckford, et al. 2020, for an analysis of individual variation in this foraging strategy). In a positive feedback loop, this contributes to the low rates of nutrient cycling and primary productivity of the boreal biome (Pastor and Naiman 1992; Pastor, Dewey, et al. 1993; Pastor, Cohen, and Hobbs 2006).

In addition to their direct, consumptive effects, consumers can elicit indirect influences on ecosystem functions and dynamics (Schmitz, Wilmers, et al. 2018), from contrasting (e.g., Holdo, Sinclair, et al. 2009) or compounding with (e.g., MacSween, Leroux, and Oakes 2019) the effects of natural disturbances, to changing nutrient cycling dynamics (e.g., Bump, Tischler, et al. 2009). In the Serengeti, as the wildebeest population increased following eradication of a crippling disease, higher rates of herbivory reduced the susceptibility of this savannah ecosystem to seasonal fires and turned what used to be a carbon source into a net carbon sink (Holdo, Holt, and Fryxell 2009; Holdo, Holt, Sinclair, et al. 2011). In boreal systems, moose move over the landscape and change their space use under the influence of multiple stimuli, from forage stoichiometry (Leroux, Vander Wal, et al. 2017; Balluffi-Fry, Leroux, Wiersma, Heckford, et al. 2020) to predation risk (Bump, Peterson, and Vucetich 2009; Montgomery et al. 2014). As they move to find higher-quality resources to forage on, moose trample the soil, increasing compaction and fostering anaerobic conditions in the organic horizons, and thus dampen nutrient mineralization (Tuomi et al. 2021). Conversely, carcass deposition following predation by the wolf (*Canis lupus*) may lead to enhanced local nutrient availability that can persist through time (Bump, Peterson, and Vucetich 2009; Bump, Webster, et al. 2009). Finally, consumers "on-the-move" indirectly pair ecosystem processes over space and time, contributing to meta-ecosystem dynamics (Gounand, Harvey, et al. 2018). At continental scales, migratory snow geese (*Chen caerulenscens*) seasonally connect fertilized agricultural fields in New Mexico (USA) to the wetlands of the Canadian tundra, transporting human-derived nutrients and pairing ecosystem functions across habitat types and more than 4500 km (Jefferies, Rockwell, and Abraham 2004). Similar, albeit smaller-scale, effects can be found in boreal systems where beaver (*Castor canadensis*) and moose link ponds and streams, respectively, to the nearby forests stands (Rosell et al. 2005; Bump, Tischler, et al. 2009).

As the above examples show, consumers can mediate indirect, unintuitive effects among diverse ecosystems and across vast spatio-temporal scales. Yet, the potentially strong influence of consumers on the complex machinery of the biosphere is still only rarely accounted for—particularly in terrestrial ecosystems (Schmitz, Raymond, et al. 2014; Enquist et al. 2020). Earth-system models routinely do not incorporate consumers in their simulations of planet-wide dynamics (but see Dangal et al. 2017), or do so in a limited, simplified manner that does not capture their diverse roles as intermediaries of local and meta-ecosystem dynamics (e.g., Harfoot et al. 2014, but see Hoeks et al. 2020, for a biomass-based study accounting for the role of carnivorous consumers). Excluding consumers from large-scale models aimed at investigating or predicting the state of our planet in the face of Anthropogenic change is problematic for both ecological research and mitigation and conservation efforts. The high level of abstraction of these models (Gounand, Harvey, et al. 2018), complexity of consumer-related behaviours and interactions with other ecosystem components (e.g., Ebel et al. 2015), and mathematical tractability (e.g., Gravel, Guichard, et al. 2010) have all been invoked as hurdles standing in the way of a more nuanced, realistic representation of consumer-mediated ecosystem effects in local and meta-ecosystem models.

I surmise that, to advance research on the role and effects of consumers in ecosystem functions and services, two lines of inquiry will offer helpful contributions. In particular, (i) describing vertebrate consumers, and especially terrestrial species, using units of measurement and currencies shared among biotic and abiotic components of ecosystems and the processes that connect them, and (ii) developing new, flexible, and study system-agnostic conceptual tools to represent the variety of ways consumers interact with and modify their environment, its functions, and its services. In this thesis, I offer a two-pronged approach to tackle these issues and develop a more comprehensive framework for consumer-mediated ecosystem effects.

1.1 What unites us: a stoichiometric approach to consumer ecology

Advancing our understanding of the role consumers play in shaping ecosystem processes and functions requires grounding this work in common currencies and units of measurement. For all its impressive variety of forms, life uses a relatively small subset of chemical elements to assemble them ($\simeq$25 out of 118; Sterner and Elser 2002; Kaspari and Powers 2016). Excluding oxygen and hydrogen, carbon (C), nitrogen (N), and phosphorus (P) are the most common among these shared “building blocks”, and their relative balance among organisms and the environment is a key trait of ecological systems (Sterner and Elser 2002). Availability of elements in abiotic environmental pools—e.g., as soil minerals or water-suspended nutrients—determines rates of primary productivity in ecosystem worldwide, with stark and consistent differences across different ecosystems (e.g, between freshwater and terrestrial; Elser et al. 2000). Experimental evidence shows that different environmental nutrient availability mediates the effects of herbivory on inorganic pools of C and N (e.g., in grassland ecosystems; Sitters, Wubs, et al. 2020). Furthermore, consumers appear to respond to the stoichiometry of their resources, as shown using fertilization experiments in the boreal forests of Scandinavia (Ball, Danell, and Sunesson 2000) and with cafeteria-style forage choice studies in boreal Canada (Balluffi-Fry, Leroux, Wiersma, Heckford, et al. 2020). As these examples show, ecological stoichiometry—the study of the arrangement and dynamics of chemical elements in natural systems—offers a unifying conceptual and quantitative approach to investigate organism-environment interactions across levels of biological organization (Sterner and Elser 2002).

As a framework, ecological stoichiometry stems from biogeochemistry and studies of freshwater and marine ecosystems (Sperfeld et al. 2016). Primary producers are stoichiometrically plastic in the relative amounts of key elemental nutrients that they contain compared to those available in their environment (Sterner and Elser 2002). This plasticity is mediated by the cellular biology of autotrophs, which allows primary producers to store excess nutrients in a dedicated type of organelle (i.e., vacuoles; Sterner and Elser 2002). The ability to decouple environmental uptake of nutrients from maintaining their internal homeostasis grants primary producers the ability to thrive in stoichiometrically heterogeneous environments (Ågren and Weih 2012; Rivas-Ubach et al. 2012; Martiny et al. 2013). Conversely, consumers generally show limited stoichiometric plasticity (Sterner and Elser 2002). Consumers constantly regulate the amount of certain elements circulating in their system—e.g., the dynamics of skeletal and circulating P in vertebrates (Sterner and Elser 2002). As well, consumers move among environments to escape unfavourable stoichiometry conditions: from this perspective, foraging is a stoichiometric decision for some consumers, dictated by the need to prioritize uptake of certain elements and not others (see below, Section 1.2; Sterner and Elser 2002; Nie et al. 2015). Exceptions to the general rule of low consumer stoichiometric plasticity can be found, for instance, in species that undergo ontogenic changes to reach their adult form (Ebel et al. 2016) or following physiological changes induced by, e.g., predation risk (El-Sabaawi et al. 2012; Rinehart and Hawlena 2020). For instance, organismal content of P and other elements in Atlantic salmon varies among individuals at different life stages (Ebel et al. 2016). In addition to the life history or behavioural changes that it entails—i.e., the ocean-bound migration of post-spawn individuals from their spawning freshwater streams—it is this intraspecific variation that is key to determine whether Atlantic salmon act as P sources or sinks for the freshwater ecosystems they spawn in (Ebel et al. 2015).

Little is known, however, about the organismal elemental composition of terrestrial, vertebrate consumers—especially mammals. A sizeable body of literature exists on the nutritional composition—i.e., the content of proteins, carbohydrates, and other macromolecules—of mammalian species of economic or recreational interest (e.g., caribou, *Rangifer tarandus,* Gerhart et al. 1996, or roe deer, *Capreolus capreoulus*, Hewison et al. 1996). Indeed, following the development of the nutritional geometry framework (see review in Raubenheimer 2011), nutritional composition analyses are experiencing a renaissance of sorts with new analyses focusing on wildlife species (e.g., the giant panda, *Ailuropoda melanoleuca*; Nie et al. 2015). However, elements contained in macromolecules are constrained in precise, invariant proportions and do not necessarily represent an organism's whole pool for a given element (Mariotti, Tomé, and Mirand 2008). Furthermore, macromolecules are themselves composite currencies subject to anabolic and catabolic processes, and thus lacking the kind of transferability across biological groups that is inherent to elements. Macromolecular content data are thus better suited as tools to study trophic interactions rather than ecosystem processes (Sperfeld et al. 2016).

However, aside from rare examples involving smaller-bodied species (e.g., desert lizards; González, Fariña, et al. 2011), our knowledge of the ecological stoichiometry of terrestrial vertebrate consumers is still in its infancy. This dearth of information effectively precludes investigating the finer scales and facets of consumer-environment relationships not only in terrestrial ecosystems, but also at the interface between terrestrial and aquatic environments (Sitters, Bakker, et al. 2017; Schmitz, Wilmers, et al. 2018). This knowledge gap can have real-world consequences, for instance, leading to incorrectly accounting for a species' contributions to the ecosystem budget of a limiting nutrient (e.g., P; Ebel et al. 2015). Furthermore, dietary needs of key chemical elements shape consumers' dietary needs just as much as energetic requirements (Sterner and Elser 2002; Simpson et al. 2004; González, Dézerald, et al. 2017; Anderson et al. 2020), potentially shaping multiple aspects of their ecology (Sterner 2004; Jean et al. 2015; Leroux, Vander Wal, et al. 2017). Expanding our knowledge of consumer ecology with empirical stoichiometry data is thus a necessary step towards a better understanding of the zoogeochemistry of our planet (*sensu* Schmitz, Wilmers, et al. 2018). As well, integrating new insights arising from this endeavour into existing frameworks and models will be instrumental in further assessing the magnitude and reduction of past and present consumers' influences on ecosystem functioning (Doughty et al. 2016; Doughty 2017).

1.2 Step into space: meta-ecology of consumers

Consumers exist within the context of their environment, so that the study of how they fit in ecosystem processes and functions can advance both our understanding of consumer ecology and ecosystem dynamics. Interactions with their environment define consumers, their ecology and life histories. The very names with which we partition consumers among eaters of plants, flesh, carrion or waste stem from their relationships with environmental features—their food sources, in this case. Literature is replete with examples of how consumers interact with their environment, for instance, resource (e.g., Jean et al. 2015; Duparc et al. 2020) or habitat (e.g., Zweifel-Schielly et al. 2009; Bjørneraas et al. 2012) selection. However, this wealth of information often exists in isolated nuggets, without a common framework that integrates general, shared details into a larger ecological picture. Meta-extensions of classic areas of ecology—i.e., population (Hanski 1998), community (Leibold et al. 2004), and ecosystem ecology (Loreau, Mouquet, and Holt 2003), collectively referred to as meta-ecology (Schiesari et al. 2019)—have brought an integrative, spatially aware, multi-disciplinary approach to the forefront. Meta-ecology has proven effective at expanding ecology's field of inference, leading to new insights on the way structure and variability in natural systems vary with context and scale (Levin 1992). For instance, how fragmented landscapes can support species persistence (Haddad et al. 2015), or how flows of elemental currencies enable planet-wide connections among far-flung ecosystems (Gounand, Little, et al. 2018). Yet, meta-ecology often relies on simplistic representations of consumer-resource interactions, space, and time in its theoretical constructs, limiting the applicability and relevance of its hypotheses and predictions for real-world scenarios (Gounand, Harvey, et al. 2018; Schiesari et al. 2019).

Consumers interact with and experience their surroundings through multiple perceptual layers, each defined by its own currency, that together produce the spatial maps used to navigate their environment (*sensu* Powell and Mitchell 2012). Integrating across these different layers and currencies, consumers engage in iterative, progressive space selection processes in which different stimuli inform decisions at different spatial scales (Johnson 1980). For instance, in Isle Royale National Park (USA) landscape use by moose changes among different seasons, with moose prioritizing use of shorelines in winter months due to these areas' better foraging opportunities and lower snow cover (Bump, Peterson, and Vucetich 2009). This pattern of space use also increases encounter rates with wolves, producing clustered carcass deposition that mediates ecosystem effects (see above, Section 1.1; Bump, Tischler, et al. 2009; Montgomery et al. 2014). Landscape heterogeneity, then, is a key element to consider when investigating consumer-resources interactions. In a zoogeochemical framework (Schmitz, Wilmers, et al. 2018), elements are the currency of choice and their variability in space is the spring that powers ecosystem processes and functions at multiple spatio-temporal scales (Schmitz and Leroux 2020). Recent contributions to ecological stoichiometry allow for explicit consideration of space in the dynamics of elemental nutrient exchanges between consumers and resources (Leroux, Vander Wal, et al. 2017; Soranno et al. 2019). In doing so, spatial ecological stoichiometry brings an ecosystem ecology perspective to the study of trophic relationships. However, the question remains of whether consumer can indeed perceive and respond to variation in the elemental phenotype (*sensu* Leal, Seehausen, and Matthews 2017) of their resources.

In addition to expanding the way we represent consumer-resources interactions in our theoretical constructs, accounting for how consumers navigate complex, realistic spatial configurations of resources and ecosystems remains a major challenge in meta-ecology (Gounand, Harvey, et al. 2018; McLeod and Leroux 2021). Consumers move in space and time, crossing ecosystem borders and acting as vessels for a host of ecological currencies that cannot move on their own. As well, consumers are adapting to the Anthropocene, changing the way they move and use space in relation to anthropogenic modifications of their environments (Tucker et al. 2018). Meta-ecology has long adopted simple representations of space (e.g., two-patch models; Marleau, Guichard, et al. 2010; Leroux and Loreau 2012) and consumer movement across them (e.g., diffusion-like movement; Gravel, Guichard, et al. 2010; Gravel, Mouquet, et al. 2010). However, movement is a complex phenomenon, shaped and influenced by a host of variables—both endogenous and exogenous to the consumer moving (Nathan et al. 2008). Movement is also an economical process, in which consumers seek the highest possible fitness return from the energetic investment done when initiating the move, thus differing substantially from other types of connections across ecosystems that do not entail energetic costs (McInturf et al. 2019). Finally, movement ability is also an ecological trait, subject to evolution and change over time, and through this trait consumers can manifest pervasive effects on local and regional processes and functions of ecosystems (Schmitz, Wilmers, et al. 2018; Hartfelder et al. 2020). In this context, developing new, more realistic and flexible mathematical representations of consumer movement is a fundamental step towards a more empirically relevant meta-ecology (Gounand, Harvey, et al. 2018; McInturf et al. 2019; Schiesari et al. 2019).

1.3 The boreal forest biome: brief description and overview

My thesis combines an empirical case study of the zoogeochemistry of herbivores in the boreal forests of Canada with a mathematical model of consumer movement in a meta-ecosystem. Here, I describe the boreal biome, one of the largest on Earth, to provide additional context to my two empirical data-based chapters, Chapter 2 and Chapter 3. I refer the interested reader to the works cited here for more detailed descriptions of this biome.

The boreal forest is the largest terrestrial biome on Earth, a circumpolar belt that spans the northern reaches of Eurasia and North America between 45°N–90°N (Brandt 2009). Caught between the arctic tree line to the North and the temperate forest to the South, the boreal forest has a subarctic climate with average temperature ranging from 0 °C (6–9 months per year) to 10 °C (1–3 months per years; Brandt 2009; Brandt et al. 2013). Coniferous—e.g., spruce, fir, and pines—and deciduous—e.g., aspen, birch, maples—tree species cover the majority of the landscape in the boreal forest (Worrell 1996; Brandt 2009). Below the canopy, lichens (e.g., *Cladonia* spp.), feather-mosses, and shrubs (e.g., *Vaccinium* spp.) dominate the forest floor community. Rivers, lakes, and wetlands break up the vegetation cover, leading to the high levels of ground humidity that characterize the boreal forest. Cold climate, frozen soils, dominant coniferous tree species, and high levels of humidity all compound to limit the nutrient availability and uptake by higher trophic levels—i.e., consumers (Naiman et al. 1994; Jones 1999; Gower et al. 2001).

The strong nutrient limitation of the boreal forest drives the relationship between plants and herbivores by shaping the fundamental mismatch in the dietary needs of these two trophic compartments (Bryant, Reichardt, and Clausen 1992; Sterner and Elser 2002; Pastor, Cohen, and Hobbs 2006). N is fundamental for the synthesis of the C-heavy molecules that plants rely on for structural support and growth, as well as for the protein-based development and energy production of herbivores. Plants, being stoichiometrically plastic, can finely regulate their internal elemental balance—i.e., their homeostasis—to offset environmental nutrient limitation (Sterner and Elser 2002). Herbivores, lacking the homeostatic plasticity of autotrophs, must prioritize access to N and other limiting nutrients in order to survive (e.g., P, K, Na; Sterner and Elser 2002; Kaspari and Powers 2016). The ensuing arms race influences not only the trophic interactions between plants and herbivores, but also ecosystem processes and functions (e.g., nutrient cycling; Leroux and Schmitz 2015). Furthermore, because of this pervasive nutrient limitation, herbivores have disproportionate effects on nutrient cycles and ecosystem functions in the boreal forest—variously mediated through both direct and indirect pathways (Leroux, Wiersma, and Vander Wal 2020). Owing to their relevance for human activities and wellbeing, several keystone boreal herbivores have been extensively studied (Rosell et al. 2005; Pastor, Cohen, and Hobbs 2006; Krebs, Boonstra, and Boutin 2018). Indeed, tentative theoretical constructs describing the feedback loops that link herbivory, environmental nutrient limitation, and primary productivity in the boreal forest have been proposed (Pastor, Cohen, and Hobbs 2006) and contested (Sitters and Olde Venterink 2015). This combination of strong nutrient limitation, well studied herbivores, and short trophic pathways makes the boreal forest a well-suited system to investigate the effects of consumers—herbivores in particular—on ecosystem processes and functions.

1.4 Thesis Overview

My thesis combines empirical studies and mathematical modeling to investigate the role terrestrial vertebrate consumers play in shaping ecosystem functions. Overall, my thesis is an example of how infusing wildlife, landscape, and ecosystem ecology with an ecological stoichiometry approach can lead to new insights on the mechanisms that underlie the ecosystem services humankind benefits from and strives to preserve.

In Chapter 2, I investigate the intraspecific variability in the organismal elemental composition of a keystone herbivore in the North American boreal biome, the snowshoe hare (*Lepus americanus*). Here, I assemble one of the first datasets on the C, N, and P whole-body content of a terrestrial vertebrate. I show that terrestrial vertebrates have higher intraspecific variation in the content of key elemental nutrients than previously expected. Furthermore, I demonstrate that this variability is mostly independent of a suite of ecological variables commonly identified as drivers of intraspecific stoichiometric differences in invertebrates. In addition to challenging long-held assumptions on the ecological stoichiometry of terrestrial vertebrates, in this chapter I highlight the need to consider a broader set of potential predictors of organismal elemental composition for this group of organisms.

In Chapter 3, I bridge landscape and wildlife ecology with ecological stoichiometry to investigate the responses of consumers to their environment. Specifically, I analyse how spatial variability in the stoichiometry of foraging resources changes the space use of herbivores. I use empirically assembled datasets on the spatial stoichiometry of three preferred forage species of snowshoe hares (*L. americanus*) to show that herbivore spatial ecology can vary in response to the spatial distribution of elements in their food. Snowshoe hares in areas where forage species have lower or more variable content of key elements—i.e., C, N, and P—have larger home range size than hares in areas with higher or less variable nutrient availability.

Building on the results of the previous two chapters, in Chapter 4 I develop a mathematical framework to integrate different types of consumer movement into meta-ecosystem models and explore their influences on local and meta-ecosystem functions. I demonstrate how different types of consumer movement can have different, and at times opposite, effects on local and meta-ecosystem functions. Furthermore, I show how the characteristics of local species assemblages—e.g., plant communities—can modulate the effects of consumer movement and even reverse them. Expanding meta-ecosystem models to account for multiple types of consumer movement can drastically alter the predictions of meta-ecosystem ecology and offer new insights on the dynamics of ecosystems connected in space and time.

In Chapter 5, I briefly summarize the main findings of my dissertation. I then discuss potential future directions arising from this work.

My thesis spans multiple areas of ecological research, woven together through the common threads of ecological stoichiometry and ecosystem ecology. Taken together, my thesis makes a major contribution to ecosystem ecology and should help improve predictions of the effects of organismal loss on ecosystem functions. In particular, my thesis highlights the importance of terrestrial vertebrate consumers for ecosystem functioning. First, I show that organisms are key, elementally diverse actors in ecosystem functions, and that they can elicit both direct and indirect influences on ecosystem processes. Second, I highlight conceptual and methodological issues in current models of meta-ecosystem dynamics built around a single type of flows—that is, diffusive flows—and offer an alternative approach that can accomodate a more diverse array of exchanges happening within and across ecosystem borders. Finally, I show that elements can act as a common currency across levels of ecological investigation in a manner akin to energy. As humankind continues to introduce, disperse, and otherwise modify the availability of elemental nutrients around the globe, infusing current and future research with an elementally aware approach may offer us new, unintuitive insights into ways of mitigating anthropogenic change.

Information to access the data and code used in this thesis can be found in the data accessibility section of each chapters, in the form of a hyper-textual link to an online repository.

1.5 Co-authorship Statement

This thesis is the result of my independent research. Throughout my work, I benefitted from collaborating with a cohesive, supportive, and dedicated group of co-authors. The breakdown of contributions to each chapter by co-authors is as follows:

Chapter 2

Myself, S. Leroux, E. Vander Wal, and Y. Wiersma devised the project; myself, T. Heckford, J. Balluffi-Fry, S. Leroux, Y. Wiersma, and E. Vander Wal collected the data; myself and S. Leroux analyzed the data; myself, T. Heckford, J. Balluffi-Fry, S. Leroux, Y. Wiersma, and E. Vander Wal interpreted the data. I led the writing of the manuscript. All authors contributed critically to the drafts and gave final approval for publication.

A version of this paper was published in *Ecology and Evolution* as:

M. Rizzuto, S. J. Leroux, E. Vander Wal, Y. F. Wiersma, T. R. Heckford, and J. Balluffi-Fry (2019). “Patterns and potential drivers of intraspecific variability in the body C, N, and P composition of a terrestrial consumer, the snowshoe hare (*Lepus americanus*)”. *Ecology and Evolution* 9 (24), pp. 14453–14464. DOI: `10.1002/ece3.5880`

Chapter 3

Myself, S. Leroux, Y. Wiersma, and E. Vander Wal designed the project; myself, T. Heckford, J. Balluffi-Fry, I. Richmond, Y. Wiersma, and S. Leroux collected the data; myself, S. Leroux, and I. Richmond analyzed the data. All authors contributed to interpreting the results. I led the writing of the manuscript and all authors read and approved the final version.

A version of this paper was published in *Oecologia* as:

M. Rizzuto, S. J. Leroux, E. Vander Wal, I. C. Richmond, T. R. Heckford, J. Balluffi-Fry, and Y. F. Wiersma (2021). "Forage stoichiometry predicts the home range size of a small terrestrial herbivore". *Oecologia* 197 (2), pp. 327–338. DOI: `10.1007/s00442-021-04965-0`

Chapter 4

Myself and S. Leroux designed the project; myself, S. Leroux, and O. Schmitz developed the model; myself and S. Leroux conducted the analyses. I wrote the manuscript. All authors contributed to revising the manuscript and approved the final version.

A version of this paper will be submitted to *The American Naturalist* as:

M. Rizzuto, S. J. Leroux, O. J. Schmitz, E. Vander Wal, Y. F. Wiersma, and T. H. Heckford (in prep.). "Animal-vectored nutrient flow along different resource gradients influences the nature of local and meta-ecosystem functioning."

1.6 Achievements

I disseminated the results presented in this thesis in the form of peer-reviewed journal articles (listed above, Section 1.5), as well as conference presentations and posters. Furthermore, this study is part of a long-term research project jointly led by Y. Wiersma, S. Leroux, and E. Vander Wal and collectively known as the Terrestrial Ecology Research Group (henceforth, TERG). TERG aims at disentangling the ecosystem dynamics of the boreal forest biome with an ecological stoichiometry-infused approach that bridges wildlife, landscape, and ecosystem ecology. As part of TERG, I collaborated on a number of papers led by other graduate students in the group; these are listed below. Additionally, by attending conferences and during a three months placement as visiting scholar at the Yale University School of the Environment funded by the Mitacs Globalink Research Internship program, I developed an extensive network of collaborators outside Memorial University and TERG. Engaging with this network of world-class researchers from diverse backgrounds and disciplines led to the development and publication of two separate papers. The details of these additional contributions are listed below. Please, see Section 1.5 for full citations of the peer-reviewed papers that arose from this dissertation.

1.6.1 Peer-reviewed papers

The following is a comprehensive list of peer-reviewed papers I was involved in—either as lead or co-author—throughout my Ph.D. but that are not part of this dissertation. I report the abstracts for these papers in Appendix D. For papers where I am lead author, I led ideas development, study design, data collection and analysis if applicable, and manuscript writing. For papers where I am fourth author or later, I contributed to ideas, data collection, and writing. An asterisk (*) denotes authors who contributed equally to a project.

- with the Terrestrial Ecology Research Group
    - J. Balluffi-Fry, S. J. Leroux, Y. F. Wiersma, T. R. Heckford, M. Rizzuto, I. C. Richmond, and E. Vander Wal (2020). "Quantity-quality trade-offs revealed using a multiscale test of herbivore resource selection on elemental landscapes". *Ecology and Evolution* 10.24, pp. 13847–13859. DOI: `10.1002/ece3.6975`
    - J. Balluffi-Fry, S. J. Leroux, Y. F. Wiersma, I. C. Richmond, T. R. Heckford, M. Rizzuto, J. L. Kennah, and E. Vander Wal (2021). "Integrating plant stoichiometry and feeding experiments: state-dependent forage choice and its implications on body mass". *Oecologia*. DOI: `10.1007/s00442-021-05069-5`
    - I. C. Richmond, S. J. Leroux, T. R. Heckford, E. Vander Wal, M. Rizzuto, J. Balluffi-Fry, J. L. Kennah, and Y. F. Wiersma (2021). "Temporal variation and its drivers in the elemental traits of four boreal plant species". *Journal of Plant Ecology* 14.3, pp. 398–413. DOI: `10.1093/jpe/rtaa103`
    - I. C. Richmond, J. Balluffi-Fry, E. Vander Wal, S. J. Leroux, M. Rizzuto, T. R. Heckford, J. L. Kennah, G. R. Riefesel, and Y. F. Wiersma (2021). "Individual snowshoe

hares manage risk differently: Integrating stoichiometric distribution models and foraging ecology." *Journal of Mammalogy*. Accepted, manuscript id: JMAMM–2021–026.R2

  - T. R. Heckford, S. J. Leroux, E. Vander Wal, M. Rizzuto, J. Balluffi-Fry, I. C. Richmond, and Y. F. Wiersma (2021). "Does where you live influence what you are made of? Spatial correlates of chemical traits across commonly occurring boreal plants". *Landscape Ecology*. DOI: `10.1007/s10980-021-01334-3`
  - T. R. Heckford, S. J. Leroux, E. Vander Wal, M. Rizzuto, J. Balluffi-Fry, I. C. Richmond, and Y. F. Wiersma (*in revision*). "Foliar elemental niche responses of balsam fir (*Abies balsamea*) and white birch (*Betula papyrifera*) to differing community types across geographic scales." *Functional Ecology*. manuscript id: FE-2020-00432.

- as visiting scholar at the Yale University School of the Environment
  - D. Ellis-Soto*, K. M. Ferraro*, M. Rizzuto, E. Briggs, J. D. Monk, and O. J. Schmitz (2021). "A methodological roadmap to quantify animal-vectored spatial ecosystem subsidies". *Journal of Animal Ecology* 90.7, pp. 1605–1622. DOI: `10.1111/1365-2656.13538`
- from other collaborations
  - C. J. Little*, M. Rizzuto*, T. M. Luhring, J. D. Monk, R. Nowicki, R. E. Paseka, J. Stegen, C. C. Symons, F. B. Taub, and J. Yen (*in review*). "Filling the Information Gap in Meta-Ecosystem Ecology". *Oikos*. manuscript id: OIK-08892.R1. EcoEvoRxiv preprint. DOI: `10.32942/osf.io/hc83u`

1.6.2 Conference contributions

- Rizzuto, M., Leroux, S. J., Schmitz, O. J., Vander Wal, E., Wiersma, Y. F., Heckford, T. R. *Going against the flow: non-diffusive organismal movement influences local and meta-*

ecosystem functioning. 02–06 August 2021. Contributed talk. Ecological Society of America Virtual Annual Meeting, Long Beach, CA, USA.

- Rizzuto, M., Leroux, S. J., Vander Wal, E., Wiersma, Y., Heckford, T. R., Balluffi-Fry, J. *Beyond Diffusion: Animal-Mediated Nutrient Transport at Different Spatial Scales.* 21–27 July 2018. Poster. “Unifying Ecology Across Scales” Gordon Research Seminar and Conference, Biddeford, ME, USA.

- Rizzuto, M., Leroux, S. J., Vander Wal, E., Wiersma, Y., Heckford, T. R., Balluffi-Fry, J. *Ontogeny and Ecological Stoichiometry of Snowshoe hares (Lepus americanus) in the Boreal Forests of Newfoundland.* 18–21 July 2018. Contributed talk. Canadian Society for Ecology and Evolution Annual General Meeting, Guelph, ON, Canada.

1.7 References

Ågren, G. I. and M. Weih (2012). “Plant stoichiometry at different scales: element concentration patterns reflect environment more than genotype”. *New Phytologist* 194 (4), pp. 944–952. DOI: `10.1111/j.1469-8137.2012.04114.x`.

Anderson, T. R. et al. (2020). “Geometric Stoichiometry: Unifying Concepts of Animal Nutrition to Understand How Protein-Rich Diets Can Be “Too Much of a Good Thing””. *Frontiers in Ecology and Evolution* 8.July, pp. 1–12. DOI: `10.3389/fevo.2020.00196`.

Ball, J. P., K. Danell, and P. Sunesson (2000). “Response of a herbivore community to increased food quality and quantity: an experiment with nitrogen fertilizer in a boreal forest”. *Journal of Applied Ecology* 37 (2), pp. 247–255. DOI: `10.1046/j.1365-2664.2000.00487.x`.

Balluffi-Fry, J., S. J. Leroux, Y. F. Wiersma, T. R. Heckford, et al. (2020). “Quantity-quality trade-offs revealed using a multiscale test of herbivore resource selection on elemental landscapes”. *Ecology and Evolution* 10.24, pp. 13847–13859. DOI: `10.1002/ece3.6975`.

Balluffi-Fry, J., S. J. Leroux, Y. F. Wiersma, I. C. Richmond, et al. (2021). “Integrating plant stoichiometry and feeding experiments: state-dependent forage choice and its implications on body mass”. *Oecologia*. DOI: `10.1007/s00442-021-05069-5`.

Bjørneraas, K. et al. (2012). “Habitat quality influences population distribution, individual space use and functional responses in habitat selection by a large herbivore”. *Oecologia* 168 (1), pp. 231–243. DOI: `10.1007/s00442-011-2072-3`.

Brandt, J. P. (2009). “The extent of the North American boreal zone”. *Environmental Reviews* 17.NA, pp. 101–161. DOI: `10.1139/A09-004`.

Brandt, J. P. et al. (2013). “An introduction to Canada’s boreal zone: ecosystem processes, health, sustainability, and environmental issues”. *Environmental Reviews* 21.4, pp. 207–226. DOI: `10.1139/er-2013-0040`.

Bryant, J. P., P. B. Reichardt, and T. P. Clausen (1992). “Chemically Mediated Interactions between Woody Plants and Browsing Mammals”. *Journal of Range Management* 45.1, p. 18. DOI: `10.2307/4002520`.

Bump, J. K., R. O. Peterson, and J. A. Vucetich (2009). “Wolves modulate soil nutrient heterogeneity and foliar nitrogen by configuring the distribution of ungulate carcasses”. *Ecology* 90.11, pp. 3159–3167. DOI: `10.1890/09-0292.1`.

Bump, J. K., K. B. Tischler, et al. (2009). “Large herbivores and aquatic-terrestrial links in southern boreal forests”. *Journal of Animal Ecology* 78.2, pp. 338–345. DOI: `10.1111/j.1365-2656.2008.01498.x`.

Bump, J. K., C. R. Webster, et al. (2009). “Ungulate carcasses perforate ecological filters and create biogeochemical hotspots in forest herbaceous layers allowing trees a competitive advantage”. *Ecosystems* 12.6, pp. 996–1007. DOI: `10.1007/s10021-009-9274-0`.

Currie, W. S. (2011). “Units of nature or processes across scales? The ecosystem concept at age 75”. *New Phytologist* 190.1, pp. 21–34. DOI: `10.1111/j.1469-8137.2011.03646.x`.

Dangal, S. R. S. et al. (2017). “Integrating Herbivore Population Dynamics Into a Global Land Biosphere Model: Plugging Animals Into the Earth System”. *Journal of Advances in Modeling Earth Systems* 9.8, pp. 2920–2945. DOI: `10.1002/2016MS000904`.

Díaz, S. et al. (2015). “The IPBES Conceptual Framework — connecting nature and people”. *Current Opinion in Environmental Sustainability* 14, pp. 1–16. DOI: `10.1016/j.cosust.2014.11.002`.

Doughty, C. E. (2017). “Herbivores increase the global availability of nutrients over millions of years”. *Nature Ecology & Evolution* 1.12, pp. 1820–1827. DOI: `10.1038/s41559-017-0341-1`.

Doughty, C. E. et al. (2016). “Global nutrient transport in a world of giants”. *Proceedings of the National Academy of Sciences of the United States of America* 113.4, pp. 868–873. DOI: `10.1073/pnas.1502549112`.

Duparc, A. et al. (2020). “Through the taste buds of a large herbivore: foodscape modeling contributes to an understanding of forage selection processes”. *Oikos* 129 (2), pp. 170–183. DOI: `10.1111/oik.06386`.

Ebel, J. D. et al. (2015). “Ontogenetic differences in Atlantic salmon phosphorus concentration and its implications for cross ecosystem fluxes”. *Ecosphere* 6.8, art136. DOI: `10.1890/ES14-00516.1`.

— (2016). “Whole body-element composition of Atlantic salmon *Salmo salar* influenced by migration direction and life stage in three distinct populations”. *Journal of Fish Biology* 89.5, pp. 1–10. DOI: `10.1111/jfb.13123`.

Elser, J. J. et al. (2000). “Nutritional constraints in terrestrial and freshwater food webs”. *Nature* 408.6812, pp. 578–580. DOI: `10.1038/35046058`.

Enquist, B. J. et al. (2020). “The megabiota are disproportionately important for biosphere functioning”. *Nature Communications* 11.1, p. 699. DOI: `10.1038/s41467-020-14369-y`.

Garland, G. et al. (2021). “A closer look at the functions behind ecosystem multifunctionality: A review”. *Journal of Ecology* 109.2, pp. 600–613. DOI: `10.1111/1365-2745.13511`.

Gerhart, K. L. et al. (1996). “Body composition and nutrient reserves of arctic caribou”. *Canadian Journal of Zoology* 74.1, pp. 136–146. DOI: `10.1139/z96-018`.

González, A. L., O. Dézerald, et al. (2017). “The Multidimensional Stoichiometric Niche”. *Frontiers in Ecology and Evolution* 5.September, pp. 1–17. DOI: `10.3389/fevo.2017.00110`.

González, A. L., J. M. Fariña, et al. (2011). “Exploring patterns and mechanisms of interspecific and intraspecific variation in body elemental composition of desert consumers”. *Oikos* 120.8, pp. 1247–1255. DOI: `10.1111/j.1600-0706.2010.19151.x`.

Gounand, I., E. Harvey, et al. (2018). “Meta-Ecosystems 2.0: Rooting the Theory into the Field”. *Trends in Ecology & Evolution* 33.1, pp. 36–46. DOI: `10.1016/j.tree.2017.10.006`.

Gounand, I., C. J. Little, et al. (2018). “Cross-ecosystem carbon flows connecting ecosystems worldwide”. *Nature Communications* 9.1, p. 4825. DOI: `10.1038/s41467-018-07238-2`.

Gower, S. T. et al. (2001). “Net primary production and carbon allocation patterns of boreal forest ecosystems”. *Ecological Applications* 11.5, pp. 1395–1411. DOI: `10.1890/1051-0761(2001)011[1395:NPPACA]2.0.CO;2`.

Gravel, D., F. Guichard, et al. (2010). “Source and sink dynamics in meta-ecosystems”. *Ecology* 91.7, pp. 2172–2184. DOI: `10.1890/09-0843.1`.

Gravel, D., N. Mouquet, et al. (2010). “Patch Dynamics, Persistence, and Species Coexistence in Metaecosystems”. *The American Naturalist* 176.3, pp. 289–302. DOI: `10.1086/655426`.

Haddad, N. M. et al. (2015). “Habitat fragmentation and its lasting impact on Earth’s ecosystems”. *Science Advances* 1.2, pp. 1–10. DOI: `10.1126/sciadv.1500052`.

Hanski, I. (1998). “Metapopulation dynamics”. *Nature* 396.6706, pp. 41–49. DOI: `10.1038/23876`.

Harfoot, M. B. J. et al. (2014). “Emergent Global Patterns of Ecosystem Structure and Function from a Mechanistic General Ecosystem Model”. *PLoS Biology* 12.4. DOI: `10.1371/journal.pbio.1001841`.

Hartfelder, J. et al. (2020). “The allometry of movement predicts the connectivity of communities”. *Proceedings of the National Academy of Sciences of the United States of America* 117.36, pp. 22274–22280. DOI: `10.1073/pnas.2001614117`.

Heckford, T. R. et al. (2021). “Does where you live influence what you are made of? Spatial correlates of chemical traits across commonly occurring boreal plants”. *Landscape Ecology*. DOI: `10.1007/s10980-021-01334-3`.

— (*in revision*). “Foliar elemental niche responses of balsam fir (*Abies balsamea*) and white birch (*Betula papyrifera*) to differing community types across geographic scales.” *Functional Ecology*. manuscript id: FE-2020-00432.

Hewison, A. J. M. et al. (1996). “Annual variation in body composition of roe deer (*Capreolus capreolus*) in moderate environmental conditions”. *Canadian Journal of Zoology* 74.2, pp. 245–253. DOI: `10.1139/z96-031`.

Hoeks, S. et al. (2020). “Mechanistic insights into the role of large carnivores for ecosystem structure and functioning”. *Ecography* 43.12, pp. 1752–1763. DOI: `10.1111/ecog.05191`.

Holdo, R. M., R. D. Holt, and J. M. Fryxell (2009). “Grazers, browsers, and fire influence the extent and spatial pattern of tree cover in the Serengeti”. *Ecological Applications* 19.1, pp. 95–109. DOI: `10.1890/07-1954.1`.

Holdo, R. M., R. D. Holt, A. R. Sinclair, et al. (2011). “Migration impacts on communities and ecosystems: empirical evidence and theoretical insights”. In: *Animal Migration*. Ed. by E. J. Milner-Gulland, J. M. Fryxell, and A. R. E. Sinclair. Oxford: Oxford University Press. Chap. Chapter 9, pp. 130–143. DOI: `10.1093/acprof:oso/9780199568994.003.0009`.

Holdo, R. M., A. R. Sinclair, et al. (2009). “A disease-mediated trophic cascade in the Serengeti and its implications for ecosystem C”. *PLoS Biology* 7.9. DOI: `10.1371/journal.pbio.1000210`.

Jean, P.-O. et al. (2015). “Combining near infrared spectra of feces and geostatistics to generate forage nutritional quality maps across landscapes”. *Ecological Applications* 25 (6), pp. 1630–1639. DOI: `10.1890/14-1347.1`.

Jefferies, R. L., R. F. Rockwell, and K. F. Abraham (2004). “Agricultural Food Subsidies, Migratory Connectivity and Large-Scale Disturbance in Arctic Coastal Systems: A Case Study”. *Integrative and Comparative Biology* 44, pp. 130–139. DOI: `10.1093/icb/44.2.130`.

Johnson, D. H. (1980). “The Comparison of Usage and Availability Measurements for Evaluating Resource Preference”. *Ecology* 61.1, pp. 65–71. DOI: `10.2307/1937156`.

Jones, H. G. (1999). “The ecology of snow-covered systems: a brief overview of nutrient cycling and life in the cold”. *Hydrological Processes* 13.1415, pp. 2135–2147. DOI: `10.1002/(SICI)1099-1085(199910)13:14/15<2135::AID-HYP862>3.3.CO;2-P`.

Kaspari, M. and J. S. Powers (2016). “Biogeochemistry and Geographical Ecology: Embracing All Twenty-Five Elements Required to Build Organisms”. *The American Naturalist* 188 (S1), S62–S73. DOI: `10.1086/687576`.

Krebs, C. J., R. Boonstra, and S. Boutin (2018). “Using experimentation to understand the 10-year snowshoe hare cycle in the boreal forest of North America”. *Journal of Animal Ecology* 87.1. Ed. by K. Wilson, pp. 87–100. DOI: `10.1111/1365-2656.12720`. eprint: `0608246v3`.

Leal, M., O. Seehausen, and B. Matthews (2017). “The ecology and evolution of stoichiometric phenotypes”. *Trends in Ecology & Evolution* 32.2, pp. 108–117. DOI: `10.1016/j.tree.2016.11.006`.

Leibold, M. A. et al. (2004). “The metacommunity concept: A framework for multi-scale community ecology”. *Ecology Letters* 7.7, pp. 601–613. DOI: `10.1111/j.1461-0248.2004.00608.x`. eprint: `2042`.

Leroux, S. J. and M. Loreau (2012). “Dynamics of Reciprocal Pulsed Subsidies in Local and Meta-Ecosystems”. *Ecosystems* 15.1, pp. 48–59. DOI: `10.1007/s10021-011-9492-0`.

Leroux, S. J. and O. J. Schmitz (2015). “Predator-driven elemental cycling: the impact of predation and risk effects on ecosystem stoichiometry”. *Ecology and Evolution* 5.21, pp. 4976–4988. DOI: `10.1002/ece3.1760`.

Leroux, S. J., E. Vander Wal, et al. (2017). “Stoichiometric distribution models: ecological stoichiometry at the landscape extent”. *Ecology Letters* 20 (12), pp. 1495–1506. DOI: `10.1111/ele.12859`.

Leroux, S. J., Y. F. Wiersma, and E. Vander Wal (2020). “Herbivore Impacts on Carbon Cycling in Boreal Forests”. *Trends in Ecology & Evolution* 35.11, pp. 1001–1010. DOI: `10.1016/j.tree.2020.07.009`.

Levin, S. A. (1992). “The Problem of Pattern and Scale in Ecology: The Robert H. MacArthur Award Lecture”. *Ecology* 73.6, pp. 1943–1967. DOI: `10.2307/1941447`.

Loreau, M., N. Mouquet, and R. D. Holt (2003). “Meta-ecosystems: A theoretical framework for a spatial ecosystem ecology”. *Ecology Letters* 6.8, pp. 673–679. DOI: `10.1046/j.1461-0248.2003.00483.x`.

MacSween, J., S. J. Leroux, and K. D. Oakes (2019). “Cross-ecosystem effects of a large terrestrial herbivore on stream ecosystem functioning”. *Oikos* 128.1, pp. 135–145. DOI: `10.1111/oik.05331`.

Mariotti, F., D. Tomé, and P. P. Mirand (2008). “Converting Nitrogen into Protein—Beyond 6.25 and Jones’ Factors”. *Critical Reviews in Food Science and Nutrition* 48.2, pp. 177–184. DOI: `10.1080/10408390701279749`.

Marleau, J. N., F. Guichard, et al. (2010). “Nutrient flows between ecosystems can destabilize simple food chains”. *Journal of Theoretical Biology* 266.1, pp. 162–174. DOI: `10.1016/j.jtbi.2010.06.022`.

Marleau, J. N., T. Peller, et al. (2020). “Converting Ecological Currencies: Energy, Material, and Information Flows”. *Trends in Ecology & Evolution* 35.12, pp. 1068–1077. DOI: `10.1016/j.tree.2020.07.014`.

Martiny, A. C. et al. (2013). “Strong latitudinal patterns in the elemental ratios of marine plankton and organic matter”. *Nature Geoscience* 6 (4), pp. 279–283. DOI: `10.1038/ngeo1757`.

McInturf, A. G. et al. (2019). “Vectors with autonomy: what distinguishes animal-mediated nutrient transport from abiotic vectors?” *Biological Reviews* 94, pp. 1761–1773. DOI: `10.1111/brv.12525`.

McLeod, A. M. and S. J. Leroux (2021). “Incorporating abiotic controls on animal movements in metacommunities”. *Ecology* 102.7, pp. 1–15. DOI: `10.1002/ecy.3365`.

Montgomery, R. A. et al. (2014). “Where Wolves Kill Moose: The Influence of Prey Life History Dynamics on the Landscape Ecology of Predation”. *PLoS One* 9.3, e91414. DOI: `10.1371/journal.pone.0091414`.

Naiman, R. J. et al. (1994). “Beaver Influences on the Long-Term Biogeochemical Characteristics of Boreal Forest Drainage Networks”. *Ecology* 75.4, pp. 905–921. DOI: `10.2307/1939415`.

Nathan, R. et al. (2008). “A movement ecology paradigm for unifying organismal movement research”. *Proceedings of the National Academy of Sciences of the United States of America* 105.49, pp. 19052–19059. DOI: `10.1073/pnas.0800375105`.

Nie, Y. et al. (2015). “Obligate herbivory in an ancestrally carnivorous lineage: The giant panda and bamboo from the perspective of nutritional geometry”. *Functional Ecology* 29 (1), pp. 26–34. DOI: `10.1111/1365-2435.12302`.

Pastor, J., Y. Cohen, and N. T. Hobbs (2006). “The roles of large herbivores in ecosystem nutrient cycles”. In: *Large herbivore ecology. Ecosystem dynamics and conservation*. Ed. by K. Danell et al. Conservation Biology. Cambridge University Press, pp. 289–325. DOI: `10.1017/CBO9780511617461.012`.

Pastor, J., B. Dewey, et al. (1993). “Moose Browsing and Soil Fertility in the Boreal Forests of Isle Royale National”. *Ecology* 74.2, pp. 467–480. DOI: `10.2307/1939308`.

Pastor, J. and R. J. Naiman (1992). “Selective Foraging and Ecosystem Processes in Boreal Forests”. *The American Naturalist* 139.4, pp. 690–705. DOI: `10.1086/285353`.

Powell, R. A. and M. S. Mitchell (2012). “What is a home range?” *Journal of Mammalogy* 93 (4), pp. 948–958. DOI: `10.1644/11-MAMM-S-177.1`.

Raubenheimer, D. (2011). “Toward a quantitative nutritional ecology: the right-angled mixture triangle”. *Ecological Monographs* 81.3, pp. 407–427. DOI: `10.1890/10-1707.1`.

Richmond, I. C., J. Balluffi-Fry, et al. (2021). “Individual snowshoe hares manage risk differently: Integrating stoichiometric distribution models and foraging ecology.” *Journal of Mammalogy*. Accepted, manuscript id: JMAMM–2021–026.R2.

Richmond, I. C., S. J. Leroux, et al. (2021). “Temporal variation and its drivers in the elemental traits of four boreal plant species”. *Journal of Plant Ecology* 14.3, pp. 398–413. DOI: `10.1093/jpe/rtaa103`.

Rinehart, S. and D. Hawlena (2020). “The effects of predation risk on prey stoichiometry: a meta-analysis”. *Ecology* 101.7, pp. 1–12. DOI: `10.1002/ecy.3037`.

Rivas-Ubach, A. et al. (2012). “Strong relationship between elemental stoichiometry and metabolome in plants”. *Proceedings of the National Academy of Sciences of the United States of America* 109.11, pp. 4181–4186. DOI: `10.1073/pnas.1116092109`.

Rizzuto, M., S. J. Leroux, E. Vander Wal, Y. F. Wiersma, et al. (2019). “Patterns and potential drivers of intraspecific variability in the body C, N, and P composition of a terrestrial consumer, the snowshoe hare (*Lepus americanus*)”. *Ecology and Evolution* 9 (24), pp. 14453–14464. DOI: `10.1002/ece3.5880`.

Roman, J., J. A. Estes, et al. (2014). “Whales as marine ecosystem engineers”. *Frontiers in Ecology and the Environment* 12, pp. 377–385. DOI: `10.1890/130220`.

Roman, J. and J. J. McCarthy (2010). “The whale pump: Marine mammals enhance primary productivity in a coastal basin”. *PLoS One* 5.10. DOI: `10.1371/journal.pone.0013255`.

Rosell, F. et al. (2005). “Ecological impact of beavers castor fiber and castor canadensis and their ability to modify ecosystems”. *Mammal Review* 35.3-4, pp. 248–276. DOI: `10.1111/j.1365-2907.2005.00067.x`.

El-Sabaawi, R. W. et al. (2012). “Widespread intraspecific organismal stoichiometry among populations of the Trinidadian guppy”. *Functional Ecology* 26.3, pp. 666–676. DOI: `10.1111/j.1365-2435.2012.01974.x`.

Schiesari, L. et al. (2019). “Towards an applied metaecology”. *Perspectives in Ecology and Conservation* 17.4, pp. 172–181. DOI: `10.1016/j.pecon.2019.11.001`.

Schmitz, O. J. and S. J. Leroux (2020). “Food Webs and Ecosystems: Linking Species Interactions to the Carbon Cycle”. *Annual Review of Ecology, Evolution, and Systematics* 51.1, pp. 271–295. DOI: `10.1146/annurev-ecolsys-011720-104730`.

Schmitz, O. J., P. A. Raymond, et al. (2014). “Animating the carbon cycle”. *Ecosystems* 17.2, pp. 344–359. DOI: `10.1007/s10021-013-9715-7`.

Schmitz, O. J., C. C. Wilmers, et al. (2018). “Animals and the zoogeochemistry of the carbon cycle”. *Science* 362 (6419), eaar3213. DOI: `10.1126/science.aar3213`.

Simpson, S. J. et al. (2004). "Optimal foraging when regulating intake of multiple nutrients". *Animal Behaviour* 68.6, pp. 1299–1311. DOI: `10.1016/j.anbehav.2004.03.003`.

Sitters, J., C. L. Atkinson, et al. (2015). "Spatial stoichiometry: cross-ecosystem material flows and their impact on recipient ecosystems and organisms". *Oikos* 124.7, pp. 920–930. DOI: `10.1111/oik.02392`.

Sitters, J., E. S. Bakker, et al. (2017). "The Stoichiometry of Nutrient Release by Terrestrial Herbivores and Its Ecosystem Consequences". *Frontiers in Earth Science* 5.April, pp. 1–8. DOI: `10.3389/feart.2017.00032`.

Sitters, J. and H. Olde Venterink (2015). "The need for a novel integrative theory on feedbacks between herbivores, plants and soil nutrient cycling". *Plant and Soil* 396.1-2, pp. 421–426. DOI: `10.1007/s11104-015-2679-y`.

Sitters, J., E. R. Wubs, et al. (2020). "Nutrient availability controls the impact of mammalian herbivores on soil carbon and nitrogen pools in grasslands". *Global Change Biology* 26.4, pp. 2060–2071. DOI: `10.1111/gcb.15023`.

Soranno, P. A. et al. (2019). "Spatial and temporal variation of ecosystem properties at macroscales". *Ecology Letters* 22 (10), pp. 1587–1598. DOI: `10.1111/ele.13346`.

Sperfeld, E. et al. (2016). "Bridging Ecological Stoichiometry and Nutritional Geometry with homeostasis concepts and integrative models of organism nutrition". *Functional Ecology*, pp. 1–11. DOI: `10.1111/1365-2435.12707`.

Sterner, R. W. (2004). "A one-resource "stoichiometry"". *Ecology* 85 (7), pp. 1813–1816. URL: `https://www.jstor.org/stable/3450351`.

Sterner, R. W. and J. J. Elser (2002). *Ecological stoichiometry: the biology of elements from molecules to the biosphere*. 1st ed. Princeton University Press, p. 464. URL: `https://www.jstor.org/stable/j.ctt1jktrp3`. Accessed 26 July 2021.

Tucker, M. A. et al. (2018). "Moving in the Anthropocene: Global reductions in terrestrial mammalian movements". *Science* 359.6374, pp. 466–469. DOI: `10.1126/science.aam9712`.

Tuomi, M. et al. (2021). “Stomping in silence: Conceptualizing trampling effects on soils in polar tundra”. *Functional Ecology* 35.2, pp. 306–317. DOI: `10.1111/1365-2435.13719`.

Worrell, R. (1996). *The boreal forests of Scotland*. Edinburgh: Forestry Commission Edinburgh, p. 42. URL: `https://www.forestry.gov.uk/PDF/FCTP014.pdf`.

Yang, H. and J. Chen (2018). “Integrating landscape system and meta-ecosystem frameworks to advance the understanding of ecosystem function in heterogeneous landscapes: An analysis on the carbon fluxes in the Northern Highlands Lake District (NHLD) of Wisconsin and Michigan”. *PLoS One* 13.2, e0192569. DOI: `10.1371/journal.pone.0192569`.

Zweifel-Schielly, B. et al. (2009). “Habitat selection by an Alpine ungulate: The significance of forage characteristics varies with scale and season”. *Ecography* 32 (1), pp. 103–113. DOI: `10.1111/j.1600-0587.2008.05178.x`.

Chapter 2

Patterns and potential drivers of intraspecific variability in the body C, N, P composition of a terrestrial consumer, the snowshoe hare (*Lepus americanus*).

Authors: Matteo Rizzuto[1], Shawn J. Leroux[1], Eric Vander Wal[1], Yolanda F. Wiersma[1], Travis R. Heckford[1], and Juliana Balluffi-Fry[2]

Authors' Affiliations

1: Department of Biology, Memorial University of Newfoundland and Labrador, St. John's, Canada

2: Department of Biological Sciences, University of Alberta, Edmonton, Canada

A version of this paper was published in *Ecology and Evolution* as:

M. Rizzuto, S. J. Leroux, E. Vander Wal, Y. F. Wiersma, T. R. Heckford, and J. Balluffi-Fry (2019). "Patterns and potential drivers of intraspecific variability in the body C, N, and P composition of a terrestrial consumer, the snowshoe hare (*Lepus americanus*)". *Ecology and Evolution* 9 (24), pp. 14453–14464. DOI: `10.1002/ece3.5880`

2.1 Introduction

The elemental composition of an organism is an important ecological trait subject to variation within and across species (Jeyasingh, Cothran, and Tobler 2014; Leal, Seehausen, and Matthews 2017). Primary producers (e.g., plants, algae), owing to the presence of dedicated storage structures in their cells, are plastic in their elemental composition (Sterner and Elser 2002; Borer et al. 2013): individual stoichiometric variability can at times be as large as that found among different genotypes (Ågren and Weih 2012). Marine phytoplankton and terrestrial plants show large variability in their carbon (C), nitrogen (N), and phosphorus (P) concentrations, at both large (Martiny et al. 2013; Sardans et al. 2016) and small spatio-temporal extents (Rivas-Ubach et al. 2012). Conversely, intraspecific variability in the chemical composition of consumers is generally considered smaller than variability observed in autotrophs, due to strict homeostasis requirements—particularly for terrestrial consumers (Sterner and Elser 2002; Elser, Bracken, et al. 2007; Leroux and Schmitz 2015). However, studies of invertebrates (González, Fariña, et al. 2011) or aquatic consumers (e.g., fish; Ebel et al. 2015, 2016) recently challenged this view, showing evidence of intraspecific stoichiometric variability in these species. For terrestrial vertebrates, much research has focused on their nutritional body composition (Hewison et al. 1996), differential use of chemical elements among conspecifics (Atwood and Weeks 2002), or body condition (Peig and Green 2010). We know little, however, about their organismal elemental composition, how it interacts with other ecological traits, and whether it varies among individuals. Given the very different patterns of energy and nutrient flows in aquatic and terrestrial ecosystems, which are driven primarily by the greater resource investments in structural support structures by terrestrial autotrophs (Shurin, Gruner, and Hillebrand 2006), we may expect differences in vertebrate consumer body composition in different ecosystems. Further, knowledge of the patterns and drivers of terrestrial vertebrate body elemental composition may shed light on how they shape a species' ecological niche (González, Dézerald, et al. 2017; González, Céréghino, et al. 2018; Peñuelas et al. 2019). Further, it may improve our ability to predict the relationship between consumers and ecosystem processes (e.g., carbon cycling; Schmitz, Raymond, et al. 2014).

Herbivores have the potential to exert top-down control on primary producers and can also affect their predators' ecology (Leroux and Schmitz 2015). They rely on resources whose organismal stoichiometry is markedly different from their own: terrestrial plants and algae are rich in C-heavy structural molecules, while herbivores rely on N and P to fuel their growth (Fagan et al. 2002; Sterner and Elser 2002). This mismatch, especially evident in terrestrial food webs, creates a strong bottleneck to nutrient flow in ecosystems (Boersma et al. 2008; Leroux and Schmitz 2015). As such, investigating the drivers of intraspecific variability in elemental composition of terrestrial herbivores can help shed light on both trophic dynamics and ecosystem processes, such as nutrient cycling (Sterner and Elser 2002; Leroux and Schmitz 2015; Schmitz, Wilmers, et al. 2018). Previous studies showed that consumers' elemental composition may vary under the effect of a wide range of variables and, in particular, as a function of an individual's age, sex, or body size and condition (El-Sabaawi, Zandona, et al. 2012; El-Sabaawi, Travis, et al. 2014; Ebel et al. 2015). Here, we investigate how these three variables influence the C, N, P body composition of a terrestrial consumer common across North America's boreal forest, the snowshoe hare (*Lepus americanus*). We focus on C, N, and P, as these are three of the most commonly studied and important elements for an organism (Sterner and Elser 2002, but see Jeyasingh, Cothran, and Tobler 2014). Owing to the strong nutrient limitation of boreal ecosystems (Pastor, Cohen, and Hobbs 2006), their unique ecology (Feldhamer, Thompson, and Chapman 2003), and their role as keystone herbivores in the boreal forest (Krebs, Boonstra, and Boutin 2018), snowshoe hares are well-suited to address these questions.

Organismal elemental content can vary throughout an individual's life. For instance, early life stages of *Daphnia lumholtzi* show higher concentrations of P and lower N:P than older ones, that appear to more strongly influence their growth rate than their body size (Main, Dobberfuhl, and Elser 1997). Evidence shows this pattern holds true among freshwater insects as well (Back and King 2013). Furthermore, similar intraspecific differences in elemental concentrations between life stages also exist among vertebrates (El-Sabaawi, Kohler, et al. 2012; El-Sabaawi, Zandona, et al. 2012; El-Sabaawi, Travis, et al. 2014). At times, this ontogenic variation in elemental composition of conspecifics is as large as that found among different genera (e.g., *Pimephales promelas* and *Cyprinodon variegatus*; Boros, Sály, and Vanni 2015). This allows for describing life stage-specific elemental signatures, as recently done for pre- and post-spawn adult Atlantic salmon (*Salmo salar*) during their annual spawning migration up- and downstream, respectively (Ebel et al. 2016). Similarly, the transition from newborn to adult in mammals involves a wide range of developmental changes, e.g., skeletal development and gonadal maturation, that could influence the elemental requirements and composition of an individual as it grows. For instance, Sterner and Elser (2002) hypothesize that, as bone tissue should contain most of its P reserves, a vertebrate's P content should increase with age given skeletal growth. Snowshoe hares develop quickly from newborn to adult but live in a strongly nutrient-limited environment: the trade-offs they face in acquiring necessary nutrients throughout their lifetime makes them well-suited to investigate how age may affect vertebrate intraspecific stoichiometry.

In a similar way, sex could affect relative content of key elements, due to differences in reproductive strategies and roles between males and females. Female mayflies, for instance, tend to have higher %P than males and slower %P decline with age (Back and King 2013). Among vertebrates, three-spined stickleback (*Gasterosteus aculeatus*) populations sampled from different lakes showed opposing trends in %P and N:P between sexes (Durston and El-Sabaawi 2017). Among mammals, differences in elemental composition related to sex arise mostly because of either parental care or mate search. Lactation and parental care exert costs due to increased foraging requirements in the parent administering to the newborns, as is the case among small mammals such as the big brown bat (*Eptesicus fuscus*; Hood, Oftedal, and Kunz 2006). Similarly, the development of secondary sexual characteristics, for instance the yearly production of antlers in some ungulate species, dramatically increases the need of a few selected elements in one of the two sexes (Atwood and Weeks 2002). While snowshoe hares are weakly sexually dimorphic (Feldhamer, Thompson, and Chapman 2003), and lack specialized secondary sexual characteristics, they can produce up to four litters per year, each comprising between 4–6 leverets. Females are larger than males, on average, likely as a strategy to offset this large reproductive investment (Feldhamer, Thompson, and Chapman 2003). Consequently, differences in the organismal content of C, N, or P could arise between sexes in hares following varying nutritional needs due to different reproductive strategies and efforts (Morehouse et al. 2010).

Organismal elemental composition can also vary with an individual's body size, as well as with its related condition metrics (body condition indexes, BCI; Stevenson and Woods 2006). For instance, P content tends to scale with an organism's size, particularly among vertebrates (González, Fariña, et al. 2011; Back and King 2013; but see Gillooly et al. 2005). While widespread, the sign of this relationship differs strongly among different groups, such as invertebrates and vertebrates. Among invertebrates, P content decreases with size, as they lack internal repositories of this element (Sterner and Elser 2002; González, Fariña, et al. 2011). Conversely, among vertebrates the majority of P stocks are found in bone tissue, so the P-body size allometric relationship should be positive (Sterner and Elser 2002). That is, all else being equal, P concentration should increase as the body size of an individual increases. However, modeling approaches show that P content should initially decrease and eventually approach an asymptotic relationship with vertebrate body size (Gillooly et al. 2005). Yet, empirical evidence suggests vertebrates' organismal P content increases with body size among indeterminate growers: for instance, in the tropical stream fish *Rivulus hartii*, larger individuals have higher concentrations of P than their smaller conspecifics (El-Sabaawi, Kohler, et al. 2012). Likewise, in the Atacama Desert of Chile, two species of lizards show a similar pattern of %P increasing with body size (González, Fariña, et al. 2011). In turn, this variability in the content of fundamental nutrients with body size could influence the overall condition of an individual—which ultimately determines its fitness and nutritional value for its predators (Stevenson and Woods 2006). In a strongly N- and P-limited environment like the boreal forest, snowshoe hares need access to large quantities of both N and P to develop muscle mass and skeleton over the course of a relatively short time (Pilati and Vanni 2007). Thus, larger individuals could indeed show higher concentrations of N and P as they may prioritize or have easier access to these limiting nutrients over C or other elements (Kay et al.

2005).

From all of the above it follows that, during an individual's lifetime, its content of C, N, P likely varies as a result of age (Ebel et al. 2016), sex (Durston and El-Sabaawi 2017), or body size (El-Sabaawi, Kohler, et al. 2012). Following previous works and theory on both consumer stoichiometry (González, Fariña, et al. 2011; Boros, Sály, and Vanni 2015; Ebel et al. 2016) and snowshoe hare ecology (Krebs, Boonstra, and Boutin 2018), we predict that (i) snowshoe hare organismal concentration of N and P increases as individuals grow older, whereas C content should decrease. We also expect (ii) female hares to have higher overall concentration of N and P than males, due to higher reproductive costs, and lower C. Finally, we expect (iii) larger snowshoe hares and those in better body condition to have higher concentrations of N and P. We provide predictions for C:N, C:P, and N:P ratios in Appendix A.2. We present one of the first assessments of the C, N, P body stoichiometry of a terrestrial vertebrate and discuss how intraspecific stoichiometric variability might influence trophic dynamics and ecosystem processes.

2.2 Methods

2.2.1 Study Species

Snowshoe hares (Figure 2.1) are a keystone herbivore in the boreal forests of North America, with a geographic range extending from Alaska to New Mexico (Feldhamer, Thompson, and Chapman 2003). Average total body length of snowshoe hares varies 36–52 cm and mean adult body weight is 1.3 kg (range: 0.9–2.3 kg): of this, only about 5% is fat, with both seasonal and annual fluctuations (Murray 2002). Females are usually 10–25% larger than males (Feldhamer, Thompson, and Chapman 2003).

Snowshoe hares are mostly nocturnal and do not hibernate over winter (Feldhamer, Thompson, and Chapman 2003). For these reasons, they are most often found in habitats with dense understory vegetation, allowing for more efficient thermo-regulation and predator avoidance (Litvaitis, Sherburne, and Bissonette 1985). Snowshoe hares populations cycle throughout the continent, with peaks every 8–11 years and densities ranging 5 to 25 fold (Reynolds et al. 2017). These abundance cycles are a defining characteristic of the boreal forest, affecting the ecology of many boreal species, from the plants the snowshoe hares consume, to their competitors and predators (Krebs, Boonstra, and Boutin 2018).

Snowshoe hares were introduced in Newfoundland in 1864 and quickly spread across the island (Strong and Leroux 2014). Studies conducted in the 1960s investigated their population dynamics, diet composition, and competition with another introduced herbivore, the moose (*Alces alces*; Dodds 1960, 1965). Compared to areas of Canada further west, Newfoundland has a fluctuating snowshoe hare population, with shorter and less regular periodicity (8–9 years; Reynolds et al. 2017). Their diet varies among seasons and areas of the island of Newfoundland (Dodds 1960): black spruce (*Picea mariana*) and balsam fir (*Abies balsamea*) comprise most of the winter forage, whereas during the summer they forage almost exclusively on deciduous plants and shrubs (e.g., *Vaccinium* spp.; *Trifolium* spp.; *Viburnum* spp.; Dodds 1960).

2.2.2 Data Collection

2.2.2.1 Snowshoe hare morphology, age, and sex

In October 2016, we purchased 50 whole, wild-caught snowshoe hares from a local trapper and stored them in individual plastic bags at −20 °C. These wild-caught specimens came from four snaring locations in the Eastern Avalon peninsula, over a small 21.5 km^2 trapping area around the towns of Chapel Arm (NL, 47°31’0” N, 53°40’0” W) and Long Harbour (NL, 47°25’46” N, 53°51’30” W). Individuals were snared without baiting with snares that do not select for age or sex, and thus likely reflect the age and sex distribution of the wild population they were taken from. In the laboratory, we thawed and weighed each specimen to the closest 0.1 g. We collected data on total body length, left hind foot length, and skull length and width for each hare to the closest mm, repeating each measurement 3 times and using their arithmetic mean in all subsequent analyses (see Appendix A.3.1). The Animal Care Committee of Memorial University approved our animal handling protocol with permit number 18-02-EV.

Like rodents, the teeth of lagomorphs grow continuously during their life, making conventional aging techniques based on dentine and cement inapplicable (Morris 1972). To account for this, we aged our specimens using a mixed approach involving counting bone tissue growth lines deposited after each winter in the mandibular bone. We used an ageing method developed for mountain hares (*Lepus timidus*) to select the area of the bone from which to count the growth lines (Iason 1988). For all 50 snowshoe hares in our sample, we extracted the complete mandibular bone, cleaned it of all soft tissues, and shipped the clean bones to Matson's Laboratory (Manhattan, MT, USA) for age determination (see Appendix A.3.2).

Sex determination in wild-caught snowshoe hares can be difficult. While visual approaches are available, these can be challenging when used on young, not yet fully developed individuals (as was the case in this study, see Results below). Genitalia are often not apparent in individuals younger than 6–12 months old and, even among not actively reproducing adults, they can be difficult to find. For these reasons, we chose to determine specimen sex using a DNA-based approach (Shaw, Wilson, and White 2003; see Appendix A.3.3). As the snowshoe hare genome is not yet completely sequenced, we chose a widely used set of primers for genetic sex determination in mammals to amplify the genetic material extracted from our specimens and from two control snowshoe hares of known sex (Shaw, Wilson, and White 2003). In cases when this DNA-based approach failed to detect an individual's sex (n = 3), we determined it by visual inspection and palpation of the genital area.

2.2.2.2 Body Size Metrics

We investigate the relationship between body size and organismal chemical composition of snowshoe hares using two different metrics: body condition and average body length. Body condition is a widely used metric to assess the overall health and quality, or "plumpness", of animals (Stevenson and Woods 2006; Peig and Green 2010). Snowshoe hares, however, differ from other mammals in that they do not rely on fat tissue to store energy (see Section 2.2.1 above). Consequently, body condition indexes that rely on body fat content may not capture the real body condition of our sample of wild-caught hares. For this reason, we estimate body condition using the scaled mass index (SMI; Peig and Green 2009, 2010). The SMI standardizes an individual's measure of body size with respect to another, thus accounting for scaling relationships (Peig and Green 2009). In particular, the SMI uses the average value of the length measurement (L) with the strongest relationship with body weight (M) as the standardizing variable, as established by a Standardized Major Axis regression (Peig and Green 2009; see Appendix A.3.4). The SMI formula is:

$$\hat{M}_i = M_i \left[\frac{L_0}{L_i} \right]^{b_{SMA}} \tag{2.1}$$

where $\hat{M}_i$ is the SMI of individual i, M_i is its body weight, L_i is the linear measure of body size of i, b_{SMA} is the exponent (i.e. slope) of a Standardized Major Axis Regression of $\ln(M)$ over $\ln(L)$, and L_0 is the study population's average value of L_i. Therefore, the SMI is the expected weight of individual i if its length measurement L_i was equal to the population's average value L_0. In this study, we used the length of the left hind foot to calculate the SMI. From the SMI value, we then computed the relative body condition (K_n) of an individual as the ratio of M_i to $\hat{M}_i$ (Stevenson and Woods 2006). This provided us with a simple metric to assess how good or bad an individual's condition was, compared to what it should be.

As the SMI is sensitive to the length measurement used to calculate it, we ran a separate set of models using a SMI produced using skull length, which also showed a strong relationship with body weight (see Appendix A.3.4 and Figure A.1). Furthermore, we considered average body length as a separate estimate of the effect of body size on the C, N, P stoichiometry of snowshoe hares (see Section 2.2.2.1 above).

2.2.2.3 Snowshoe hare C, N, P Body Stoichiometry

After collecting both morphological data and bone samples required for ageing, we individually blended our specimens to a homogeneous paste using a Retsch GM300 knife mill (Retsch GmbH, Haan, Germany). Through preliminary tests conducted on road-killed individuals not included in our sample of 50, we noticed that elastic or fine tissues, such as fur, skin, ears, and the walls of the digestive tract, were particularly difficult to homogenize with our equipment. Consequently, we removed fur, skin, and ears from all specimens: as such, our definition of body here does not include fur, skin, and ears. For the digestive tract, instead, we removed, cleaned, and finely chopped it before adding it back into the mixture. For each specimen, we collected a sample of the homogenized mixture, weighed it for wet weight (g), and oven dried it to constant weight for an average of 4 nights at 50 °C. After drying, we further ground each sample to as fine a powder as possible using mortar and pestle, and weighed it again for dry weight (g). On average, we required 50 g of wet homogenized material to produce 10 g of dry material for determining elemental concentration. We transferred all ground samples to glass vials and stored them in desiccators to prevent moisture accumulation and mold formation.

We sent the 50 dried samples to the Agriculture and Food Laboratory (AFL) at the University of Guelph for determination of the body content of C, N, and P as % of each sample's dry weight. At AFL, each sample was further ground before stoichiometric analyses. Concentrations of C and N were obtained following standard practices with an Elementar Vario MACRO cube (Elementar Analysensysteme GmbH, Langenselbold, Germany). For P, homogenized samples were first digested with nitric acid and hydrochloric acid using a closed-vessel microwave (CEM Marsxpress, CEM Corporation, Matthews, NC, USA). The microwave-digested sample was then brought to volume with nanopure water and P content quantified using Inductively-coupled Plasma-Optical Emission Spectroscopy using a Varian Vista Pro and a pneumatic nebulizer (Varian Inc., Palo Alto, CA, USA). This method was based on AOAC 2011.14.

Given that few studies have measured the C, N, P body stoichiometry of terrestrial vertebrates, we ran pilot tests to assess within-sample variability. These showed some within-sample variability in %C and %N (Figures A.2 and A.3). To account for this, each sample was analyzed three times for C and N content. Conversely, %P was relatively invariant within samples. Because of this, only 5 samples were run in duplicate to assess within-sample variability in %P (see Appendix A.3.5). In addition, to capture variability within individuals due to our homogenization protocol, we selected 5 random specimens for which we sent 2 additional samples (n = 10) of the homogenized paste to AFL (see Appendix A.3.5). Upon receiving the results back from AFL, to obtain C, N, P stoichiometry and molar ratios for each hare, we calculated each hare's dry body weight and converted the concentration of each element to molar mass using atomic weights. As variation among samples taken from each individual was negligible for all three elements, we used average values of %C, %N and %P for each individual in subsequent analyses (see Appendix A.3.6).

2.2.3 Statistical Analyses

We used General Linear Models (GLMs) in R (v. 3.4.4; R Core Team 2018) to investigate age, sex, body size and condition as potential drivers of hare stoichiometry. We used the concentration of each element of interest (i.e. %C, %N, %P), as well as the ratios C:N, C:P, and N:P as our response variables. We chose to focus on both elemental concentrations and ratios as these different measurements convey different but complementary information on body composition: quantity of elements of interest and their relationship to each other and importance to the animal, respectively. Age (continuous), sex (categorical), relative body condition (K_n, continuous), and average body length (ABL, continuous) were our explanatory variables. To test our predictions, we considered the effects of each of our predictor variables alone and their additive and 2-way interactive effects. We tested for multicollinearity among our explanatory variables using variance inflation factor analysis (VIF). As expected, VIF showed that relative body condition and average body length were highly correlated (VIF > 3). Therefore, we did not include these two variables in the same model (see Appendix A.4). We fit a set of 22 competing models, including an intercept-only model, and used the function `AICc` from the `AICmodavg` R package to select the most parsimonious model based on the Akaike Information Criterion corrected for small sample size (AICc; Burnham and Anderson 2002; Mazerolle 2017). We assessed that the assumptions of GLMs were met using standard approaches (Zuur, Ieno, and Elphick 2010). We then removed models with uninformative parameters from the model set of each response variable (Leroux

2019; see Appendix A.5.1).

2.3 Results

Snowshoe hares in our sample varied in age between 0 (“young-of-the-year”) and 6 years old, the majority (74%) being between 0 and 1 years old. Only one individual, a female, was 6 years old. Males were more common (31 out of 50) than females (19). Average (±SD) wet body weight was 1374.81 g (±186.59, range: 914.30–1776.50 g), with average dry weight being 399.11 g (±74.70, range: 241.76–567.86 g). Water made up to 72% of body weight. Average body length was 42.49 cm (±2.07, range: 36.67–46.67 cm; Table A.16). Average left hind foot length (L_0) for our snowshoe hare population was 12.88 cm (±0.58, range: 11.40–14.10 cm). The slope of the Standardized Major Axis Regression of average left hind foot length on body weight (i.e., the exponent b_{SMA} in eq. 2.1) was 3.18. Overall, young snowshoe hares appeared more variable in relative body condition than older individuals (mean: 1.01 ±0.14; Figure A.5).

Snowshoe hares were, on average, composed of 43.60% C (±2.59, range: 37.46%–51.29%), 11.20% N (±0.78, range: 9.42%–12.68%), and 2.97% P (±0.52, range: 2.00%–4.29%; Figure 2.2 and Table A.17). The most parsimonious model for %N included only age ($R^2 = 0.066$): %N was negatively related to the age of individual snowshoe hares (Table 2.1). Evidence for this relationship is, however, weak as the intercept-only model was within 2ΔAICc of the top ranked model (Table 2.1). For %P, the two top ranked models included relative body condition and average body length, respectively (Table 2.1). %P was positively related to relative body condition ($R^2 = 0.073$; Figure 2.3) and average body length ($R^2 = 0.047$). Again, evidence for these relationships is weak as the intercept-only model was the third-best performing model and within 2ΔAICc of the top ranked models (Table 2.1). We also observed a qualitative pattern of higher %P among older males (Figure 2.4), but found no statistical support for it (Table 2.1). For %C, the top ranked model was the intercept-only model, which provides no evidence of a relationship between variation in %C and age, sex, or body size and condition of individuals (Table 2.1).

For the stoichiometric ratios, the top ranked model for C:N included only age, which had a positive relationship with C:N ratio ($R^2 = 0.074$; Table 2.2). For this relationship too, evidence is weak as the intercept-only model was within 2ΔAICc of the best-performing one. We found no evidence for a relationship between age, sex, body size and condition, and either C:P or N:P as the top ranked model for both these ratios was the intercept-only model (Table 2.2). Using skull length instead of left hind foot length to calculate K_n did not qualitatively change our results (see Tables A.1 and A.2).

2.4 Discussion

We provide one of few assessments of the C, N, P body stoichiometry of a terrestrial vertebrate and investigate potential drivers of this fundamental ecological trait. Overall, we find variation in the concentrations of C, N, P, and in their ratios within our sample of snowshoe hares. However, age, sex, and body size or condition provide little or no explanation of this variation. Our models highlight a weak negative relationship between an individual's age and its N concentration and, symmetrically, a weak and positive trend of C:N and age. Likewise, we find weak support for a relationship between an individual's body size and condition and its P concentration. Together, these results provide some of the first evidence for intraspecific variability in the C, N, P body stoichiometry of a terrestrial vertebrate but raise the need to consider a broader suite of potential drivers. As well, our data provide a starting point for comparisons of vertebrate species stoichiometry across ecological realms (e.g. aquatic-terrestrial).

We found weak evidence in support of our prediction that age might drive variability in the C, N, P body stoichiometry of snowshoe hares. In particular, contrary to our predictions, we find weak evidence of young individuals (0–1 years old) having higher N concentrations than older ones—with a more pronounced decrease among males than among females (Figure 2.4). As would be expected from this pattern, C:N values show an opposite, positive trend with age (Figure 2.4)—reflecting the lower amounts of N compared to C in older hares and lending further support to this result. Younger individuals may show higher %N as a result of increased N allocation to muscle tissue production (Boros, Sály, and Vanni 2015). Snowshoe hares experience strong predation pressure from a large cohort of predators, both land-based and avian, from the earliest life stages (Krebs, Boonstra, and Boutin 2018). A higher N content among young hares could be a sign of early-life investments in production of N-rich protein to develop the muscle mass necessary for their hide and run anti-predator response. We also observed a qualitative pattern of increasing %P with age among males. While our models do not offer support for it (Table 2.1), similar patterns have been described for other vertebrate species. Boros, Sály, and Vanni (2015) found a similar trend between %P and age in two species of laboratory-reared minnows. Similarly, Sterrett, Maerz, and Katz (2015) found that older individuals had higher %P in four species of turtles. This pattern could result from bone tissue development as the individual ages (Sterner and Elser 2002). In turn, by actively sequestering P in their bones, vertebrates could influence nutrient ecosystem dynamics by acting as "walking" repositories of a limiting element (Pastor, Cohen, and Hobbs 2006; Sterrett, Maerz, and Katz 2015). Given the large number of young individuals in our sample, and the relative rarity of snowshoe hares older than 3 years, it may be that access to P during a hare's ageing process is fundamental for its survival. Future studies investigating the link between N and P availability and long-term survival in wild herbivore populations may further our understanding of both population dynamics and ecosystem impacts mediated by these consumers.

Contrary to our predictions, we find no evidence for a relationship between hare stoichiometry and sex (Figure 2.2). This may not be surprising given the low sexual dimorphism shown by our study species. Several studies that investigated the relationship between sex and organismal stoichiometry among more strongly sexually dimorphic species provide similarly contradictory evidence. Among guppies, for instance, sex had no relationship with stoichiometry when considered alone, yet it had significant interactions with the fish's stream of origin—likely an indirect consequence of different predation levels experienced by males and females in different streams (El-Sabaawi, Zandona, et al. 2012). Conversely, among *Hyalella* amphipods, strong sexual dimorphism in the concentrations and patterns of variation of multiple elements underlays sexual dimorphism in traits as different as foraging behaviour, nutritional physiology, and sex-specific selection of genomic loci (Goos, Cothran, and Jeyasingh 2017). Among antler-producing ungulates, males and females differ in both content and use of certain elements (e.g., calcium; Atwood and Weeks 2002). Finally, as hares undergo morpho-physiological changes during their reproductive season, investigating the relationship between C, N, P body stoichiometry and sex among actively reproducing hares might produce different results (Hood, Oftedal, and Kunz 2006). These contrasting lines of evidence highlight the need of further research, involving a wider range of species from a variety of environments, to reduce the uncertainty around the role of sex as a driver of variation in organismal stoichiometry.

Consistent with our predictions, our results indicate body size and condition as potential drivers for variability in P concentration in our sample. The two top models for this element included relative body condition and average body length, and both variables had a positive relationship with %P. In particular, the observed body weight of snowshoe hares with higher %P matched or exceeded the predicted value obtained from the SMI formula (eq. 2.1). Snowshoe hare body condition fluctuates throughout the year (Murray 2002), with peaks in the months leading up to the boreal winter, during which hares remain active and face increased levels of stress due to both lack of optimal forage and increased predation (Krebs, Boonstra, and Boutin 2018). As body condition declines over the winter months (Murray 2002), one could test if the weak relationship we observe between P and body condition would vary in a similar way. Additionally, we observe a qualitatively larger variability in relative body condition among young hares in our sample than among older specimens (Figure A.5). Snowshoe hares produce multiple litters per year (up to four; Feldhamer, Thompson, and Chapman 2003), yet a large number of leverets does not survive their first winter (Krebs, Boonstra, and Boutin 2018). While we do not find evidence for a relationship between age and P content, a potential question to ask is whether birth date within a year could explain part of this variability. Our results, albeit weakly supported by our statistical analyses, appear to confirm the potential role P plays within the internal chemical machinery of an animal, and its importance for its survival (Elser, Bracken, et al. 2007; Boersma et al. 2008).

A large amount of variability in our sample remains unexplained and, overall, we find only weak support for our initial hypothesis of variation in organismal stoichiometry among snowshoe hares. Indeed, other vertebrate species show much stronger patterns of intraspecific variation in elemental content. Ebel et al. (2015, 2016), for instance, showed that migratory Atlantic salmon (*S. salar*) at different ontogenic stages have distinct stoichiometric signatures, particularly before and after their first migration from their freshwater nurseries to the open ocean. The reason for these differences in the magnitude of the effects mediated by ontogeny could be found in the life history of snowshoe hares. Snowshoe hares do not undergo dramatic life events like migratory salmon, or the metamorphosis of certain insect species, which clearly separate different life stages. Rather, they are characterized by short gestation periods (≃30–40 days) and quick maturation of leverets into adults (≃6 months; Feldhamer, Thompson, and Chapman 2003). It is possible, in this scenario, that we investigated the effects of age at a time in the life of snowshoe hares when most of the changes in chemical composition had already taken place. It is also interesting to note the larger proportion of young individuals in our sample, consistent with current knowledge about snowshoe hare survival beyond their first winter (Krebs, Boonstra, and Boutin 2018) and likely representative of the age distribution of the particular wild population we used in this study. Thus, a potentially interesting and rewarding research avenue would be to further investigate differences in hare stoichiometry in earlier life stages.

Before homogenization, we removed fur, skin, and ears of our snowshoe hare specimens as these tissues proved challenging to homogenize. While we consistently applied this protocol to all 50 hares included in our sample, excluding these tissues from analyses may have influenced the amount of stoichiometric variability we detected. Ears are made of cartilage, which consists mostly of polysaccharides and proteoglycans, thus being C-rich. Additionally, on average, ears accounted for 0.74% of a hare's body weight in our sample. As for fur and skin, in humans and other mammalian species, hair is made up of up to ∼17%N (Block and Schein 1939). While we could not find accounts of the chemical composition of snowshoe hare hair, it is possible that the production, maintenance, and molting processes of this species' fur impose further stoichiometric requirements—ultimately influencing the relative concentrations of C, N, and P in a snowshoe hare body throughout its life. Finally, although our samples were collected from a small area, fine scale forage quality may also be a driver of the stoichiometric variability we observed. As well, snowshoe hare populations sampled from different areas of Newfoundland and North America or in different times of the year may differ in their elemental composition from the specimens investigated here (as is the case for some fish species; El-Sabaawi, Zandona, et al. 2012). Future work could investigate spatio-temporal variation in individual, habitat, and forage quality as a driver of consumer body elemental composition (Leroux, Vander Wal, et al. 2017) and interpopulation variability.

The variation in hare body composition we observe could have repercussions beyond the stoichiometry of this species, and influence ecosystem processes such as nutrient cycling, transport, and primary productivity (Pastor, Cohen, and Hobbs 2006). Snowshoe hares are a keystone herbivore in the boreal forest, a markedly nutrient-limited environment (Pastor, Cohen, and Hobbs 2006). They are characterized by strong, decade-long fluctuations in their population abundance and serve as primary food source for multiple predator species (Krebs, Boonstra, and Boutin 2018). Paucity of nutrients, and the well-known stoichiometric mismatch between plants and herbivores (Elser, O'brien, et al. 2000; Sterner and Elser 2002), prompted boreal forest herbivores to evolve browsing strategies allowing them to extract as many nutrients as possible from their food (Pastor, Cohen, and Hobbs 2006). Thus, the appearance of a large number of young snowshoe hares over the landscape during a population peak could have strong dampening effects on elemental cycling in the boreal forest—as well as in adjacent ecosystems—possibly reducing N or P availability to primary producers as they become locked within the herbivores' biomass. By infusing ongoing ecological research with stoichiometric data, future studies could address this potential interplay between a species' stoichiometry and the ecosystem processes it contributes to (Leal, Seehausen, and Matthews 2017). In turn, this would allow for shedding light on fine-grain mechanisms with far-reaching consequences, such as cross-ecosystem nutrient mobilization (Schmitz, Wilmers, et al. 2018) and nutrient recycling (Schmitz, Raymond, et al. 2014), as well as on their influence on ecosystem services fundamental for humans.

Ecological stoichiometry has a long history in marine and freshwater ecosystems and has been shaped by detailed studies of algae, plants and invertebrates. In recent years, researchers started investigating the stoichiometry of more complex organisms in aquatic ecosystems, particularly fish (Atkinson et al. 2017). This expanded the reach of ecological stoichiometry in exciting new directions, integrating it with other subfields of ecology, such as metabolic ecology (Rivas-Ubach et al. 2012), ecosystem ecology (Abbas et al. 2012), and landscape ecology (Sardans et al. 2016; Leroux, Vander Wal, et al. 2017). Yet, terrestrial species other than plants and insects remain relatively unexplored in terms of their stoichiometry. Our results suggest that a greater focus on terrestrial vertebrates and consumers could provide novel insights and potentially question well-known concepts in this field.

2.5 Data Availability

All data and code used in the analyses are available via a figshare online repository at:

https://doi.org/10.6084/m9.figshare.7884854

2.6 References

Abbas, F. et al. (2012). “Roe deer may markedly alter forest nitrogen and phosphorus budgets across Europe”. *Oikos* 121.8, pp. 1271–1278. DOI: `0.1111/j.1600-0706.2011.20103.x`.

Ågren, G. I. and M. Weih (2012). “Plant stoichiometry at different scales: element concentration patterns reflect environment more than genotype”. *New Phytologist* 194 (4), pp. 944–952. DOI: `10.1111/j.1469-8137.2012.04114.x`.

Atkinson, C. L. et al. (2017). “Consumer-driven nutrient dynamics in freshwater ecosystems: from individuals to ecosystems”. *Biological Reviews* 92.4, pp. 2003–2023. DOI: `10.1111/brv.12318`.

Atwood, T. C. and H. P. Weeks (2002). “Sex- and Age-specific Patterns of Mineral Lick Use by White-tailed Deer (*Odocoileus virginianus*)”. *The American Midland Naturalist* 148.2, pp. 289–296. DOI: `10.1674/0003-0031(2002)148[0289:SAASPO]2.0.CO;2`.

Back, J. A. and R. S. King (2013). “Sex and size matter: ontogenetic patterns of nutrient content of aquatic insects”. *Freshwater Science* 32.3, pp. 837–848. DOI: `10.1899/12-181.1`.

Block, R. and A. Schein (1939). “The composition of keratins: the amino acid composition of hair, wool, horn, and other eukeratins”. *Journal of Biological Chemistry*, pp. 181–186. DOI: `10.1016/S0021-9258(18)73740-X`.

Boersma, M. et al. (2008). “Nutritional limitation travels up the food chain”. *International Review of Hydrobiology* 93, pp. 479–488. DOI: `10.1002/iroh.200811066`.

Borer, E. T. et al. (2013). “Global biogeography of autotroph chemistry: is insolation a driving force?” *Oikos* 122.8, pp. 1121–1130. DOI: `10.1111/j.1600-0706.2013.00465.x`.

Boros, G., P. Sály, and M. J. Vanni (2015). “Ontogenetic variation in the body stoichiometry of two fish species”. *Oecologia* 179.2, pp. 329–341. DOI: `10.1007/s00442-015-3349-8`.

Burnham, K. P. and D. R. Anderson (2002). *Model Selection and Multimodel Inference: A Practical Information-Theoretic Approach (2nd ed)*. 2nd ed. Springer-Verlag New York, pp. XXVI, 488.

Dodds, D. G. (1960). “Food Competition and Range Relationships of Moose and Snowshoe hare in Newfoundland”. *The Journal of Wildlife Management* 24 (1), pp. 52–60. DOI: `10.2307/3797356`.

— (1965). “Reproduction and Productivity of Snowshoe Hares in Newfoundland”. *The Journal of Wildlife Management* 29.2, pp. 303–315. DOI: `10.2307/3798435`.

Durston, D. J. and R. W. El-Sabaawi (2017). “Bony traits and genetics drive intraspecific variation in vertebrate elemental composition”. *Functional Ecology* 31.11, pp. 2128–2137. DOI: `10.1111/1365-2435.12919`.

Ebel, J. D. et al. (2015). “Ontogenetic differences in Atlantic salmon phosphorus concentration and its implications for cross ecosystem fluxes”. *Ecosphere* 6.8, art136. DOI: `10.1890/ES14-00516.1`.

— (2016). “Whole body-element composition of Atlantic salmon *Salmo salar* influenced by migration direction and life stage in three distinct populations”. *Journal of Fish Biology* 89.5, pp. 1–10. DOI: `10.1111/jfb.13123`.

Elser, J. J., M. E. S. Bracken, et al. (2007). “Global analysis of nitrogen and phosphorus limitation of primary producers in freshwater, marine and terrestrial ecosystems”. *Ecology Letters* 10.12, pp. 1135–1142. DOI: `10.1111/j.1461-0248.2007.01113.x`.

Elser, J. J., W. J. O’brien, et al. (2000). “The evolution of ecosystem processes: growth rate and elemental stoichiometry of a key herbivore in temperate and arctic habitats”. *Journal of Evolutionary Biology* 13.5, pp. 845–853. DOI: `10.1046/j.1420-9101.2000.00215.x`.

Fagan, W. F. et al. (2002). “Nitrogen in insects: Implications for trophic complexity and species diversification”. *The American Naturalist* 160.6, pp. 784–802. DOI: `10.1086/343879`.

Feldhamer, G. A., B. C. Thompson, and J. A. Chapman (2003). *Wild mammals of North America: biology, management, and conservation*. JHU Press.

Gillooly, J. F. et al. (2005). “The metabolic basis of whole-organism RNA and phosphorus content”. *Proceedings of the National Academy of Sciences of the United States of America* 102.33, pp. 11923–11927. DOI: `10.1073/pnas.0504756102`.

González, A. L., R. Céréghino, et al. (2018). “Ecological mechanisms and phylogeny shape invertebrate stoichiometry: A test using detritus-based communities across Central and South America”. *Functional Ecology* 32.10. Ed. by S. J. Leroux, pp. 2448–2463. DOI: `10.1111/1365-2435.13197`.

González, A. L., O. Dézerald, et al. (2017). “The Multidimensional Stoichiometric Niche”. *Frontiers in Ecology and Evolution* 5.September, pp. 1–17. DOI: `10.3389/fevo.2017.00110`.

González, A. L., J. M. Fariña, et al. (2011). “Exploring patterns and mechanisms of interspecific and intraspecific variation in body elemental composition of desert consumers”. *Oikos* 120.8, pp. 1247–1255. DOI: `10.1111/j.1600-0706.2010.19151.x`.

Goos, J. M., R. D. Cothran, and P. D. Jeyasingh (2017). “Within-population variation in the chemistry of life: the stoichiometry of sexual dimorphism in multiple dimensions”. *Evolutionary Ecology* 31.5, pp. 1–17. DOI: `10.1007/s10682-017-9900-9`.

Hewison, A. J. M. et al. (1996). “Annual variation in body composition of roe deer (*Capreolus capreolus*) in moderate environmental conditions”. *Canadian Journal of Zoology* 74.2, pp. 245–253. DOI: `10.1139/z96-031`.

Hood, W. R., O. T. Oftedal, and T. H. Kunz (2006). “Variation in body composition of female big brown bats (*Eptesicus fuscus*) during lactation”. *Journal of Comparative Physiology B* 176.8, pp. 807–819. DOI: `10.1007/s00360-006-0102-y`.

Iason, G. R. (1988). “Age determination of mountain hares (*Lepus timidus*): a rapid method and when to use it”. *Journal of Applied Ecology* 25 (2), pp. 389–395. DOI: `10.2307/2403831`.

Jeyasingh, P. D., R. D. Cothran, and M. Tobler (2014). “Testing the ecological consequences of evolutionary change using elements”. *Ecology and Evolution* 4.4, pp. 528–538. DOI: `10.1002/ece3.950`.

Kay, A. D. et al. (2005). “Toward a stoichiometric framework for evolutionary biology”. *Oikos* 109.1, pp. 6–17. DOI: `10.1111/j.0030-1299.2005.14048.x`.

Krebs, C. J., R. Boonstra, and S. Boutin (2018). “Using experimentation to understand the 10-year snowshoe hare cycle in the boreal forest of North America”. *Journal of Animal Ecology* 87.1. Ed. by K. Wilson, pp. 87–100. DOI: `10.1111/1365-2656.12720`. eprint: `0608246v3`.

Leal, M., O. Seehausen, and B. Matthews (2017). “The ecology and evolution of stoichiometric phenotypes”. *Trends in Ecology & Evolution* 32.2, pp. 108–117. DOI: `10.1016/j.tree.2016.11.006`.

Leroux, S. J. (2019). “On the prevalence of uninformative parameters in statistical models applying model selection in applied ecology”. *PLoS One* 14 (2), pp. 1–12. DOI: `10.1371/journal.pone.0206711`.

Leroux, S. J. and O. J. Schmitz (2015). “Predator-driven elemental cycling: the impact of predation and risk effects on ecosystem stoichiometry”. *Ecology and Evolution* 5.21, pp. 4976–4988. DOI: `10.1002/ece3.1760`.

Leroux, S. J., E. Vander Wal, et al. (2017). “Stoichiometric distribution models: ecological stoichiometry at the landscape extent”. *Ecology Letters* 20 (12), pp. 1495–1506. DOI: `10.1111/ele.12859`.

Litvaitis, J. A., J. A. Sherburne, and J. A. Bissonette (1985). “Influence of Understory Characteristics on Snowshoe Hare Habitat Use and Density”. *The Journal of Wildlife Management* 49.4, pp. 866–873. DOI: `10.2307/3801359`.

Main, T. M., D. R. Dobberfuhl, and J. J. Elser (1997). “N:P stoichiometry and ontogeny of crustacean zooplankton: a test of the growth rate hypothesis”. *Limnology and Oceanography* 42.6, pp. 1474–1478. DOI: `10.4319/lo.1997.42.6.1474`.

Martiny, A. C. et al. (2013). “Strong latitudinal patterns in the elemental ratios of marine plankton and organic matter”. *Nature Geoscience* 6 (4), pp. 279–283. DOI: `10.1038/ngeo1757`.

Mazerolle, M. J. (2017). *AICcmodavg: Model selection and multimodel inference based on (Q)AIC(c)*. URL: `https://cran.r-project.org/package=AICcmodavg`.

Morehouse, N. I. et al. (2010). “Sex in a Material World: Why the Study of Sexual Reproduction and Sex-Specific Traits Should Become More Nutritionally-Explicit”. *Oikos* 119.5, pp. 766–778. DOI: `10.1111/j.1600-0706.2009.18569.x`.

Morris, P. (1972). “A review of mammalian age determination methods”. *Mammal Review* 2.3, pp. 69–104. DOI: `10.1111/j.1365-2907.2012.00221.x`.

Murray, D. L. (2002). “Differential body condition and vulnerability to predation in snowshoe hares”. *Journal of Animal Ecology* 71 (4), pp. 614–625. DOI: `10.1046/j.1365-2656.2002.00632.x`.

Pastor, J., Y. Cohen, and N. T. Hobbs (2006). “The roles of large herbivores in ecosystem nutrient cycles”. In: *Large herbivore ecology. Ecosystem dynamics and conservation*. Ed. by K. Danell et al. Conservation Biology. Cambridge University Press, pp. 289–325. DOI: `10.1017/CBO9780511617461.012`.

Peig, J. and A. J. Green (2009). “New perspectives for estimating body condition from mass/length data: The scaled mass index as an alternative method”. *Oikos* 118.12, pp. 1883–1891. DOI: `10.1111/j.1600-0706.2009.17643.x`.

— (2010). “The paradigm of body condition: A critical reappraisal of current methods based on mass and length”. *Functional Ecology* 24.6, pp. 1323–1332. DOI: `10.1111/j.1365-2435.2010.01751.x`.

Peñuelas, J. et al. (2019). “The bioelements, the elementome, and the biogeochemical niche”. *Ecology* 100.5, e02652. DOI: `10.1002/ecy.2652`.

Pilati, A. and M. J. Vanni (2007). “Ontogeny, diet shifts, and nutrient stoichiometry in fish”. *Oikos* 116.10, pp. 1663–1674. DOI: `10.1111/j.2007.0030-1299.15970.x`.

R Core Team (2018). *R: A Language and Environment for Statistical Computing*. R Foundation for Statistical Computing. Vienna, Austria. URL: `https://www.R-project.org/`.

Reynolds, J. J. et al. (2017). “Does prey density predict characteristics of primiparity in a solitary and specialized predator, the Canada lynx (*Lynx canadensis*)?” *Canadian Journal of Zoology* 95.10, pp. 779–785. DOI: `10.1139/cjz-2016-0269`.

Rivas-Ubach, A. et al. (2012). “Strong relationship between elemental stoichiometry and metabolome in plants”. *Proceedings of the National Academy of Sciences of the United States of America* 109.11, pp. 4181–4186. DOI: `10.1073/pnas.1116092109`.

Rizzuto, M. et al. (2019). “Patterns and potential drivers of intraspecific variability in the body C, N, and P composition of a terrestrial consumer, the snowshoe hare (*Lepus americanus*)”. *Ecology and Evolution* 9 (24), pp. 14453–14464. DOI: `10.1002/ece3.5880`.

El-Sabaawi, R. W., T. J. Kohler, et al. (2012). “Environmental and organismal predictors of intraspecific variation in the stoichiometry of a neotropical freshwater fish”. *PLoS One* 7.3, e32713. DOI: `10.1371/journal.pone.0032713`.

El-Sabaawi, R. W., J. Travis, et al. (2014). “Intraspecific variability modulates interspecific variability in animal organismal stoichiometry”. *Ecology and Evolution* 4.9, pp. 1505–1515. DOI: `10.1002/ece3.981`.

El-Sabaawi, R. W., E. Zandona, et al. (2012). “Widespread intraspecific organismal stoichiometry among populations of the Trinidadian guppy”. *Functional Ecology* 26.3, pp. 666–676. DOI: `10.1111/j.1365-2435.2012.01974.x`.

Sardans, J. et al. (2016). “Foliar and soil concentrations and stoichiometry of nitrogen and phosphorous across European *Pinus sylvestris* forests: Relationships with climate, N deposition and tree growth”. *Functional Ecology* 30, pp. 676–689. DOI: `10.1111/1365-2435.12541`.

Schmitz, O. J., P. A. Raymond, et al. (2014). “Animating the carbon cycle”. *Ecosystems* 17.2, pp. 344–359. DOI: `10.1007/s10021-013-9715-7`.

Schmitz, O. J., C. C. Wilmers, et al. (2018). “Animals and the zoogeochemistry of the carbon cycle”. *Science* 362 (6419), eaar3213. DOI: `10.1126/science.aar3213`.

Shaw, C. N., P. J. Wilson, and B. N. White (2003). “A Reliable Molecular Method of Gender Determination for Mammals”. *Journal of Mammalogy* 84.1, pp. 123–128. DOI: `10.1644/1545-1542(2003)084<0123:ARMMOG>2.0.CO;2`.

Shurin, J. B., D. S. Gruner, and H. Hillebrand (2006). “All wet or dried up? Real differences between aquatic and terrestrial food webs”. *Proceedings of the Royal Society B Biological Sciences* 273.1582, pp. 1–9. DOI: `10.1098/rspb.2005.3377`.

Sterner, R. W. and J. J. Elser (2002). *Ecological stoichiometry: the biology of elements from molecules to the biosphere*. 1st ed. Princeton University Press, p. 464. URL: `https://www.jstor.org/stable/j.ctt1jktrp3`. Accessed 26 July 2021.

Sterrett, S. C., J. C. Maerz, and R. A. Katz (2015). “What can turtles teach us about the theory of ecological stoichiometry?” *Freshwater Biology* 60.3, pp. 443–455. DOI: `10.1111/fwb.12516`.

Stevenson, R. D. and W. A. Woods (2006). “Condition indices for conservation: New uses for evolving tools”. *Integrative and Comparative Biology* 46.6, pp. 1169–1190. DOI: `10.1093/icb/icl052`.

Strong, J. S. and S. J. Leroux (2014). “Impact of Non-Native Terrestrial Mammals on the Structure of the Terrestrial Mammal Food Web of Newfoundland, Canada”. *PLoS One* 9.8. Ed. by S. S. Romanach, e106264. DOI: `10.1371/journal.pone.0106264`.

Zuur, A. F., E. N. Ieno, and C. S. Elphick (2010). “A protocol for data exploration to avoid common statistical problems”. *Methods in Ecology and Evolution* 1.1, pp. 3–14. DOI: `10.1111/j.2041-210X.2009.00001.x`.

2.7 Tables

Table 2.1: Top ranking GLMs for %C, %N, and %P based on ΔAICc values. We report only models that ranked better than the null model, together with the null model. k, number of parameters in the model, LL, log-likelihood, K_n, relative body condition, ABL, average body length. We provide coefficient values as estimate (±SE).

%N top models				**Coefficients**			
k	LL	ΔAICc	R^2	Intercept	Age	K_n	ABL
3	−56.599	0.000	0.066	11.367 (±0.141)	−0.160 (±0.087)		
2	−58.306	1.147	0.000	11.200 (±0.111)			

%P top models				**Coefficients**			
k	LL	ΔAICc	R^2	Intercept	Age	K_n	ABL
3	−35.556	0.000	0.073	1.962 (±0.526)		1.006 (±0.518)	
3	−36.252	1.391	0.047	0.687 (±1.495)			0.054 (±0.035)
2	−37.444	1.508	0.000	2.974 (±0.073)			

%C top models				**Coefficients**			
k	LL	ΔAICc	R^2	Intercept	Age	K_n	ABL
2	−118.090	0.000	0.000	43.606 (±0.367)			

Table 2.2: Top ranking GLMs for C:N, C:P, and N:P based on ΔAICc values. All specifications as in Table 2.1.

C:N top models				**Coefficients**			
k	LL	ΔAICc	R^2	Intercept	Age	K_n	ABL
3	−27.818	0.000	0.074	4.465 (±0.079)	0.095 (±0.049)		
2	−29.731	1.559	0.000	4.564 (±0.063)			

C:P top models				**Coefficients**			
k	LL	ΔAICc	R^2	Intercept	Age	K_n	ABL
2	−178.30	0.000	0.000	39.205 (±1.223)			

N:P top models				**Coefficients**			
k	LL	ΔAICc	R^2	Intercept	Age	K_n	ABL
2	−94.153	0.000	0.000	8.580 (±0.227)			

2.8 Figures

Figure 2.1: A snowshoe hare, *Lepus americanus*, with its summer livery. Photo courtesy of Travis R. Heckford.

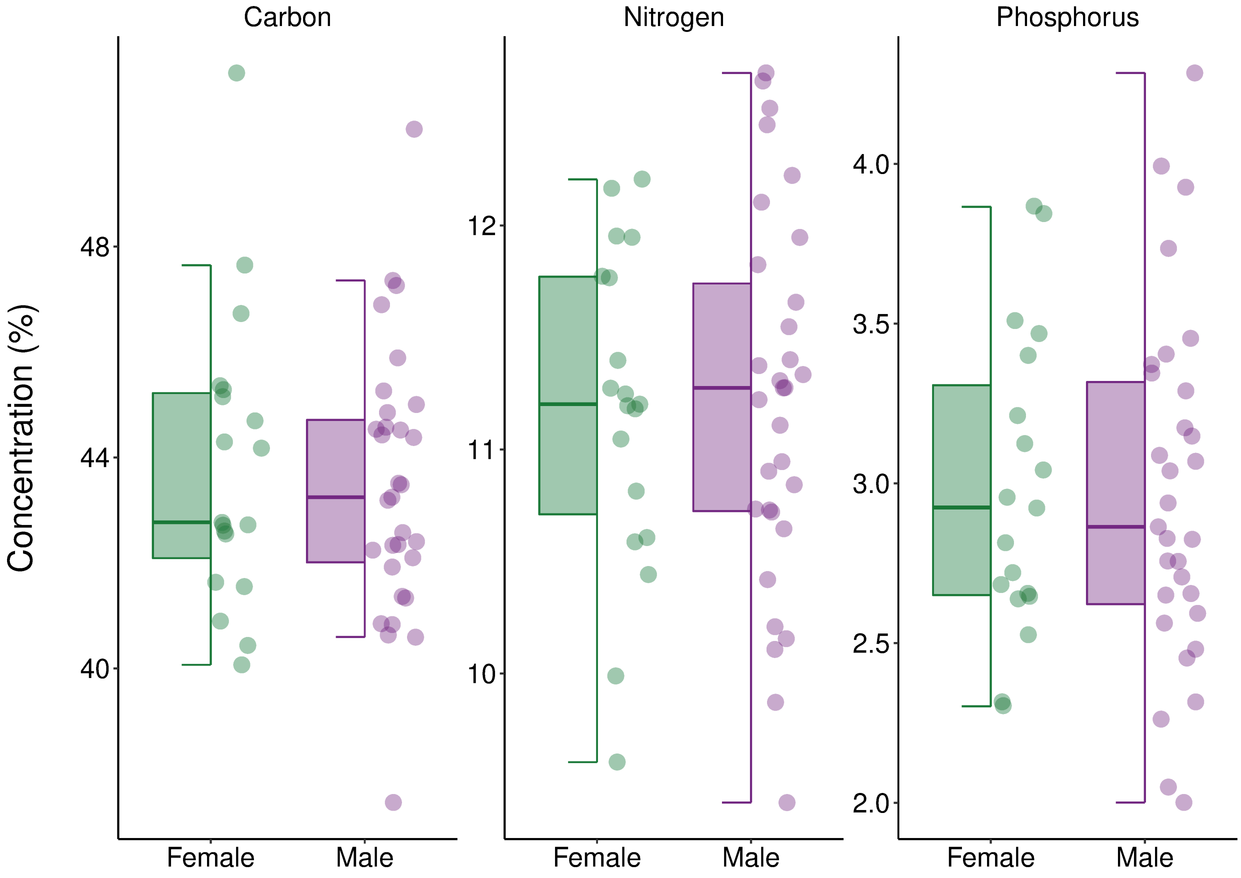

Figure 2.2: Sex-related variability in the concentrations of carbon (C), nitrogen (N), and phosphorus (P) among 50 snowshoe hares. The lower and upper boundaries of the box are the first and third quartiles, respectively. The thick horizontal line inside the box is the median, i.e., the second quartile. The whiskers extend from either boundary to no further than the largest (or smallest) value × 1.5 IQR (interquartile range). Female snowshoe hares show higher median values of %P than males. Males, on the other hand, appear consistently more variable than females in their content of both N and P. Note the different scales of the y-axis among the three panels.

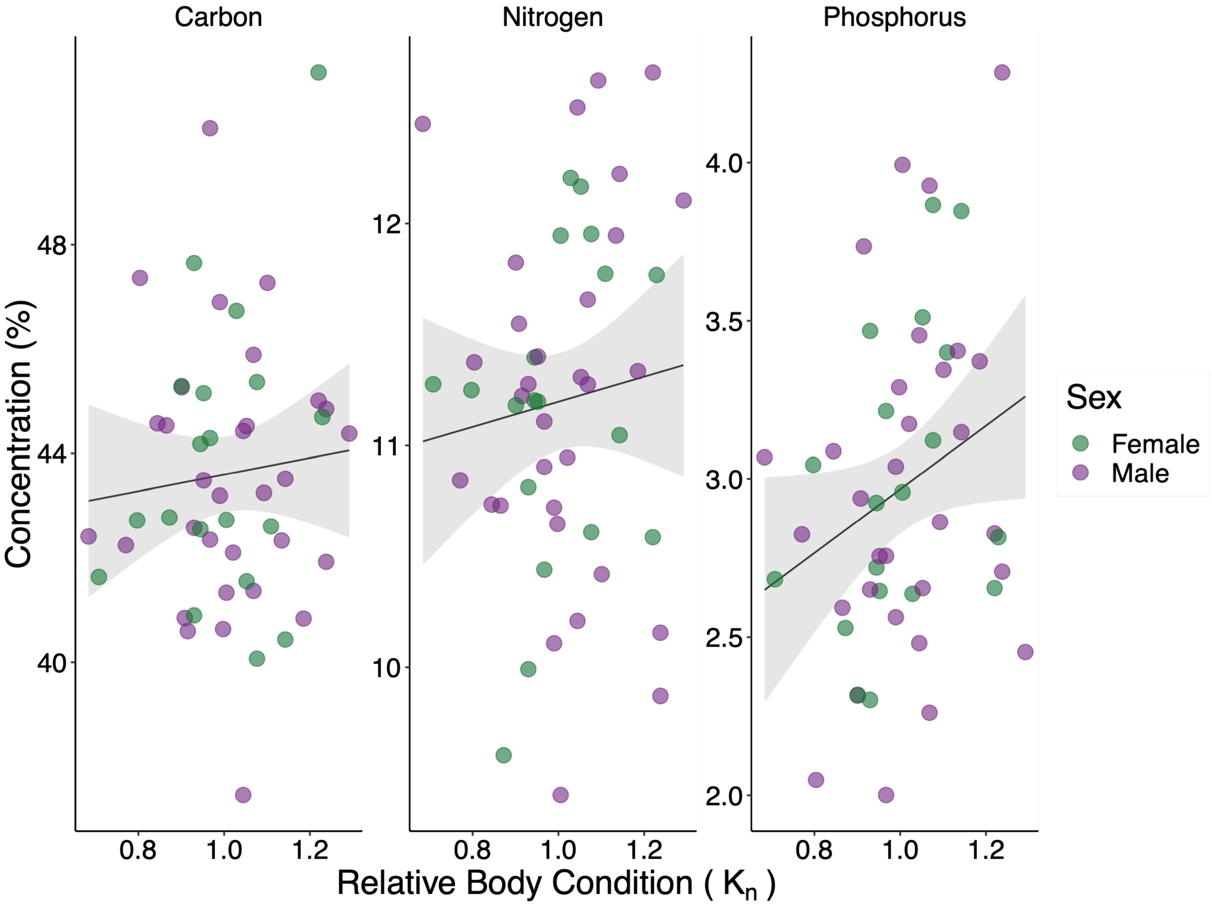

Figure 2.3: Variability in the concentrations of C, N, and P with increasing relative body condition. The positive trend for P is evident, and is weakly supported by the results of our modeling. Conversely, there is no visual evidence of a relationship between %C or %N and relative body condition, which is further confirmed by the results of our modeling (Table 2.1). Solid lines are ordinary least square regression lines, shaded areas represent 95% confidence intervals around them. Regression lines are drawn to aid in pattern visualization only and are from top-ranked models within 2ΔAICc of the null, intercept-only model.

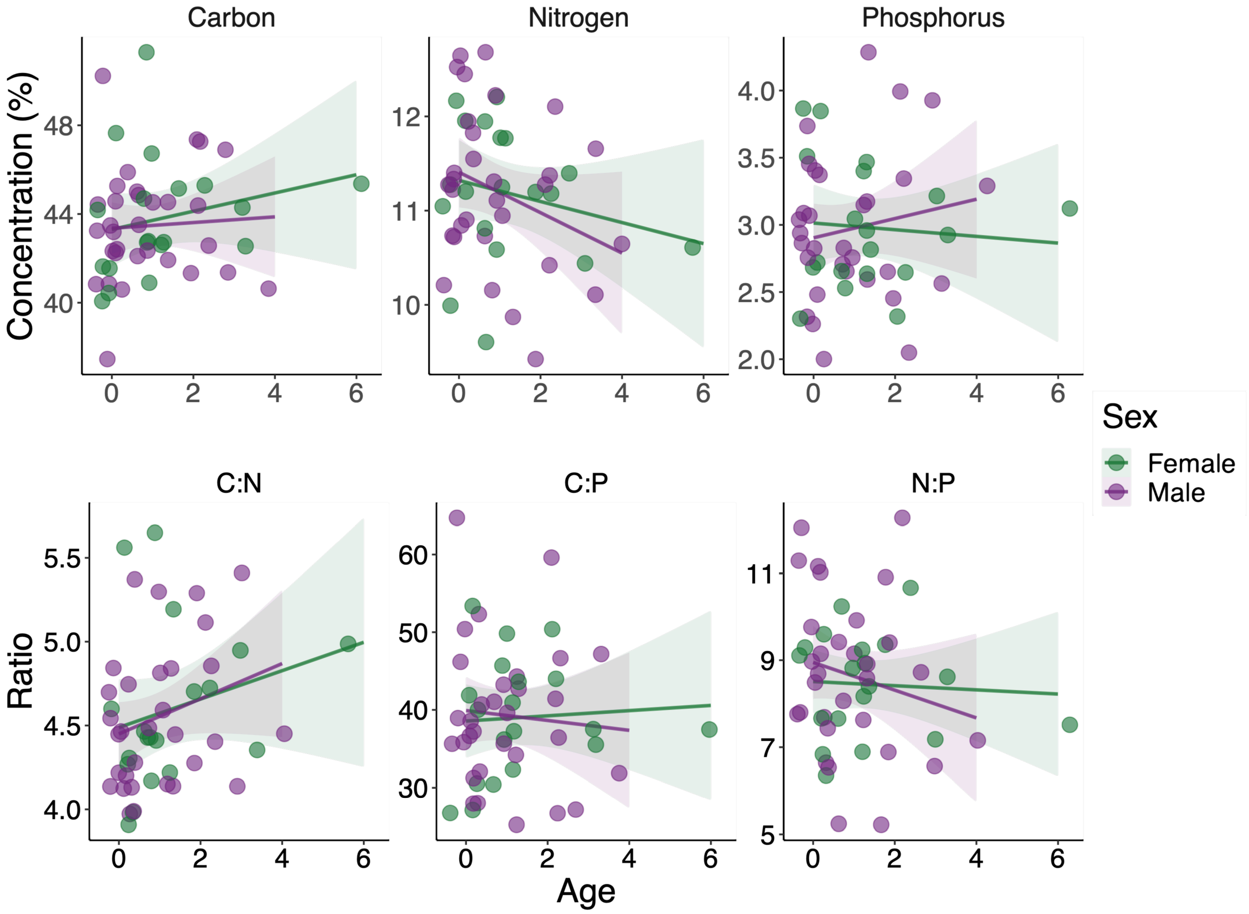

Figure 2.4: Variability in C, N, P concentrations and their stoichiometric ratios with increasing age among 50 snowshoe hares. **Upper panels**: while concentrations of P appear largely invariant as age increases, we notice a negative trend for N concentration for both sexes. This is further supported by the weak relationship found between age and %N through our modeling approach. Conversely, our modeling does not provide any support for the seemingly increasing trend we observe for %C. **Lower panels**: values of C:N appear to increase with age, for both males and females, as would be expected given the negative relationship between %N and age. Conversely, the values of N:P seem to decrease as males get older, which might mean that %N is more strongly influencing the variability of this ratio than %P is. No trend appears evident for C:P, which is in line with the lack of pattern in the variability of %C. We added a jitter of 0.4 to both axes to improve readability of the graphs. Regression lines are drawn to aid in pattern visualization only and are from top-ranked models within 2ΔAICc of the null, intercept-only model. All other specifications as in Figure 2.3.

Chapter 3

Forage stoichiometry predicts the home range size of a small terrestrial herbivore

Authors: Matteo Rizzuto[1], Shawn J. Leroux[1], Eric Vander Wal[1], Isabella C. Richmond[1], Travis R. Heckford[1], Juliana Balluffi-Fry[2], and Yolanda F. Wiersma[1]

Authors' Affiliation

1: Department of Biology, Memorial University of Newfoundland and Labrador, St. John's, Canada

2: Department of Biological Sciences, University of Alberta, Edmonton, Canada

A version of this paper was published in *Oecologia* as:

M. Rizzuto, S. J. Leroux, E. Vander Wal, I. C. Richmond, T. R. Heckford, J. Balluffi-Fry, and Y. F. Wiersma (2021). "Forage stoichiometry predicts the home range size of a small terrestrial herbivore". *Oecologia* 197 (2), pp. 327–338. DOI: `10.1007/s00442-021-04965-0`

3.1 Introduction

Environmental and organismal variability within ecosystems are tightly interconnected. Geochemical, atmospheric, and biological factors drive differences in the elemental composition of primary producers across landscapes (Ågren and Weih 2012; Borer et al. 2015). For example, elemental ratios in marine phytoplankton can vary widely across latitudinal gradients of environmental variables (e.g., ocean temperature; Martiny et al. 2013). Indeed, environmental variability in the supply of key elements like phosphorus (P) and nitrogen (N) is the single best predictor of differences in cellular concentrations of these elements among phytoplankton (Galbraith and Martiny 2015). As well, species composition of local producer and consumer communities can influence carbon (C) and N concentrations in foliar tissues of plant species (Borer et al. 2015). This variability in elemental composition of autotrophs produces areas of high- and low-quality resources for herbivores across landscapes (Jean et al. 2015; Leroux et al. 2017). In turn, spatial heterogeneity in resource elemental composition—i.e., their stoichiometry (Sterner and Elser 2002)—can influence consumers' foraging strategies (Ball, Danell, and Sunesson 2000; Youngentob et al. 2011). However, few studies to date have investigated how consumers' space use varies in response to variability in resource stoichiometry (but see McNaughton et al. 1989; Balluffi-Fry et al. 2020). Here, we investigate how this mosaic of hot- and cold-spots in resource elemental composition (*sensu* Bernhardt et al. 2017) may influence the home range size of a small terrestrial mammal, the snowshoe hare (*Lepus americanus*).

The home range, the area an animal routinely uses to meet its daily needs (Powell and Mitchell 2012), varies in size within and across species under the effect of multiple variables (Table 3.1; Tamburello, Côté, and Dulvy 2015). Forage resource inter- and intra-specific variability—e.g., in quantity, quality, and/or spatial distribution—plays a pivotal role in shaping the cost-benefit trade-offs that regulate animals' dietary balances (Ball, Danell, and Sunesson 2000; van Beest et al. 2011; Duparc et al. 2020). For instance, resource productivity is a well-known driver of home range size among herbivores: individuals tend to have larger home ranges in low productivity areas, because they need to move more to find enough food to avoid starvation (Bjørneraas et al. 2012; Tucker, Ord, and Rogers 2014). Home ranges size also varies with resource quality: home range size tends to be smaller where food quality is higher, and vice versa (Saïd and Servanty 2005; Saïd, Gaillard, et al. 2009; McClintic et al. 2014). Indeed, recent studies have shown that terrestrial herbivores respond to variability in both quantity and quality of their preferred resources at multiple spatio-temporal scales (e.g., van Beest et al. 2011; Nie et al. 2015; Balluffi-Fry et al. 2020). Yet, studies often use an array of different definitions and proxies to measure variability in resource quality (Felton et al. 2018). Thus, one study may define and measure resource quality using forage species identity (van Beest et al. 2011), whereas another may measure their macronutrients content (e.g., proteins, carbohydrates, fibers; Saïd, Gaillard, et al. 2009), or their availability in the environment (Duparc et al. 2020). Within the framework of ecological stoichiometry, resource quality is often defined based on the elemental composition of the resource—that is, its content of key nutrients such as C, N, and P (Sterner and Elser 2002; Kaspari and Powers 2016). Here, we argue that spatial variability in a resource's elemental composition may inform consumer space use by influencing its home range size and potentially act as a common currency across studies.

Animals make space use decisions at multiple spatio-temporal scales, from which food items to consume in a patch to where to establish their geographic range (Johnson 1980). Within a patch, available food items vary in their quality and quantity and animals, in turn, forage only on some of these food items (4th order selection; Johnson 1980). Koalas (*Phascolarctos cinereus*) and greater gliders (*Petauroides volans*) prioritize use of high-quality *Eucalyptus* spp. patches in different ways: koalas search for and forage longer on trees whose leaves have high N concentrations (Marsh et al. 2014), while greater gliders avoid trees with high levels of N-based secondary metabolites in their leaves (Youngentob et al. 2011). Thus, animals tend to use some areas of the landscape more than others (3rd order selection; Johnson 1980). For instance, moose (*Alces alces*) and mountain hare (*Lepus timidus*) visited N-fertilized forest plots more frequently than unfertilized controls (Ball, Danell, and Sunesson 2000). Home ranges arise from these patch use patterns. For example, bamboo-exclusive giant pandas (*Ailuropoda melanoleuca*) seasonally shift their range and vary their home range size in response to variation in N, P, and calcium content in their food—consistently foraging on the highest-quality food available as a result (Nie et al. 2015). Here, we focus on Johnson (1980)'s 2nd order of selection—that is, the home range of an individual—and investigate how spatial variability in resource quality influences home range size of a small mammalian herbivore.

As these examples show, resource elemental composition can play an important role in determining how animals use their space: where they forage, what they forage on, for how long, and when. In turn, this preferential use of high forage quality areas appears to be related to reproductive and physiological benefits (Mcart et al. 2009) or to population dynamics (Merkle et al. 2015). With the recent development of new statistical methods to predict resource stoichiometry at landscape extents (e.g., Galbraith and Martiny 2015; Leroux et al. 2017; Soranno et al. 2019), we can investigate how resource elemental composition influences consumers' space use beyond the local patch. For example, stoichiometric distribution models—henceforth, StDMs—can predict element distributions over landscapes and allow identification of hot- and cold-spots of resource elemental composition across spatial extents (Leroux et al. 2017). StDMs allow for studying patterns of consumers' space use and distribution in a stoichiometrically informed way. For instance, Leroux et al. (2017) used StDMs predictions to investigate the spatial distribution of moose (*A. alces*) at the landscape extent, in the boreal forests of northern Newfoundland, Canada. Spatial distribution models of moose performed consistently better when including a measure of forage elemental composition (e.g., elemental g dry weight, % content, or ratios), providing evidence that spatial gradients in plant stoichiometry may influence herbivores' distribution and habitat selection (Leroux et al. 2017). Consequently, as in the case of the giant panda (*A. melanoleuca*) mentioned above (Nie et al. 2015), spatial variability in forage elemental composition may also drive an animal's home range size. While the above studies provide some evidence for a relationship between food elemental composition and consumer home range size, whether this relationship exists across diverse consumer-resource systems remains unclear.

Here, we use elemental distribution models—i.e., StDMs—to investigate the relationship between summer home range size and resource elemental composition in snowshoe hares (*L. americanus*). Snowshoe hares are keystone herbivores in the boreal forests of North America, a strongly N- and P-limited habitat (Feldhamer, Thompson, and Chapman 2003; Price et al. 2013). Nutrient limitation influences snowshoe hare ecology, behavior, and physiology (Murray 2002), making snowshoe hares well suited to address questions of food quality and space use. Snowshoe hares may respond to the overall forage quality of an area, one metric of which may be the average quality of forage, or to heterogeneity in an area's forage quality (Zweifel-Schielly et al. 2009). We use stoichiometric ratios—i.e., C:N, C:P, N:P ratios—as proxies for resource quality for snowshoe hares. High C:N or C:P forage tends to be woody, hence less digestible, whereas consumption of high N:P forage—that is, low P-content forage—may not offset the boreal forest's strong P-limitation (Leroux et al. 2017). Hence, we consider food items with low C:N, C:P, and N:P ratios as higher quality resources than those with high C:N, C:P, or N:P ratios. Using these stoichiometric ratios, we test the hypothesis that spatial differences in average resource quality, the variability of resource quality, or both, influence snowshoe hare home range size (Figure 3.1). We predict (i) that snowshoe hares in areas of homogeneous resource quality (low variability) will have smaller home ranges than individuals in areas with more spatially heterogeneous resources. We further predict (ii) that in areas with low and spatially homogeneous stoichiometric ratios (low mean and low variation), snowshoe hares will have smaller home ranges compared to areas where these metrics are both high or where one is high and the other is low. As well, we predict (iii) that snowshoe hares in areas of lower average forage C:N or C:P ratio will have smaller home ranges than individuals in areas in which these forage ratios are higher. Finally, for N:P ratio, we predict (iv) that snowshoe hares will have larger home ranges in areas of high N:P ratio, i.e., P-limited, than in areas of low N:P ratio, i.e., N-limited.

3.2 Methods

3.2.1 Study area and spatial study design

We conducted our study in four boreal forest stands in eastern Newfoundland, Canada, in and around Terra Nova National Park (48°31'50" N, 53°55'41" W; Figure B.1). We selected forest stands based on snowshoe hare habitat preferences and along a forest stand age chronosequence with four categories; 20–40 years old, 41–60 y. o., 61–80 y. o., and 81–100 y. o. (see Appendix B.3 for more details). In all four forest stands, black spruce (*Picea mariana*) dominates the canopy, which also comprises balsam fir (*Abies balsamea*), red maple (*Acer rubrum*), white birch (*Betula papyrifera*), and white spruce (*Picea glauca*). Lowbush blueberry (*Vaccinium angustifolium*), Sheep laurel (*Kalmia angustifolia*), and Labrador tea (*Rhododendrum groenlandicum*) dominate the understory.

In May 2016, we established a $500\,\mathrm{m}\times500\,\mathrm{m}$ snowshoe hare live trapping grid housing 50 Tomahawk live traps (Tomahawk Live Trap Company, Hazelhurst, WI) along a meandering transect in each of the four forest stands (see Appendix B.3 and Figure B.2). Live traps were spaced 75 m apart, except for turning points in the transect where the distance was smaller (Figure B.2). Each trap location was also the center of a circular sampling plot with a 11.3 m radius and a $401.15\,\mathrm{m}^2$ area that we used for collecting plant tissue samples (see below). While our plant tissue sampling effort involved all four live-trapping grids, during our first live-trapping season in summer 2016 we had consistent snowshoe hare captures only in one of the four grids, the youngest one (20–40 y. o.). We thus focused our live-trapping efforts on this grid in the following live-trapping seasons (see Appendix B.5 for further details).

3.2.2 Spatial variability in food stoichiometry

We collected plant samples, $\sim$20 g wet weight, in the sampling plot centered on each trap location in the four live trapping grids during the summer months of 2016 and 2017. We focused on three important summer forage species for snowshoe hares (Dodds 1960): lowbush blueberry (*V.*

angustifolium), red maple (*A. rubrum*), and white birch (*B. papyrifera*). Our sampling tried to replicate hare browsing by collecting only new growth material—that is, new leaves and terminal ends of branches. We shipped 10 g dry weight from each sample to the Agriculture and Food Laboratory at the University of Guelph to measure content of C, N, and P for each of our three plant species of interest (listed above; henceforth, SOI). In Appendix B.4 we report a detailed breakdown of the number of samples collected for each plant SOI (Table B.4 and Figure B.7).

In our analyses, we used quantitative predictions of foliar C:N, C:P, and N:P ratios obtained from fitting StDMs to the stoichiometry data obtained from plant samples from all four grids. We built nine plant SOI stoichiometry predictive surfaces, one for each combination of plant SOI and stoichiometric ratio. Here we briefly describe the procedure behind building and fitting StDMs (for general rationale behind StDMs and detailed methods see Leroux et al. 2017; Heckford et al. 2021, respectively). To build each StDM, we used three types of plant SOI data: (i) sampling plot density data from a shrub belt sampled along the South-North diameter (22.6 m long, 1 m wide) of the plot, divided into 4 height classes (0–50, 51–100, 101–150, 151–200 cm, respectively); (ii) elemental percentages, i.e., % C, N, P, extracted from foliar samples; and (iii) biomass data collected in randomly selected areas adjacent to our sampling grids. We collected new-growth-only biomass samples from 50 individuals per species, stratified by the aforementioned 4 height classes. In the laboratory, we dried the biomass samples at 50 °C until we reached constant weight (2–3 days; see Heckford et al. 2021, for detailed plant SOI sampling protocols). We first fit allometric models for each study species using the formula: $log(biomass) \sim log(basal\ diameter) + log(height)$. At the sampling plot level, this allowed us to estimate density of plant SOI by height class based on shrub belt data, and to use these estimates to predict plant SOI biomass by height class in each sampling plot. We then calculated C, N, P foliar content per SOI per plot by dividing a SOI's total plot biomass by the product of plot area and foliar elemental content (% dry weight). We obtained C, N, P quantity estimates by dividing elements' foliar content by their molar weight, and stoichiometric ratios from these estimates (C:N, C:P, N:P; Leroux et al. 2017).

Each StDM included spatially explicit covariates, grouped into four categories: land cover, productivity, biotic, and abiotic factors (see Appendix B.4). Preliminary analyses of yearly variation in plant SOI stoichiometry showed negligible variability between 2016 and 2017 (Richmond et al. 2021). Hence, we did not include year of sampling as a covariate in our StDMs. We fit a set of 16 General Linear Models based on *a priori* hypotheses (see Appendix B.4), including a null model, to plot-level data of three response variables (C:N, C:P, and N:P ratios) for each plant SOI using function `glm` in the `stats` R package (R Core Team 2020). We used the Akaike Information Criterion corrected for small sample size (AICc; Burnham and Anderson 2002) to assess the weight of evidence supporting each model. After removing uninformative parameters (*sensu* Leroux 2019), we used the top-ranked model for each plant SOI-stoichiometric ratio pair to produce plant SOI stoichiometry predictive surfaces as proxies for resource quality available within hare home ranges (Table B.5).

3.2.3 Home range size estimation

In May-November of 2016 through 2019, we live-trapped and radio-collared snowshoe hares in one of our study grid, the youngest forest stand (henceforth, hare study area). We baited each trap at dusk with apple slices, alfalfa, and rabbit chow, and checked them the following dawn. We collected body weight (g) and other demographic data of each hare, before fitting it with a 25 g radio collar (M1555, Advanced Telemetry Systems, Isanti, MN) and releasing it. We did not fit individuals with radio-collars when the weight of the collar was ≥5% of the hare's own body weight. Further details on our live trapping protocol can be found in Appendix B.5. The Animal Care Committee of Memorial University approved our animal handling protocol with permit number 18-02-EV.

In May-September of 2017 through 2019, we located snowshoe hares using handheld receivers (Biotracker, Lotek, Ontario, CA) and VHF antennas (RA–23K, Telonics, AZ). We collected three or more azimuths per hare per day between 0500–2100, storing them in an electronic data collection form on an iPad (FileMaker Pro Advanced, v. 14; Claris International Inc. 2015) and using digital maps (Avenza Maps, v. 3.7; Avenza Systems Inc. 2020) to check the triangulation polygon's size (see Appendix B.6 for further details on triangulation protocols). We estimated home range size and ran all subsequent analyses in R (v. 4.0.1; R Core Team 2020). For each hare in our sample (n = 30), we used package `razimuth` to estimate collar location based on the Azimuthal Telemetry Model (Gerber et al. 2018, see Appendix B.6 for more details). From these locations, we estimated the Utilization Distribution (UD) of our snowshoe hares using the Autocorrelated Kernel Density Estimator corrected for small sample size (AKDEc) from the `ctmm` R package (Fleming and Calabrese 2017; Fleming, Noonan, et al. 2019; Fleming and Calabrese 2020). From the UDs, we estimated home range area in hectares (ha) at the 50%, 75%, and 90% isopleths. While we did not collect nighttime relocations from our snowshoe hares, we would expect nighttime movements of individuals to influence use patterns within the home range rather than home range placement over the landscape or home range size. Thus, we are confident we captured summer home range size for our snowshoe hare sample. For more details on our home range estimation workflow, see Appendix B.7 and the Supporting Code document in the online data repository.

3.2.4 Stoichiometry of home range size

We used function `extract` from the `raster` R package (Hijmans 2020) to overlay the boundary of each snowshoe hare's home range area estimate, i.e., the 50%, 75%, 90% UD isopleths, on the stoichiometric surfaces and get C:N, C:P, and N:P ratios values for every pixel covered by the home range (see Supporting Code for more details). From these data, for each home range, we estimated (i) each stoichiometric ratio's mean value and (ii) its coefficient of variation. The coefficient of variation (henceforth, CV), the ratio of a sample's standard deviation to its mean value, provides an easy-to-interpret assessment of how variable the predicted SOI stoichiometry of a given home range is, compared to its mean value.

We used linear models to investigate the effects of resource stoichiometry, i.e., mean, CV, and their interactive effects, and body weight on the size of the home range of snowshoe hares estimated at the 50% (i.e., the core area; Börger et al. 2006), 75%, and 90% isopleths. We included body weight to capture potential intraspecific variability in home range size due to an individual's ecology and physiology (Peters 1983). Conversely, we did not include year of sampling, as preliminary analyses provided no evidence it influenced home range size of our snowshoe hares (see Appendix B.7.2 and Supporting Code for models' output; Börger et al. 2006). As well, we did not include sex in our models as evidence for snowshoe hares points to this variable being correlated with body weight (Feldhamer, Thompson, and Chapman 2003) and it does not appear to influence the elemental composition of snowshoe hares (Rizzuto, Leroux, Vander Wal, Wiersma, et al. 2019). For each combination of plant SOI and C:N, C:P, and N:P ratio (n = 5, see below), to test prediction (i) we fit a model including each stoichiometric ratio's CV (Table 3.2). Likewise, to test predictions (ii) and (iii) we fit a model including the ratios' mean values (Table 3.2). To test prediction (iv) we fit a model including the additive effects and a model including the additive and interactive effects of the ratios' mean and coefficient of variation (Table 3.2). For each model, we also fit a version that included the hares' body weight at capture (Table 3.2). We fit this set of 8 models, plus a null model, to our dataset using function `lm` in the `stats` R package (R Core Team 2020), and we visually checked that models met assumptions using standard approaches (Zuur, Ieno, and Elphick 2010). We used function `AICc` in the `AICcmodavg` R package to select top models based on parsimony (Burnham and Anderson 2002; Mazerolle 2017). Following Leroux (2019), we removed uninformative parameters from the model set of each plant SOI-stoichiometric ratio pair. Below, we present the summary AICc table for analyses at the 50% UD slice. In Appendix B.9 we present summary tables of the analyses at the 75% and 90% UD, as well as the full AICc tables.

3.3 Results

StDMs of red maple C:N, N:P ratios and lowbush blueberry C:N, C:P, and N:P ratios all ranked above the null model whereas all other StDMs (i.e., red maple C:P ratio, white birch C:N, C:P, and N:P ratios) were not supported by the data (Heckford et al. 2021). We used this suite of five StDMs to produce geo-referenced predictions of resources' spatial variability in and around our hare study area (see Table B.5 for details on models fit to the data and parameters' slope estimates).

Our sample of radiocollared snowshoe hares included 30 individuals: 4 followed during summer 2017, 6 in summer 2018, and 20 during summer 2019. We followed four snowshoe hares for two consecutive sampling years: three in the 2018 and 2019 sampling seasons and one in the 2017 and 2018 sampling seasons. For the individuals sampled in more than one year, we included in the analyses only the home range size estimate from the year with the most telemetry points. Our results are not sensitive to this decision (see Appendix B.7.1 and our code repository for more details). Our sample included 14 females, 12 males, and 4 individuals of unknown sex. Adult hares comprised the majority of our sample (n = 27), with two young-of-the-year and one individual of unknown age. Mean core area size was 4.21 ha (range: 0.70–11.19) in 2017, 3.39 ha (range: 1.37–7.21) in 2018, and 2.69 ha (range: 0.53–6.33) in 2019 (3-year mean ± SD: 3.03 ha ± 2.32). For lowbush blueberry, within the core area, predicted C:N ratio ranged from 45.32 to 49.18 (median: 47.13), predicted C:P ratio ranged from 1201.35 to 2277.46 (median: 1275.88), and predicted N:P ratio from 25.15 to 45.42 (median: 28.08). For red maple, predicted C:N ratio ranged from 23.26 to 39.79 (median: 30.89) and predicted N:P ratio ranged from 28.39 to 39.09 (median: 34.14).

We found mixed support for prediction (i), resource quality heterogeneity influencing home range size. The CV of lowbush blueberry C:N ratio appeared in the top model for home range core area size (slope = 3.96 ± 0.55, $R^2 = 0.70$; Table 3.3 and Figure 3.3). This trend holds at all UD isopleths (Tables B.1 and B.2). Indeed, the CV of lowbush blueberry C:N ratio explained a higher portion of the variation in snowshoe hare home range size, compared to the mean value of this ratio (CV-only model $R^2 = 0.45$, mean-only model $R^2 = 0.12$; Table 3.3). We found a similar relationship for both red maple ratios, C:N (slope = 0.16 ± 0.09, $R^2 = 0.11$; Table 3.3) and N:P (slope = 0.73 ± 0.35, $R^2 = 0.14$; Table 3.3). This trend holds at all UD isopleths for red maple C:N, but only at the 75% isopleth for red maple N:P (Tables B.1 and B.2). Evidence supporting the red maple C:N and N:P relationships is weak, however, as these models were consistently within 2ΔAICc from the null model (Table 3.3, and Tables B.1 and B.2). We found no evidence of this relationship for the CV of lowbush blueberry C:P and N:P ratios (Table 3.3, and Tables B.1 and B.2). Additionally, we found some support for prediction (ii) at the 50% UD isopleth for red maple N:P ratio only (slope = 0.40 ± 0.23, $R^2 = 0.24$; Table 3.3). However, as this model ranked below the CV-only model for this ratio and within 2ΔAICc from the null, the evidence supporting prediction (ii) is weak.

We found mixed support for our prediction (iii) on the effects of average C:N ratio and C:P ratio on home range size. The mean values for lowbush blueberry foliage C:N ratio (slope = 5.14 ± 1.11, $R^2 = 0.70$; Table 3.3 and Figure 3.3) and C:P ratio appeared in top models (slope = 0.01 ± 0.004, $R^2 = 0.10$; Table 3.3), with the trend holding at all three isopleths (Tables B.1 and B.2). While the top model included both mean and CV of lowbush blueberry C:N ratio, the mean-only model was ranked 3rd overall and explained ∼11% of the variation in hare home range size (Table 3.3). No support for this prediction came from models using average red maple C:N ratio (Table 3.3, and Tables B.1 and B.2). As well, we found weak evidence supporting prediction (iv), home range size increasing as resources' N:P ratio increases, for lowbush blueberry foliage (slope = 0.38 ± 0.24, $R^2 = 0.08$; Table 3.3) with the trend holding at larger UD isopleths (Tables B.1 and B.2).

3.4 Discussion

Animals forage on a variety of resources whose elemental composition may influence space use and foraging patterns at multiple spatial scales (Lima and Zollner 1996; van Beest et al. 2011; Duparc et al. 2020). We set out to test whether a keystone boreal herbivore, the snowshoe hare (*L. americanus*), changes its home range size in response to variability in the content of key elemental nutrients in two preferred summer forage species, lowbush blueberry and red maple. We found evidence that spatial differences in a preferred resource's elemental composition variability and its average correlate with herbivore home range size. Additionally, forage species identity may also play a role, further influencing these relationships. Together, our results provide evidence supporting the role that resources' elemental content plays in influencing consumers' spatial ecology. The approach we adopt here suggests that exploring fundamental questions of animal spatial ecology through an elemental lens may allow researchers to better resolve one component of the feedbacks between animals and ecosystem functions, e.g., elemental cycling (Schmitz et al. 2018).

The boreal forest is a strongly N- and P-limited ecosystem (Price et al. 2013). Snowshoe hares need to carefully balance their intake of C-heavy plant food against their N and P growth requirements (Sterner and Elser 2002). Our results provide explicit evidence of this elemental trade-off at the home range scale and highlight how differences in resource elemental content within and across areas used by snowshoe hares underlie variation in home range size in a heterogeneous landscape. Results for lowbush blueberry foliage C:N ratio and both red maple foliage C:N and N:P ratio support prediction (i), that variability in plant N and P relative content can drive home range core area size (Table 3.3). For lowbush blueberry C:N, this is evident at larger UD isopleths too (Tables B.1 and B.2). Lowbush blueberry is a preferred summer forage of snowshoe hare (Dodds 1960), as well as more abundant than red maple in our study area (Figure B.8). Thus, a higher sensitivity to variation in the quality of blueberry may be the most adaptive strategy for snowshoe hares to fulfill their high dietary requirements (Murray 2002). Consequently, spatial variability in lowbush blueberry stoichiometry may exert a significant influence on this herbivore's space use. Evidence from other studies strongly suggests that variability in the chemistry of a consumer's diet main components can influence both their spatial and temporal distribution over the environment (McNaughton et al. 1989; Nie et al. 2015; Balluffi-Fry et al. 2020).

Furthermore, we find evidence that elements can influence home range core area size even when considering an area's average quality—i.e., when smoothing the variation to a single value—supporting predictions (ii) and (iii). Low average values of C:N ratio for lowbush blueberry consistently correspond to smaller home range size (Table 3.3 and Figure 3.3). This held true for C:N ratio whether we estimated home range size from the core area or from larger UD slices, suggesting that resource quality may influence space use decisions at a higher order of selection (i.e., landscape or 1st order of selection; Johnson 1980). Results from lowbush blueberry C:P and N:P ratios suggest a similar, but weaker relationship (Table 3.3). Taken together, our results for both the mean and coefficient of variation of lowbush blueberry C:N ratio point to hares living in areas of high mean and high coefficient of variation for this ratio having larger home ranges than those living in areas where mean values are high but the coefficient of variation is small (Figure 3.2). Thus, spatial heterogeneity in the relative content of key elemental nutrient of preferred forage species may influence consumers' home range placement and size (Powell and Mitchell 2012).

Several study systems provide evidence of resource quality influence on consumer spatial ecology, corroborating our results (e.g., Saïd, Gaillard, et al. 2009; van Beest et al. 2011; Nie et al. 2015). Indeed, most snowshoe hares in this study appeared to live in areas of relatively high N and P content in the foliage of both red maple and lowbush blueberry (Figure 3.2). The few home ranges in areas with high resource heterogeneity may result from population dynamics, particularly the increase in hare numbers from 2017 to 2019. In 2017, our collared snowshoe hares all had home ranges in relatively high-quality areas for lowbush blueberry. As more snowshoe hares appeared on the landscape in 2018 and 2019, new individuals increasingly established larger home ranges that extended beyond the areas of lower heterogeneity or higher mean N or P availability. The high degree of overlap between home range estimates calculated for hares with more than one year of telemetry data may point to a certain ability of older snowshoe hares to retain their range across years (Table B.3 and Figures B.3 to B.6). Other herbivores show similar colonization of less-favorable areas of a landscape that depends on growth. For example, among bison (*Bison bison*), individuals appeared to expand their population range to include areas of lower resource quality and establish larger home ranges in them as population density increased over time (Merkle et al. 2015). The elemental composition of foraging resources, then, may not only influence the size of a consumer's home range, but also its placement over the landscape. However, to our knowledge, this study is the first to show that the spatial distribution of key chemical elements can influence where and how large a home range an animal may establish and maintain.

We modeled our measure of forage quality, forage stoichiometry, based on a suite of environmental, biotic, and abiotic covariates. This approach may help investigate direct drivers of consumer spatial ecology and shed light on ecosystem characteristics allowing high-quality resources to persist in an area. Further, StDMs allow accounting for multiple ecological currencies shaping a consumer's ecology at varying spatio-temporal scales (Levin 1992; Lima and Zollner 1996). Thus, applying stoichiometric measures of forage to model consumer space use may be a fundamental tool in bridging metabolic, nutritional, landscape, and behavioural ecology (Sterner 2004). Furthermore, our StDM-driven approach explains a large portion of the variance observed in our sample, albeit with some variability among model sets (see Tables B.1 and B.2). Indeed, the elemental composition of resources has been shown to accurately describe and predict the spatial distribution patterns of consumers in a variety of biomes, from boreal (this study), to temperate (Nie et al. 2015; Merems et al. 2020), to tropical (McNaughton et al. 1989).

We take a stoichiometry-based perspective on food quality and combine it with a novel modeling approach to investigate herbivore spatial ecology. We assume—like most other studies that use other quality metrics—that we have captured quality. Indeed, not all the N or P of a resource are available to consumers, as structural or defensive compounds may sequester some portions of these elements in undigestible macromolecules, e.g., cellulose or lignin, thus influencing the quality of a given food item (Felton et al. 2018; Champagne et al. 2020). Our review of two recent meta-analyses on herbivores and food quality (Felton et al. 2018; Champagne et al. 2020) suggests that—across 14 studies reporting data from 12 broadleaved and 5 coniferous plants—structural compound content, i.e., lignin and cellulose, decreased as N content increased (more details in Appendix B.8 and Figure B.9). Taken together with our results, this suggests that elemental N may be a good indicator of food quality across multiple species and environments. Nitrogen may be a particularly useful indicator of food quality in N-limited systems such as the boreal forest (Price et al. 2013). Furthermore, integration of multiple elements into stoichiometric ratios—like the C:N, C:P, and N:P ratios used in our study—may prove useful for capturing different components of food limitation or quality (Sterner and Elser 2002), particularly at landscape extents where herbivores make trade-offs in food quality and quantity (Balluffi-Fry et al. 2020). Given that the majority of research on the role of food on animal spatial ecology employs non-elemental measures of food quality, future work should seek to measure both elemental content and nutritional content of food items and relate these to animal use (Wilder and Jeyasingh 2016).

Large portions of variance remain unexplained in our models suggesting that, while useful, focusing on a few key elements and their ratios only captures one part of animal space use decisions. Macromolecules (e.g., protein, fibers; Seccombe-Hett and Turkington 2008) also play a role in influencing snowshoe hare space use, alongside other elements (e.g., Na, Ca, K; Kaspari and Powers 2016). Further, population dynamics and predation risk may add layers to the cost-benefit trade-offs faced by herbivores foraging in heterogeneous landscapes. These layers, in turn, may influence the spatial maps mammals create to navigate their environment—for instance, potentially leading to different home range shapes and size when considering foraging vs. breeding opportunities (Powell and Mitchell 2012). We offer our StDMs-driven approach as a complementary framework to existing wildlife and nutritional ecology based approaches (for an overview of the limitations of a StDMs-based approach, see Leroux et al. 2017). We see much value in, for instance, combining StDMs with more traditional nutritional ecology techniques, e.g., macronutrients analysis or foodscape approaches, to more fully address questions pertaining to animal space use—as recently done for European hares (*Lepus europaeus*; Weterings et al. 2018) and koalas (*P. cinereus*; Marsh et al. 2014). Furthermore, herbivores rarely experience their foraging landscape as a collection of individual resources. Spatial stoichiometry and its applications to animal foraging ecology are in their infancy and we see exciting potential in developing StDMs beyond the single-species models used in the present study. We can envision several ways to conceptualize multi-species StDMs, from stacking predictions from multiple single-species StDMs (Ferrier and Guisan 2006) to developing Joint Species Distribution

Models (*sensu* Pollock et al. 2014) for elements. Progress in this direction means confronting additional layers of assumptions tied to predicting the spatial distribution of multiple elemental response variables—e.g., uneven sample size across species and elements—but promising tools recently emerged in community ecology that could be useful to overcome these challenges (e.g., Ovaskainen et al. 2017).

Overall, our results provide evidence that ecological stoichiometry may help researchers understand fundamental components of consumers' spatial ecology. Based on the emergent field of spatial stoichiometry (Galbraith and Martiny 2015; Leroux et al. 2017; Soranno et al. 2019) and our own results, we argue that using the elemental composition of resources to investigate patterns of consumer spatial distribution and habitat use has several advantages. First, it may provide a parsimonious approach to resource selection analysis that complements other, more widespread methods—e.g., habitat classification (Zweifel-Schielly et al. 2009), forage species identity (van Beest et al. 2011), or availability (Duparc et al. 2020). Second, using elemental currencies would allow for consistency in defining and measuring metrics, such as food quality, across studies and study systems, even when not used in a spatial stoichiometry framework (Van Der Graaf et al. 2006; Weterings et al. 2018). Third, it would reduce reliance on elemental conversion factors, increasingly recognized as problematic due to their lack of generality across different food items and outdated estimation methods (Mariotti, Tomé, and Mirand 2008). Fourth, stoichiometric currencies may help investigate the different experiential layers that make up an animal's home range (*sensu* Powell and Mitchell 2012), further refining how researchers measure, describe, and interpret animal space use at multiple spatio-temporal scales (Levin 1992). Finally, rooting theoretical models of ecological processes in stoichiometric units may make them more widely applicable to real world scenarios (Schmitz et al. 2018).

Life builds itself using a limited subset of elements (Kaspari and Powers 2016). These elements are continuously transformed and exchanged, both globally, among organisms and their abiotic environment, and more locally within and across ecosystem borders. Our results show that the spatial distribution of elements over the landscape plays a key role in shaping where and how organisms interact with their environment. Ecological stoichiometry may thus offer a highly parsimonious approach that, by providing common units of measurement with which to describe both actors and currencies involved in these spatial relationships, may offer researchers a holistic perspective to explore animal spatial ecology.

3.5 Data Availability

All data and code used in the analyses are available via a figshare online repository at: https://doi.org/10.6084/m9.figshare.12798296.

3.6 References

Ågren, G. I. and M. Weih (2012). “Plant stoichiometry at different scales: element concentration patterns reflect environment more than genotype”. *New Phytologist* 194 (4), pp. 944–952. DOI: `10.1111/j.1469-8137.2012.04114.x`.

Avenza Systems Inc. (2020). *Avenza Maps*. Toronto, ON. URL: `https://www.avenzamaps.com`.

Ball, J. P., K. Danell, and P. Sunesson (2000). “Response of a herbivore community to increased food quality and quantity: an experiment with nitrogen fertilizer in a boreal forest”. *Journal of Applied Ecology* 37 (2), pp. 247–255. DOI: `10.1046/j.1365-2664.2000.00487.x`.

Balluffi-Fry, J. et al. (2020). “Quantity-quality trade-offs revealed using a multiscale test of herbivore resource selection on elemental landscapes”. *Ecology and Evolution* 10.24, pp. 13847–13859. DOI: `10.1002/ece3.6975`.

Bernhardt, E. S. et al. (2017). “Control Points in Ecosystems: Moving Beyond the Hot Spot Hot Moment Concept”. *Ecosystems* 20.4, pp. 665–682. DOI: `10.1007/s10021-016-0103-y`.

Bjørneraas, K. et al. (2012). “Habitat quality influences population distribution, individual space use and functional responses in habitat selection by a large herbivore”. *Oecologia* 168 (1), pp. 231–243. DOI: `10.1007/s00442-011-2072-3`.

Borer, E. T. et al. (2015). “Food-web composition and plant diversity control foliar nutrient content and stoichiometry”. *Journal of Ecology* 103 (6), pp. 1432–1441. DOI: `10.1111/1365-2745.12461`.

Börger, L. et al. (2006). “Effects of sampling regime on the mean and variance of home range size estimates”. *Journal of Animal Ecology* 75 (6), pp. 1393–1405. DOI: `10.1111/j.1365-2656.2006.01164.x`.

Burnham, K. P. and D. R. Anderson (2002). *Model Selection and Multimodel Inference: A Practical Information-Theoretic Approach (2nd ed)*. 2nd ed. Springer-Verlag New York, pp. XXVI, 488.

Champagne, E. et al. (2020). “Phytochemicals Involved in Plant Resistance to Leporids and Cervids: a Systematic Review”. *Journal of Chemical Ecology* 46 (1), pp. 84–98. DOI: `10.1007/s10886-019-01130-z`.

Claris International Inc. (2015). *FileMaker Pro Advanced*. Santa Clara, CA. URL: `https://www.claris.com/filemaker/pro/`.

Dodds, D. G. (1960). “Food Competition and Range Relationships of Moose and Snowshoe hare in Newfoundland”. *The Journal of Wildlife Management* 24 (1), pp. 52–60. DOI: `10.2307/3797356`.

Duparc, A. et al. (2020). “Through the taste buds of a large herbivore: foodscape modeling contributes to an understanding of forage selection processes”. *Oikos* 129 (2), pp. 170–183. DOI: `10.1111/oik.06386`.

Feldhamer, G. A., B. C. Thompson, and J. A. Chapman (2003). *Wild mammals of North America: biology, management, and conservation*. JHU Press.

Felton, A. M. et al. (2018). “The complexity of interacting nutritional drivers behind food selection, a review of northern cervids”. *Ecosphere* 9 (5). DOI: `10.1002/ecs2.2230`.

Ferrier, S. and A. Guisan (2006). “Spatial modelling of biodiversity at the community level”. *Journal of Applied Ecology* 43.3, pp. 393–404. DOI: `10.1111/j.1365-2664.2006.01149.x`.

Fleming, C. H. and J. M. Calabrese (2017). “A new kernel density estimator for accurate home-range and species-range area estimation”. *Methods in Ecology and Evolution* 8 (5), pp. 571–579. DOI: `10.1111/2041-210X.12673`.

— (2020). *ctmm: Continuous-Time Movement Modeling*. v. 0.5.10. URL: `https://cran.r-project.org/package=ctmm`.

Fleming, C. H., M. J. Noonan, et al. (2019). “Overcoming the challenge of small effective sample sizes in home-range estimation”. *Methods in Ecology and Evolution* 10 (10), pp. 1679–1689. DOI: `10.1111/2041-210X.13270`.

Galbraith, E. D. and A. C. Martiny (2015). “A simple nutrient-dependence mechanism for predicting the stoichiometry of marine ecosystems”. *Proceedings of the National Academy of Sciences of the United States of America* 112 (27), p. 201423917. DOI: `10.1073/pnas.1423917112`.

Gerber, B. D. et al. (2018). “Accounting for location uncertainty in azimuthal telemetry data improves ecological inference”. *Movement Ecology* 6 (1), pp. 1–14. DOI: `10.1186/s40462-018-0129-1`.

Heckford, T. R. et al. (2021). “Does where you live influence what you are made of? Spatial correlates of chemical traits across commonly occurring boreal plants”. *Landscape Ecology*. DOI: `10.1007/s10980-021-01334-3`.

Hijmans, R. J. (2020). *raster: Geographic Data Analysis and Modeling*. v. 3.0-12.

Jean, P.-O. et al. (2015). “Combining near infrared spectra of feces and geostatistics to generate forage nutritional quality maps across landscapes”. *Ecological Applications* 25 (6), pp. 1630–1639. DOI: `10.1890/14-1347.1`.

Johnson, D. H. (1980). “The Comparison of Usage and Availability Measurements for Evaluating Resource Preference”. *Ecology* 61.1, pp. 65–71. DOI: `10.2307/1937156`.

Kaspari, M. and J. S. Powers (2016). “Biogeochemistry and Geographical Ecology: Embracing All Twenty-Five Elements Required to Build Organisms”. *The American Naturalist* 188 (S1), S62–S73. DOI: `10.1086/687576`.

Leroux, S. J. (2019). “On the prevalence of uninformative parameters in statistical models applying model selection in applied ecology”. *PLoS One* 14 (2), pp. 1–12. DOI: `10.1371/journal.pone.0206711`.

Leroux, S. J. et al. (2017). “Stoichiometric distribution models: ecological stoichiometry at the landscape extent”. *Ecology Letters* 20 (12), pp. 1495–1506. DOI: `10.1111/ele.12859`.

Levin, S. A. (1992). “The Problem of Pattern and Scale in Ecology: The Robert H. MacArthur Award Lecture”. *Ecology* 73.6, pp. 1943–1967. DOI: `10.2307/1941447`.

Lima, S. L. and P. A. Zollner (1996). “Towards a behavioral ecology of ecological landscapes”. *Trends in Ecology & Evolution* 11 (3), pp. 131–135. DOI: `10.1016/0169-5347(96)81094-9`.

Mariotti, F., D. Tomé, and P. P. Mirand (2008). “Converting Nitrogen into Protein—Beyond 6.25 and Jones’ Factors”. *Critical Reviews in Food Science and Nutrition* 48.2, pp. 177–184. DOI: `10.1080/10408390701279749`.

Marsh, K. J. et al. (2014). “Feeding rates of a mammalian browser confirm the predictions of a ’foodscape’ model of its habitat”. *Oecologia* 174 (3), pp. 873–882.

Martiny, A. C. et al. (2013). “Strong latitudinal patterns in the elemental ratios of marine plankton and organic matter”. *Nature Geoscience* 6 (4), pp. 279–283. DOI: `10.1038/ngeo1757`.

Mazerolle, M. J. (2017). *AICcmodavg: Model selection and multimodel inference based on (Q)AIC(c)*. URL: `https://cran.r-project.org/package=AICcmodavg`.

Mcart, S. H. et al. (2009). “Summer dietary nitrogen availability as a potential bottom-up constraint on moose in south-central Alaska”. *Ecology* 90 (5), pp. 1400–1411. DOI: `10.1890/08-1435.1`.

McClintic, L. F. et al. (2014). “Effects of spatiotemporal resource heterogeneity on home range size of american beaver”. *Journal of Zoology* 293.2, pp. 134–141. DOI: `10.1111/jzo.12128`.

McNaughton, S. J. et al. (1989). “Ecosystem-level patterns of primary productivity and herbivory in terrestrial habitats”. *Nature* 341, pp. 142–144. DOI: `10.1038/341142a0`.

Merems, J. L. et al. (2020). “Nutritional-Landscape Models Link Habitat Use to Condition of Mule Deer (*Odocoileus hemionus*)”. *Frontiers in Ecology and Evolution* 8 (98), pp. 1–13. DOI: `10.3389/fevo.2020.00098`.

Merkle, J. A. et al. (2015). “Bison distribution under conflicting Foraging strategies: Site fidelity vs. Energy maximization”. *Ecology* 96 (7), pp. 1793–1801. DOI: `10.1890/14-0805.1`.

Murray, D. L. (2002). "Differential body condition and vulnerability to predation in snowshoe hares". *Journal of Animal Ecology* 71 (4), pp. 614–625. DOI: `10.1046/j.1365-2656.2002.00632.x`.

Nie, Y. et al. (2015). "Obligate herbivory in an ancestrally carnivorous lineage: The giant panda and bamboo from the perspective of nutritional geometry". *Functional Ecology* 29 (1), pp. 26–34. DOI: `10.1111/1365-2435.12302`.

Ofstad, E. G. et al. (2016). "Home ranges, habitat and body mass: simple correlates of home range size in ungulates". *Proceedings of the Royal Society B Biological Sciences* 283 (1845). DOI: `10.1098/rspb.2016.1234`.

Ovaskainen, O. et al. (2017). "How to make more out of community data? A conceptual framework and its implementation as models and software". *Ecology Letters* 20.5. Ed. by J. Chave, pp. 561–576. DOI: `10.1111/ele.12757`.

Peters, R. H. (1983). *The ecological implications of body size*. 1st. Cambridge: Cambridge University Press.

Pollock, L. J. et al. (2014). "Understanding co-occurrence by modelling species simultaneously with a Joint Species Distribution Model (JSDM)". *Methods in Ecology and Evolution* 5.5. Ed. by J. McPherson, pp. 397–406. DOI: `10.1111/2041-210X.12180`.

Powell, R. A. and M. S. Mitchell (2012). "What is a home range?" *Journal of Mammalogy* 93 (4), pp. 948–958. DOI: `10.1644/11-MAMM-S-177.1`.

Price, D. T. et al. (2013). "Anticipating the consequences of climate change for Canada's boreal forest ecosystems". *Environmental Reviews* 21 (4), pp. 322–365. DOI: `10.1139/er-2013-0042`.

R Core Team (2020). *R: A Language and Environment for Statistical Computing*. R Foundation for Statistical Computing. Vienna, Austria. URL: `https://www.R-project.org/`.

Richmond, I. C. et al. (2021). "Temporal variation and its drivers in the elemental traits of four boreal plant species". *Journal of Plant Ecology* 14.3, pp. 398–413. DOI: `10.1093/jpe/rtaa103`.

Rizzuto, M., S. J. Leroux, E. Vander Wal, Y. F. Wiersma, et al. (2019). “Patterns and potential drivers of intraspecific variability in the body C, N, and P composition of a terrestrial consumer, the snowshoe hare (*Lepus americanus*)”. *Ecology and Evolution* 9 (24), pp. 14453–14464. DOI: `10.1002/ece3.5880`.

Saïd, S., J. M. Gaillard, et al. (2009). “What shapes intra-specific variation in home range size? A case study of female roe deer”. *Oikos* 118 (9), pp. 1299–1306. DOI: `10.1111/j.1600-0706.2009.17346.x`.

Saïd, S. and S. Servanty (2005). “The influence of landscape structure on female roe deer home-range size”. *Landscape Ecology* 20.8, pp. 1003–1012. DOI: `10.1007/s10980-005-7518-8`.

Schmitz, O. J. et al. (2018). “Animals and the zoogeochemistry of the carbon cycle”. *Science* 362 (6419), eaar3213. DOI: `10.1126/science.aar3213`.

Seccombe-Hett, P. and R. Turkington (2008). “Summer diet selection of snowshoe hares: a test of nutritional hypotheses”. *Oikos* 117.12, pp. 1874–1884. DOI: `10.1111/j.1600-0706.2008.16773.x`.

Soranno, P. A. et al. (2019). “Spatial and temporal variation of ecosystem properties at macroscales”. *Ecology Letters* 22 (10), pp. 1587–1598. DOI: `10.1111/ele.13346`.

Sterner, R. W. (2004). “A one-resource ”stoichiometry””. *Ecology* 85 (7), pp. 1813–1816. URL: `https://www.jstor.org/stable/3450351`.

Sterner, R. W. and J. J. Elser (2002). *Ecological stoichiometry: the biology of elements from molecules to the biosphere*. 1st ed. Princeton University Press, p. 464. URL: `https://www.jstor.org/stable/j.ctt1jktrp3`. Accessed 26 July 2021.

Tamburello, N., I. M. Côté, and N. K. Dulvy (2015). “Energy and the scaling of animal space use”. *The American Naturalist* 186 (2), pp. 196–211. DOI: `10.1086/682070`.

Tucker, M. A., T. J. Ord, and T. L. Rogers (2014). “Evolutionary predictors of mammalian home range size: Body mass, diet and the environment”. *Global Ecology and Biogeography* 23 (10), pp. 1105–1114. DOI: `10.1111/geb.12194`.

van Beest, F. M. et al. (2011). "What determines variation in home range size across spatiotemporal scales in a large browsing herbivore?" *Journal of Animal Ecology* 80 (4), pp. 771–785. DOI: `10.1111/j.1365-2656.2011.01829.x`.

Van Der Graaf, S. et al. (2006). "Surfing on a green wave - How plant growth drives spring migration in the Barnacle Goose Branta leucopsis". *Ardea* 94.3, pp. 567–577.

Weterings, M. J. A. et al. (2018). "Food quality and quantity are more important in explaining foraging of an intermediate-sized mammalian herbivore than predation risk or competition". *Ecology and Evolution* 17.3, pp. 8419–8432. DOI: `10.1002/ece3.4372`.

Wilder, S. M. and P. D. Jeyasingh (2016). "Merging elemental and macronutrient approaches for a comprehensive study of energy and nutrient flows". *Journal of Animal Ecology* 85.6. Ed. by G. Hays, pp. 1427–1430. DOI: `10.1111/1365-2656.12573`.

Youngentob, K. N. et al. (2011). "Foliage chemistry influences tree choice and landscape use of a gliding marsupial folivore". *Journal of Chemical Ecology* 37 (1), pp. 71–84. DOI: `10.1007/s10886-010-9889-9`.

Zuur, A. F., E. N. Ieno, and C. S. Elphick (2010). "A protocol for data exploration to avoid common statistical problems". *Methods in Ecology and Evolution* 1.1, pp. 3–14. DOI: `10.1111/j.2041-210X.2009.00001.x`.

Zweifel-Schielly, B. et al. (2009). "Habitat selection by an Alpine ungulate: The significance of forage characteristics varies with scale and season". *Ecography* 32 (1), pp. 103–113. DOI: `10.1111/j.1600-0587.2008.05178.x`.

3.7 Tables

Table 3.1: Environmental and ecological drivers of home range size among mammals.

Variable	Effect	References
Body Size	larger body mass corresponds to larger home ranges	Ofstad et al. (2016), Peters (1983), and Tucker, Ord, and Rogers (2014)
Habitat	richer habitats usually corresponds to smaller home ranges	Ofstad et al. (2016) and Tucker, Ord, and Rogers (2014)
Information	previous knowledge of an area's distribution of resources, risk sources, mates, and refugia varies how individuals use available space	Merkle et al. (2015), Powell and Mitchell (2012), and Zweifel-Schielly et al. (2009)
Diet	carnivores have larger home ranges than herbivores and omnivores	Tamburello, Côté, and Dulvy (2015) and Tucker, Ord, and Rogers (2014)
Energy	increasing energetic demands lead to larger home ranges	Mcart et al. (2009) and Merkle et al. (2015)
Behaviour	sociality can influence where and on what to forage on	Merkle et al. (2015)

Table 3.2: Models' formulation and predictions tested. For each combination of plant SOI and stoichiometric ratio, we fit this set of 8 competing models plus a null model. The Mean Ratio and Ratio CV terms are the average and the coefficient of variation (CV) of the StDM-predicted stoichiometric ratios. The Ratio Mean * CV term is the interaction of these two measures of food quality variability over space. Body Weight refers to the body weight of the radio-collared snowshoe hares at point of capture. Models listed in descending level of complexity.

Model	Explanatory variables	Prediction tested
1	~ Mean Ratio + Ratio CV + Ratio Mean * CV + Body Weight	iv
2	~ Mean Ratio + Ratio CV + Ratio Mean * CV	iv
3	~ Mean Ratio + Ratio CV + Body Weight	iv
4	~ Mean Ratio + Ratio CV	iv
5	~ Mean Ratio + Body Weight	ii, iii
6	~ Ratio CV + Body Weight	i
7	~ Mean Ratio	ii, iii
8	~ Ratio CV	i
9	~ Null	

Table 3.3: Top ranking GLMs describing the relationship between home range core area size and resource stoichiometry, after removing uninformative parameters (see Table 3.2 for a list of variables included in each model and Appendix B.9.1 for full AICc tables). For each plant SOI and stoichiometric ratio pair, we report the top model, any model above the intercept, and the intercept. For coefficients, we report values estimates and 95% Confidence Intervals. Mean and coefficient of variation (CV) refer to the metrics calculated for the relevant stoichiometric ratio within the home range core area (see text for details). Column headers: k, number of parameters in the model; LL, log-likelihood; Mean:CV, interaction between a ratio's mean and CV.

				Coefficients			
k	ΔAICc	LL	R^2	Intercept	Mean	CV	Mean:CV
Lowbush blueberry C:N top models							
4	0.00	−49.43	0.70	−242.48 (−349.82– −135.14)	5.14 (2.86–7.41)	3.96 (2.83–5.10)	
3	14.87	−58.21	0.45	−0.19 (−1.71–1.33)		3.43 (1.97–4.90)	
3	29.19	−65.37	0.12	−161.71 (−336.47–13.06)	3.50 (−0.21–7.21)		
2	30.47	−67.25	0.00	3.03 (2.16–3.89)			
Lowbush blueberry N:P top models							
3	0.00	−65.99	0.08	−7.91 (−22.30–6.43)	0.38 (−0.12–0.87)		
2	0.03	−67.25	0.00	3.03 (2.16–3.89)			
Lowbush blueberry C:P top models							
3	0.00	−65.64	0.10	−7.04 (−18.67–4.59)	0.01 (−0.00–0.02)		
2	0.73	−67.25	0.00	3.03 (2.16–3.89)			
Red maple N:P top models							
3	0.00	−65.07	0.14	0.62 (−1.87–3.12)		0.73 (0.01–1.45)	
5	1.72	−63.14	0.24	44.06 (−24.59–112.70)	−1.32 (−3.34–0.71)	−12.43 (−28.43–3.57)	0.40 (−0.08–0.88)
2	1.87	−67.25	0.00	3.03 (2.16–3.89)			
Red maple C:N top models							
3	0.00	−65.57	0.11	1.55 (−0.31–3.41)		0.16 (−0.02–0.35)	
2	0.86	−67.25	0.00	3.03 (2.16–3.89)			

3.8 Figures

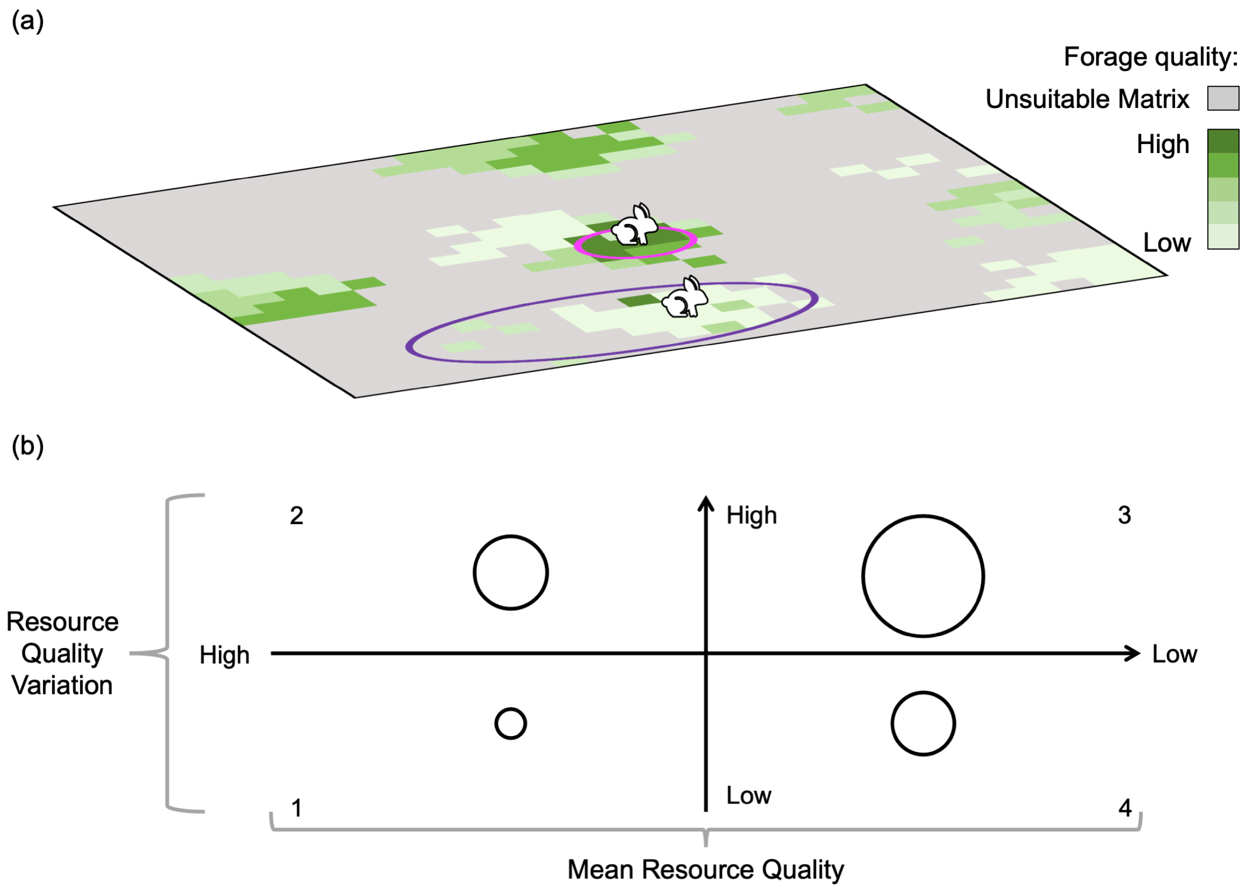

Figure 3.1: Predictions of the relationship between resource elemental composition and home range size in snowshoe hares. **Panel (a)**: in heterogeneous landscapes, resource quality varies from low (light green) to high (dark green). Herbivores space use is, in part, shaped by their foraging needs: in areas of higher overall resource quality, or where resource quality is less heterogeneous, herbivore home range size will likely be small as it is easier to meet their dietary requirements within a smaller area (pink circle). Conversely, in areas of lower overall resource quality, or higher heterogeneity, herbivore home ranges will be larger to offset the lower returns of each foraging event (purple circle). **Panel (b)**: we can imagine mean resource quality and its variability as two axes of a cartesian plane. In this resource quality space, high average resource quality and low variability lead to small herbivore home range size (quadrant 1). Conversely, high variability and low average quality will produce large home range size (quadrant 3). When either average quality is high and its variability is low, or vice versa, home range size will be intermediate between the two extremes (quadrants 2 and 4).

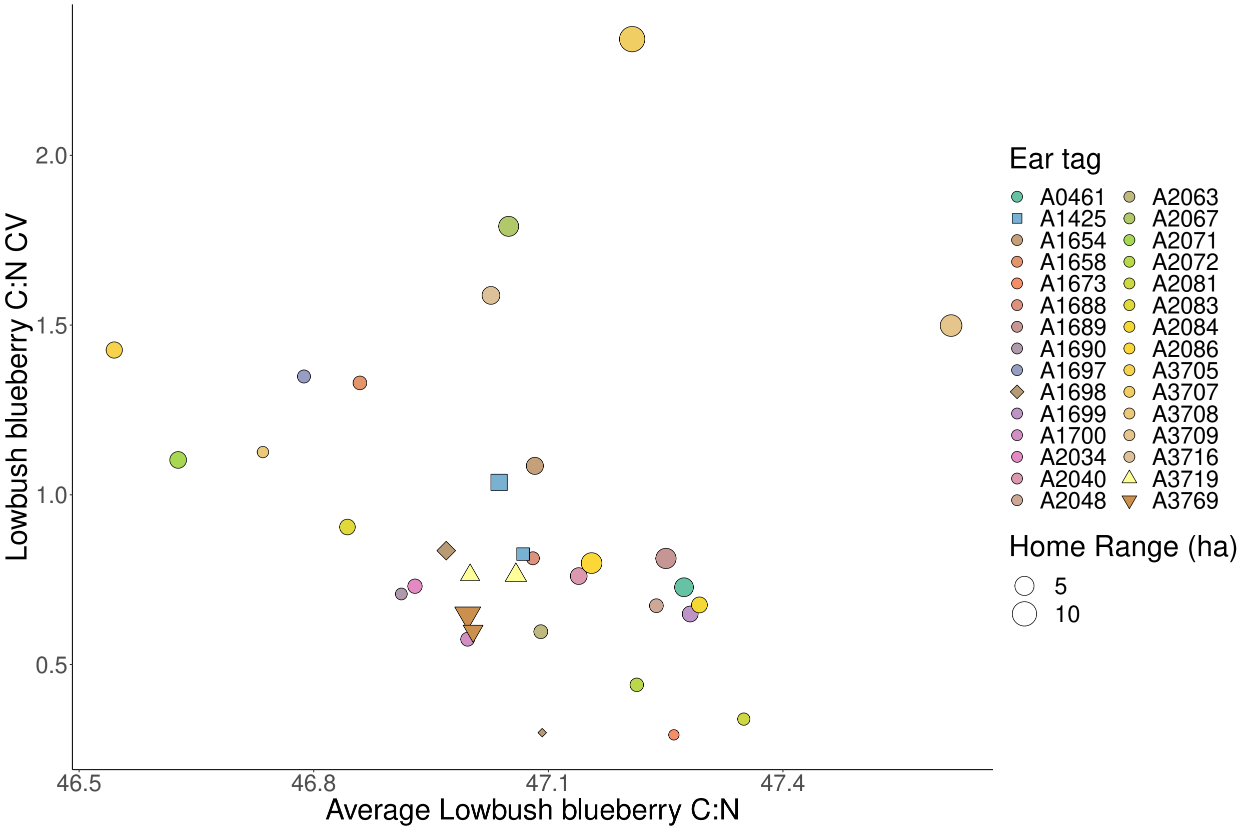

Figure 3.2: Distribution of snowshoe hare home range size estimates (ha) from this study (n = 30) in lowbush blueberry resource quality space, defined by foliage C:N ratio.
Most hares in our sample live in areas of moderate lowbush blueberry C:N content and variability. Some individuals maintain small home ranges in areas of relatively homogeneous, medium-to-high lowbush blueberry foliage C:N ratio (e.g., A1673, A2702, A2081). Conversely, a few snowshoe hares with large home ranges live in areas of heterogeneous, low-quality lowbush blueberry (e.g., A3705). The empty lower left corner may indicate that no areas of high and homogenous resource quality are available in our study area, or that no hares are using them if present. Data point size reflects 50% UD home range size; colors identify different individuals. Different shapes separate individuals with more than one year of telemetry sampling (squares, A1425; diamonds, A1698; triangles, A3719; upside-down triangles, A3769) from individuals with only one year of telemetry (circles). The Supplementary Information contains additional details on the degree of overlap between home ranges from consecutive years for these four individuals (Table B.3 and Figures B.3 to B.6).

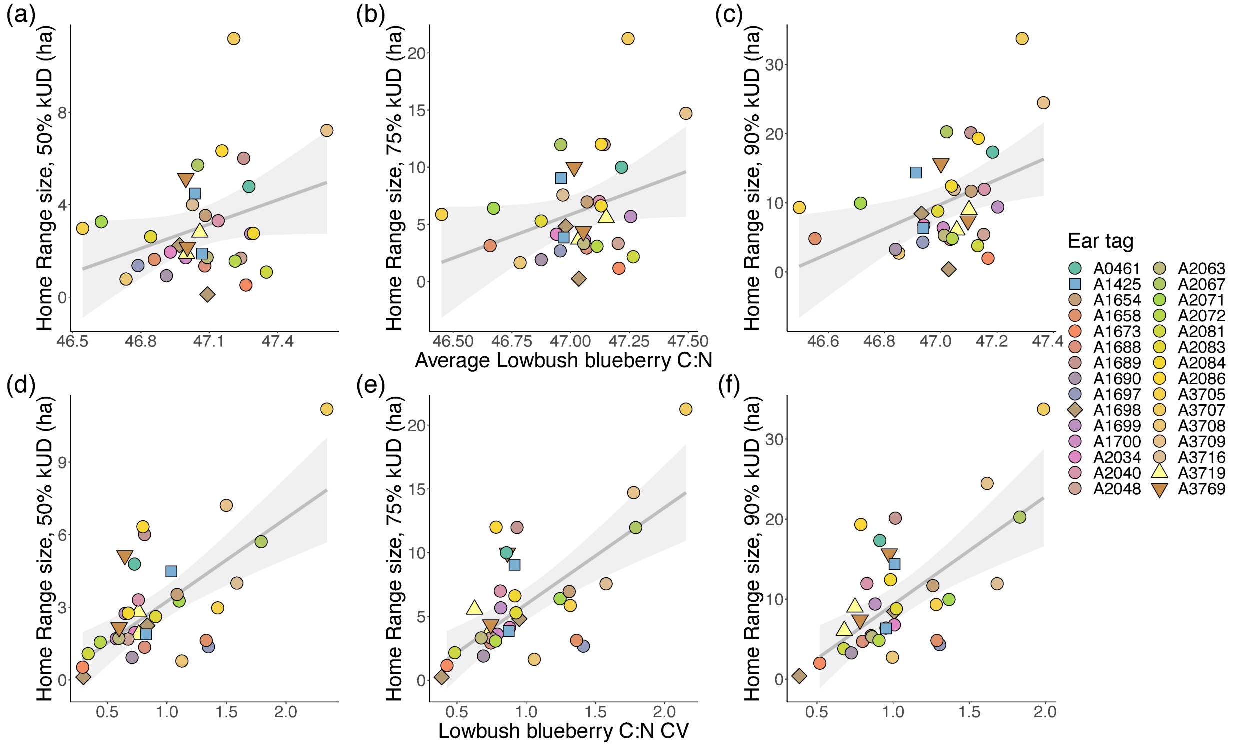

Figure 3.3: Relationship between lowbush blueberry foliage C:N ratio quality metrics and home range size, at 50%, 75%, and 90% UD. **Upper panels**: the size of home range core area for our snowshoe hares is smaller in areas of lower mean lowbush blueberry foliage C:N ratio and increases with the ratio's mean value (panel (a)). Home range sizes estimated at the 75% and 90% UD isopleths show similar trends (panels (b) and (c), respectively). Higher values of C:N ratio point towards lower availability of N in blueberries, so that individuals living in such areas (e.g., A2084) may have to forage over larger areas to meet their dietary requirements of N to survive (Sterner and Elser 2002). **Lower panels**: at increasing values of variability in lowbush blueberry foliage C:N ratio corresponds a sharp increasing in home range core area size of snowshoe hares (panel (d)). We find a similar trend at the 75% and 90% UD isopleths (panels (e) and (f), respectively). Snowshoe hares in areas of high variability of lowbush blueberry N content may resort to foraging over much larger areas than individuals that have access to food items of less variable quality—regardless of whether this is high or low quality. Grey lines are regression lines drawn from the top-ranking model for lowbush blueberry C:N ratio at the relevant UD isopleth (Tables 3.2 and 3.3 and Tables B.1 and B.2) and light grey shaded areas around them represent 95% Confidence Intervals. All other specifications as in Figure 3.1.

Chapter 4

Animal-vectored nutrient flow along different resource gradients influences the nature of local and meta-ecosystem functioning

Authors: Matteo Rizzuto[1], Shawn J. Leroux[1], Oswald J. Schmitz[2], Eric Vander Wal[1], Yolanda F. Wiersma[1], Travis R. Heckford[1]

Authors' Affiliations

1: Department of Biology, Memorial University of Newfoundland and Labrador, St. John's, Canada

2: School of the Environment, Yale University, New Haven, USA

A version of this paper will be submitted to *The American Naturalist* as:

M. Rizzuto, S. J. Leroux, O. J. Schmitz, E. Vander Wal, Y. F. Wiersma, and T. H. Heckford (in prep.). "Animal-vectored nutrient flow along different resource gradients influences the nature of local and meta-ecosystem functioning."

4.1 Introduction

Ecosystems are intrinsically open systems connected by exchanges of multiple currencies (e.g., energy, matter, information; Loreau, Mouquet, and Holt 2003; Marleau, Peller, et al. 2020). Abiotic and biotic vectors—for instance, rivers or migratory animals—drive these exchanges and thus influence ecosystem functioning at multiple spatial extents (Gravel, Guichard, et al. 2010; Schiesari et al. 2019). While the influences of abiotic vectors on ecosystem dynamics have been extensively studied (Gravel, Guichard, et al. 2010; Gravel, Mouquet, et al. 2010; Loreau, Daufresne, et al. 2013; Gounand, Mouquet, et al. 2014), less is known about how flows mediated by biotic vectors affect ecosystem processes and functions (Gounand, Harvey, et al. 2018; but see Schmitz, Wilmers, et al. 2018; Subalusky, Dutton, Njoroge, et al. 2018). Evidence from both the fossil record and present-day events shows that biotic drivers of ecosystem flows affect ecosystem functions at extents ranging from local to continental (Bauer and Hoye 2014; Schmitz, Raymond, et al. 2014; Doughty 2017; MacSween, Leroux, and Oakes 2019). However, organism-driven exchanges have diminished over time, partly as humankind began modifying the biosphere (from the late Quaternary onwards; Doughty et al. 2016). Mathematical models can play an increasingly key role in predicting causes and consequences of human-driven changes to biotic flows connecting ecosystems over space and time (McCann et al. 2021). Yet, most models and theory on organismal movement focus on the effects of these movements on patterns of populations and communities (reviewed in Bauer and Hoye 2014), without addressing their ecosystem effects. Thus, a conceptual and practical gap exists that hampers the study of how organismal movement impacts ecosystem functions, in particular biogeochemical cycling, at local and regional extents (i.e., zoogeochemistry; *sensu* Schmitz, Wilmers, et al. 2018).

Organisms can mobilize large quantities of nutrients across ecosystems' borders, influencing donor and recipient ecosystems (Earl and Zollner 2014; Hobbie and Villóeger 2015; Earl and Zollner 2017). For instance, migratory Pacific salmon (*Oncorhynchus* spp.) transfer ocean-derived nutrients to the riparian forests surrounding their spawning streams in north-western

North America (Helfield and Naiman 2001; Francis, Schindler, and Moore 2006). Similar productivity-enhancing effects of animal-mediated subsidies benefit ocean surface waters (Roman and McCarthy 2010). In terrestrial ecosystems, ungulates are well-known vectors of nutrient exchanges (Seagle 2003; Frank 2008; Abbas et al. 2012). Daily foraging movement of hippopotamuses (*Hippopotamus amphibius*) and seasonal mass drownings of migrating wildebeest (*Connochaetes taurinus*) transfer large quantities of nitrogen from grassland plains to the Mara River, Kenya (Subalusky, Dutton, Rosi-Marshall, et al. 2015; Subalusky, Dutton, Rosi, et al. 2017). Analogous flows, mediated by local and migratory animals, act in circumpolar (Jefferies, Rockwell, and Abraham 2004), boreal (Seagle 2003; Bump et al. 2009), and temperate (Abbas et al. 2012) biomes. These organismal nutrient subsidies affect fundamental ecosystem processes, such as primary productivity (Helfield and Naiman 2001; Subalusky, Dutton, Njoroge, et al. 2018) and nutrient cycling (Bump et al. 2009; Abbas et al. 2012), and connect ecosystems into higher-order organizational units—so that local changes elicit regional responses, and vice versa (Loreau, Mouquet, and Holt 2003; Loreau 2010). Human activities have and will continue to modify these widespread but delicate organismal pathways across ecosystems as we progress in the Anthropocene. Yet, we currently lack the tools to predict the consequences of our influence on these pathways.

Meta-ecosystem theory—which studies how flows of energy, matter, and organisms connect ecosystems over space and time (Loreau, Mouquet, and Holt 2003; Gounand, Harvey, et al. 2018)—provides a useful framework to place the empirical evidence for organismal pathways across ecosystems in the broader context of an interconnected biosphere. Organism-mediated spatial exchanges of nutrients bridge ecosystem processes and functions, thus changing the structure and properties of local and meta-ecosystems (Leroux and Loreau 2012; Massol, Altermatt, et al. 2017). Regional, consumer-mediated flows of nutrients across ecosystems can interact with local biomass recycling processes to influence primary and secondary production and ecosystem stability (Marleau, Guichard, Mallard, et al. 2010; Marleau, Guichard, and Loreau 2014). For instance, these interactions can sustain autotroph populations in ecosystems with low nutrient availability and allow them to thrive (Gravel, Guichard, et al. 2010), as in the hippopotamus example above (Subalusky, Dutton, Rosi-Marshall, et al. 2015). Through modifications of regional source-sink dynamics, biotic flows can thus shift the distribution of biotic populations and abiotic stocks across space and time (Gravel, Guichard, et al. 2010; Gounand, Mouquet, et al. 2014). Organismal movement can further benefit primary producers by redistributing excess nutrients over regional spatial extents, alleviating the effects of excessive nutrient availability (i.e., ameliorating the Paradox of Enrichment; Gounand, Mouquet, et al. 2014). Finally, through the movement of organisms, trophic interactions in one ecosystem can influence those of adjacent ones and produce spatial trophic cascades (*sensu* Knight et al. 2005), whereby apical trophic compartments from a donor ecosystem influence basal compartments in a recipient ecosystem (Massol, Altermatt, et al. 2017).

However, meta-ecosystem theory has been criticized for weak linkages to empirical research (Gounand, Harvey, et al. 2018; Schiesari et al. 2019). We surmise that one of the reasons for this is that most meta-ecosystem theory models organismal movements as diffusive flows along environmental gradients—e.g., from high to low resource availability (Gravel, Guichard, et al. 2010; Marleau, Guichard, Mallard, et al. 2010; but see Leroux and Loreau 2012). Assuming diffusive movement of organisms implicitly assumes that it occurs among patches within the same ecosystem, because the *same* organisms are moving within the *same* compartment from one patch to another (*sensu* Massol, Altermatt, et al. 2017). However, organisms routinely cross the boundaries of different ecosystem types—that is, of different patches—in against-gradient or gradient-neutral ways (i.e., from low to high resource availability, or in the absence of a gradient, respectively; Gounand, Harvey, et al. 2018). Through these movements, organism biomass is often converted from one compartment to another (Gounand, Harvey, et al. 2018), for instance, via ontogenic niche shifts (e.g., juvenile insectivorous salmons in rivers evolve to adult piscivore salmons in the ocean; Ebel et al. 2015) or senescence (e.g., leaves falling into freshwater bodies). Assuming diffusive organismal movement also means glossing over evidence from wildlife and behavioral ecology that describes organismal movement as driven by pervasive fitness trade-offs

(Hugie and Dill 1994; Nathan et al. 2008). As organisms move over landscapes, short-term (e.g., avoiding predation, competition, starvation) and long-term (e.g., growth, reproduction) needs influence the processes of looking for, entering, and foraging in a new patch. The matrix that surrounds local ecosystems also matters, as organisms traversing it are removed from ecosystem dynamics that may be influenced by their absence (Weisser and Hassell 1996).

Here, we aim to enhance the ecological realism of meta-ecosystem theory by integrating multiple types of organismal movement with respect to resource availability gradients into a classic meta-ecosystem model and investigate their influence on ecosystem functions at local and regional extents. We focus on three types of consumer movement with respect to resource availability gradients: movement in the absence of a gradient (henceforth, gradient-neutral), along-gradient movement, and against-gradient movement. We combine a classic, two-patch meta-ecosystem model with an intermediate “dispersers’ pool” compartment to represent the ecosystem-matrix mosaic that consumers face when traveling across the landscape (Weisser and Hassell 1996; Gounand, Harvey, et al. 2018). While this is a two-patch model which is not spatially explicit, the inclusion of the inhospitable matrix consumers travel through while moving between the two patches echoes the “patch-matrix mosaic” model that landscape ecologist frequently use to describe real-world matrix landscapes (Castilla et al. 2009; Wu 2013). Following other meta-ecosystem models (Ludwig, Jones, and Holling 1978; Menge, Pacala, and Hedin 2009; Menge, Hedin, and Pacala 2012), we use time scales separation to investigate the complex temporal dynamics of our model (Otto and Day 2011). We investigate how these different biotic movement types influence local and meta-ecosystem functions, e.g., biomass and nutrient stock accumulation, nutrient flux, and primary and secondary productivity. We expect that different types of consumer movement will influence local and regional ecosystem functions, albeit not necessarily in the same direction or with the same magnitude (Table 4.1 and Figure 4.1; Marleau, Guichard, Mallard, et al. 2010). We explore how against-gradient consumer movement influences the degree of heterogeneity in resource availability at regional extents, relative to along-gradient and gradient-neutral consumer movement. We further explore how the effects on heterogeneity due to consumer movement along different environmental gradients depends on differences in the recycling rates of primary producers.

4.2 Ecosystem Model

4.2.1 Model Derivation

We derive a meta-ecosystem model comprising two ecosystems (Figure 4.2), connected by dispersal of consumers mediated through a dispersers' pool (*sensu* Weisser and Hassell 1996). Each ecosystem contains a food web composed of three trophic compartments: inorganic nutrients (N_i), primary producers (P_i), and consumers (C_i)—where $i \in (1, 2)$ indicates the two ecosystems. The meta-ecosystem obeys mass balance constraints, and both ecosystems are open at the basal level through a constant input of inorganic nutrients, I_i. Inorganic nutrients leach from the basal level at rate l. Biotic compartments lose biomass at rate h_i for producers and at rate d_i for consumers. Following Gravel, Guichard, et al. (2010), we assume all biomass lost from higher trophic levels (P_i, C_i) re-enters each ecosystem at the basal level (N_i). Producers uptake nutrients from the basal level of each ecosystem at rate u_i. We assume a Type I functional response (Holling 1959): consumers uptake producer biomass at rate a_i and convert it to new consumer biomass with efficiency ϵ_i.

We model the fraction of consumers moving between the two ecosystems using a dispersers' pool Q (eq. 4.1g; Weisser and Hassell 1996). Q can be thought of as a stopover compartment, in which consumers enter as they leave the donor ecosystem and from which they depart once they enter a recipient ecosystem. Thus, Q provides a first approximation for the role of the unsuitable matrix in which ecosystems are embedded. We use Q to explicitly investigate three types of movement happening in one direction, from ecosystem 1 to ecosystem 2: gradient-neutral, along-, and against-gradient movement. Consumers move from ecosystem 1 towards the dispersers' pool Q with rate g, and leave Q towards ecosystem 2 with rate m. As Q is only used to move from one ecosystem to the next, no production of consumer biomass takes place in it, but individual consumers can die while in Q and do so at rate c. The following set of ordinary differential equations describes the meta-ecosystem dynamics:

Ecosystem 1:

$$\frac{dN_1}{dt} = I_1 - u_1 \cdot N_1 \cdot P_1 - l \cdot N_1 + h_1 \cdot P_1 + d_1 \cdot C_1 \tag{4.1a}$$

$$\frac{dP_1}{dt} = u_1 \cdot N_1 \cdot P_1 - a_1 \cdot P_1 \cdot C_1 - h_1 \cdot P_1 \tag{4.1b}$$

$$\frac{dC_1}{dt} = \epsilon_1 \cdot a_1 \cdot P_1 \cdot C_1 - d_1 \cdot C_1 - g \cdot C_1 \tag{4.1c}$$

Ecosystem 2:

$$\frac{dN_2}{dt} = I_2 - u_2 \cdot N_1 \cdot P_2 - l \cdot N_2 + h_2 \cdot P_2 + d_2 \cdot C_2 \tag{4.1d}$$

$$\frac{dP_2}{dt} = u_2 \cdot N_2 \cdot P_2 - a_2 \cdot P_2 \cdot C_2 - h_2 \cdot P_2 \tag{4.1e}$$

$$\frac{dC_2}{dt} = \epsilon_2 \cdot a_2 \cdot P_2 \cdot C_2 - d_2 \cdot C_2 + m \cdot Q \tag{4.1f}$$

Dispersers' pool:

$$\frac{dQ}{dt} = g \cdot C_1 - m \cdot Q - c \cdot Q \tag{4.1g}$$

To capture gradient-neutral, along-, and against-gradient consumer movement we keep the structure of the model (eq. 4.1) constant and vary the relative values of parameter I_i, thus varying the nutrient availability in the two ecosystems. That is, we vary the inorganic nutrients inputs into each ecosystem: this varies their availability for primary producers and hence the availability of forage for consumers. For gradient-neutral consumer movement, we set $I_1 = I_2$, so that consumers effectively move among homogeneous ecosystems. To reproduce along-gradient consumer movement, we consider a scenario where $I_1 >> I_2$. Finally, for against-gradient consumer movement, we set $I_1 << I_2$. Table 4.2 summarizes the model's state variable and parameters, their units of measurement, and any constraints on their values.

We use time scales separation to investigate the dynamics of this meta-ecosystem (Otto and Day 2011). Time scales separation accounts for the different timings that processes may have in an ecosystem. It works by keeping *slow* processes constant while solving for *fast* ones, and then maintaining *fast* processes at their quasi-equilibrium while solving for the *slow* ones (Otto and Day 2011; Menge, Hedin, and Pacala 2012). Studies analyzing ecological processes involving multiple time scales routinely employ this technique, e.g., insect outbreaks (Ludwig, Jones, and Holling 1978). Recently, ecosystem models of nutrient limitation and ecosystem development successfully employed time scales separation to disentangle the effects of concurring factors acting at different time scales (Menge, Pacala, and Hedin 2009; Menge, Hedin, and Pacala 2012). Fundamental to this technique is identifying the different time scales at which different processes take place, particularly which ones happen over long (i.e., *slow*) and which ones over short (i.e., *fast*) time scales. We turned to natural history to identify *slow* and *fast* processes in our model. Two fundamental processes influence the dynamics of each ecosystem in the model: biomass production and consumers' movement. Biomass production takes place on the scale of months and seasons, whereas consumer movement often happens on the scale of hours to days. Briefly, we assume that, over the time scale at which movement to and from Q takes place, biomass production in either ecosystem is effectively invariant and constant. Thus, we solve eq. 4.1g first, finding the quasi-equilibrium Q^*:

$$Q^* = \frac{g \cdot C_1}{c + m} \tag{4.2}$$

Substituting eq. 4.2 in eq. 4.1f allows us to solve for the meta-ecosystem equilibria (i.e., N_i^*, P_i^*, C_i^*) and to investigate the dynamics of the system as we allow the *slow* processes to vary over time while the *fast* process is at quasi-equilibrium. Finally, we use these meta-ecosystem equilibria to obtain the equilibrium for the dispersers' pool Q. See Appendix C.2 for full model equilibria.

4.2.2 Model Analyses

4.2.2.1 Ecosystem functions

Using the quasi-equilibrium for Q^* (eq. 4.2), we solve eq. 4.1 for feasible equilibria—that is, the equilibria where the biomass of all trophic compartments is > 0 (see Appendix C.2 for mathematical expressions). We then use these equilibria to calculate biomass and nutrient stocks, primary and secondary productivity, and nutrient flux at both local and meta-ecosystem scales. Table 4.3 shows the general formulae used to calculate these ecosystem metrics. At the local ecosystem scale, biomass stock is defined by each state variable equilibrium equation because the model's units are biomass (second column in Table 4.3). We calculate the local ecosystem's primary and secondary productivity using the equilibrium functional responses of primary producers and consumers, respectively—i.e., the flow of resources from one trophic level to the next trophic level (third column in Table 4.3). We measure nutrient flux using the loss terms from each trophic compartment at equilibrium (fourth column in Table 4.3). To obtain meta-ecosystem values for the three functions of interest, we sum together the values obtained for the local ecosystems (bottom rows in Table 4.3). Note that, at the meta-ecosystem scale, nutrient flux also includes the rate at which consumers' biomass is lost while in Q—i.e., the parameter c. Consumer biomass lost while in Q does not re-enter the recycling pathways of either local ecosystem, and is thus lost from the meta-ecosystem. Appendix C.2 provides the formulae for the equilibria used to calculate biomass and nutrient stock.

4.2.2.2 Numerical analyses

We first investigate how local and meta-ecosystem metrics vary as consumers move between two ecosystems that differ in their local environmental nutrient availability conditions (i.e., I_i). We compare three cases: equal nutrient availability ($I_1 = I_2$), higher nutrient availability in the donor ecosystem ($I_1 >> I_2$), and higher nutrient availability in the recipient ecosystem ($I_1 << I_2$). These three scenarios help us establish whether different types of consumers movement—neutral, along-, and against-gradient, respectively—influence local and meta-ecosystem dynamics.

We then investigate whether varying the ecological characteristics of biological communities in local ecosystems influences how consumer movement affects ecosystem functions. To achieve this, we use the same three movement scenarios listed above—i.e., neutral, along-, and against-gradient consumer movement—and vary the recycling rates of autotrophs to be alternatively higher in the donor or in the recipient ecosystem. This leads to a total of n = 9 competing scenarios. After setting fixed values for the nutrient availability of each local ecosystem (i.e., the parameters I_1, I_2), we measure the equilibrium values of the state variables and estimate ecosystem functions for 1000 random sets of parameter values drawn from a uniform distribution and fed to the single feasible equilibrium of the model (*sensu* Leroux and Schmitz 2015). Performing these simulations with 10 000 random sets of parameter values did not qualitatively change our results (see Appendix C.3, Figures C.4 to C.9).

We evaluate the effects of consumer movement on local and meta-ecosystem functions using the log response ratio of the function's value in each scenario to the function's value in the baseline condition. Our baseline condition is the case of equal nutrient availability across ecosystems and no manipulation of the primary producers recycling rates. The ratio's formula is:

$$LRR = log_{10}\left(\frac{X_{i,I_1 \neq I_2, h_1 \neq h_2}}{X_{i,I_1 = I_2}}\right) \tag{4.3}$$

Where $X \in [N, P, C]$ is the trophic compartment of interest, i is either the local or meta-ecosystem, and $I_1 \neq I_2$ and $h_1 \neq h_2$ represent the relationships between environmental nutrient availability and primary producers recycling rates across local ecosystems, respectively. Values of *LRR* > 0 indicate that the numerator of the ratio is larger than the denominator, and thus that the value of the function of interest calculated in a given scenario is larger than in the baseline condition. Conversely, values of *LRR* < 0 indicate a larger denominator and a larger value of the function as calculated in the baseline condition than in the given scenario. Following White et al. (2014)'s advice to not conduct frequentist statistical analyses on data from large numerical simulations, we focus on reporting median *LRR* effect sizes and their ranges.

4.3 Results

4.3.1 Consumer movement and ecosystem functions

Consumer movement establishes a spatial trophic cascade across local ecosystems, influencing local and meta-ecosystem functions in all nutrient availability scenarios (Figure 4.3 and Figure C.1). The effects of consumer movement, however, change based on the direction of the nutrient availability gradient between local ecosystems.

At the meta-ecosystem scale, against-gradient consumer movement does not appear to influence neither nutrient flux (primary producers *LRR* = 0.01, range: 0.00–0.89; consumers *LRR* = 0.07, range: −0.72–0.28) nor productivity (primary producers *LRR* = 0.03, range: −0.31–0.85; consumers *LRR* = 0.04, range: −0.72–0.28), compared to along-gradient movement (compare yellow and red boxplots in Figure 4.3b, c). Likewise, trophic compartment biomass and nutrient stock appear unchanged in the meta-ecosystem when movement happens against nutrient availability gradient (primary producers biomass *LRR* = 0.01, range: 0.00–0.88; consumers biomass *LRR* = 0.08, range: −0.72–0.28; nutrient stock *LRR* = 0.03, range: −0.63–0.25; red boxplots, right-most column, Figure 4.3a). However, at the local ecosystem scale, we observe a different situation. Consumers moving against gradient lead to the recipient ecosystem having higher primary (*LRR* = 0.18, range: 0.01–2.27) and secondary productivity (*LRR* = 0.22, range: 0.03–2.41) than in the along-gradient scenario (Figure 4.3c, compare the left and central panels). Likewise, nutrient flux in the recipient ecosystem when consumers move against gradient is higher than in the competing scenario for consumers (*LRR* = 0.16, range: −0.70–0.48) but not for primary producers (*LRR* = 0.04, range: 0.00–2.11) (Figure 4.3b). In turn, the donor ecosystem shows reduced values for consumer-mediated functions (productivity *LRR* = −0.72, range: −2.60– −0.70; nutrient flux *LRR* = −0.72, range: −2.60– −0.70; biomass *LRR* = −0.72, range: −2.60– −0.70), primary productivity (*LRR* = −0.16, range: −0.69–0.00), and nutrient stock (*LRR* = −0.16, range: −0.69–0.00).

Along-gradient consumer movement does not appear to elicit marked changes with respect to the equal nutrient availability scenario at the meta-ecosystem scale (Figure 4.3). For all three meta-ecosystem functions, biomass and nutrient stock accumulation, nutrient flux, and primary and secondary productivity, we observe no change with respect to the equal nutrient availability scenario—i.e., median *LRR* values are ~ 0—with the exception of consumer biomass (*LRR* = -0.10, range: -1.12–0.28). At the local ecosystem scale, however, along-gradient movement elicits effects that are somewhat specular to those of against-gradient movement. Along-gradient consumer movement leads to an increase in secondary productivity (*LRR* = 0.26, range: 0.26–0.67) and consumer nutrient flux (*LRR* = 0.26, range: 0.25–0.67) in the donor ecosystem, compared with the gradient-neutral movement scenarios (yellow boxplots in Figure 4.3b, c). As well, we note a reduction of both functions for consumers (productivity *LRR* = −0.46, range: −2.09– −0.03; nutrient flux *LRR* = −0.26, range: −1.16–0.26) and for primary producer nutrient flux (*LRR* = −0.13, range: −1.68–0.00) and primary productivity (*LRR* = −0.34, range: −1.90– −0.03) in the recipient ecosystem compared to the equal nutrient availability scenarios (Figure 4.3b, c).

4.3.2 Synergies between consumer movement and environmental context

Next, we vary the recycling rates of primary producers in the two ecosystems. We thus establish a gradient of autotrophs recyclability on top of the nutrient availability one, and compare results with those of a model with gradient-neutral movement and no manipulation of recycling rates. This gradient of recycling rates appears to more clearly affect primary producers in the donor ecosystem, regardless of the direction of the gradient or the type of consumer movement connecting the two ecosystems.

When consumers move against the nutrient availability gradient, higher primary producers recycling rates in the donor ecosystem (ecosystem 1, yellow boxplots in Figure 4.4) compound with higher ecosystem functioning in the recipient ecosystem (ecosystem 2). This leads to higher autotroph nutrient flux (*LRR* = 0.28, range: 0.28–0.28) and primary productivity (*LRR* = 0.09, range: −0.69–0.28) in ecosystem 1, whereas ecosystem 2 shows close to no difference from the baseline scenario in nutrient flux (*LRR* = 0.08, range: −2.44–2.79) and an increase in primary productivity (*LRR* = 0.20, range: −1.40–2.27) (yellow boxplots in Figure 4.4b, c). Curiously, nutrient stock increases not in the donor (ecosystem 1, *LRR* = 0.09, range: −0.69–0.28) but in the recipient (ecosystem 2, *LRR* = 0.13, range: −1.56–1.52) (yellow boxplots, Figure 4.4a). As a result, the meta-ecosystem is richer in nutrients (*LRR* = 0.11, range: −1.18–0.70), has higher primary productivity (*LRR* = 0.15, range: −1.35–1.61), and higher autotroph nutrient flux (*LRR* = 0.26, range: -2.00–1.64; yellow boxplots in right-most panel, Figure 4.4). Note that this is the opposite of what happens in the absence of a gradient of autotrophs recycling rates (Figure 4.3). Conversely, when autotrophs are more easily recycled in the recipient ecosystem (ecosystem 2, red boxplots in Figure 4.4), against-gradient consumer movement leads to a strong reduction in both autotroph nutrient flux (*LRR* = −1.00, range: −1.00– −1.00) and primary productivity (*LRR* = −0.86, range: −1.00– −0.70) in the donor ecosystem compared to gradient-neutral movement (compare red to yellow and blue boxplots, Figure 4.4b, c). This reduces nutrient stock in the donor ecosystem (*LRR* = −0.86, range: −1.00– −0.70; Figure 4.4a). As above, these changes appear to scale up to affect the meta-ecosystem, and even reverse the effects of consumer movement. Higher ecosystem functioning in the recipient ecosystem is not enough to offset the reduction in the donor, leading the meta-ecosystem to lower primary productivity (*LRR* = −0.11, range: −1.38–1.61), lower autotroph nutrient flux (*LRR* = −0.51, range: −2.40–1.64), but apparently unchanged nutrient stock accumulation (*LRR* = −0.04, range: −1.38–0.61; red boxplots in right-most panel, Figure 4.4). Figure C.2 reports the untransformed response ratio data, that corroborate these findings.

When the donor ecosystem (ecosystem 1) is more fertile—i.e., consumers move along-gradient—and contains more easily recyclable autotrophs, we observe an increase in autotroph nutrient flux (*LRR* = 0.28, range: 0.28–0.28) and primary productivity (*LRR* = 0.27, range: 0.26–0.28) in this ecosystem compared to gradient-neutral movement, that scales up regional extents (yellow boxplots in Figure 4.5b, c). In turn, these contribute to increasing the nutrient stock in the donor ecosystem (ecosystem 1, *LRR* = 0.27, range: 0.26–0.28) compared to gradient-neutral movement (Figure 4.5a), but to a limited effect at regional extents (*LRR* = 0.03, range: −0.91–0.70).

When more easily recyclable autotrophs are found in the recipient ecosystem, along-gradient movement of consumers appears to reduce autotroph nutrient flux (*LRR* = −1.00, range: −1.00–−1.00) and primary productivity (*LRR* = −0.12, range: −0.99–0.25) in the donor ecosystem compared to gradient-neutral movement (ecosystem 1, red boxplots in Figure 4.5b, c). Note that the primary productivity reduction is less pronounced than when consumers move against-gradient (compare Figure 4.5c with Figure 4.4c). This movement-induced reduction appears to scale up to reduce meta-ecosystem autotroph nutrient flux (*LRR* = −0.70, range: −2.40–1.09) and primary productivity (*LRR* = −0.24, range: −1.42–1.06; right-most column in Figure 4.5b, c). Nutrient stock accumulation falls in the donor ecosystem (*LRR* = −0.12, range: −0.99–0.25), leading to an overall reduction in the availability of nutrients in the meta-ecosystem (*LRR* = −0.15, range: −1.08–0.59). These effects are more pronounced when ecosystem 2 has higher recycling rates of primary producers (compare yellow and red boxplots in the right-most panel; Figure 4.5a). The untransformed data corroborate these findings (Figure C.3).

4.4 Discussion

Organismal movement connects ecosystem functions and processes across space and time, mediating exchanges of disparate currencies (Marleau, Peller, et al. 2020; Little et al. *in review*) and linking ecosystems together into meta-ecosystems (Massol, Gravel, et al. 2011; Massol, Altermatt, et al. 2017). Meta-ecosystem models generally account for organismal movement as a diffusive process not dissimilar from abiotic nutrient flows across ecosystems (but see Leroux and Loreau 2012; Häussler, Ryser, and Brose 2021). Consumer movement, however, is a multifaceted process (Nathan et al. 2008; Earl and Zollner 2017) and a diffusion-like approach may not capture the variety of organism movement types observed in nature (Gounand, Harvey, et al. 2018; McInturf et al. 2019). We integrate non-diffusive movement into a novel meta-ecosystem model and investigate how different consumer movement types may influence ecosystems functions. Our results show that diffusive and non-diffusive movements of organisms can exert a pervasive, direct and indirect influence on biomass and stock accumulation, productivity, and nutrient flux at local and meta-ecosystem extents. We offer our model as a flexible tool to provide testable predictions for common consumer movement scenarios observed in nature, to help bridge empirical and theoretical meta-ecology, and we discuss ways to further expand it and test predictions arising from it in both controlled and real-world scenarios.

Irrespective of gradients, consumers moving in meta-ecosystems directly influence consumer biomass, secondary productivity, and nutrient flux in both donor and recipient ecosystems (Figures 4.3 to 4.5). Against-gradient, non-diffusive consumer movement results in an unbalanced meta-ecosystem where local functioning is highly skewed towards the recipient ecosystem (Figures 4.3 and 4.4). Notwithstanding—or perhaps because of—the stark difference we observe at local scales, a regional overview shows the meta-ecosystem being overall more productive and nutrient-rich (right-most panels, Figures 4.3 and 4.4). Ecosystems occupied by central-place foragers provide a real-world example of these dynamics. Central-place foragers transport material from peripheral ecosystems into a central area—whether through ecosystem engineering (e.g., beavers, *Castor* spp.; Rosell et al. 2005) or excretion and egestion (e.g., humpback whales, *Megaptera novaeangliae*; Roman and McCarthy 2010; Friedlaender et al. 2016). Central-place foraging can elicit pervasive effects on the dynamics of local and meta-ecosystems that may last beyond the disappearance of the foragers, from increased nutrient availability and mineralization in the central area, to higher nutrient cycling in peripheral and adjacent ecosystems (see reviews in Rosell et al. 2005; Roman, Estes, et al. 2014). Conversely, along-gradient, diffusion-like consumer movement leads to somewhat opposite effects. Specifically, when the recipient ecosystem (ecosystem 2 in Figures 4.3 and 4.5) has lower nutrient availability but consumers move into it, this local ecosystem acts as a sink for consumer biomass with reduced secondary productivity and nutrient flux (yellow boxplots, Figure 4.3b, c; yellow and red boxplots, Figure 4.5b, c). However, consumer movement from the donor ecosystem (ecosystem 1 in Figures 4.3 and 4.5)—which has higher nutrient availability—offset these changes in the recipient ecosystem: at the meta-ecosystem scale, biomass, productivity, and nutrient flux are similar to those found in an homogeneous landscape (yellow boxplots in Figure 4.3 and compare yellow and blue boxplots in the right-most panels in Figure 4.5). Thus, we predict that the "resource pooling" effect mediated by non-diffusive, against-gradient consumer movement may be instrumental in the emergence of temporal hot-spots of nutrient availability over the landscape (*sensu* Bernhardt et al. 2017), or in facilitating habitat turnover dynamics (McNaughton 1990)—as opposed to along-gradient consumer movement leading to landscape homogenization.

Moving between the two ecosystems, consumers couple trophic interactions and ecosystem functions in time and space through mechanisms akin to those of spatial trophic cascades (*sensu* Knight et al. 2005), with indirect effects on other trophic compartments that vary with the type of consumer movement—i.e., along- or against-gradient (Figures 4.3 to 4.5). Somewhat counterintuitively, the trophic cascade arising from against-gradient, non-diffusive immigration into the recipient ecosystem stimulates primary productivity and nutrient flux while keeping local autotroph biomass low (ecosystem 2 in Figures 4.3 and 4.4). In turn, this leads to nutrient accumulation in the meta-ecosystem. That is, against-gradient consumer immigration in the recipient ecosystem maintains and exacerbates ecosystem heterogeneity: nutrient flux and production grow, leading the recipient ecosystem to become progressively richer in nutrients and biomass. For instance, in Figure 4.1a, dark green ecosystem 3 would become darker and light green ecosystem 1 would get paler. Environmental conditions can further modulate these effects, as shown by how different recycling rates of primary producers in the two ecosystems can reduce—and even overturn—the effects of against-gradient consumer movement (compare red and yellow boxplots in Figure 4.4). Our model predictions provide some theoretical support to empirical evidence of synergies between an ecosystem's autotroph community and the way consumers move over the landscape as observed, for example, in the boreal forests and circumpolar regions of North America (Pastor and Naiman 1992; Pastor, Dewey, et al. 1993; Jefferies, Rockwell, and Abraham 2004). Conversely, along-gradient, diffusive consumer movement reduces nutrient flux and ultimately nutrient accumulation in the recipient ecosystem, again producing meta-ecosystem dynamics that resemble those of an homogeneous landscape (yellow boxplots, Figures 4.3 and 4.5). These results further highlight the importance of context (*sensu* Subalusky and Post 2019) in modulating ecosystems dynamics at multiple spatial extents, through the physical (e.g., Gounand, Mouquet, et al. 2014; Sitters et al. 2020) and biological (e.g., Leroux and Schmitz 2015; Daskin and Pringle 2016; Schmitz, Miller, et al. 2017) characteristics of the environment in which a process takes place.

We surmise that a primary reason for the abundance of simple and diffusion-based meta-ecosystems models is that representing movement in different ways leads to challenges in mathematical model analysis (Massol, Altermatt, et al. 2017). As such, a major contribution of our work is the development of a modeling framework to consider more diverse types of consumer movement while maintaining some level of analytical tractability. We achieve this by integrating two novel approaches into a meta-ecosystem model. First, we model the movement of consumers in our meta-ecosystem using a dynamical variable for a "dispersers' pool", Q (*sensu* Weisser and Hassell 1996). This dispersers' pool lets us explicitly account for spatial heterogeneity in ecosystem components (Figures 4.1 and 4.2). In turn, this allows us to clearly separate between local and regional dynamics, and to quantify the influence of consumer movement across spatial scales. Organisms can often make active decisions on where to move in a landscape, and these can vary with spatial scales (Johnson 1980). Stimuli and information collected from both the surrounding environment and the internal state of a consumer can influence the trade-offs that regulate these active decisions (Nathan et al. 2008; Earl and Zollner 2017; Subalusky and Post 2019). As well, through the use of increasingly accurate bio-loggers (e.g., radio-collars combining GPS and Accelerometer; Friedlaender et al. 2016), these movements can be described by one or more states such as foraging, transit, or birthing (Ellis-Soto et al. 2021). The dispersers' pool we introduce may allow us to incorporate these different movement states into future meta-ecosystem models. Our initial model uses Q simply as a transit state: consumers move from one ecosystem to the next, and they can do so only through Q. Future models could incorporate additional elements in the formulation of Q (eq. 4.1g), to account for qualitative or quantitative heterogeneity in the movement of consumers and the landscape it takes place in. For example, by making emigration from Q towards a recipient ecosystem dependent on some metric of patch quality (Subalusky and Post 2019) or of biotic and abiotic connectivity (McLeod and Leroux 2021).

Consumer movement and activities occur over diverse time frames, that further differ from those of, e.g., primary productivity. Thus, time is a key variable for meta-ecosystem dynamics, defining and influencing both ephemeral (e.g., Bernhardt et al. 2017) and long-term processes (e.g., Ludwig, Jones, and Holling 1978; Menge, Hedin, and Pacala 2012). There is a long history of using time scales separation (Otto and Day 2011) to study processes that occur over different temporal scales in ecosystems. For example, time scales separation has been used to model the dynamics of insect outbreaks in the boreal forests of North America (Ludwig, Jones, and Holling 1978). When parameterized with general empirical data from a spruce budworm (*Choristoneura fumiferana*) system, their model predicted ecosystem dynamics that closely matched those of a typical spruce budworm outbreak (Ludwig, Jones, and Holling 1978). Similarly, time scales separation helped to shed light on the emergence of autotroph plasticity in nutrient uptake and limitation (Menge, Ballantyne IV, and Weitz 2011). Competing nutrient uptake strategies vary in their adaptive value over time based on the degree of environmental heterogeneity, in turn influencing primary producers community dynamics and nutrient cycling (Menge, Ballantyne IV, and Weitz 2011). However, to our knowledge, our study is the first to apply time scale separation to a meta-ecosystem model to tease apart the relative timing of local and regional events. We can envision fruitful applications of the combined approach involving Q and time scale separation in future ecosystem ecology research, from increasing generality by varying the timing of events, to connecting more than two patches, to accounting for a more diverse matrix among patches.

Meta-ecosystem ecology theory—and, indeed, meta-ecology at large—have historically focused on local and meta-ecosystem stability as the response variable of interest (Gravel, Guichard, et al. 2010; Marleau, Guichard, Mallard, et al. 2010; Marleau, Guichard, and Loreau 2014; Marleau, Peller, et al. 2020). However, ecosystem functions are diverse and encompass a broad range of processes that enable and complement ecosystem stability. The modeling framework we propose allows us to pivot from a focus on stability, to consider instead how consumer movement influences some of these ecosystem functions—namely, primary and secondary productivity and nutrient flux—in local and meta-ecosystems. Crucially, these ecosystem functions are commonly measured in empirical studies (Garland et al. 2021). For instance, measuring gross primary production and respiration rates of freshwater autotrophs was instrumental in disentangling the effects of subsidies on ecosystem functions mediated by different types of consumer movement in the Mara River, Kenya (Subalusky, Dutton, Njoroge, et al. 2018). As well, data on organic matter flow and secondary productivity from the Horonai Stream, Japan, helped show that consumer-mediated subsidies may elicit opposite effects on ecosystem functions at different temporal scales (Marcarelli et al. 2020). We hope that, by allowing integration of widespread measurements of ecosystem function in mathematical models, our approach will foster the development of feedbacks between empirical and theoretical meta-ecology—with the potential for real-world applications. For instance, how might the removal or alteration of organismal movement pathways (e.g., through road or hydro-electric dam construction, Tucker et al. 2018) impact ecosystem primary productivity at local and regional extents in, e.g., the meta-ecosystem formed by salmon-spawning rivers and tropical boreal forests of the North American Pacific North-West. Or, in the wake of the COVID-19 pandemic, how widespread, rapid, and long-term changes in humankind's habitat use patterns (e.g., the COVID-19 Anthropause; *sensu* Rutz et al. 2020) may in turn vary consumer movement pathways and the connections among, e.g., agricultural and forested areas in the Central European landscape mosaic (Abbas et al. 2012).

In our model, we focus on reproducing key dynamics of a complex phenomenon (i.e., movement of medium-to-large land mammals; Nathan et al. 2008) and make several simplifying assumptions. While open at the basal level, our model does not feature ecosystem flows other than consumer movement (Figure 4.2). By focusing only on apical flows, our work complements and expands on earlier studies of passive ecosystem exchanges of abiotic and biotic resources (e.g., Leroux and Loreau 2008; Gravel, Guichard, et al. 2010; Gravel, Mouquet, et al. 2010; Marleau, Guichard, Mallard, et al. 2010) and consumer influence on ecosystem dynamics (e.g., Leroux and Loreau 2010; Leroux, Hawlena, and Schmitz 2012; Leroux and Schmitz 2015), offering new insights on the mechanisms that may regulate ecosystem functions and their scale-dependency (Levin 1992). We see developing and analyzing models that include both types of flow—diffusive and non-diffusive—as a natural extension of this work. Indeed, as our analyses of consumer movement in the presence of both nutrient availability and autotrophs recycling rates gradients show (Figures 4.4 and 4.5), synergies or antagonisms with other landscape processes and features may modulate the effects described here (Subalusky and Post 2019). Concepts and tools from landscape ecology, where space is often treated explicitly, may be useful to integrate into future development of our approach. For example, mapping the patch compartments into a spatially explicitly cellular automata model would be useful to test how landscape features might influence consumer movement (see Crespo-Pérez et al. 2011, for an example of a model of moth pests between "patches" of storage silos within an agricultural landscape). As well, further integrating landscape ecology in our model may help to explicitly account for the spatial relationship among different ecosystems—thus informing how Q is modeled—and to identify spatial extents at which the model's predictions may no longer be viable, for instance, for movement of small-bodied terrestrial or aquatic organisms.

Integrating additional movement pathways, e.g., allowing bidirectional movement, and an ecosystem "preference" parameter would greatly enhance the realism of our model, and thus help bridge the gap with more complex, Earth-system models (for an example of an Earth-system model, see Harfoot et al. 2014). Consumers routinely move in both one-way and two-way fashion in real-world scenarios—for instance, during continental migration or when moving from resting to foraging areas (Gounand, Harvey, et al. 2018)—and the decision to move itself entails complex trade-offs on part of the organism (Charnov 1976; Nathan et al. 2008). Furthermore, moving in the unsuitable matrix exposes consumers to a host of inputs and environmental features that may play a role in shaping both the direction of movement and its ecosystem consequences. The spatial configuration of habitat patches within an inhospitable matrix can influence movement, and the ability to move through a matrix can vary depending on how the landscape has been altered and the species' tolerance of anthropogenic features; these features of the matrix could be parameterized in a spatial model with, for instance, different friction values (e.g., Coulon et al. 2015). In particular, we see scope to expand our model to account for human modifications of landscapes. For instance, habitat fragmentation (Haddad et al. 2015), sensory pollution (Sanders et al. 2021), and movement barriers (Tucker et al. 2018) can potentially greatly influence the trajectory and scale of organismal movement. Our model's ability to account for these modifications by changing the simple functions that govern movement into and from Q, while maintaining mathematical tractability, may be instrumental in developing new hypotheses and predictions to investigate their effects on both organismal movement and ecosystem functions.

Meta-ecosystem ecology encourages and challenges researchers to expand their focus and look at general, emerging properties of ecosystems. Here, we develop a novel, flexible approach to investigate the influence of different types of consumer movement in meta-ecosystems. Key predictions arising from our initial, simple model include (i) along- and against-gradient consumer movement has different, at times opposite influences on local and meta-ecosystem stocks, productivity, and nutrient flux, (ii) a spatial trophic cascade, whereby consumers from the donor ecosystem influence the trophic interactions in the recipient ecosystem, mediate these effects, and (iii) functional traits, such as plant recycling rates, can further modulate the effects of consumer movement on ecosystem functions. Furthermore, our results conform to earlier expectations about the effects of more complex movement representations in meta-ecosystem models (Massol, Altermatt, et al. 2017). As humankind adopts new actions and strategies to mitigate the effects of anthropogenic environmental change, accounting for the myriad moving pieces that shape ecosystem functioning has never been more pressing.

4.5 Data Availability

All data and code used in the analyses are available via a figshare online repository at:

https://doi.org/10.6084/m9.figshare.16479933

4.6 References

Abbas, F. et al. (2012). “Roe deer may markedly alter forest nitrogen and phosphorus budgets across Europe”. *Oikos* 121.8, pp. 1271–1278. DOI: `0.1111/j.1600-0706.2011.20103.x`.

Bauer, S. and B. J. Hoye (2014). “Migratory Animals Couple Biodiversity and Ecosystem Functioning Worldwide”. *Science* 344.6179, p. 1242552. DOI: `10.1126/science.1242552`.

Bernhardt, E. S. et al. (2017). “Control Points in Ecosystems: Moving Beyond the Hot Spot Hot Moment Concept”. *Ecosystems* 20.4, pp. 665–682. DOI: `10.1007/s10021-016-0103-y`.

Bump, J. K. et al. (2009). “Large herbivores and aquatic-terrestrial links in southern boreal forests”. *Journal of Animal Ecology* 78.2, pp. 338–345. DOI: `10.1111/j.1365-2656.2008.01498.x`.

Castilla, G. et al. (2009). “The impact of thematic resolution on the patch-mosaic model of natural landscapes”. *Landscape Ecology* 24.1, pp. 15–23. DOI: `10.1007/s10980-008-9310-z`.

Charnov, E. L. (1976). “Optimal foraging, the marginal value theorem”. *Theoretical Population Biology* 9.2, pp. 129–136. DOI: `10.1016/0040-5809(76)90040-X`.

Coulon, A. et al. (2015). “A stochastic movement simulator improves estimates of landscape connectivity”. *Ecology* 96.8, pp. 2203–2213. DOI: `10.1890/14-1690.1`.

Crespo-Pérez, V. et al. (2011). “Modeling invasive species spread in complex landscapes: the case of potato moth in Ecuador”. *Landscape Ecology* 26.10, pp. 1447–1461. DOI: `10.1007/s10980-011-9649-4`.

Daskin, J. H. and R. M. Pringle (2016). “Does primary productivity modulate the indirect effects of large herbivores? A global meta-analysis”. *Journal of Animal Ecology* 85.4, pp. 857–868. DOI: `10.1111/1365-2656.12522`.

Doughty, C. E. (2017). “Herbivores increase the global availability of nutrients over millions of years”. *Nature Ecology & Evolution* 1.12, pp. 1820–1827. DOI: `10.1038/s41559-017-0341-1`.

Doughty, C. E. et al. (2016). “Global nutrient transport in a world of giants”. *Proceedings of the National Academy of Sciences of the United States of America* 113.4, pp. 868–873. DOI: `10.1073/pnas.1502549112`.

Earl, J. E. and P. A. Zollner (2014). “Effects of animal movement strategies and costs on the distribution of active subsidies across simple landscapes”. *Ecological Modelling* 283, pp. 45–52. DOI: `10.1016/j.ecolmodel.2014.03.020`.

— (2017). “Advancing research on animal-transported subsidies by integrating animal movement and ecosystem modelling”. *Journal of Animal Ecology* 86.5, pp. 987–997. DOI: `10.1111/1365-2656.12711`.

Ebel, J. D. et al. (2015). “Ontogenetic differences in Atlantic salmon phosphorus concentration and its implications for cross ecosystem fluxes”. *Ecosphere* 6.8, art136. DOI: `10.1890/ES14-00516.1`.

Ellis-Soto, D. et al. (2021). “A methodological roadmap to quantify animal-vectored spatial ecosystem subsidies”. *Journal of Animal Ecology* 90.7, pp. 1605–1622. DOI: `10.1111/1365-2656.13538`.

Francis, T. B., D. E. Schindler, and J. W. Moore (2006). “Aquatic insects play a minor role in dispersing salmon-derived nutrients into riparian forests in southwestern Alaska”. *Canadian Journal of Fisheries and Aquatic Sciences* 63.11, pp. 2543–2552. DOI: `10.1139/f06-144`.

Frank, D. A. (2008). “Ungulate and topographic control of nitrogen: phosphorus stoichiometry in a temperate grassland; soils, plants and mineralization rates”. *Oikos* 117.4, pp. 591–601. DOI: `10.1111/j.0030-1299.2008.16220.x`.

Friedlaender, A. S. et al. (2016). “Multiple-stage decisions in a marine central-place forager”. *Royal Society Open Science* 3.5, p. 160043. DOI: `10.1098/rsos.160043`.

Garland, G. et al. (2021). “A closer look at the functions behind ecosystem multifunctionality: A review”. *Journal of Ecology* 109.2, pp. 600–613. DOI: `10.1111/1365-2745.13511`.

Gounand, I., E. Harvey, et al. (2018). “Meta-Ecosystems 2.0: Rooting the Theory into the Field”. *Trends in Ecology & Evolution* 33.1, pp. 36–46. DOI: `10.1016/j.tree.2017.10.006`.

Gounand, I., N. Mouquet, et al. (2014). “The Paradox of Enrichment in Metaecosystems”. *The American Naturalist* 184.6, pp. 752–763. DOI: `10.1086/678406`.

Gravel, D., F. Guichard, et al. (2010). “Source and sink dynamics in meta-ecosystems”. *Ecology* 91.7, pp. 2172–2184. DOI: `10.1890/09-0843.1`.

Gravel, D., N. Mouquet, et al. (2010). “Patch Dynamics, Persistence, and Species Coexistence in Metaecosystems”. *The American Naturalist* 176.3, pp. 289–302. DOI: `10.1086/655426`.

Haddad, N. M. et al. (2015). “Habitat fragmentation and its lasting impact on Earth’s ecosystems”. *Science Advances* 1.2, pp. 1–10. DOI: `10.1126/sciadv.1500052`.

Harfoot, M. B. J. et al. (2014). “Emergent Global Patterns of Ecosystem Structure and Function from a Mechanistic General Ecosystem Model”. *PLoS Biology* 12.4. DOI: `10.1371/journal.pbio.1001841`.

Häussler, J., R. Ryser, and U. Brose (2021). “Invasive spread in meta-food-webs depends on landscape structure, fertilization and species characteristics”. *Oikos*, oik.07503. DOI: `10.1111/oik.07503`.

Helfield, J. M. and R. J. Naiman (2001). “Effects of Salmon-Derived Nitrogen on Riparian Forest Growth and Implications for Stream Productivity”. *Ecology* 82.9, pp. 2403–2409. DOI: `10.1890/0012-9658(2001)082[2403:EOSDNO]2.0.CO;2`.

Hobbie, S. E. and S. Villóeger (2015). “Interactive effects of plants, decomposers, herbivores, and predators on nutrient cycling”. In: *Trophic Ecology: Bottom-Up and Top-Down Interactions across Aquatic and Terrestrial Systems*. Ed. by T. C. Hanley and K. J. La Pierre. Ecological Reviews. Cambridge University Press, pp. 233–259. DOI: `10.1017/CBO9781139924856.010`.

Holling, C. S. (1959). “The Components of Predation as Revealed by a Study of Small-Mammal Predation of the European Pine Sawfly”. *The Canadian Entomologist* 91.5, pp. 293–320. DOI: `10.4039/Ent91293-5`.

Hugie, D. M. and L. M. Dill (1994). “Fish and game: a game theoretic approach to habitat selection by predators and prey”. *Journal of Fish Biology* 45.Suplement A, pp. 151–169. DOI: `10.1006/jfbi.1994.1220`.

Jefferies, R. L., R. F. Rockwell, and K. F. Abraham (2004). “Agricultural Food Subsidies, Migratory Connectivity and Large-Scale Disturbance in Arctic Coastal Systems: A Case Study”. *Integrative and Comparative Biology* 44, pp. 130–139. DOI: `10.1093/icb/44.2.130`.

Johnson, D. H. (1980). “The Comparison of Usage and Availability Measurements for Evaluating Resource Preference”. *Ecology* 61.1, pp. 65–71. DOI: `10.2307/1937156`.

Knight, T. M. et al. (2005). “Trophic cascades across ecosystems”. *Nature* 437.7060, pp. 880–883. DOI: `10.1038/nature03962`.

Leroux, S. J., D. Hawlena, and O. J. Schmitz (2012). “Predation risk, stoichiometric plasticity and ecosystem elemental cycling”. *Proceedings of the Royal Society B Biological Sciences* 279.1745, pp. 4183–4191. DOI: `10.1098/rspb.2012.1315`.

Leroux, S. J. and M. Loreau (2008). “Subsidy hypothesis and strength of trophic cascades across ecosystems”. *Ecology Letters* 11.11, pp. 1147–1156. DOI: `10.1111/j.1461-0248.2008.01235.x`.

— (2010). “Consumer-mediated recycling and cascading trophic interactions”. *Ecology* 91.7, pp. 2162–2171. DOI: `10.1890/09-0133.1`.

— (2012). “Dynamics of Reciprocal Pulsed Subsidies in Local and Meta-Ecosystems”. *Ecosystems* 15.1, pp. 48–59. DOI: `10.1007/s10021-011-9492-0`.

Leroux, S. J. and O. J. Schmitz (2015). “Predator-driven elemental cycling: the impact of predation and risk effects on ecosystem stoichiometry”. *Ecology and Evolution* 5.21, pp. 4976–4988. DOI: `10.1002/ece3.1760`.

Levin, S. A. (1992). “The Problem of Pattern and Scale in Ecology: The Robert H. MacArthur Award Lecture”. *Ecology* 73.6, pp. 1943–1967. DOI: `10.2307/1941447`.

Little, C. J. et al. (*in review*). “Filling the Information Gap in Meta-Ecosystem Ecology”. *Oikos*. manuscript id: OIK-08892.R1. EcoEvoRxiv preprint. DOI: `10.32942/osf.io/hc83u`.

Loreau, M. (2010). *From populations to ecosystems: Theoretical foundations for a new ecological synthesis*. Princeton University Press, p. 320. DOI: `10.1515/9781400834167`.

Loreau, M., T. Daufresne, et al. (2013). “Unifying sources and sinks in ecology and Earth sciences”. *Biological Reviews* 88.2, pp. 365–379. DOI: `10.1111/brv.12003`.

Loreau, M., N. Mouquet, and R. D. Holt (2003). “Meta-ecosystems: A theoretical framework for a spatial ecosystem ecology”. *Ecology Letters* 6.8, pp. 673–679. DOI: `10.1046/j.1461-0248.2003.00483.x`.

Ludwig, D., D. Jones, and C. S. Holling (1978). “Qualitative Analysis of Insect Outbreak Systems: The Spruce Budworm and Forest”. *Journal of Animal Ecology* 47.1, pp. 315–332. DOI: `10.2307/3939`.

MacSween, J., S. J. Leroux, and K. D. Oakes (2019). “Cross-ecosystem effects of a large terrestrial herbivore on stream ecosystem functioning”. *Oikos* 128.1, pp. 135–145. DOI: `10.1111/oik.05331`.

Marcarelli, A. M. et al. (2020). “Magnitude and direction of stream–forest community interactions change with timescale”. *Ecology* 101.8, pp. 1–10. DOI: `10.1002/ecy.3064`.

Marleau, J. N., F. Guichard, and M. Loreau (2014). “Meta-ecosystem dynamics and functioning on finite spatial networks”. *Proceedings of the Royal Society B Biological Sciences* 281.1777, p. 20132094. DOI: `10.1098/rspb.2013.2094`.

Marleau, J. N., F. Guichard, F. Mallard, et al. (2010). “Nutrient flows between ecosystems can destabilize simple food chains”. *Journal of Theoretical Biology* 266.1, pp. 162–174. DOI: `10.1016/j.jtbi.2010.06.022`.

Marleau, J. N., T. Peller, et al. (2020). “Converting Ecological Currencies: Energy, Material, and Information Flows”. *Trends in Ecology & Evolution* 35.12, pp. 1068–1077. DOI: `10.1016/j.tree.2020.07.014`.

Massol, F., F. Altermatt, et al. (2017). “How life-history traits affect ecosystem properties: effects of dispersal in meta-ecosystems”. *Oikos* 126.4, pp. 532–546. DOI: `10.1111/oik.03893`.

Massol, F., D. Gravel, et al. (2011). “Linking community and ecosystem dynamics through spatial ecology”. *Ecology Letters* 14.3, pp. 313–323. DOI: `10.1111/j.1461-0248.2011.01588.x`.

McCann, K. S. et al. (2021). “Landscape modification and nutrient-driven instability at a distance”. *Ecology Letters* 24.3, pp. 398–414. DOI: `10.1111/ele.13644`.

McInturf, A. G. et al. (2019). “Vectors with autonomy: what distinguishes animal-mediated nutrient transport from abiotic vectors?” *Biological Reviews* 94, pp. 1761–1773. DOI: `10.1111/brv.12525`.

McLeod, A. M. and S. J. Leroux (2021). “Incorporating abiotic controls on animal movements in metacommunities”. *Ecology* 102.7, pp. 1–15. DOI: `10.1002/ecy.3365`.

McNaughton, S. J. (1990). “Mineral nutrition and seasonal movements of African migratory ungulates”. *Nature* 345.6276, pp. 613–615. DOI: `10.1038/345613a0`.

Menge, D. N. L., F. Ballantyne IV, and J. S. Weitz (2011). “Dynamics of nutrient uptake strategies: Lessons from the tortoise and the hare”. *Theoretical Ecology* 4.2, pp. 163–177. DOI: `10.1007/s12080-010-0110-0`.

Menge, D. N. L., L. O. Hedin, and S. W. Pacala (2012). “Nitrogen and Phosphorus Limitation over Long-Term Ecosystem Development in Terrestrial Ecosystems”. *PLoS One* 7.8. Ed. by C. P. Slomp, e42045. DOI: `10.1371/journal.pone.0042045`.

Menge, D. N. L., S. W. Pacala, and L. O. Hedin (2009). “Emergence and maintenance of nutrient limitation over multiple timescales in terrestrial ecosystems”. *The American Naturalist* 173.2, pp. 164–175. DOI: `10.1086/595749`.

Nathan, R. et al. (2008). “A movement ecology paradigm for unifying organismal movement research”. *Proceedings of the National Academy of Sciences of the United States of America* 105.49, pp. 19052–19059. DOI: `10.1073/pnas.0800375105`.

Otto, S. P. and T. Day (2011). *A biologist’s guide to mathematical modeling in ecology and evolution*. Princeton University Press, p. 744. DOI: `10.1515/9781400840915`.

Pastor, J., B. Dewey, et al. (1993). “Moose Browsing and Soil Fertility in the Boreal Forests of Isle Royale National”. *Ecology* 74.2, pp. 467–480. DOI: `10.2307/1939308`.

Pastor, J. and R. J. Naiman (1992). “Selective Foraging and Ecosystem Processes in Boreal Forests”. *The American Naturalist* 139.4, pp. 690–705. DOI: `10.1086/285353`.

Roman, J., J. A. Estes, et al. (2014). “Whales as marine ecosystem engineers”. *Frontiers in Ecology and the Environment* 12, pp. 377–385. DOI: `10.1890/130220`.

Roman, J. and J. J. McCarthy (2010). “The whale pump: Marine mammals enhance primary productivity in a coastal basin”. *PLoS One* 5.10. DOI: `10.1371/journal.pone.0013255`.

Rosell, F. et al. (2005). “Ecological impact of beavers castor fiber and castor canadensis and their ability to modify ecosystems”. *Mammal Review* 35.3-4, pp. 248–276. DOI: `10.1111/j.1365-2907.2005.00067.x`.

Rutz, C. et al. (2020). “COVID-19 lockdown allows researchers to quantify the effects of human activity on wildlife”. *Nature Ecology & Evolution* 4.9, pp. 1156–1159. DOI: `10.1038/s41559-020-1237-z`.

Sanders, D. et al. (2021). “A meta-analysis of biological impacts of artificial light at night”. *Nature Ecology & Evolution* 5.1, pp. 74–81. DOI: `10.1038/s41559-020-01322-x`.

Schiesari, L. et al. (2019). “Towards an applied metaecology”. *Perspectives in Ecology and Conservation* 17.4, pp. 172–181. DOI: `10.1016/j.pecon.2019.11.001`.

Schmitz, O. J., J. R. B. Miller, et al. (2017). “Toward a community ecology of landscapes: predicting multiple predator-prey interactions across geographic space”. *Ecology* 98.9, pp. 2281–2292. DOI: `10.1002/ecy.1916`. eprint: `0608246v3`.

Schmitz, O. J., P. A. Raymond, et al. (2014). “Animating the carbon cycle”. *Ecosystems* 17.2, pp. 344–359. DOI: `10.1007/s10021-013-9715-7`.

Schmitz, O. J., C. C. Wilmers, et al. (2018). “Animals and the zoogeochemistry of the carbon cycle”. *Science* 362 (6419), eaar3213. DOI: `10.1126/science.aar3213`.

Seagle, S. W. (2003). “Can ungulates foraging in a multiple-use landscape alter forest nitrogen budgets?” *Oikos* 103.1, pp. 230–234. DOI: `10.1034/j.1600-0706.2003.12287.x`.

Sitters, J. et al. (2020). "Nutrient availability controls the impact of mammalian herbivores on soil carbon and nitrogen pools in grasslands". *Global Change Biology* 26.4, pp. 2060–2071. DOI: `10.1111/gcb.15023`.

Subalusky, A. L., C. L. Dutton, L. Njoroge, et al. (2018). "Organic matter and nutrient inputs from large wildlife influence ecosystem function in the Mara River, Africa". *Ecology* 99.11, pp. 2558–2574. DOI: `10.1002/ecy.2509`.

Subalusky, A. L., C. L. Dutton, E. J. Rosi, et al. (2017). "Annual mass drownings of the Serengeti wildebeest migration influence nutrient cycling and storage in the Mara River". *Proceedings of the National Academy of Sciences of the United States of America* 114.29, pp. 7647–7652. DOI: `10.1073/pnas.1614778114`.

Subalusky, A. L., C. L. Dutton, E. J. Rosi-Marshall, et al. (2015). "The hippopotamus conveyor belt: Vectors of carbon and nutrients from terrestrial grasslands to aquatic systems in sub-Saharan Africa". *Freshwater Biology* 60.3, pp. 512–525. DOI: `10.1111/fwb.12474`.

Subalusky, A. L. and D. M. Post (2019). "Context dependency of animal resource subsidies". *Biological Reviews* 94.2, pp. 517–538. DOI: `10.1111/brv.12465`.

Tucker, M. A. et al. (2018). "Moving in the Anthropocene: Global reductions in terrestrial mammalian movements". *Science* 359.6374, pp. 466–469. DOI: `10.1126/science.aam9712`.

Weisser, W. W. and M. P. Hassell (1996). "Animals 'on the move' stabilize host-parasitoid systems". *Proceedings of the Royal Society B Biological Sciences* 263.1371, pp. 749–754. DOI: `10.1098/rspb.1996.0112`.

White, J. W. et al. (2014). "Ecologists should not use statistical significance tests to interpret simulation model results". *Oikos* 123.4, pp. 385–388. DOI: `10.1111/j.1600-0706.2013.01073.x`.

Wu, J. (2013). "Key concepts and research topics in landscape ecology revisited: 30 years after the Allerton Park workshop". *Landscape Ecology* 28.1, pp. 1–11. DOI: `10.1007/s10980-012-9836-y`.

4.7 Tables

Table 4.1: Predictions of the effects of consumer movement at the ecosystem scale, under three scenarios of nutrient availability. Column headers indicate the nutrient availability scenarios we use to compare the effects of different types of consumer movement (see text). Numbers in each row indicate in which of the two ecosystems (1, 2) we expect a given metric to be higher.

Metric	Along-gradient	Equal	Against-gradient
Biomass and Nutrient Stock	1	1	2
Primary productivity	1	2	2
Nutrient flux	2	2	2

Table 4.2: The model state variables, parameters, definitions, units of measurements, and range of values. See Figure 4.2 for a diagram.

Variable	Definition	Units	Range
N_i	Inorganic nutrient stock in patch i	g	> 0
P_i	Primary producer stock in patch i	g	> 0
C_i	Consumer stock in patch i	g	> 0
Q	Dispersers' pool	g	> 0
Parameter			
I_i	Inorganic nutrient input rate to patch i	$g * t^{-1}$	> 0
l	Inorganic nutrient output rate	$g * t^{-1}$	> 0
u_i	Producer uptake rate in patch i	$(g * t)^{-1}$	> 0
a_i	Consumer attack rate in patch i	$(g * t)^{-1}$	> 0
ϵ_i	Consumer assimilation efficiency in patch i	dimensionless	$[0, 1]$
h_i	Biomass loss rate from Producer stock in patch i	t^{-1}	> 0
d_i	Biomass loss rate from Consumer stock in patch i	t^{-1}	> 0
g_i	Movement rate from Consumer stock in patch i towards Dispersers' pool	t^{-1}	$[0, 1]$
m_i	Movement rate from Dispersers' pool towards Consumer stock in patch i	t^{-1}	$[0, 1]$
c_i	Biomass loss rate from Dispersers' pool	t^{-1}	> 0

Table 4.3: Formulas to calculate ecosystem and meta-ecosystem functions. See Table 4.2 for variable and parameter definitions. An asterisk * indicates the feasible equilibrium value of a variable, whereas $i \in (1, 2)$ indicates either local ecosystem.

Compartment	**Stock**	**Productivity**	**Nutrient Flux**
Ecosystem i			$\sum(h_i \cdot P_i^*, d_i \cdot C_i^*)$
Nutrients	N_i^*		
Producers	P_i^*	$u_i \cdot N_i^* \cdot P_i^*$	$h_i \cdot P_i^*$
Consumers	C_i^*	$\epsilon_i \cdot a_i \cdot P_i^* \cdot C_i^*$	$d_i \cdot C_i^*$
Meta-ecosystem			$\sum_i (h_i \cdot P_i^*, d_i \cdot C_i^*) - c \cdot Q^*$
Nutrients	$\sum_i (N_i^*)$		
Producers	$\sum_i (P_i^*)$	$\sum_i (u_i \cdot N_i^* \cdot P_i^*)$	$\sum_i (h_i \cdot P_i^*)$
Consumers	$\sum_i (C_i^*)$	$\sum_i (\epsilon_i \cdot a_i \cdot P_i^* \cdot C_i^*)$	$\sum_i (d_i \cdot C_i^*)$

4.8 Figures

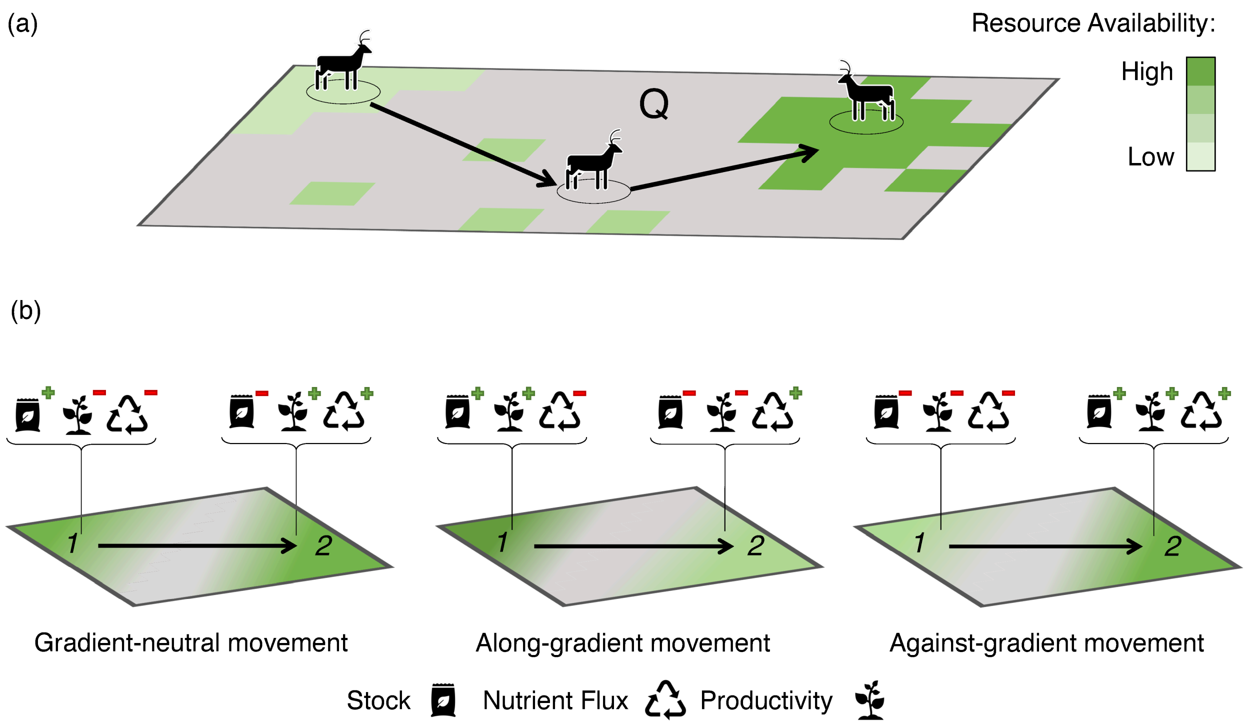

Figure 4.1: Panel (a): conceptual diagram of the model. Organisms move among ecosystems (green polygons) by traveling across the matrix, Q (grey-shaded areas). In doing so, organisms connect ecosystems with different resource availability (shades of green) across the landscape, potentially influencing ecosystem functions in each local ecosystem and in the meta-ecosystem. **Panel (b)**: Our analyses consider three scenarios of background environmental nutrient availability—the parameter I_i in the model (Table 4.2)—here shown in green. Organisms move from ecosystem 1 to ecosystem 2 in all scenarios (black arrow). The grey-shaded area in the middle of each scenario represents the unsuitable matrix Q between donor and recipient ecosystems. In the first scenario, on the left, the two ecosystems have equivalent environmental nutrient availability ($I_1 = I_2$); organisms movement is gradient-neutral. In the second scenario, center, the donor ecosystem has higher nutrient availability than the recipient ecosystem ($I_1 >> I_2$); organisms move along gradient. In the third scenario, on the right, the recipient ecosystem has higher nutrient availability than the donor ecosystem ($I_1 << I_2$); organisms move against gradient. The cartoons above each scenario show the hypothesized local influence of consumer movement on each of the three ecosystem functions of interest, i.e., biomass and nutrient accumulation (sack icon), primary and secondary productivity (sapling icon), and nutrient flux (recycling icon), respectively. Green plus signs represent an enhanced process, red minus signs stand for a reduced process.

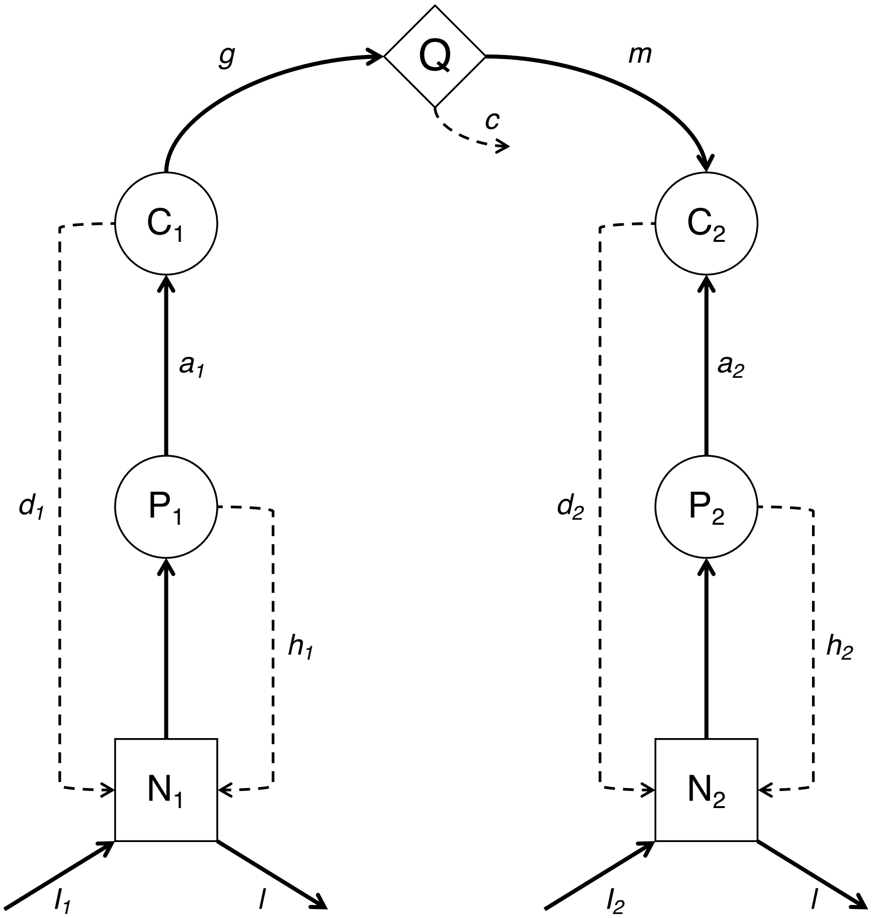

Figure 4.2: Model diagram, showing the two ecosystems and the pool of dispersers connecting them through unidirectional movement. Boxes and circles represent nutrient stock, primary producers, and consumers biomass, respectively. Solid arrows connecting trophic compartment (i.e., Nutrients N_i, Primary Producers P_i, and Consumers C_i) represent trophic interactions, whereas dashed arrows represent recycling pathways. See Table 4.2 for variables and parameters definitions.

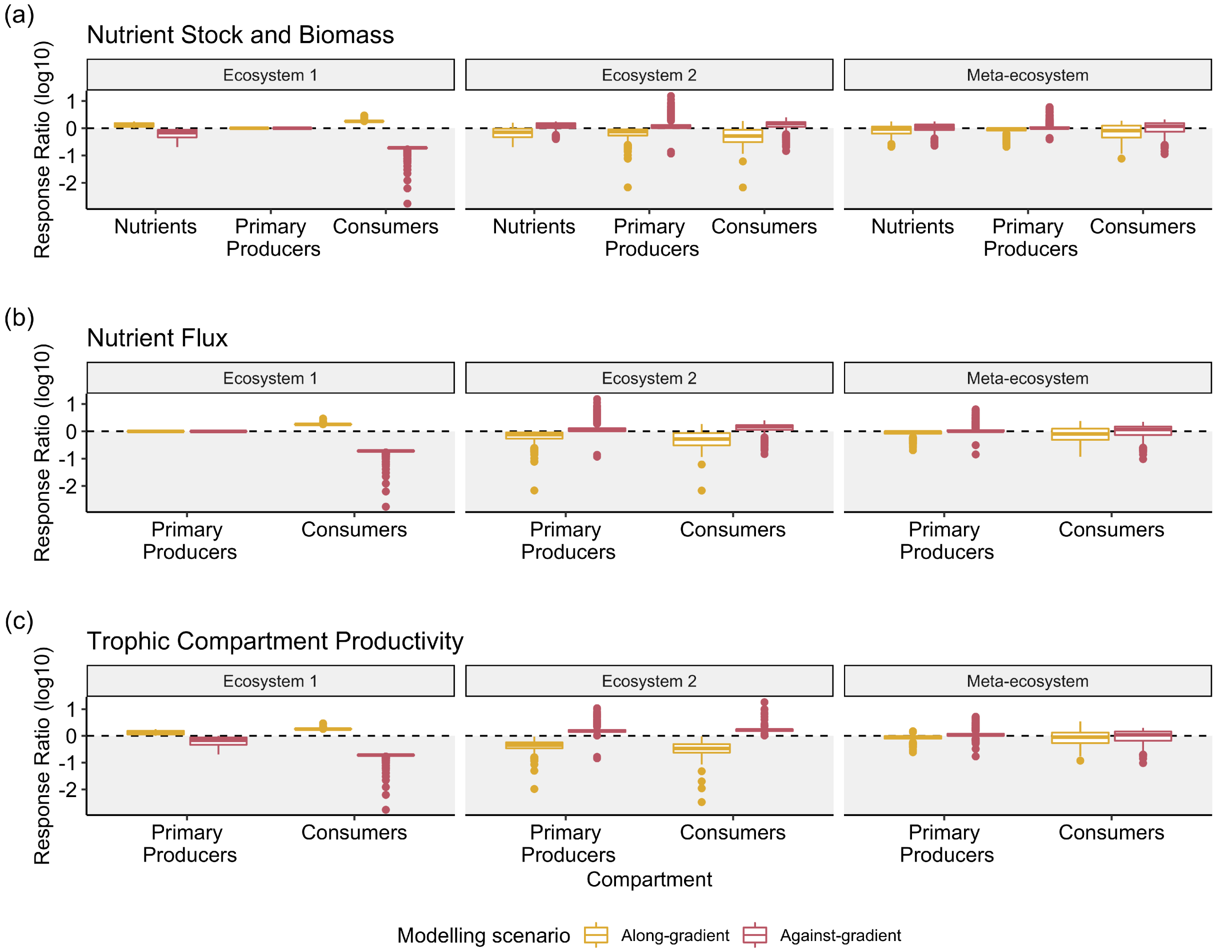

Figure 4.3: Comparison of log_{10} response ratio values for (a) nutrient stock and biomass, (b) nutrient flux, and (c) trophic compartment productivity when consumers move in an heterogeneous meta-ecosystem. Consumer movement happens from ecosystem 1 to ecosystem 2. The log_{10} response ratio (*LRR*, eq. 4.3) on the ordinate captures the change in local and meta-ecosystem functions in the two nutrient availability scenarios ($I_1 >> I_2$ and $I_1 << I_2$) with respect to the baseline, homogeneous scenario ($I_1 = I_2$). Against-gradient, non-diffusive consumer movement (red boxplots, $I_1 << I_2$) mediates higher levels of Consumers nutrient flux and primary and secondary productivity in the recipient ecosystem 2 that scale up to the meta-ecosystem. In turn, at regional spatial extents, these values offset reductions of the same ecosystem functions in the donor ecosystem (right-most panels). Conversely, along-gradient, diffusive consumer movement (yellow boxplots, $I_1 >> I_2$) elicits a reduction of ecosystem functions in ecosystem 2, the recipient, compared to both the against-gradient ($I_1 << I_2$) and the gradient-neutral ($I_1 = I_2$) consumer movement scenarios. Conversely, higher values of these ecosystem functions in the donor ecosystem offset the reductions at the regional spatial scale. Note the log_{10} scale on the ordinate. For each ecosystem function, thick lines inside the boxes represent median values, the upper and lower hinges correspond to the first (25%) and third (75%) quartiles, and the upper and lower whiskers extend from the respective hinge to the largest and smaller value no further than 1.5 × interquartile range.

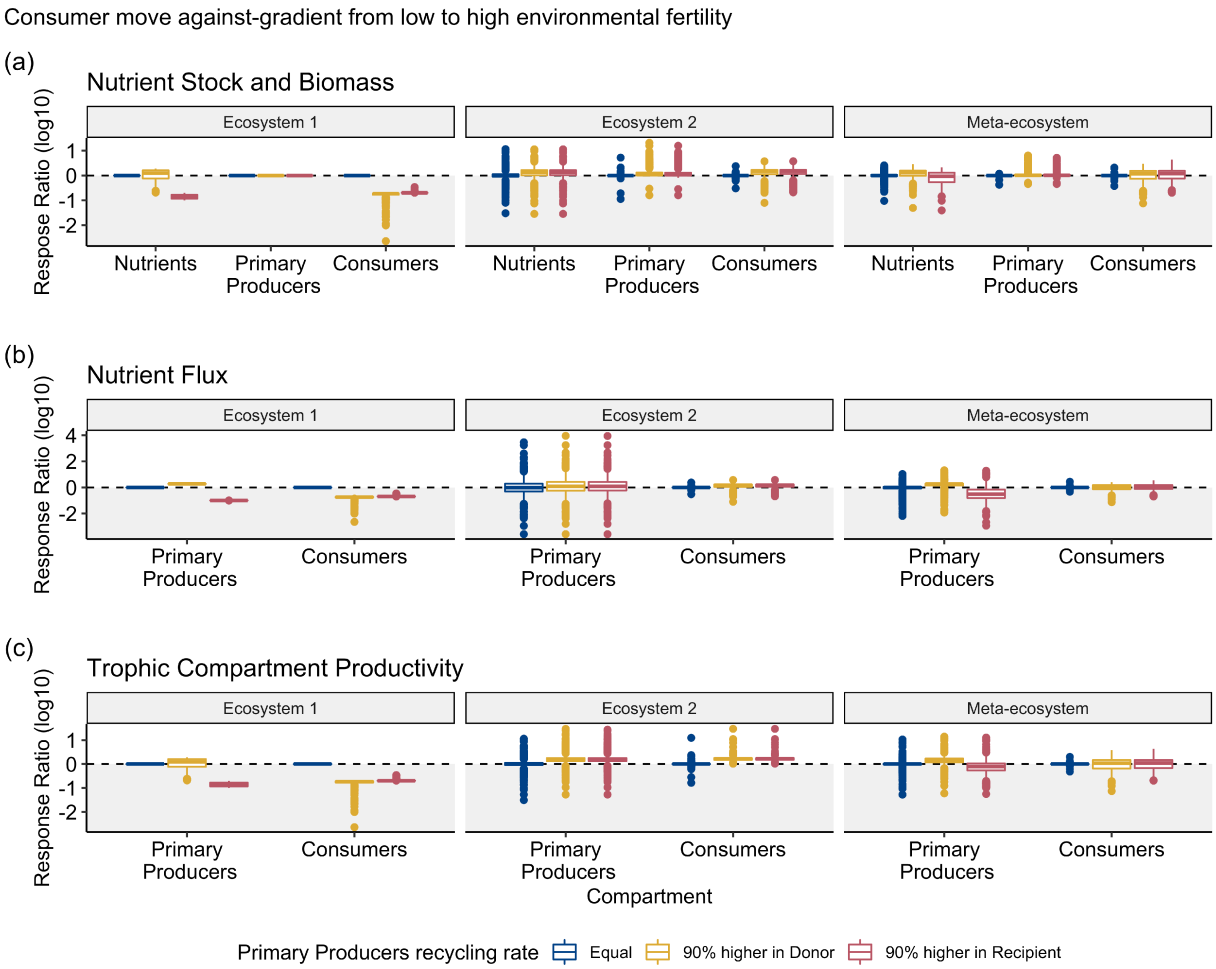

Figure 4.4: Comparison of log_{10} response ratio values for (a) nutrient stock and biomass, (b) nutrient flux, and (c) trophic compartment productivity when consumers move against nutrient availability gradient, in the presence of an autotroph recycling rate gradient. We use the log_{10} response ratio (LRR, eq. 4.3) to compare scenarios where autotroph recyclability is equal ($h_1 = h_2$), higher in ecosystem 1 ($h_1 >> h_2$), higher in ecosystem 2 ($h_1 << h_2$) with a baseline scenario where we do not manipulate it (i.e., random h_i values). When consumers move against both the nutrient availability and autotroph recycling rate gradients (red boxplots), ecosystem functions in the donor ecosystem 1 are strongly reduced and the effect appears to scale to the regional spatial extent. In this scenario, the spatial trophic cascade established by consumer movement leads to a counterintuitive increase in primary productivity (panel (c)) and nutrient flux (panel (c)) with no corresponding increase in primary producers' biomass at either spatial scale (center and right-most panels in (a)). Conversely, consumers moving against nutrient availability gradient but along a gradient of autotroph recycling rate appear to enhance ecosystem functions in both ecosystems (yellow boxplots). Autotrophs release in ecosystem 1 leads to higher productivity and nutrient flux there (panels (b), (c)), but no change in autotroph biomass values (panel (a)). Both ecosystems experience nutrient stock accumulation in this scenario, leading to the meta-ecosystem being more nutrient-rich than other cases (yellow boxplots, right-most panels in (a)). See Figure C.2 for untransformed data trends. All specifications as in Figure 4.3.

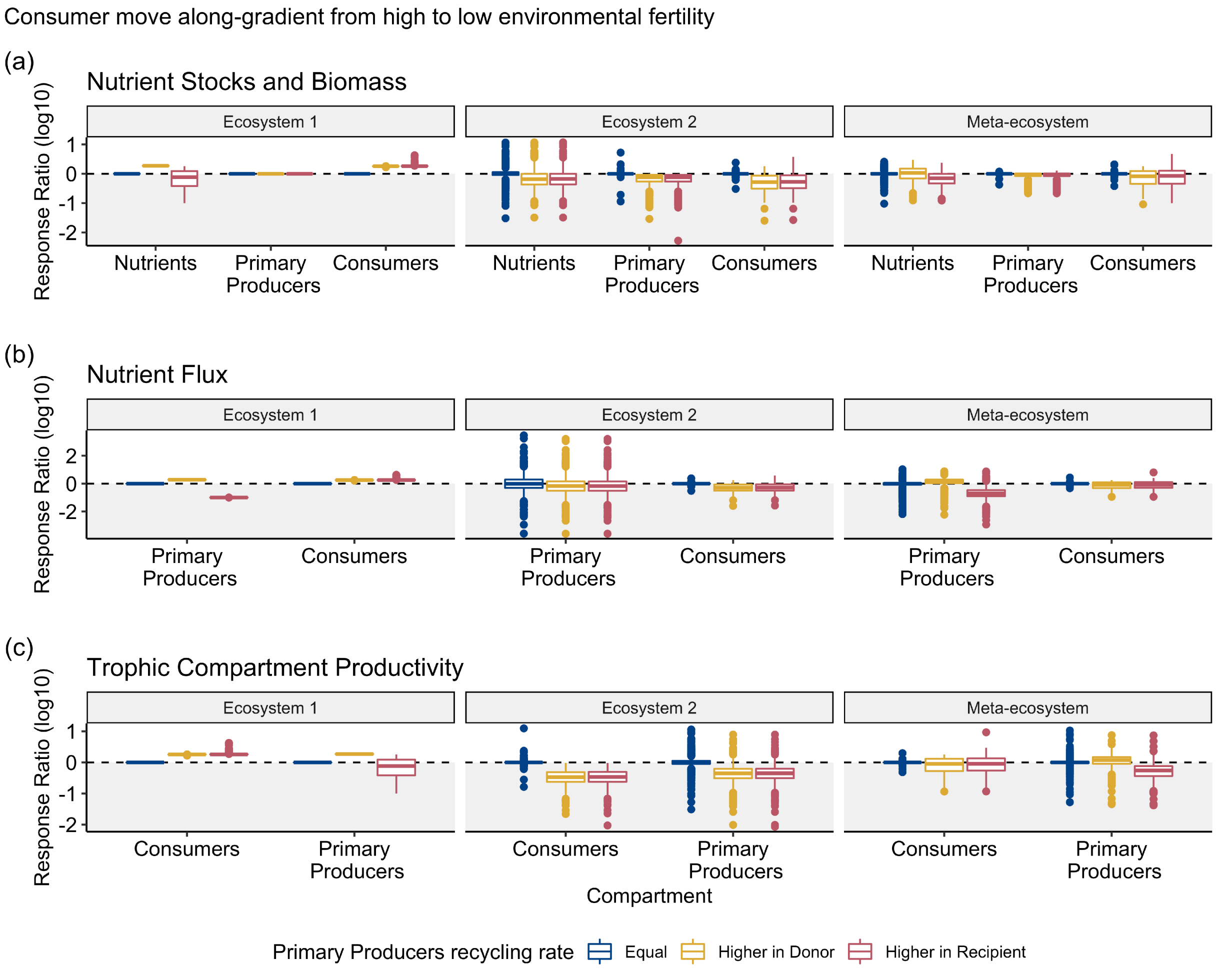

Figure 4.5: Comparison of log_{10} response ratio values for (a) nutrient stock and biomass, (b) nutrient flux, and (c) trophic compartment productivity when consumers move along nutrient availability gradient, in the presence of an autotroph recycling rate gradient. Along-gradient consumer movement mediates an increase in primary productivity (panel (c)) and nutrient flux (panel (b)) when recycling rates are higher in ecosystem 1, compared to the baseline scenario (compare blue and yellow boxplots). In turn, nutrient stock increases at local spatial extents in ecosystem 1, albeit without a corresponding increase in nutrient stocks in the meta-ecosystem (right-most panel) or in consumer biomass, as would be expected in a classic trophic cascade (yellow boxplot, panel (a)). Like the against-gradient scenarios (Figure 4.4), when recycling rates are higher in ecosystem 2, along-gradient consumer movement reduces primary productivity and autotroph nutrient flux in ecosystem 1 (red boxplots, panels (b), (c); compare with Figure 4.4b, c). However, we observe higher secondary productivity and nutrient flux in ecosystem 1 (red boxplots, panels (b), (c)), which were absent from the against-gradient scenarios (compare red boxplots for consumers in panels (b), (c) with those in Figure 4.4b, c). In turn, nutrient stocks diminish at local and regional spatial extents (red boxplots for nutrients, panel (a)). See Figure C.3 for untransformed data trends. All specifications as in Figures 4.3 and 4.4.

Chapter 5

Summary

Ecosystems are complex systems whose existence relies on interactions among their diverse components (Currie 2011) and with other ecosystems across spatio-temporal scales (i.e., meta-ecosystems; Loreau, Mouquet, and Holt 2003). Mapping and understanding what drives these ubiquitous relationships between organic and inorganic ecosystem components is a prime objective of ecology, made more pressing by anthropogenic environmental change (Schiesari et al. 2019). In ecosystem ecology, consumers have historically received less attention than other ecosystem compartments, such as primary producers or decomposers and detritivores (Schmitz, Raymond, et al. 2014). This is particularly true for terrestrial vertebrates other than *Homo sapiens*, as they account for a small portion of Earth's extant biomass and are generally assumed to have a limited influence on ecosystem functioning (but see Schmitz, Raymond, et al. 2014; Schmitz, Wilmers, et al. 2018). However, a growing body of literature points to the relationship between biomass and ecosystem influences being non-linear and multi-faceted, with increasing calls to re-evaluate how consumers fit into local and meta-ecosystem processes and functions (Enquist et al. 2020; Leroux, Wiersma, and Vander Wal 2020; Schmitz and Leroux 2020; Leroux, Charron, et al. 2021). For instance, fossil-record analyses show high-magnitude effects of consumers on ecosystem nutrient budgets and primary productivity patterns in past geological ages, with reductions starting around the late Quaternary (Doughty et al. 2016; Doughty 2017). Furthermore, present-day evidence from disparate ecosystems shows that, while reduced in both numbers and diversity, terrestrial vertebrate consumers are still instrumental in mediating ecosystems' resilience (e.g., response to natural disturbances; Leroux, Charron, et al. 2021), functions (e.g., nutrient cycling; Rosell et al. 2005; Pastor, Cohen, and Hobbs 2006), and services (e.g., carbon sequestration; Holdo, Sinclair, et al. 2009; Strickland et al. 2013).

Accounting for consumers in ecosystem studies, or doing so in more nuanced ways, is challenging. Consumers have complex ecologies and behaviours (e.g., Felton et al. 2018; Gounand et al. 2018), that are difficult to include in mathematical models and theoretical frameworks of ecosystem functioning (but see Leroux and Loreau 2010; Leroux and Schmitz 2015, building on work by DeAngelis 1992; Loreau 2010). The goals of my thesis were to (i) describe a keystone boreal vertebrate using stoichiometric units of measurement, (ii) examine its interactions with the environment within a spatial ecological stoichiometry framework, and (iii) develop mathematical tools able to account for the multiple ways consumers' can influence local and meta-ecosystem functioning at multiple spatial scales. To achieve these goals, I adopted a multidisciplinary approach that combined empirical data collection in both laboratory and field settings, spatial statistical analyses, and mathematical modeling, woven together through an ecological stoichiometry lens. I found that:

(i) Contrary to expectations, snowshoe hares (*L. americanus*) showed variability in their content of key elements, irrespective of the metrics—absolute or relative—used. A set of commonly used, invertebrate-derived predictors, e.g., age, sex, and body condition indices, explained little of this intraspecific elemental variation. I found weak evidence supporting a decrease in body content of nitrogen with age, which could be consistent with the escape-based anti-predator strategy of snowshoe hares, which are heavily preyed-upon in the boreal biome. As well, I found weak evidence supporting higher content of phosphorus (P) among hares in better overall body condition, consistent with both stoichiometric expectations for vertebrates and the strong P-limitation of the boreal biome. Taken together, these results suggest three insights. First, snowshoe hares demonstrate plasticity in whole-body stoichiometry, posing new questions about the stoichiometry of vertebrates that require further study. Second, while constrained by stricter homeostasis requirements, stoichiometrically variable vertebrates may play more substantial roles in the elemental budgets of ecosystems than previously thought. Third, identifying proximate and remote causes of vertebrate intraspecific elemental variability will require accounting for multiple endo- and exogenous potential drivers that do not necessarily transfer across taxa.

(ii) Consumers are aware of the elemental composition of their resources and its spatial variability, and this contributes to their space use and spatial ecology. Snowshoe hares appeared to vary their space use based on two different facets of food stoichiometry. One of these was the overall difference in quality between two areas (i.e., the mean content of key elements), while the other one was the variation within a given area (i.e., the variation around the mean quality). Snowshoe hares had smaller home range sizes in areas of the landscape where quality of preferred forage species was either overall higher or more homogeneous. Curiously, this meant that some hares had relatively small home ranges in areas of overall lower, but homogeneous, forage quality. Conversely, hares maintained larger home ranges where forage quality was overall poor or highly heterogeneous. These results demonstrate that intraspecific variability at the most fundamental, atomic level can traverse scales of biological organization to influence scale-dependent, iterative processes such as habitat and resource selection.

(iii) The multiple ways in which consumers can move over the landscape elicit different effects in local and meta-ecosystems, changing how ecosystem functions and processes play out at multiple spatial extents. Expanding on existing conceptual models of meta-ecosystem connectivity, I demonstrate that consumers moving against gradients of resource availability can directly alter the balance of functions such as productivity and nutrient cycling among local ecosystems. In turn, these alterations scale up to change the overall functional profile of meta-ecosystems. Furthermore, I show that the effects of consumer movement may be further modulated, and even reversed, by the functional traits of biological communities they interact with in either the donor or recipient ecosystem. The novel mathematical modeling framework I develop here allows for inference beyond local and meta-ecosystem stability, opening new research avenues to study the dynamics of these ubiquitous ecological units. As well, it offers a way to develop future meta-ecosystem models beyond the classic, two-patch approach, to include more complex and realistic spatial layouts, as well as additional currencies and scales.

Overall, my thesis offers empirical evidence and theoretical tools to re-evaluate the role of consumers in the dynamics of ecosystems. Unified by a common stoichiometric framework, the disparate topics of my thesis coalesce around two main themes to explore in future studies. First, by showing how terrestrial vertebrates are both stoichiometrically variable and able to respond to stoichiometric variation in their environment, my thesis offers support to an expansion of existing paradigms in both ecological stoichiometry and ecosystem ecology to better integrate consumers and their interactions with other biotic and abiotic compartments into ecosystem processes and functions (Schmitz, Wilmers, et al. 2018; Harvey et al. 2021; Leroux, Charron, et al. 2021). As well, my thesis offers evidence supporting the development of ecology towards multi-currency models that comprise energy, matter (i.e., elements; Sterner 2004), and other currencies (e.g., information; O'Connor et al. 2019; Marleau et al. 2020) to paint a more refined picture of the actors and interactions shaping ecosystem functions and services.

5.1 Come together: integrating consumers into ecosystem ecology

In recent years, integrating consumers into existing paradigms became a focus for ecosystem ecology (Schmitz, Raymond, et al. 2014; Gounand et al. 2018; Schmitz, Wilmers, et al. 2018). Part of the challenge lies in consumers being, like ecosystems, complex systems that show a high degree of variability in their interactions with the environment; this is particularly true for vertebrates. Consumers continuously experience endogenous stimuli—e.g., energetic (Carbone et al. 1999) and dietary (Nie et al. 2015) requirements, but also memory (Powell and Mitchell 2012; Spencer 2012). As well, they constantly collect exogenous inputs—e.g., environmental variability (Marsh et al. 2014; Nie et al. 2015), competition (Schradin et al. 2010), risk and safety (Lima and Zollner 1996; Laundré et al. 2014). In turn, intelligent behaviour arises from consumers integrating these disparate types of information (*sensu* Fronhofer, Hovestadt, and Poethke

2013; Harfoot et al. 2014). This set of condition-informed actions and reactions then shapes consumers' relationships with their habitats and environments (Powell and Mitchell 2012; Bernhardt, O'Connor, et al. 2020). How to distill and account for the salient properties of this biological complexity within the ecosystem ecology framework, rooted in trophic or functional groupings of organisms, remains an open question.

At times, long-term empirical studies have succeeded in this endeavour by employing multidisciplinary approaches, synthesizing data and insights from disparate ecological disciplines. For instance, in Isle Royale National Park (Michigan), bridging animal and plant ecology through combined physiological and behavioural approaches led to insights into moose influence on nutrient cycling and other ecosystem functions (Pastor and Naiman 1992; Pastor, Dewey, et al. 1993). In turn, integrating individual-scale results with spatial data from movement ecology, population dynamics, and forest distribution patterns, helped define a framework to predict how large herbivores alter the balance of limiting nutrients in ecosystems via feedback processes (see synthesis in Pastor, Cohen, and Hobbs 2006). In turn, by introducing stoichiometric approaches, new studies (Bump, Peterson, and Vucetich 2009; Bump, Tischler, et al. 2009; Bump, Webster, et al. 2009; Montgomery et al. 2014) uncovered the ecosystem influences of trophic interactions, e.g., moose-wolf, and of their outcomes, e.g., carcass deposition, on the distribution of ecosystem control points that further mediate nutrient cycling and soil fertility (*sensu* Bernhardt, Blaszczak, et al. 2017). Recently, the distilled insights arising from this diverse literature led to studies addressing applied ecology questions—e.g., how rewilding efforts impact nutrient subsidies (Bump 2018). Similar examples from well-known study systems include the northern boreal forests of Kluane (Yukon; Krebs, Boonstra, and Boutin 2018), the grasslands of the Serengeti (Tanzania and Kenia; McNaughton et al. 1989; McNaughton 1990; Holdo, Holt, et al. 2011; Subalusky et al. 2018), and a few others (reviewed in Schmitz, Wilmers, et al. 2018; Schmitz and Leroux 2020).

On the other hand, theoretical studies of ecosystems and the interactions among their compartments have lagged behind, mostly eschewing the complexity of consumers' ecology and of their interactions with each other and the environment (Massol et al. 2017; Gounand et al. 2018; Schiesari et al. 2019). Simplifying approaches and assumptions are commonly used in theoretical models of ecosystem functioning (reviewed in Massol et al. 2017, see also Chapter 4 for further examples). As well, Earth-system models aimed at simulating and predicting the current and future dynamics of our planet under varying scenarios are just beginning to include consumer-mediated effects (e.g., the Madingley Model; Harfoot et al. 2014). While mostly centered around direct measures of consumers' ecosystem effects, e.g., biomass or body size, recent works on Earth-system models have produced compelling evidence of consumers' influences on terrestrial ecosystem functioning being detectable even at continental scales (Enquist et al. 2020; Hoeks et al. 2020). Yet, consumers elicit effects on ecosystem functioning—and thus Earth's state and conditions—through a host of other mechanisms that do not necessarily depend on their body size or biomass, or even their presence (Lima and Zollner 1996; Strickland et al. 2013; Wirsing et al. 2021). Functional traits, the morphological, behavioural, or physiological characteristics of an organism, can account for both direct and indirect consumers' effects and may thus be instrumental in capturing their contributions to ecosystem processes (reviewed in Schmitz and Leroux 2020).

Stoichiometric ratios, e.g., the Carbon:Nitrogen, Carbon:Phosphorus, or Nitrogen:Phosphorus ratios of an organism or substrate, can be considered functional traits (Leal, Seehausen, and Matthews 2017) and thus allow for investigating how organisms may fit into biogeochemical processes and models of ecosystem functioning (Sterner and Elser 2002). While further studies are necessary to identify what drives their variability, throughout my thesis I offer evidence that terrestrial mammals show and are sensitive to variation in stoichiometric traits. In turn, this opens the door to future studies of terrestrial mammals' role in ecosystem functioning, rooted in the combined use of stoichiometric and functional traits. For instance, in the context of the snowshoe hare-based case study presented here, infusing stoichiometric and functional traits into future studies could lead to new insights in the role of snowshoe hares in the dynamics of boreal forests. While showing some overlap in diet with the moose (Dodds 1960) and sharing some physiological adaptations with beavers (e.g., hindgut fermenting; Rosell et al. 2005), snowshoe hares differ from either these larger herbivores in their foraging strategies, space use patterns, and population dynamics (Krebs, Boonstra, and Boutin 2018). Snowshoe hares exhibit boom-bust population dynamics with distinct, multi-year periodicity driven mainly by food availability (Krebs, Boonstra, and Boutin 2018). Building on the results I present in Chapters 2 and 3, future studies in this system could pair population and community ecology approaches with stoichiometric distribution models (StDMs; Leroux, Vander Wal, et al. 2017) to investigate how successive peaks and valleys in the hares' abundance cycle influence the stoichiometry of their ecosystem's functions and processes by, for example, increasing or decreasing amounts of faeces, litter, and carcasses available for decomposition.

Functional traits can also help resolve the interplay among consumers, their resources, and other organismal and environmental variables. In Chapter 3, I showed how snowshoe hares respond to variability in stoichiometric traits of their forage and consequently vary aspects of their ecology—space use, in this case. Crucially, my stoichiometric trait-based approach produced insights that would have been lost otherwise—namely, that spatial heterogeneity in forage stoichiometric traits may be as or more important than their averages in shaping the space use of some individuals. Conversely, focusing on ecosystem functions such as primary productivity and nutrient cycling, in Chapter 4 I demonstrated that these are sensitive to differences in consumers' traits—movement capabilities, in this case. However, while my thesis points to stoichiometric and functional traits of consumers and resources interacting to shape multiple aspects of organisms' ecology and ecosystem functioning, it stops short of integrating these separate lines of evidence into a unified investigation of these feedback processes. Consequently, a way to expand and advance the results presented here would be to integrate ecological traits of both consumers and resources into the meta-ecosystem model presented in Chapter 4. For instance, consumer movement could be adaptive to the environmental, climatic, or biological conditions of an area—e.g., forage quality (Chapter 4), but also predation risk (Richmond et al. 2021) and temperature (Balluffi-Fry, Leroux, Wiersma, Richmond, et al. 2021)—by including a preference parameter in the formulation of movement functions to determine which ecosystem consumers move towards from the dispersers' pool Q.

A consumer-aware paradigm rooted into stoichiometric and functional traits may also account for effects that consumers mediate by changing the environment around them. For instance, while examples reported so far implicitly assumed consumers are present in the ecosystem, consumers can also influence ecosystem functions through their absence. Movement of consumers in Chapter 4 influences functions and processes in both donor and recipient ecosystems—that is, through both absence and presence. Studies abound that describe and investigate the ecosystem influences of consumers' indirect effects, such as the non-consumptive influences that predators can exert on their prey through their mere presence or absence (Leroux, Hawlena, and Schmitz 2012; Strickland et al. 2013). For instance, risk of predation is a well-known cause of stress in prey, leading to distinct physiological responses (Hawlena and Schmitz 2010) that can alter how prey experience and interact with their environment (Richmond et al. 2021) and, ultimately, modify nutrient cycles (Schmitz, Hawlena, and Trussell 2010; Strickland et al. 2013). For instance, considering the mostly aerial predation risk present in my study system (Richmond et al. 2021), stoichiometric and functional traits could allow for capturing alterations of ecosystem functions and processes arising from the landscape of fear (Laundré et al. 2014; Schmitz, Miller, et al. 2017) created by aerial predation on snowshoe hares—both empirically (e.g., Richmond et al. 2021) and theoretically (see above). Additionally, such an approach could be transferred to other systems where the main source of predation is different (e.g., lynx, *Lynx canadensis*; Krebs, Boonstra, and Boutin 2018), allowing for comparisons of dynamics among the core and periphery of the snowshoe hare's geographic range. Thus, an inclusive paradigm, rooted in the use of functional and stoichiometric traits, may be instrumental in accounting for both direct and indirect effects of consumers occupying different trophic positions in an ecosystem. In turn, this approach could help resolve a few more pieces of the ecosystem functioning puzzle and improve our ability to forecast the fate of key ecosystem functions and services at local and planetary spatial scales (Harfoot et al. 2014).

5.2 A multi-currency approach to ecosystem ecology

Developing and adopting an inclusive, trait-based paradigm that re-evaluates the influences of consumers in the ecology of ecosystems entails a wider shift in perspective—from single- to multi-currency approaches. Single-currency approaches focus on one resource that links individuals to ecosystems and limits their biological activities; energy being the most common (Brown et al. 2004). Indeed, single-currency approaches can lead to resolving patterns that span scales of biological organization, such as the well-known ¾ scaling of metabolic rate to body size (Brown et al. 2004) that underlies a host of other allometric relationships (Carbone et al. 1999; Tucker, Ord, and Rogers 2014; Rizzuto, Carbone, and Pawar 2018). However, a single-currency framework compresses much of the inherent complexity arising from the interactions of multiple resources and from their effects on organisms (e.g., energy, elements, information; Marleau et al. 2020). Importantly, a single-currency approach also implies that the same currency is the sole limiting factor across widely different biological activities and ecosystem processes—whereas evidence shows that different limiting currency may be species- or landscape-specific (e.g., Chapter 3; Sterner and Elser 2002; Sterner 2004). In turn, this limits investigation of processes involving other currencies whose qualities differ from energy (e.g., nutrient cycling; Sterner 2004), as well as of the relationships among different currencies (but see Marleau et al. 2020).

The trade-off between simplicity and complexity that underlies the switch from a single- to multi-currency approaches can lead to unveiling new generalities, such as the relatively consistent Carbon:Nitrogen:Phosphorus ratio of the world oceans (Sterner and Elser 2002), the nutrient limitation of food webs (Boersma et al. 2008), or the latitudinal patterns in the stoichiometric ratios of autotrophs (Borer et al. 2013; Martiny et al. 2013; Galbraith and Martiny 2015). Indeed, examples of multi-currency approaches already exist in ecology, particularly among empirical subdisciplines (Sterner and Elser 2002; Raubenheimer 2011). For instance, nutritional geometry, which investigates the connections between physiology and behavioural ecology, developed alongside and complements ecological stoichiometry, instead focused on physiology and biogeochemistry (Sperfeld et al. 2016). Rooted into the multiple currencies of dietary macromolecules, e.g., carbohydrates, proteins, lipids, nutritional geometry has led to key insights into the foraging process of multiple animal species—from those of conservation interest (e.g., the giant panda, *A. melanoleuca*; Nie et al. 2015) to those that are regarded as pests in certain parts of the world (e.g., the Chacma baboon, *Papio ursinus*; Johnson et al. 2013).

Multi-currency approaches are instrumental to bridge techniques and disciplines, for instance, as proposed in a recent roadmap to guide empirical assessment of animal-vectored nutrient subsidies (Ellis-Soto et al. 2021). Based on processes of interests identified using a meta-ecosystem model, the roadmap integrates biogeochemical, stoichiometric, remote sensing, macroecological, and statistical techniques (Ellis-Soto et al. 2021). Importantly, this roadmap also combines multiple currencies, suggesting that integration of energy- and element-based techniques may produce highly detailed explorations of animal-vectored subsidies (e.g., Figure 2 in Ellis-Soto et al. 2021). Initial examples of the insights this type of approach could lead to include, for instance, recent studies integrating behavioural and stoichiometric currencies to investigate the space use of moose (*A. alces*; Balluffi-Fry, Leroux, Wiersma, Heckford, et al. 2020). This fine-scale investigation revealed individual trade-offs that led to different moose adopting either quantity- or quality-maximizing strategies while foraging, and modifying their movement paths accordingly (Balluffi-Fry, Leroux, Wiersma, Heckford, et al. 2020). In turn, this individual variability may influence ecosystem processes and functions, as moose are an important terrestrial-freshwater link in boreal ecosystems (Bump, Tischler, et al. 2009). Similarly, in a study of the influence of trophic cascades on ecosystem functioning, adopting a multi-currency approach tracking both carbon isotopes and organismal biomass allowed for resolving the biogeochemical footprint of predators' non-consumptive effects on ecosystem carbon sequestration (Strickland et al. 2013).

In addition to empirical studies employing multidisciplinary, multi-currency frameworks, theoretical tools are starting to appear that investigate multiple currencies, their relationships, and their ecosystem effects. For instance, a recent ecosystem model combined energy, elements, and information to investigate how the continuous conversions among these three currencies that take place in ecosystems influence trophic and non-trophic interactions (Marleau et al. 2020). Importantly, this proposed multi-currency model allows for tracking changes in the system's emerging properties by using the same mathematical scaffolding as previous ecosystem models (Marleau et al. 2020). Incorporating this multi-currency approach into the meta-ecosystem model presented in Chapter 4 could help disentangle scales and timing of information exchanges crucial to, e.g., animal ecology (e.g., home range formation; Powell and Mitchell 2012; Spencer 2012), or simulate the consequences of artificially introduced amounts of a currency on both organismal and ecosystem processes (e.g., light, sound, and chemical pollution; see review in Little et al. *in review*).

Other than in a meta-ecological framework, multi-currency approaches may be able to improve our assessment of the disparate alterations of natural processes, pathways, and relationships triggered by anthropogenic activities. By variously introducing, sequestering, and consuming energy, matter, and information, humankind has been changing natural systems in ways that go beyond mere alterations of resource availability and distribution (Marleau et al. 2020). Humankind has been changing not only the non-random arrangement of these currencies in space and time, but also their relationships and interplay (Little et al. *in review*). Indirect effects of anthropogenic activities abound, from altering habitat connectivity (Haddad et al. 2015; Tucker, Böhning-Gaese, et al. 2018), to changing natural cycles (Bernhardt, O'Connor, et al. 2020), to disrupting information pathways (Sanders et al. 2021). In the context of rapidly increasing anthropogenic modifications of the biosphere, developing realistic, multi-faceted theoretical tools to inform empirical research and mitigation strategies is urgently needed.

5.3 Conclusions

In my thesis, I investigate the role of terrestrial consumers in ecosystem functioning, using a multi-disciplinary and multi-currency approach that merges an empirical case study with theoretical modeling. I began by describing the ecological stoichiometry of a keystone boreal herbivore, the snowshoe hare (*L. americanus*). I demonstrated that a set of invertebrate-derived predictors does not explain much of the higher-than-expected intraspecific variability I observed in this terrestrial mammal, leading me to investigate other possible factors. Using data from the same study system, I then investigated the response of snowshoe hares to intraspecific variability in the stoichiometry of their preferred forage. I found that snowshoe hares change their space use as key stoichiometric traits of their preferred forage varied in space, with hares having larger home ranges in areas of lower or more variable food content of nitrogen or phosphorus. The combined insights of high intraspecific variability in snowshoe hare ecological stoichiometry and their response to spatial variation in food elemental content led me to question whether consumers moving over the landscape can influence ecosystem processes and services. Thus, I developed a mathematical model of a meta-ecosystem, introducing a new framework to account for the multiple ways consumers traverse landscapes. I found that how consumers move over the landscape can strongly influence ecosystem functioning a multiple spatial scales, changing the biomass accumulation, productivity, and nutrient cycling profiles of local and meta-ecosystems. Taken together, my results demonstrate that expanding existing ecological frameworks to account for the role of consumers in mediating both biogeochemical cycles and ecosystem functioning can lead to unexpected, unintuitive insights into the processes and functions of these systems.

Throughout my thesis, I additionally provide evidence that chemical elements and stoichiometric traits offer a powerful unifying lens through which to investigate the myriad interactions among organic and inorganic components of ecosystems. Shared among consumers and resources, stoichiometric traits allow for describing different ecosystem compartments and measuring ecological metrics of interest using the same units of measurement—with potential benefits for comparability and reproducibility of studies, as well as transferability and collaboration across study systems. Furthermore, stoichiometric traits complement energy-based approaches, opening the way for multi-currency investigation—both empirical and theoretical—of ecosystems' functioning and emerging properties. Thus, my thesis also provides support to the development of multi-currency approaches to investigating ecosystem dynamics.

Overall, my thesis offers a two-pronged approach rooted in shared units of measurements and system-agnostic tools to address emerging questions in ecosystem ecology and meta-ecology. The two prongs—developing a consumer-aware ecosystem ecology paradigm and adopting multi-currency, system-agnostic approaches to explore ecosystem functioning—are well-positioned to integrate and expand the scope of meta-ecological and Earth-system models, which will be key to predict and address the fate of ecosystems and of the planet as the Anthropocene unfolds.

5.4 References

Balluffi-Fry, J., S. J. Leroux, Y. F. Wiersma, T. R. Heckford, et al. (2020). “Quantity-quality trade-offs revealed using a multiscale test of herbivore resource selection on elemental landscapes”. *Ecology and Evolution* 10.24, pp. 13847–13859. DOI: `10.1002/ece3.6975`.

Balluffi-Fry, J., S. J. Leroux, Y. F. Wiersma, I. C. Richmond, et al. (2021). “Integrating plant stoichiometry and feeding experiments: state-dependent forage choice and its implications on body mass”. *Oecologia*. DOI: `10.1007/s00442-021-05069-5`.

Bernhardt, E. S., J. R. Blaszczak, et al. (2017). “Control Points in Ecosystems: Moving Beyond the Hot Spot Hot Moment Concept”. *Ecosystems* 20.4, pp. 665–682. DOI: `10.1007/s10021-016-0103-y`.

Bernhardt, J. R., M. I. O’Connor, et al. (2020). “Life in fluctuating environments”. *Philosophical Transactions of the Royal Society B: Biological Sciences* 375.1814, p. 20190454. DOI: `10.1098/rstb.2019.0454`.

Boersma, M. et al. (2008). “Nutritional limitation travels up the food chain”. *International Review of Hydrobiology* 93, pp. 479–488. DOI: `10.1002/iroh.200811066`.

Borer, E. T. et al. (2013). “Global biogeography of autotroph chemistry: is insolation a driving force?” *Oikos* 122.8, pp. 1121–1130. DOI: `10.1111/j.1600-0706.2013.00465.x`.

Brown, J. H. et al. (2004). “Toward a Metabolic Theory of Ecology”. *Ecology* 85.7, pp. 1771–1789. DOI: `10.1890/03-9000`.

Bump, J. K. (2018). “Fertilizing riparian forests: nutrient repletion across ecotones with trophic rewilding”. *Philosophical Transactions of the Royal Society B: Biological Sciences* 373.1761, p. 20170439. DOI: `10.1098/rstb.2017.0439`.

Bump, J. K., R. O. Peterson, and J. A. Vucetich (2009). “Wolves modulate soil nutrient heterogeneity and foliar nitrogen by configuring the distribution of ungulate carcasses”. *Ecology* 90.11, pp. 3159–3167. DOI: `10.1890/09-0292.1`.

Bump, J. K., K. B. Tischler, et al. (2009). “Large herbivores and aquatic-terrestrial links in southern boreal forests”. *Journal of Animal Ecology* 78.2, pp. 338–345. DOI: `10.1111/j.1365-2656.2008.01498.x`.

Bump, J. K., C. R. Webster, et al. (2009). “Ungulate carcasses perforate ecological filters and create biogeochemical hotspots in forest herbaceous layers allowing trees a competitive advantage”. *Ecosystems* 12.6, pp. 996–1007. DOI: `10.1007/s10021-009-9274-0`.

Carbone, C. et al. (1999). “Energetic constraints on the diet of terrestrial carnivores”. *Nature* 402.6759, pp. 286–288. DOI: `10.1038/46266`.

Currie, W. S. (2011). “Units of nature or processes across scales? The ecosystem concept at age 75”. *New Phytologist* 190.1, pp. 21–34. DOI: `10.1111/j.1469-8137.2011.03646.x`.

DeAngelis, D. (1992). *Dynamics of Nutrient Cycling and Food Webs*. 1st ed. Springer Netherlands, p. 288. DOI: `10.1007/978-94-011-2342-6`.

Dodds, D. G. (1960). “Food Competition and Range Relationships of Moose and Snowshoe hare in Newfoundland”. *The Journal of Wildlife Management* 24 (1), pp. 52–60. DOI: `10.2307/3797356`.

Doughty, C. E. (2017). “Herbivores increase the global availability of nutrients over millions of years”. *Nature Ecology & Evolution* 1.12, pp. 1820–1827. DOI: `10.1038/s41559-017-0341-1`.

Doughty, C. E. et al. (2016). “Global nutrient transport in a world of giants”. *Proceedings of the National Academy of Sciences of the United States of America* 113.4, pp. 868–873. DOI: `10.1073/pnas.1502549112`.

Ellis-Soto, D. et al. (2021). “A methodological roadmap to quantify animal-vectored spatial ecosystem subsidies”. *Journal of Animal Ecology* 90.7, pp. 1605–1622. DOI: `10.1111/1365-2656.13538`.

Enquist, B. J. et al. (2020). “The megabiota are disproportionately important for biosphere functioning”. *Nature Communications* 11.1, p. 699. DOI: `10.1038/s41467-020-14369-y`.

Felton, A. M. et al. (2018). “The complexity of interacting nutritional drivers behind food selection, a review of northern cervids”. *Ecosphere* 9 (5). DOI: `10.1002/ecs2.2230`.

Fronhofer, E. A., T. Hovestadt, and H.-J. Poethke (2013). “From random walks to informed movement”. *Oikos* 122.6, pp. 857–866. DOI: `10.1111/j.1600-0706.2012.21021.x`.

Galbraith, E. D. and A. C. Martiny (2015). “A simple nutrient-dependence mechanism for predicting the stoichiometry of marine ecosystems”. *Proceedings of the National Academy of Sciences of the United States of America* 112 (27), p. 201423917. DOI: `10.1073/pnas.1423917112`.

Gounand, I. et al. (2018). “Meta-Ecosystems 2.0: Rooting the Theory into the Field”. *Trends in Ecology & Evolution* 33.1, pp. 36–46. DOI: `10.1016/j.tree.2017.10.006`.

Haddad, N. M. et al. (2015). “Habitat fragmentation and its lasting impact on Earth’s ecosystems”. *Science Advances* 1.2, pp. 1–10. DOI: `10.1126/sciadv.1500052`.

Harfoot, M. B. J. et al. (2014). “Emergent Global Patterns of Ecosystem Structure and Function from a Mechanistic General Ecosystem Model”. *PLoS Biology* 12.4. DOI: `10.1371/journal.pbio.1001841`.

Harvey, E. et al. (2021). “A general meta-ecosystem model to predict ecosystem function at landscape extents”. DOI: `10.22541/au.162799968.80128369/v1`.

Hawlena, D. and O. J. Schmitz (2010). “Herbivore physiological response to predation risk and implications for ecosystem nutrient dynamics”. *Proceedings of the National Academy of Sciences of the United States of America* 107.35, pp. 15503–15507. DOI: `10.1073/pnas.1009300107`.

Hoeks, S. et al. (2020). “Mechanistic insights into the role of large carnivores for ecosystem structure and functioning”. *Ecography* 43.12, pp. 1752–1763. DOI: `10.1111/ecog.05191`.

Holdo, R. M., R. D. Holt, et al. (2011). “Migration impacts on communities and ecosystems: empirical evidence and theoretical insights”. In: *Animal Migration*. Ed. by E. J. Milner-Gulland, J. M. Fryxell, and A. R. E. Sinclair. Oxford: Oxford University Press. Chap. Chapter 9, pp. 130–143. DOI: `10.1093/acprof:oso/9780199568994.003.0009`.

Holdo, R. M., A. R. Sinclair, et al. (2009). "A disease-mediated trophic cascade in the Serengeti and its implications for ecosystem C". *PLoS Biology* 7.9. DOI: `10.1371/journal.pbio.1000210`.

Johnson, C. A. et al. (2013). "30 Days in the Life: Daily Nutrient Balancing in a Wild Chacma Baboon". *PLoS One* 8.7. Ed. by T. Deschner, e70383. DOI: `10.1371/journal.pone.0070383`.

Krebs, C. J., R. Boonstra, and S. Boutin (2018). "Using experimentation to understand the 10-year snowshoe hare cycle in the boreal forest of North America". *Journal of Animal Ecology* 87.1. Ed. by K. Wilson, pp. 87–100. DOI: `10.1111/1365-2656.12720`. eprint: `0608246v3`.

Laundré, J. W. et al. (2014). "The landscape of fear: the missing link to understand top-down and bottom-up controls of prey abundance?" *Ecology* 95.5, pp. 1141–1152. DOI: `10.1890/13-1083.1`.

Leal, M., O. Seehausen, and B. Matthews (2017). "The ecology and evolution of stoichiometric phenotypes". *Trends in Ecology & Evolution* 32.2, pp. 108–117. DOI: `10.1016/j.tree.2016.11.006`.

Leroux, S. J., L. Charron, et al. (2021). "Cumulative effects of spruce budworm and moose herbivory on boreal forest ecosystems". *Functional Ecology* 35.7, pp. 1448–1459. DOI: `10.1111/1365-2435.13805`.

Leroux, S. J., D. Hawlena, and O. J. Schmitz (2012). "Predation risk, stoichiometric plasticity and ecosystem elemental cycling". *Proceedings of the Royal Society B Biological Sciences* 279.1745, pp. 4183–4191. DOI: `10.1098/rspb.2012.1315`.

Leroux, S. J. and M. Loreau (2010). "Consumer-mediated recycling and cascading trophic interactions". *Ecology* 91.7, pp. 2162–2171. DOI: `10.1890/09-0133.1`.

Leroux, S. J. and O. J. Schmitz (2015). "Predator-driven elemental cycling: the impact of predation and risk effects on ecosystem stoichiometry". *Ecology and Evolution* 5.21, pp. 4976–4988. DOI: `10.1002/ece3.1760`.

Leroux, S. J., E. Vander Wal, et al. (2017). “Stoichiometric distribution models: ecological stoichiometry at the landscape extent”. *Ecology Letters* 20 (12), pp. 1495–1506. DOI: `10.1111/ele.12859`.

Leroux, S. J., Y. F. Wiersma, and E. Vander Wal (2020). “Herbivore Impacts on Carbon Cycling in Boreal Forests”. *Trends in Ecology & Evolution* 35.11, pp. 1001–1010. DOI: `10.1016/j.tree.2020.07.009`.

Lima, S. L. and P. A. Zollner (1996). “Towards a behavioral ecology of ecological landscapes”. *Trends in Ecology & Evolution* 11 (3), pp. 131–135. DOI: `10.1016/0169-5347(96)81094-9`.

Little, C. J. et al. (*in review*). “Filling the Information Gap in Meta-Ecosystem Ecology”. *Oikos*. manuscript id: OIK-08892.R1. EcoEvoRxiv preprint. DOI: `10.32942/osf.io/hc83u`.

Loreau, M. (2010). *From populations to ecosystems: Theoretical foundations for a new ecological synthesis*. Princeton University Press, p. 320. DOI: `10.1515/9781400834167`.

Loreau, M., N. Mouquet, and R. D. Holt (2003). “Meta-ecosystems: A theoretical framework for a spatial ecosystem ecology”. *Ecology Letters* 6.8, pp. 673–679. DOI: `10.1046/j.1461-0248.2003.00483.x`.

Marleau, J. N. et al. (2020). “Converting Ecological Currencies: Energy, Material, and Information Flows”. *Trends in Ecology & Evolution* 35.12, pp. 1068–1077. DOI: `10.1016/j.tree.2020.07.014`.

Marsh, K. J. et al. (2014). “Feeding rates of a mammalian browser confirm the predictions of a ’foodscape’ model of its habitat”. *Oecologia* 174 (3), pp. 873–882.

Martiny, A. C. et al. (2013). “Strong latitudinal patterns in the elemental ratios of marine plankton and organic matter”. *Nature Geoscience* 6 (4), pp. 279–283. DOI: `10.1038/ngeo1757`.

Massol, F. et al. (2017). “How life-history traits affect ecosystem properties: effects of dispersal in meta-ecosystems”. *Oikos* 126.4, pp. 532–546. DOI: `10.1111/oik.03893`.

McNaughton, S. J. (1990). “Mineral nutrition and seasonal movements of African migratory ungulates”. *Nature* 345.6276, pp. 613–615. DOI: `10.1038/345613a0`.

McNaughton, S. J. et al. (1989). “Ecosystem-level patterns of primary productivity and herbivory in terrestrial habitats”. *Nature* 341, pp. 142–144. DOI: `10.1038/341142a0`.

Montgomery, R. A. et al. (2014). “Where Wolves Kill Moose: The Influence of Prey Life History Dynamics on the Landscape Ecology of Predation”. *PLoS One* 9.3, e91414. DOI: `10.1371/journal.pone.0091414`.

Nie, Y. et al. (2015). “Obligate herbivory in an ancestrally carnivorous lineage: The giant panda and bamboo from the perspective of nutritional geometry”. *Functional Ecology* 29 (1), pp. 26–34. DOI: `10.1111/1365-2435.12302`.

O’Connor, M. I. et al. (2019). “Principles of Ecology Revisited: Integrating Information and Ecological Theories for a More Unified Science”. *Frontiers in Ecology and Evolution* 7.June, pp. 1–20. DOI: `10.3389/fevo.2019.00219`.

Pastor, J., Y. Cohen, and N. T. Hobbs (2006). “The roles of large herbivores in ecosystem nutrient cycles”. In: *Large herbivore ecology. Ecosystem dynamics and conservation*. Ed. by K. Danell et al. Conservation Biology. Cambridge University Press, pp. 289–325. DOI: `10.1017/CBO9780511617461.012`.

Pastor, J., B. Dewey, et al. (1993). “Moose Browsing and Soil Fertility in the Boreal Forests of Isle Royale National”. *Ecology* 74.2, pp. 467–480. DOI: `10.2307/1939308`.

Pastor, J. and R. J. Naiman (1992). “Selective Foraging and Ecosystem Processes in Boreal Forests”. *The American Naturalist* 139.4, pp. 690–705. DOI: `10.1086/285353`.

Powell, R. A. and M. S. Mitchell (2012). “What is a home range?” *Journal of Mammalogy* 93 (4), pp. 948–958. DOI: `10.1644/11-MAMM-S-177.1`.

Raubenheimer, D. (2011). “Toward a quantitative nutritional ecology: the right-angled mixture triangle”. *Ecological Monographs* 81.3, pp. 407–427. DOI: `10.1890/10-1707.1`.

Richmond, I. C. et al. (2021). “Individual snowshoe hares manage risk differently: Integrating stoichiometric distribution models and foraging ecology.” *Journal of Mammalogy*. Accepted, manuscript id: JMAMM–2021–026.R2.

Rizzuto, M., C. Carbone, and S. Pawar (2018). “Foraging constraints reverse the scaling of activity time in carnivores”. *Nature Ecology & Evolution* 2.2, pp. 247–253. DOI: `10.1038/s41559-017-0386-1`.

Rosell, F. et al. (2005). “Ecological impact of beavers castor fiber and castor canadensis and their ability to modify ecosystems”. *Mammal Review* 35.3-4, pp. 248–276. DOI: `10.1111/j.1365-2907.2005.00067.x`.

Sanders, D. et al. (2021). “A meta-analysis of biological impacts of artificial light at night”. *Nature Ecology & Evolution* 5.1, pp. 74–81. DOI: `10.1038/s41559-020-01322-x`.

Schiesari, L. et al. (2019). “Towards an applied metaecology”. *Perspectives in Ecology and Conservation* 17.4, pp. 172–181. DOI: `10.1016/j.pecon.2019.11.001`.

Schmitz, O. J., D. Hawlena, and G. C. Trussell (2010). “Predator control of ecosystem nutrient dynamics”. *Ecology Letters* 13.10, pp. 1199–1209. DOI: `10.1111/j.1461-0248.2010.01511.x`.

Schmitz, O. J. and S. J. Leroux (2020). “Food Webs and Ecosystems: Linking Species Interactions to the Carbon Cycle”. *Annual Review of Ecology, Evolution, and Systematics* 51.1, pp. 271–295. DOI: `10.1146/annurev-ecolsys-011720-104730`.

Schmitz, O. J., J. R. B. Miller, et al. (2017). “Toward a community ecology of landscapes: predicting multiple predator-prey interactions across geographic space”. *Ecology* 98.9, pp. 2281–2292. DOI: `10.1002/ecy.1916`. eprint: `0608246v3`.

Schmitz, O. J., P. A. Raymond, et al. (2014). “Animating the carbon cycle”. *Ecosystems* 17.2, pp. 344–359. DOI: `10.1007/s10021-013-9715-7`.

Schmitz, O. J., C. C. Wilmers, et al. (2018). “Animals and the zoogeochemistry of the carbon cycle”. *Science* 362 (6419), eaar3213. DOI: `10.1126/science.aar3213`.

Schradin, C. et al. (2010). “Female home range size is regulated by resource distribution and intraspecific competition: a long-term field study”. *Animal Behaviour* 79.1, pp. 195–203. DOI: `10.1016/j.anbehav.2009.10.027`.

Spencer, W. D. (2012). “Home ranges and the value of spatial information”. *Journal of Mammalogy* 93.4, pp. 929–947. DOI: `10.1644/12-MAMM-S-061.1`.

Sperfeld, E. et al. (2016). “Bridging Ecological Stoichiometry and Nutritional Geometry with homeostasis concepts and integrative models of organism nutrition”. *Functional Ecology*, pp. 1–11. DOI: `10.1111/1365-2435.12707`.

Sterner, R. W. (2004). “A one-resource ”stoichiometry””. *Ecology* 85 (7), pp. 1813–1816. URL: `https://www.jstor.org/stable/3450351`.

Sterner, R. W. and J. J. Elser (2002). *Ecological stoichiometry: the biology of elements from molecules to the biosphere*. 1st ed. Princeton University Press, p. 464. URL: `https://www.jstor.org/stable/j.ctt1jktrp3`. Accessed 26 July 2021.

Strickland, M. S. et al. (2013). “Trophic cascade alters ecosystem carbon exchange”. *Proceedings of the National Academy of Sciences of the United States of America* 110.27, pp. 11035–11038. DOI: `10.1073/pnas.1305191110`.

Subalusky, A. L. et al. (2018). “Organic matter and nutrient inputs from large wildlife influence ecosystem function in the Mara River, Africa”. *Ecology* 99.11, pp. 2558–2574. DOI: `10.1002/ecy.2509`.

Tucker, M. A., K. Böhning-Gaese, et al. (2018). “Moving in the Anthropocene: Global reductions in terrestrial mammalian movements”. *Science* 359.6374, pp. 466–469. DOI: `10.1126/science.aam9712`.

Tucker, M. A., T. J. Ord, and T. L. Rogers (2014). “Evolutionary predictors of mammalian home range size: Body mass, diet and the environment”. *Global Ecology and Biogeography* 23 (10), pp. 1105–1114. DOI: `10.1111/geb.12194`.

Wirsing, A. J. et al. (2021). “The context dependence of non-consumptive predator effects”. *Ecology Letters* 24.1. Ed. by J. Chase, pp. 113–129. DOI: `10.1111/ele.13614`.

Appendices

APPENDIX A

Supplementary Information for Chapter 2: Patterns and potential drivers of intraspecific variability in the body C, N, P composition of a terrestrial consumer, the snowshoe hare (*Lepus americanus*)

A.1 Introduction

This appendix contains supplementary information on the rationale, data collection and analyses, and model selection for our study of the ecological stoichiometry of snowshoe hares (*L. americanus*) and its drivers. In Appendix A.2, we provide additional predictions for the influence of age, sex, and body size or conditions on the values of the stoichiometric ratios measured from our sample animals. Appendix A.3 describes our data collection protocol in more detail, focusing on the methods use to collect morphometric data (Appendix A.3.1), determine the age of hares in our sample (Appendix A.3.2), identify their sex (Appendix A.3.3), calculate the Scaled Mass Index (Appendix A.3.4), and on the methods used to asses intra-individual variability (Appendix A.3.5) and to calculate stoichiometric ratios (Appendix A.3.6). In Appendix A.4, we provide additional details on our Variance Inflation Factor analysis. Appendix A.5 describes in detail the process and rationale for removing uninformative parameters from our models, and provides full AICc model selection tables (Tables A.4 to A.15). Finally, in Appendix A.6 and Appendix A.7 we provide additional figures and tables, respectively.

A.2 Ratios Predictions

Based on snowshoe hare ecology, we predict that (1) older snowshoe hares would have lower C:N, C:P, and N:P than younger ones due to the larger size of their skeleton and muscle mass. We also predict that (2) male snowshoe hares would have higher C:N, C:P, and N:P than females due to their lower reproductive costs. Finally, for body size and condition, we predict (3) hares in better conditions to have lower C:N, C:P, and N:P than those in worse condition.

A.3 Data Collection

In this section, we provide details on the laboratory protocols we used to obtain data on morphology, age, sex, and body condition of the snowshoe hares in our sample. We additionally provide details on the protocols used to assess intra-individual stoichiometric variation and how we calculated molar weights and elemental ratios. At AFL, the limit of detection (henceforth, LOD) for C and N from plant or other organic material is 0.02% (N. Schrier, *personal communication*), determined using a reagent blank (i.e., the tin capsule) and calculated as:

$$LOD = 3 \times standard\ deviation\ of\ 10\ replicates \tag{A.1}$$

For P, the method detection limit is 12 ppm with a reporting limit of 100 ppm, obtained using the digestion solution as a reagent blank (CWA Methods Team 2016).

A.3.1 Morphometric Data

Following Peig and Green (2009)'s recommendation of testing a range of different length measurements before selecting the one used in the Scaled Mass Index calculations, from each of our 50 snowshoe hares we collected four different length measurements. These were total body length, left hind foot length, skull length and skull width. We measured total body length from the tip of the nose to the anus. We measured the left hind foot from the knee joint to the tip of the nail of the middle finger, while pressing down the foot and spreading the fingers. As for the skull measurements, we took length as the distance between the tip of the nose and the base of the skull and width as the width at the cheekbones. We took each measurement to the nearest 0.1 mm and repeated each measurement three times. We collected and handled data from our laboratory processing in digital format, by using a digital collection form (FileMaker Pro v. 14.0, Claris International Inc. 2015) on an iPad Mini 2 (Apple Inc., Cupertino, CA), thus removing the potential error-prone step of transferring information from physical data collection forms to digital spreadsheets.

A.3.2 Age Determination

Ageing snowshoe hares can be difficult, as their teeth grow continuously throughout their lives. Hence, traditional cementum-based ageing techniques are not available for this species. We used a mixed approach that involved combining an ageing method developed by Iason (1988) for for mountain hares (*Lepus timidus*) and standard histological procedures for examining bone sections.

For each of our 50 snowshoe hares, we extracted the complete mandibular bone. We carefully cleaned it both by hand, removing as much soft tissue as possible before drying the bones out and storing them in desiccators to prevent mold formation. To further clean each bone, we let carrion beetles (family: Dermestidae) digest all remaining soft tissue over a period of two weeks and until the bone was completely clean. Each bone was individually tagged with its specimen's ID before beetle digestion. Once we cleaned all 50 bones, we shipped them to Matson's Laboratory (Manhattan, MT, USA) for age determination.

Here, mandible specimens were prepared for histological examination following standard procedure. Each sample was decalcified in a weak acidic solution, then embedded in a paraffin block to allow sectioning at 14 µm using a microtome. We used Iason (1988) as a guideline to choose the location of the section. The resulting section was mounted, stained, coverslipped, and examined for age determination under magnification (Figures A.6 and A.7).

A.3.3 Sex Determination

Genetic sex determination followed the protocol detailed by Shaw, Wilson, and White (2003). This protocol uses mammal-specific primers that amplify an intron region of the zinc-finger regions of the X and Y chromosomes. For snowshoe hares in this study, these regions weighted approximately 1500 bp in female (*ZFNx*) and 950 bp in males (*ZFNy*). Since no complete genome sequence exists for snowshoe hare yet, we used a set of primers widely used in mammalian genetic sex determination by Shaw, Wilson, and White (2003).

The PCR used a reaction volume of 25 µL with 1 µL each of the forward and reverse primers and 10 µL of 2X Promega PCR Master Mix. The PCR consisted of one 5-minutes cycle at 95 °C. This was followed by a sequence of 30 s at 94 °C, 60 s at 52 °C, and 60 s at 72 °C, which was repeated for 35 cycles before a final cycle at 72 °C for 2 minutes. The end product was held at 4 °C before being electrophoresed on a 1.5% agarose gel in 1X TBE. The Genomics and Proteomics Laboratory at Memorial University of Newfoundland performed all DNA-based analyses and determined the sex of the individuals.

A.3.4 Scaled Mass Index Calculation

Multiple indices of body condition exist which differ in both how they define "body condition" and in how they calculate it (Peig and Green 2010). Most indices fall in one of three categories: ratios, whose units are often difficult to interpret; residuals, computed using units of mass; or non-dimensional indices (Stevenson and Woods 2006). Recent evidence also suggests that multiple regression, while not an index *per se*, provides a valuable alternative (Labocha, Schutz, and Hayes 2014). As the debate surrounding BCIs is ongoing, no clear "best" index emerged so far, and the decision on which one to apply to one's work is often heavily dependent on the history and traditions of a certain subfield of ecology (Stevenson and Woods 2006; Peig and Green 2010). In our study, we used the Scaled Mass Index developed by Peig and Green (2009).

We computed the Scaled Mass Index (SMI) following the procedure detailed by Peig and Green (2009), which consists of three steps: (1) investigate which body length measurement (L) has the strongest relationship with body weight (M) using bivariate plots, (2) fit a Standardized Major Axis (SMA) regression to the ln-transformed bivariate plots, and (3) calculate the SMI using the scaling exponent of the SMA (b_{SMA}) from the strongest length-weight relationship identified earlier and a Thorpe-Lleonart scaling model (see main text for details). We began by producing bivariate plots for each of the four length measurements we collected from our specimens (Figure A.1). From visual inspection, both average left hind foot length (HFL) and average skull length appeared to have a strong relationship with body weight. HFL also correlated strongly with average body length (ABL), as well as allowing us to compare our results with other published studies. Thus, we chose to proceed using HFL. We then used the function `sma` in R package `smatr` (Warton et al. 2012) to fit a SMA to the ln-transformed values of HFL and body weight. Finally, we extracted the slope value (b_{SMA}) and computed the SMI using Peig and Green's equation (eq. 2.1).

As the SMI presents several individual components that may vary, we tested the sensitivity of our results to changes in the length measurement used to calculate it by running the analyses again using Skull Length instead of HFL. We obtained qualitatively similar results with this alternative measure of body size (Tables A.1 and A.2).

A.3.5 Intra-individual Stoichiometric Variability

Our study is one of the first to specifically assess intraspecific variability in the content of C, N, and P in a terrestrial vertebrate. As such, no precedent existed that could inform us as to whether our hares could show significant intra-individual variability in the concentrations of the three elements of interest or not. We addressed this issue in two ways.

First, during our laboratory sample collection, we randomly selected five individuals. For each of these specimens, we collected three separate samples of the homogeneous paste resulting from our homogenization process. These three samples were identified with a progressive letter appended to their individual identifier (e.g., "TCH037_A", "TCH037_B", "TCH037_C") and underwent the same drying, hand-grinding, weighting, storing, and analysis protocol as the rest of the samples. Thus, along the 50 samples we sent to the Agriculture and Food Laboratory at the University of Guelph, we sent 10 additional samples, 2 each for specimens TCH037, TCH040, TCH042, TCH045, and TCH048. Second, at AFL, lab technicians ran the analyses in triplicate on each sample, providing us with a quantitative assessment of within-sample variability. We adopted this approach because pilot analyses performed at AFL on a subset of samples indicated that %C and %N had a potentially higher intra-individual variability than %P. For %P, we nonetheless ran 5 samples in duplicate as part of AFL's internal quality assurance protocol. The raw data we received from AFL are available online as a separate dataset and shown in Figures A.2 and A.3. None of our samples presented strong intra-individual variability in the content of C and N, so we averaged the three %C and %N values we received from each sample in subsequent analyses. As for the samples we submitted to AFL in triplicate, we computed the grand mean (mean of the mean) of the values of %C and %N, and then used these values in the analyses.

A.3.6 Obtaining Molar Weights and Elemental Ratios

To obtain molar and stoichiometric ratios for the three elements of interest, we converted the original percentage data into weight of each element. To do this, we first calculated the dry body weight of each snowshoe hare in our sample as:

$$\frac{Sample\ Dry\ Weight}{Sample\ Wet\ Weight} : \frac{Hare\ Dry\ Weight}{Hare\ Wet\ Weight} \tag{A.2}$$

We then used the atomic weights for Carbon (C), Nitrogen (N), and Phosphorus (P) to calculate the corresponding molar ratios (Meija et al. 2016). We then computed the stoichiometric ratios by dividing the molar ratio of two elements and repeated this procedure for each pair of elements. As part of this process, we also calculated each hare's water content (in g) as:

$$\left(\frac{Sample\ Wet\ Weight - Sample\ Dry\ Weight}{Sample\ Wet\ Weight}\right) \times Hare\ Wet\ Weight \tag{A.3}$$

A.4 Variance Inflation Factor Analysis

We used Variance Inflation Factor analysis to investigate collinearity among the predictor variables included in our models. We tested for independence among our variables using a VIF threshold value of <3 (Yalcin and Leroux 2018). To do so, we used function `vifstep` in R package `usdm` (Naimi et al. 2014), and ran the analyses twice, once for each of the two length measurements used to calculated the SMI and K_n (see above, Appendix A.3.4). The results of the VIF analyses indicate that, when using HFL to calculate the SMI, average body length has a collinearity problem (i.e., VIF>3). We addressed this problem by never fitting a model containing K_n and ABL at the same time. In all other cases, no collinearity issues arise (Table A.3).

A.5 Model Selection

A.5.1 Removal of Uninformative Parameters

An uninformative parameter (or "pretending variable") is a variable that does not have a relationship with the response and does not improve a model's fit to the data (i.e., its log-likelihood) or does so only marginally but, based on its AICc value, is included in a model that is ranked close to models with informative parameters (Burnham and Anderson 2002; Arnold 2010; Leroux 2019). Reporting and interpretation of results from models including uninformative parameters is a widespread, yet unappreciated, issue in ecological literature (Leroux 2019). To avoid this issue, after fitting our set of models to each response variable, we reviewed the resulting AICc table and removed models including likely uninformative parameters. We followed Leroux (2019)'s decision tree to identify and deal with uninformative parameters in our model set. We report a summarized version of each response's AICc table in the main text. Below, we report the complete AICc tables for each response variable, with models that contained uninformative parameters highlighted.

When using left hind foot length to calculate the relative body condition (K_n), for %N, K_n, sex, and average body condition (ABL) were uninformative parameters (Table A.4). For %P, both sex and age behaved as pretending variables and we thus removed them from the final AICc table (Table A.5). For %C, all parameters were uninformative (Table A.6). For the C:N ratio, all variables other than age behaved as uninformative parameters (Table A.7). For C:P and N:P ratios, we found that all variables were uninformative parameters (Tables A.8 and A.9).

When using skull length as length measurement in the SMI formula to calculate the relative body condition (SkK_n; see eq. 2.1 in main text and above, Appendix A.3.4), for %N, all variables other than age proved to be uninformative parameters and we removed all models including them (Table A.10). For %P, we found that the age, sex, and relative body condition were uninformative parameters, and thus we removed them (Table A.11). For %C, we found all parameters to be pretending variables (Table A.12). For the C:N ratio, all variables other than age were uninformative parameters (Table A.13). For C:P and N:P ratios, we removed all models other than the null model, as all variables were uninformative (Tables A.14 and A.15).

A.6 Additional Tables

In this section, we provide supplementary tables. Table A.1 shows %C, %N, and %P results for models using skull length to calculate the Scaled Mass Index (SkK_n; see eq. 2.1 in main text and above, Appendix A.3.4). Likewise, Table A.2 shows results for C:N, C:P, and N:P ratios when using skull length to calculate the SMI. Table A.3 shows the results of our Variance Inflation Factor analysis. Tables A.4 to A.9 show full AICc model selection tables when using left hind foot length to calculate the relative body condition (K_n). Tables A.10 to A.15 show full AICc model selection tables for models including relative body condition calculated using skull length as length measurement in the SMI formula. Table A.16 compares the Observed body size range in our study sample with the Expected values for snowshoe hares, as well as that of several other species for which stoichiometric composition has been published. Finally, Table A.17 shows C, N, P body stoichiometry data for our species of interest, the snowshoe hares, together with data on a range of other taxonomic groups collected from published sources.

Table A.1: Top ranking GLMs for %C, %N, and %P based on ΔAICc, when Scale Mass Index and relative body condition (K_n) calculations are based on average skull length. Only the models that scored better than the null model are reported, together with the null model. k, number of parameters in a model, LL, log-likelihood, SkK_n, skull length-derived relative body condition, ABL, average total body length. Coefficient values are presented as estimate (±SE).

%N top models				**Coefficients**			
k	LL	ΔAICc	R^2	Intercept	Age	SkK_n	ABL
3	−56.599	0.000	0.066	11.367 (±0.141)	−0.160 (±0.087)		
2	−58.306	1.147	0.000	11.200 (±0.111)			

%P top models				**Coefficients**			
k	LL	ΔAICc	R^2	Intercept	Age	SkK_n	ABL
3	−36.252	0.000	0.047	0.687 (±1.495)			0.054 (±0.035)
2	−37.444	0.118	0.000	2.974 (±0.073)			

%C top models				**Coefficients**			
k	LL	ΔAICc	R^2	Intercept	Age	SkK_n	ABL
2	−118.090	0.000	0.000	43.606 (±0.367)			

Table A.2: Top ranking GLMs for C:N, C:P, and N:P values based on ΔAICc, when Scale Mass Index and relative body condition (K_n) calculations are based on average skull length. All specification as in Table A.1.

C:N top models				**Coefficients**			
k	LL	ΔAICc	R^2	Intercept	Age	SkK_n	ABL
3	−27.818	0.00	0.074	4.465 (±0.079)	0.095 (±0.049)		
2	−29.731	1.59	0.000	4.564 (±0.063)			
C:P top models				**Coefficients**			
k	LL	ΔAICc	R^2	Intercept	Age	SkK_n	ABL
2	−178.30	0.000	0.000	39.205 (±1.223)			
N:P top models				**Coefficients**			
k	LL	ΔAICc	R^2	Intercept	Age	SkK_n	ABL
2	−94.153	0.000	0.000	8.580 (±0.227)			

Table A.3: Results of the Variance Inflation Factor analysis run on the four explanatory variables included in the set of 22 GLMs fitted to the data. Note that no model included both Relative Body Condition (K_n) and Average Body Length (ABL). The $>$ 3 result for ABL when SMI, and hence K_n, is calculated from HFL is likely due to the stronger relationship between ABL and HFL than between ABL and Skull Length.

Variable	**Did it pass the VIF <3 test?**	
	SMI from HFL	SMI from Skull Length
K_n	2.504	2.101
Age	1.572	1.432
Sex	1.034	1.064
ABL	**3.225**	2.052

Table A.4: Full AICc table for the model set fitted to the %N data. Only one model performed better than the intercept-only (i.e., null) model. The table is sorted according to the smallest ΔAICc value. In this case, relative body condition (K_n) was calculated using left hind foot length (see main text). For each model, we report the number of parameters it estimates (k), its AICc and ΔAICc values, the model's Log-Likelihood (LL) and the model's fit to the data (R^2). Relative body condition (K_n), sex, and average body length (ABL) were uninformative parameters. Accordingly, we greyed-out all models including these variables.

Model	k	AICc	ΔAICc	LL	R^2
Age	3	119.721	0.000	−56.600	0.066
Intercept	2	120.868	1.147	−58.306	0.000
Age + K_n	4	121.194	1.473	−56.153	0.083
Age + ABL	4	121.735	2.014	−56.423	0.073
Age + Sex	4	122.076	2.355	−56.594	0.066
K_n	3	122.633	2.912	−58.055	0.010
ABL	3	122.985	3.264	−58.232	0.003
Sex	3	123.112	3.391	−58.295	0.000
Age + K_n + Age:K_n	5	123.473	3.753	−56.055	0.086
Age + K_n + Sex	5	123.632	3.911	−56.134	0.083
Age + ABL + Age:ABL	5	124.016	4.295	−56.326	0.076
Age + Sex + Age:Sex	5	124.193	4.472	−56.415	0.073
Age + ABL + Sex	5	124.196	4.475	−56.416	0.073
Sex + K_n	4	124.989	5.269	−58.050	0.010
Sex + ABL	4	125.335	5.614	−58.223	0.003
Age + K_n + Sex + Sex:K_n	6	125.762	6.041	−55.904	0.092
Age + K_n + Sex + Age:K_n	6	126.006	6.285	−56.026	0.087
Age + ABL + Sex + Sex:ABL	6	126.423	6.703	−56.235	0.080
Age + ABL + Sex + Age:ABL	6	126.594	6.873	−56.320	0.076
Sex + K_n + Sex:K_n	5	126.965	7.244	−57.801	0.020
Sex + ABL + Sex:ABL	5	127.730	8.009	−58.183	0.005
Age + K_n + Sex + Sex:K_n + Age:K_n	7	128.261	8.540	−55.797	0.096
Age + ABL + Sex + Sex:ABL + Age:ABL	7	129.038	9.317	−56.186	0.081

Table A.5: Full AICc table for the model set fitted to the %P data. Two models performed better than the intercept-only (i.e., null) model. Both include proxies for body size: relative body condition and average body length, respectively. Both sex and age were uninformative parameters. All specifications as in Table A.4.

Model	k	AICc	ΔAICc	LL	R^2
K_n	3	77.635	0.000	−35.556	0.073
ABL	3	79.026	1.391	−36.252	0.047
Intercept	2	79.144	1.509	−37.444	0.000
Sex + K_n	4	79.946	2.312	−35.529	0.074
Age + K_n	4	79.970	2.335	−35.540	0.073
Age + ABL	4	81.208	3.573	−36.159	0.050
Age	3	81.266	3.632	−37.372	0.003
Sex + ABL	4	81.393	3.758	−36.252	0.047
Sex	3	81.402	3.767	−37.440	0.000
Sex + K_n + Sex:K_n	5	82.328	4.693	−35.482	0.075
Age + K_n + Sex	5	82.400	4.765	−35.518	0.074
Age + K_n + Age:K_n	5	82.403	4.768	−35.519	0.074
Age + ABL + Age:ABL	5	82.905	5.270	−35.771	0.065
Sex + ABL + Sex:ABL	5	83.583	5.949	−36.110	0.052
Age + Sex	4	83.632	5.997	−37.372	0.003
Age + ABL + Sex	5	83.678	6.043	−36.157	0.050
Age + K_n + Sex + Sex:K_n	6	84.894	7.259	−35.470	0.076
Age + K_n + Sex + Age:K_n	6	84.938	7.303	−35.492	0.075
Age + Sex + Age:Sex	5	85.418	7.783	−37.027	0.017
Age + ABL + Sex + Age:ABL	6	85.492	7.858	−35.769	0.065
Age + ABL + Sex + Sex:ABL	6	86.045	8.410	−36.046	0.054
Age + K_n + Sex + Sex:K_n + Age:K_n	7	87.556	9.921	−35.445	0.077
Age + ABL + Sex + Sex:ABL + Age:ABL	7	87.733	10.098	−35.533	0.074

Table A.6: Full AICc table for the model set fitted to the %C data. No model performed better than the intercept-only (i.e., null) model. All parameters were uninformative. All other specifications as in Table A.4.

Model	k	AICc	ΔAICc	LL	R^2
Intercept	2	240.436	0.000	−118.090	0.000
Age	3	241.703	1.268	−117.591	0.020
K_n	3	242.340	1.905	−117.909	0.007
ABL	3	242.452	2.016	−117.965	0.005
Sex	3	242.484	2.048	−117.981	0.004
Age + K_n	4	243.820	3.384	−117.465	0.025
Age + Sex	4	243.959	3.523	−117.535	0.022
Age + ABL	4	244.070	3.635	−117.591	0.020
Sex + K_n	4	244.445	4.009	−117.778	0.012
Sex + ABL	4	244.624	4.188	−117.868	0.009
Sex + K_n + Sex:K_n	5	245.787	5.351	−117.211	0.035
Sex + ABL + Sex:ABL	5	245.986	5.551	−117.311	0.031
Age + K_n + Sex	5	246.150	5.714	−117.393	0.027
Age + K_n + Age:K_n	5	246.163	5.727	−117.399	0.027
Age + Sex + Age:Sex	5	246.197	5.761	−117.416	0.027
Age + ABL + Sex	5	246.433	5.997	−117.535	0.022
Age + ABL + Age:ABL	5	246.473	6.038	−117.555	0.021
Age + K_n + Sex + Sex:K_n	6	247.534	7.098	−116.790	0.051
Age + ABL + Sex + Sex:ABL	6	248.131	7.695	−117.089	0.039
Age + K_n + Sex + Age:K_n	6	248.576	8.140	−117.311	0.031
Age + ABL + Sex + Age:ABL	6	248.947	8.511	−117.497	0.023
Age + K_n + Sex + Sex:K_n + Age:K_n	7	250.083	9.647	−116.708	0.054
Age + ABL + Sex + Sex:ABL + Age:ABL	7	250.595	10.159	−116.964	0.044

Table A.7: Full AICc table for the model set fitted to the C:N data. The age-only model was the only one that performed better than the intercept-only (i.e., null) model. All other parameters were uninformative. All specifications as in Table A.4.

Model	k	AICc	ΔAICc	LL	R^2
Age	3	62.158	0.000	−27.818	0.074
Intercept	2	63.718	1.559	−29.731	0.000
Age + ABL	4	64.391	2.233	−27.751	0.076
Age + K_n	4	64.452	2.293	−27.781	0.075
Age + Sex	4	64.507	2.349	−27.809	0.074
ABL	3	65.587	3.428	−29.533	0.008
Sex	3	65.825	3.667	−29.652	0.003
K_n	3	65.982	3.823	−29.730	0.000
Age + ABL + Age:ABL	5	66.668	4.510	−27.652	0.080
Age + ABL + Sex	5	66.849	4.690	−27.743	0.076
Age + K_n + Sex	5	66.914	4.755	−27.775	0.075
Age + K_n + Age:K_n	5	66.926	4.768	−27.781	0.075
Age + Sex + Age:Sex	5	66.938	4.779	−27.787	0.075
Sex + ABL	4	67.820	5.661	−29.465	0.011
Sex + K_n	4	68.192	6.033	−29.652	0.003
Age + ABL + Sex + Age:ABL	6	69.238	7.080	−27.642	0.080
Age + ABL + Sex + Sex:ABL	6	69.419	7.261	−27.733	0.077
Age + K_n + Sex + Sex:K_n	6	69.478	7.320	−27.762	0.076
Age + K_n + Sex + Age:K_n	6	69.503	7.345	−27.775	0.075
Sex + ABL + Sex:ABL	5	70.121	7.963	−29.379	0.014
Sex + K_n + Sex:K_n	5	70.657	8.498	−29.646	0.003
Age + ABL + Sex + Sex:ABL + Age:ABL	7	71.892	9.733	−27.613	0.081
Age + K_n + Sex + Sex:K_n + Age:K_n	7	72.191	10.033	−27.762	0.076

Table A.8: Full AICc table for the model set fitted to the C:P data. No model performed better than the intercept-only (i.e., null) model. All parameters were uninformative. All specifications as in Table A.4.

Model	k	AICc	ΔAICc	LL	R^2
Intercept	2	360.864	0.000	−178.304	0.000
K_n	3	361.583	0.719	−177.531	0.030
ABL	3	361.821	0.957	−177.650	0.026
Age	3	363.107	2.243	−178.293	0.000
Sex	3	363.111	2.247	−178.294	0.000
Sex + K_n	4	363.897	3.033	−177.504	0.032
Age + K_n	4	363.950	3.086	−177.531	0.030
Age + ABL	4	363.970	3.106	−177.541	0.030
Sex + ABL	4	364.182	3.318	−177.646	0.026
Age + Sex	4	365.460	4.596	−178.285	0.001
Age + ABL + Age:ABL	5	365.689	4.825	−177.163	0.045
Sex + ABL + Sex:ABL	5	366.249	5.385	−177.443	0.034
Age + K_n + Age:K_n	5	366.294	5.430	−177.465	0.033
Sex + K_n + Sex:K_n	5	366.351	5.487	−177.494	0.032
Age + K_n + Sex	5	366.371	5.507	−177.504	0.032
Age + ABL + Sex	5	366.425	5.561	−177.531	0.030
Age + Sex + Age:Sex	5	367.688	6.824	−178.162	0.006
Age + ABL + Sex + Age:ABL	6	368.263	7.399	−177.155	0.045
Age + ABL + Sex + Sex:ABL	6	368.688	7.824	−177.367	0.037
Age + K_n + Sex + Age:K_n	6	368.811	7.947	−177.429	0.034
Age + K_n + Sex + Sex:K_n	6	368.940	8.077	−177.494	0.032
Age + ABL + Sex + Sex:ABL + Age:ABL	7	370.355	9.492	−176.844	0.057
Age + K_n + Sex + Sex:K_n + Age:K_n	7	371.503	10.639	−177.418	0.035

Table A.9: Full AICc table for the model set fitted to the N:P data. No model performed better than the intercept-only (i.e., null) model. All parameters were uninformative. All specifications as in Table A.4.

Model	k	AICc	ΔAICc	LL	R^2
Intercept	2	192.561	0.000	−94.153	0.000
ABL	3	192.627	0.066	−93.053	0.043
K_n	3	193.015	0.454	−93.247	0.036
Age	3	193.747	1.186	−93.613	0.021
Age + K_n	4	194.546	1.985	−92.829	0.052
Sex	3	194.618	2.056	−94.048	0.004
Sex + ABL	4	194.844	2.282	−92.978	0.046
Age + ABL	4	194.856	2.294	−92.983	0.046
Sex + K_n	4	195.064	2.502	−93.088	0.042
Age + Sex	4	196.012	3.450	−93.561	0.023
Age + ABL + Age:ABL	5	196.760	4.199	−92.698	0.057
Age + K_n + Sex	5	196.830	4.269	−92.733	0.055
Age + K_n + Age:K_n	5	196.953	4.392	−92.795	0.053
Sex + ABL + Sex:ABL	5	197.122	4.561	−92.879	0.050
Age + ABL + Sex	5	197.213	4.652	−92.925	0.048
Sex + K_n + Sex:K_n	5	197.539	4.977	−93.087	0.042
Age + Sex + Age:Sex	5	197.915	5.354	−93.276	0.034
Age + ABL + Sex + Age:ABL	6	199.242	6.681	−92.644	0.059
Age + K_n + Sex + Age:K_n	6	199.326	6.764	−92.686	0.057
Age + K_n + Sex + Sex:K_n	6	199.419	6.857	−92.733	0.055
Age + ABL + Sex + Sex:ABL	6	199.552	6.991	−92.799	0.053
Age + ABL + Sex + Sex:ABL + Age:ABL	7	201.485	8.924	−92.409	0.067
Age + K_n + Sex + Sex:K_n + Age:K_n	7	202.038	9.476	−92.686	0.057

Table A.10: Full AICc table for the model set fitted to the %N data. In this case, relative body condition was calculated using skull length (SkK_n; see text for details). Only one model performed better than the intercept-only (i.e., null) model. Sex, average body length, and skull length-derived relative body condition were uninformative parameters. All other specifications as in Table A.4.

Model	k	AICc	ΔAICc	LL	R^2
Age	3	119.721	0.000	−56.600	0.066
Intercept	2	120.868	1.147	−58.306	0.000
Age + ABL	4	121.735	2.014	−56.423	0.073
Age + SkK_n	4	121.981	2.260	−56.546	0.068
Age + Sex	4	122.076	2.355	−56.594	0.066
SkK_n	3	122.773	3.052	−58.126	0.007
ABL	3	122.985	3.264	−58.232	0.003
Sex	3	123.112	3.391	−58.295	0.000
Age + SkK_n + Age:SkK_n	5	123.845	4.124	−56.241	0.079
Age + ABL + Age:ABL	5	124.016	4.295	−56.326	0.076
Age + Sex + Age:Sex	5	124.193	4.472	−56.415	0.073
Age + ABL + Sex	5	124.196	4.475	−56.416	0.073
Age + SkK_n + Sex	5	124.427	4.707	−56.532	0.069
Sex + SkK_n	4	125.099	5.378	−58.105	0.008
Sex + ABL	4	125.335	5.614	−58.223	0.003
Age + SkK_n + Sex + Sex:SkK_n	6	125.756	6.035	−55.901	0.092
Sex + SkK_n + Sex:SkK_n	5	126.389	6.668	−57.513	0.031
Age + ABL + Sex + Sex:ABL	6	126.423	6.703	−56.235	0.080
Age + SkK_n + Sex + Age:SkK_n	6	126.432	6.711	−56.239	0.079
Age + ABL + Sex + Age:ABL	6	126.594	6.873	−56.320	0.076
Sex + ABL + Sex:ABL	5	127.730	8.009	−58.183	0.005
Age + SkK_n + Sex + Sex:SkK_n + Age:SkK_n	7	128.018	8.298	−55.676	0.100
Age + ABL + Sex + Sex:ABL + Age:ABL	7	129.038	9.317	−56.186	0.081

Table A.11: Full AICc table for the model set fitted to the %P data. In this case, relative body condition was calculated using skull length (SkK_n; see text for details). Only one model performed better than the intercept-only (i.e., null) model. Age, sex, and skull length-derived relative body condition were uninformative parameters. All other specifications as in Table A.4.

Model	k	AICc	ΔAICc	LL	R^2
ABL	3	79.026	0.000	−36.252	0.047
Intercept	2	79.144	0.118	−37.444	0.000
Age + ABL	4	81.208	2.182	−36.159	0.050
Age	3	81.266	2.241	−37.372	0.003
SkK_n	3	81.364	2.339	−37.421	0.001
Sex + ABL	4	81.393	2.367	−36.252	0.047
Sex	3	81.402	2.376	−37.440	0.000
Age + ABL + Age:ABL	5	82.905	3.879	−35.771	0.065
Sex + ABL + Sex:ABL	5	83.583	4.558	−36.110	0.052
Age + Sex	4	83.632	4.606	−37.372	0.003
Age + SkK_n	4	83.632	4.607	−37.372	0.003
Age + ABL + Sex	5	83.678	4.652	−36.157	0.050
Sex + SkK_n	4	83.719	4.694	−37.415	0.001
Age + Sex + Age:Sex	5	85.418	6.392	−37.027	0.017
Age + ABL + Sex + Age:ABL	6	85.492	6.467	−35.769	0.065
Age + SkK_n + Age:SkK_n	5	85.822	6.797	−37.229	0.009
Age + ABL + Sex + Sex:ABL	6	86.045	7.020	−36.046	0.054
Age + SkK_n + Sex	5	86.105	7.079	−37.371	0.003
Sex + SkK_n + Sex:SkK_n	5	86.189	7.164	−37.413	0.001
Age + ABL + Sex + Sex:ABL + Age:ABL	7	87.733	8.707	−35.533	0.074
Age + SkK_n + Sex + Age:SkK_n	6	88.370	9.344	−37.208	0.009
Age + SkK_n + Sex + Sex:SkK_n	6	88.690	9.664	−37.368	0.003
Age + SkK_n + Sex + Sex:SkK_n + Age:SkK_n	7	91.083	12.057	−37.208	0.009

Table A.12: Full AICc table for the model set fitted to the %C data. In this case, relative body condition was calculated using skull length (SkK_n; see text for details). No model performed better than the intercept-only (i.e., null) model, and all parameters were uninformative. All other specifications as in Table A.4.

Model	k	AICc	ΔAICc	LL	R^2
Intercept	2	240.436	0.000	−118.090	0.000
SkK_n	3	241.628	1.192	−117.553	0.021
Age	3	241.703	1.268	−117.591	0.020
ABL	3	242.452	2.016	−117.965	0.005
Sex	3	242.484	2.048	−117.981	0.004
Age + SkK_n	4	243.665	3.229	−117.388	0.028
Sex + SkK_n	4	243.680	3.244	−117.396	0.027
Age + Sex	4	243.959	3.523	−117.535	0.022
Age + ABL	4	244.070	3.635	−117.591	0.020
Sex + ABL	4	244.624	4.188	−117.868	0.009
Sex + SkK_n + Sex:SkK_n	5	245.690	5.254	−117.163	0.036
Age + SkK_n + Age:SkK_n	5	245.772	5.336	−117.204	0.035
Age + SkK_n + Sex	5	245.934	5.498	−117.285	0.032
Sex + ABL + Sex:ABL	5	245.986	5.551	−117.311	0.031
Age + Sex + Age:Sex	5	246.197	5.761	−117.416	0.027
Age + ABL + Sex	5	246.433	5.997	−117.535	0.022
Age + ABL + Age:ABL	5	246.473	6.038	−117.555	0.021
Age + SkK_n + Sex + Sex:SkK_n	6	248.057	7.621	−117.052	0.041
Age + ABL + Sex + Sex:ABL	6	248.131	7.695	−117.089	0.039
Age + SkK_n + Sex + Age:SkK_n	6	248.275	7.839	−117.161	0.037
Age + ABL + Sex + Age:ABL	6	248.947	8.511	−117.497	0.023
Age + SkK_n + Sex + Sex:SkK_n + Age:SkK_n	7	250.577	10.141	−116.955	0.044
Age + ABL + Sex + Sex:ABL + Age:ABL	7	250.595	10.159	−116.964	0.044

Table A.13: Full AICc table for the model set fitted to the C:N data. In this case, relative body condition was calculated using skull length (SkK_n; see text for details). Only one model performed better than the intercept-only (i.e., null) model. Sex, average body length, and skull length-derived relative body condition were uninformative parameters. All other specifications as in Table A.4.

Model	k	AICc	ΔAICc	LL	R^2
Age	3	62.158	0.000	−27.818	0.074
Intercept	2	63.718	1.559	−29.731	0.000
Age + ABL	4	64.391	2.233	−27.751	0.076
Age + SkK_n	4	64.456	2.297	−27.783	0.075
Age + Sex	4	64.507	2.349	−27.809	0.074
SkK_n	3	64.646	2.487	−29.062	0.026
ABL	3	65.587	3.428	−29.533	0.008
Sex	3	65.825	3.667	−29.652	0.003
Age + ABL + Age:ABL	5	66.668	4.510	−27.652	0.080
Sex + SkK_n	4	66.760	4.601	−28.935	0.031
Age + ABL + Sex	5	66.849	4.690	−27.743	0.076
Age + SkK_n + Age:SkK_n	5	66.863	4.704	−27.750	0.076
Age + SkK_n + Sex	5	66.896	4.738	−27.766	0.076
Age + Sex + Age:Sex	5	66.938	4.779	−27.787	0.075
Sex + ABL	4	67.820	5.661	−29.465	0.011
Sex + SkK_n + Sex:SkK_n	5	69.015	6.856	−28.826	0.036
Age + ABL + Sex + Age:ABL	6	69.238	7.080	−27.642	0.080
Age + SkK_n + Sex + Sex:SkK_n	6	69.257	7.098	−27.652	0.080
Age + SkK_n + Sex + Age:SkK_n	6	69.380	7.221	−27.713	0.078
Age + ABL + Sex + Sex:ABL	6	69.419	7.261	−27.733	0.077
Sex + ABL + Sex:ABL	5	70.121	7.963	−29.379	0.014
Age + SkK_n + Sex + Sex:SkK_n + Age:SkK_n	7	71.889	9.731	−27.611	0.081
Age + ABL + Sex + Sex:ABL + Age:ABL	7	71.892	9.733	−27.613	0.081

Table A.14: Full AICc table for the model set fitted to the C:P data, when using skull length to calculate relative body condition (SkK_n). No model performed better than the intercept-only (i.e., null) model. All parameters were uninformative. All specifications as in Table A.4.

Model	k	AICc	ΔAICc	LL	R^2
Intercept	2	360.864	0.000	−178.304	0.000
ABL	3	361.821	0.957	−177.650	0.026
Age	3	363.107	2.243	−178.293	0.000
Sex	3	363.111	2.247	−178.294	0.000
SkK_n	3	363.124	2.260	−178.301	0.000
Age + ABL	4	363.970	3.106	−177.541	0.030
Sex + ABL	4	364.182	3.318	−177.646	0.026
Age + Sex	4	365.460	4.596	−178.285	0.001
Sex + SkK_n	4	365.469	4.605	−178.290	0.001
Age + SkK_n	4	365.474	4.610	−178.293	0.000
Age + ABL + Age:ABL	5	365.689	4.825	−177.163	0.045
Sex + ABL + Sex:ABL	5	366.249	5.385	−177.443	0.034
Age + ABL + Sex	5	366.425	5.561	−177.531	0.030
Age + SkK_n + Age:SkK_n	5	367.687	6.823	−178.162	0.006
Age + Sex + Age:Sex	5	367.688	6.824	−178.162	0.006
Sex + SkK_n + Sex:SkK_n	5	367.925	7.061	−178.281	0.001
Age + SkK_n + Sex	5	367.933	7.070	−178.285	0.001
Age + ABL + Sex + Age:ABL	6	368.263	7.399	−177.155	0.045
Age + ABL + Sex + Sex:ABL	6	368.688	7.824	−177.367	0.037
Age + SkK_n + Sex + Age:SkK_n	6	370.198	9.335	−178.122	0.007
Age + ABL + Sex + Sex:ABL + Age:ABL	7	370.355	9.492	−176.844	0.057
Age + SkK_n + Sex + Sex:SkK_n	6	370.504	9.640	−178.275	0.001
Age + SkK_n + Sex + Sex:SkK_n + Age:SkK_n	7	372.904	12.040	−178.119	0.007

Table A.15: Full AICc table for the model set fitted to the N:P data, when using skull length to calculate relative body condition (SkK_n). No model performed better than the intercept-only (i.e., null) model. All parameters were uninformative. All specifications as in Table A.4.

Model	k	AICc	ΔAICc	LL	R^2
Intercept	2	192.561	0.000	−94.153	0.000
ABL	3	192.627	0.066	−93.053	0.043
Age	3	193.747	1.186	−93.613	0.021
SkK_n	3	194.596	2.034	−94.037	0.005
Sex	3	194.618	2.056	−94.048	0.004
Sex + ABL	4	194.844	2.282	−92.978	0.046
Age + ABL	4	194.856	2.294	−92.983	0.046
Age + Sex	4	196.012	3.450	−93.561	0.023
Age + SkK_n	4	196.114	3.552	−93.612	0.021
Sex + SkK_n	4	196.711	4.150	−93.911	0.010
Age + ABL + Age:ABL	5	196.760	4.199	−92.698	0.057
Sex + ABL + Sex:ABL	5	197.122	4.561	−92.879	0.050
Age + ABL + Sex	5	197.213	4.652	−92.925	0.048
Age + SkK_n + Age:SkK_n	5	197.867	5.306	−93.252	0.035
Age + Sex + Age:Sex	5	197.915	5.354	−93.276	0.034
Age + SkK_n + Sex	5	198.485	5.924	−93.561	0.023
Sex + SkK_n + Sex:SkK_n	5	199.060	6.499	−93.848	0.012
Age + ABL + Sex + Age:ABL	6	199.242	6.681	−92.644	0.059
Age + ABL + Sex + Sex:ABL	6	199.552	6.991	−92.799	0.053
Age + SkK_n + Sex + Age:SkK_n	6	200.111	7.549	−93.079	0.042
Age + SkK_n + Sex + Sex:SkK_n	6	200.948	8.387	−93.497	0.026
Age + ABL + Sex + Sex:ABL + Age:ABL	7	201.485	8.924	−92.409	0.067
Age + SkK_n + Sex + Sex:SkK_n + Age:SkK_n	7	202.752	10.190	−93.042	0.043

Table A.16: Comparison of Observed and Expected total body length ranges between our study species, the snowshoe hare *L. americanus*, and three other freshwater vertebrate species commonly used in studies of intraspecific variability in ecological stoichiometry.

Species	**Observed range (cm)**	**Expected range (cm)**	**References**
Snowshoe hare	36.67–46.67	36.0–52.0	this study; Feldhamer, Thompson, and Chapman (2003)
Rivulus hartii	1.0–8.4	1.0–10.0	El-Sabaawi, Kohler, et al. (2012)
Poecilia reticulata	0.35–0.4	-	El-Sabaawi, Travis, et al. (2014)
Gasterosteus aculeatus	3.2–7.2	3.0–8.0	Scott and Crossman (1973) and Durston and El-Sabaawi (2017)

Table A.17: Average, minimum and maximum values for %C, %N, %P, and their respective ratios for snowshoe hares, *L. americanus*, and five other taxonomic groups.

Species	**Carbon**			**Nitrogen**			**Phosphorus**			**C:N**			**C:P**			**N:P**			**References**
	Avg.	**Min.**	**Max.**	**Avg.**	**Min.**	**Max.**	**Avg.**	**Min.**	**Max.**	**Avg.**	**Min.**	**Max.**	**Avg.**	**Min.**	**Max.**	**Avg.**	**Min.**	**Max.**	
Snowshoe hare	43.61	37.46	51.29	11.20	9.42	12.68	2.97	2.00	4.29	4.56	3.91	5.65	39.21	25.23	64.73	8.58	5.22	12.28	this study
Freshwater Fishes	44.70	30.20	53.60	10.10	6.70	13.20	2.90	1.30	5.70	5.20	3.80	7.70	44.00	15.90	95.90	8.40	2.80	15.10	McIntyre and Flecker (2010)[a]
Invertebrates	42.45	39.65	50.23	10.70	9.13	14.80	0.79	0.36	1.50	3.97	-	-	53.73	-	-	13.54	-	-	González et al. (2011)[b]
Lizards	37.88	-	-	9.75	-	-	4.56	-	-	3.89	-	-	8.31	-	-	2.14	-	-	González et al. (2011)[c]
Insects	50.26	-	-	9.29	-	-	0.85	-	-	5.91	-	-	192.95	-	-	26.42	-	-	Elser et al. (2000)[d]
Zooplankton	48.00	-	-	9.39	-	-	1.08	-	-	7.30	-	-	108.52	-	-	22.27	-	-	Elser et al. (2000)[e]

a. Average values of 100 species from Europe, North and South America
b. Average values of 22 species of terrestrial invertebrates from the Atacama Desert, Chile
c. Average values of 22 species of terrestrial invertebrates from the Atacama Desert, Chile
d. Average values of 130 species collected from published sources
e. Average values of 43 species collected from published sources

A.7 Additional Figures

In this section, we provide additional figures and graphs. Figure A.1 shows the bivariate plots used to select the best length measurement to calculate the SMI. Figures A.2 and A.3 show the amount of intra-individual variability in the C and N content of hares in our sample. Figure A.4 shows the variability in P concentration found among three repeated samples taken from 5 random snowshoe hares. Figure A.5 shows variability in relative body condition (K_n) and average body length among different hares of different age and sex. Figures A.6 and A.7 provide examples of the mandibular bone sections used to age snowshoe hares in our sample. Figure A.6 shows the section obtained by the oldest individual in our sample, a 6 years old female, whereas Figure A.7 show the same section but for a 1 year old hare.

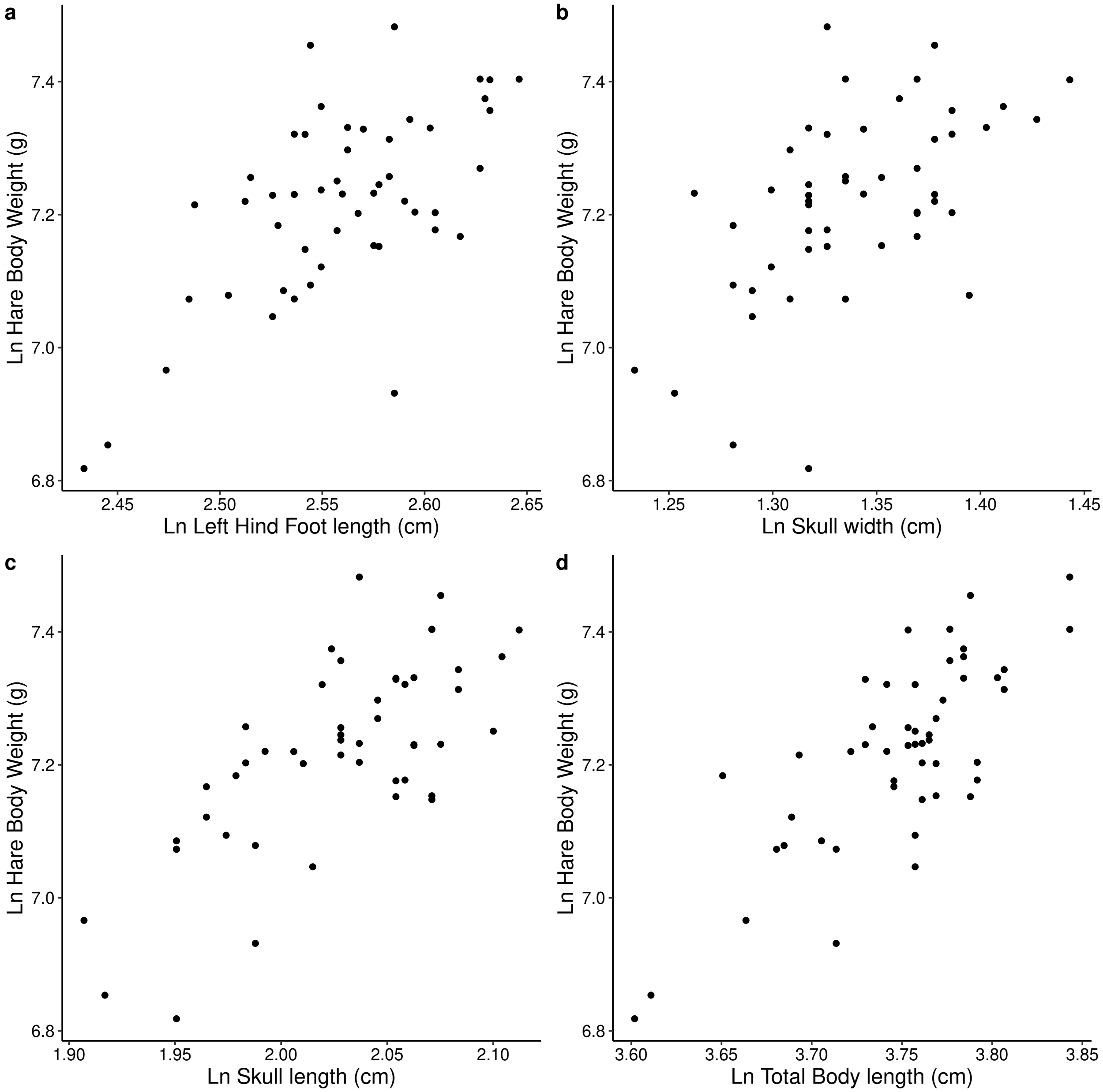

Figure A.1: Bivariate plots used to select the length measurement to calculate the SMI. On the y-axis is the ln-transformed hare body weight in g. The x- axis reports each ln-transformed length measurement: (**a**) left hind foot length, (**b**) skull width, (**c**) skull length, and (**d**) total body length. All length measurements are in mm. Note the different scales of each x-axis. Each data point is the arithmetic mean of three measurements repeated on a single specimen.

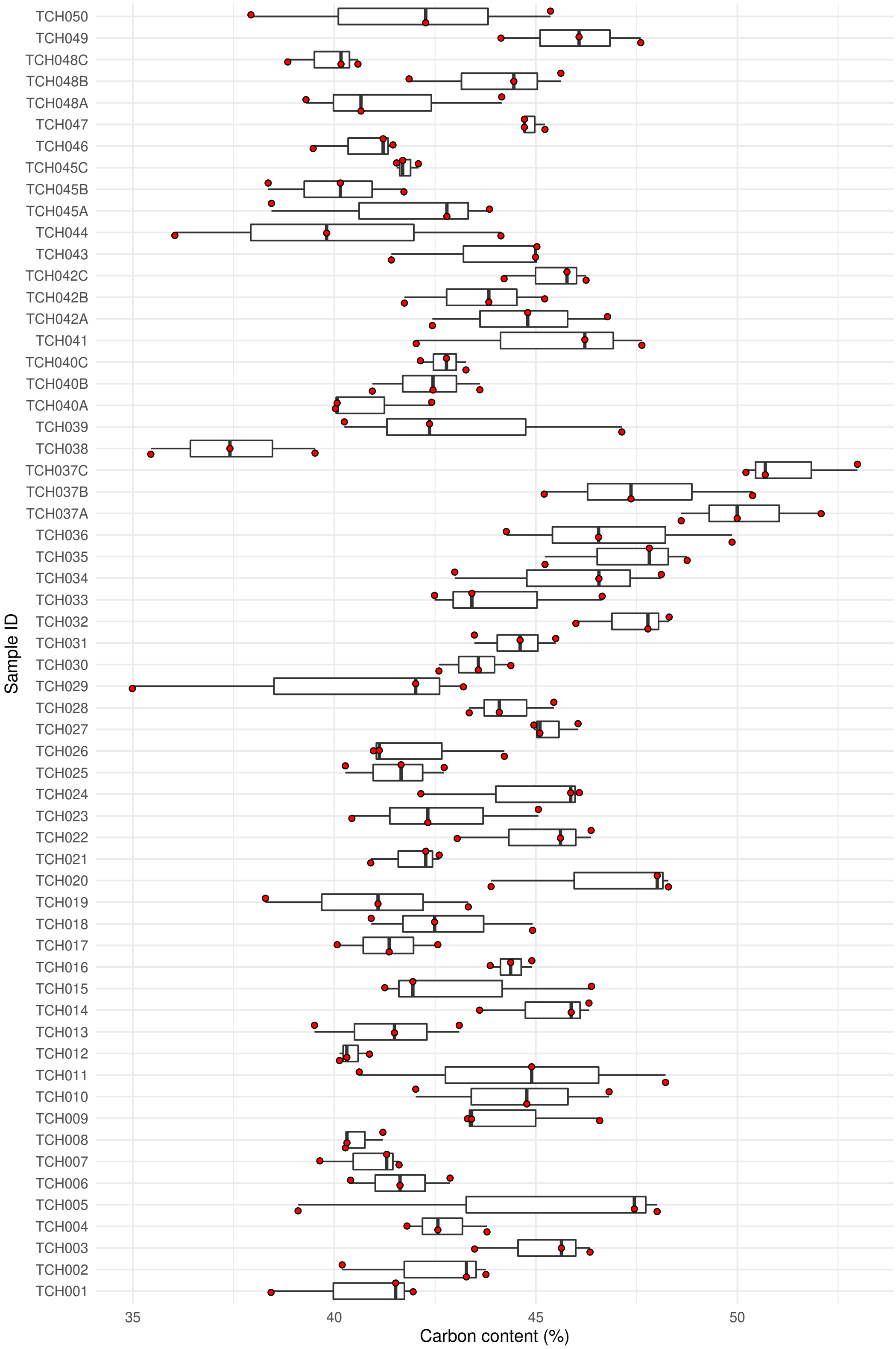

Figure A.2: Within-sample variability in the concentration of C among the 50 snowshoe hare samples sent to AFL. The dark line inside the box is the median, the upper and lower hinges represent the 75th and 25th percentile respectively, and the two whiskers extend to 1.5 × the distance between the first and third quartile.

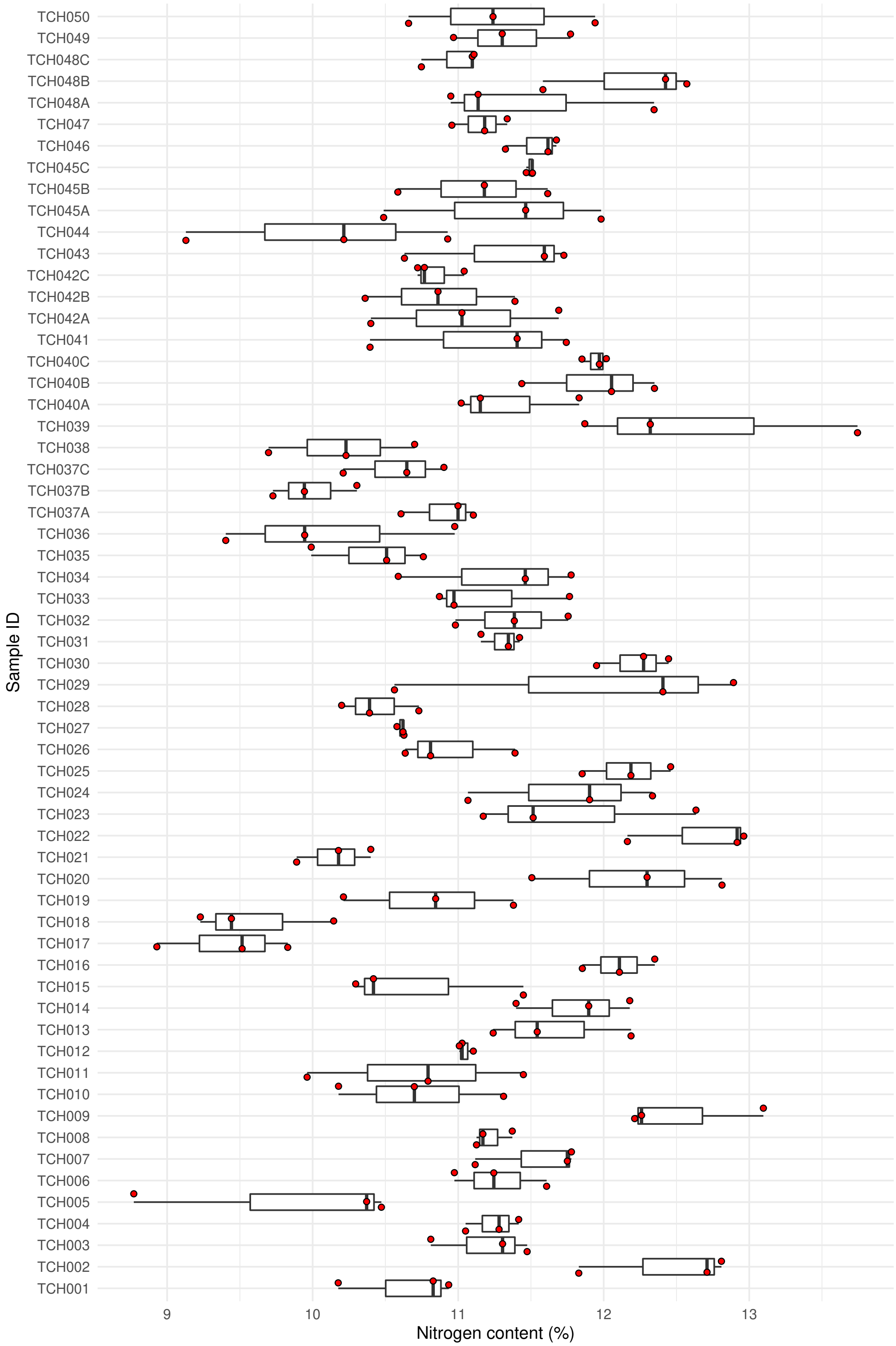

Figure A.3: Within-sample variability in the concentration of N among the 50 snowshoe hare samples sent to AFL. All specifications as in Figure A.2.

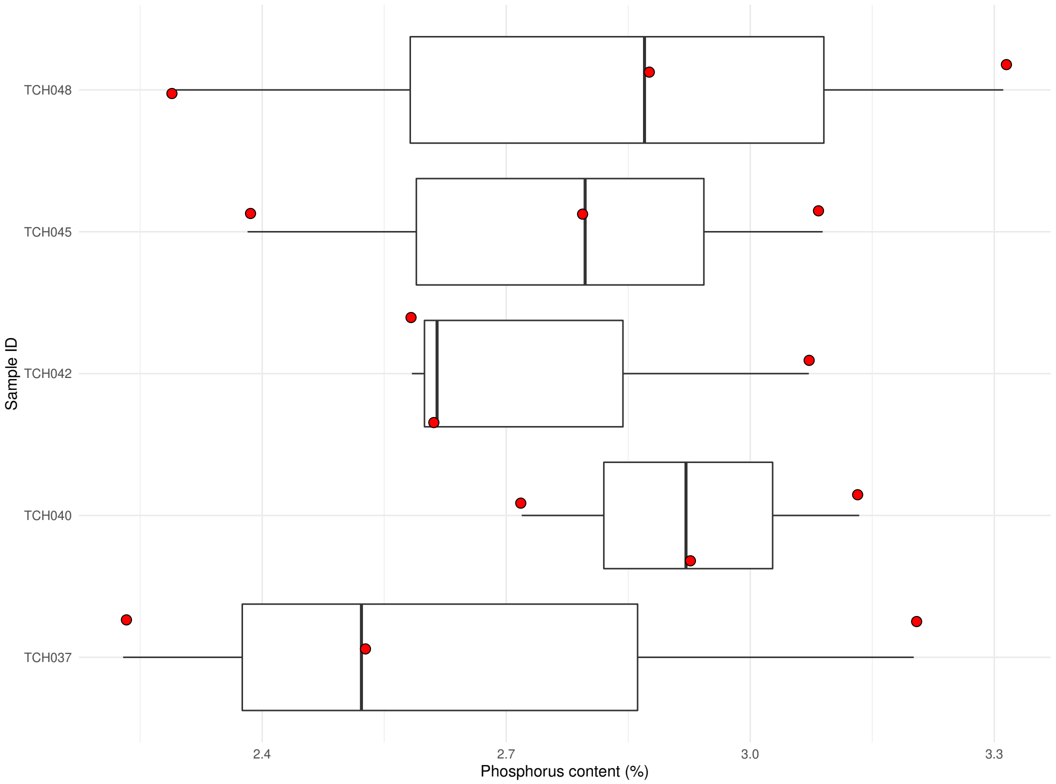

Figure A.4: Variability in P content among three repeated samples taken from 5 random snowshoe hares after homogenization.

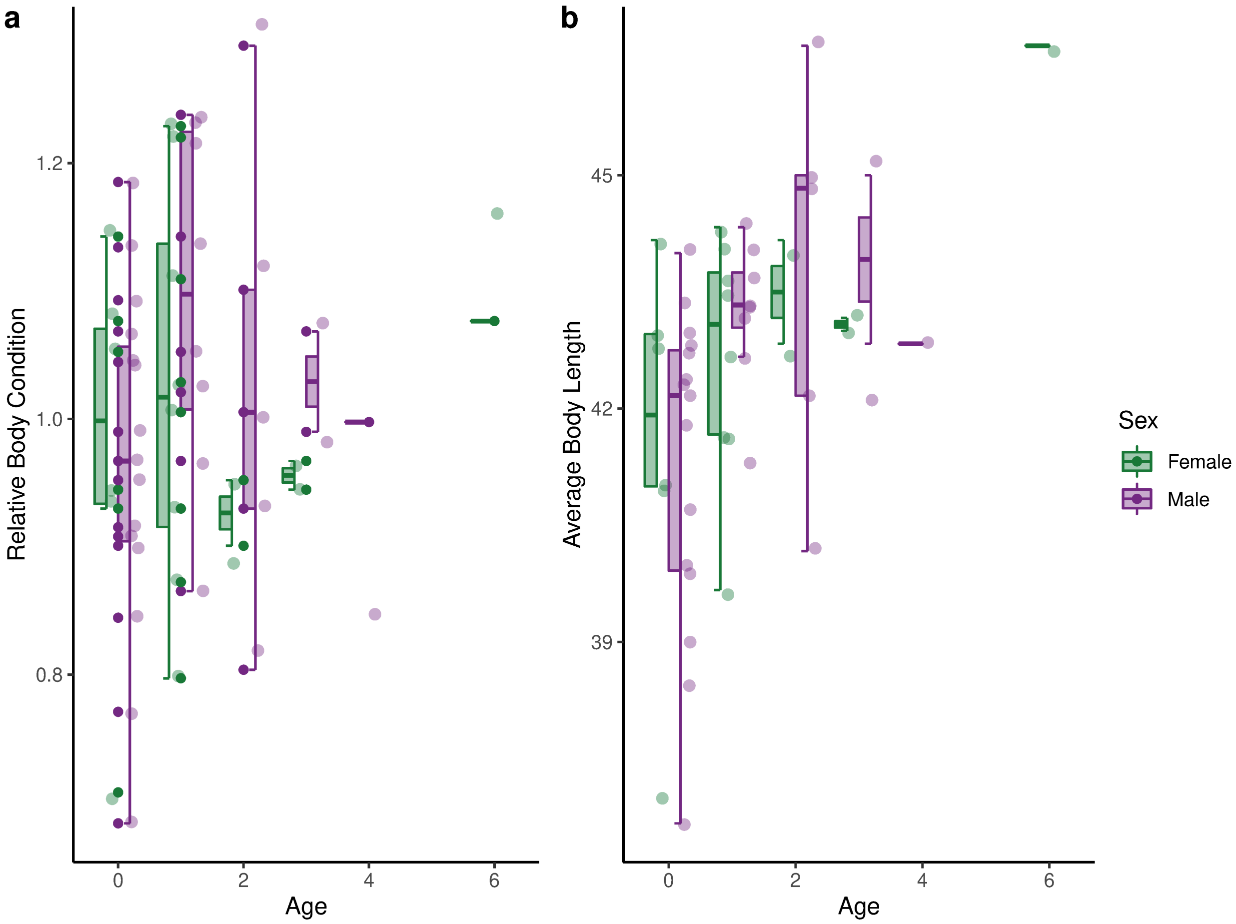

Figure A.5: Variability in relative body condition (**a**) and average body length (**b**) with age, between the two sexes. Younger individuals appeared more variable than older ones. We found no evidence of a relationship between these variables through our statistical analyses.

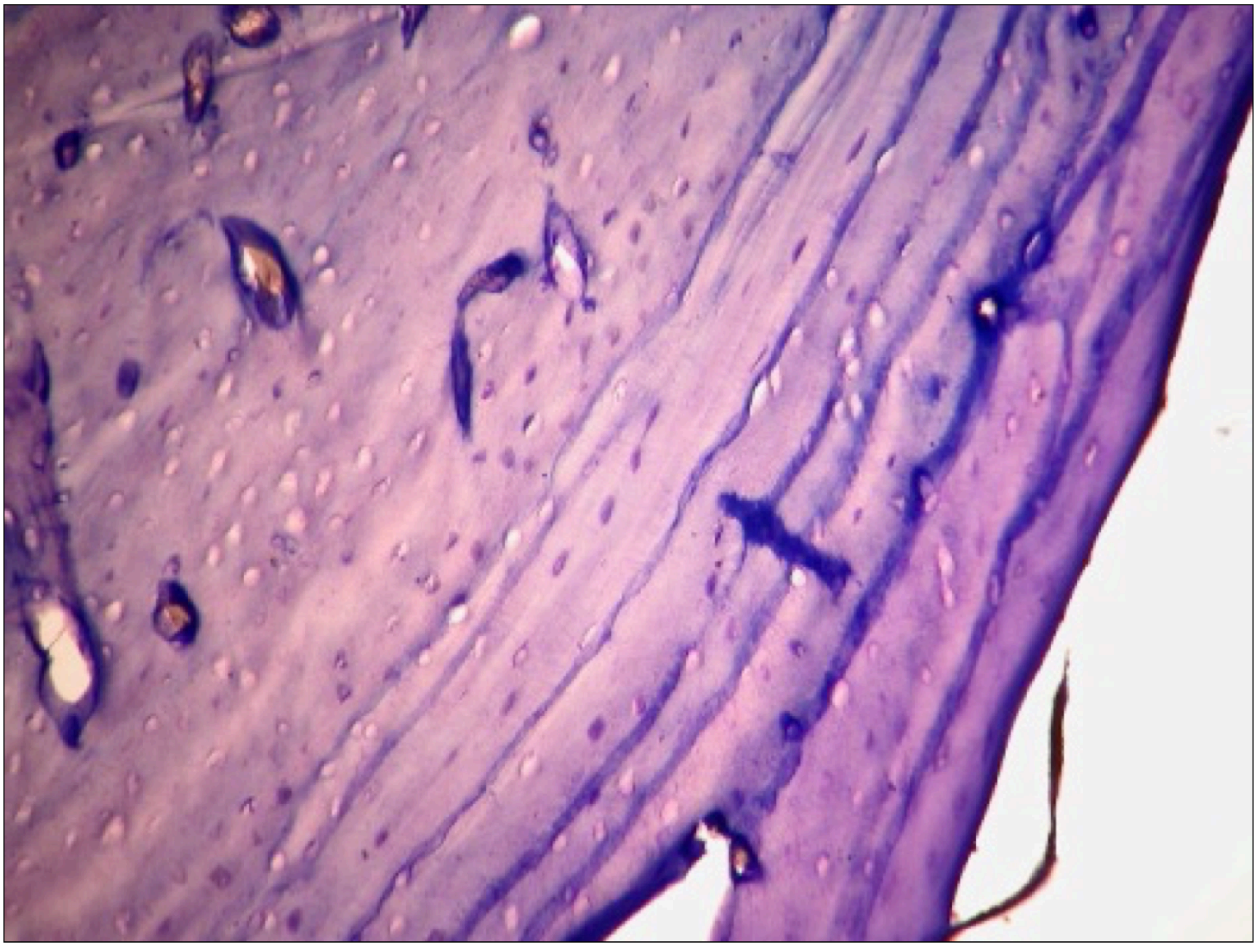

Figure A.6: Histological preparation of mandibular section from hare TCH027, magnified 160X, showing the side of the mandible near the inferior surface. Estimated age for this individual is 6 years (i.e., 6 winters survived).

Figure A.7: Histological preparation of mandibular section from hare TCH005, magnified 60X, showing the side of the mandible near the inferior mandible surface. In this case, age assessment is more difficult than in Figure A.6. As the pattern is not so clear, a conservative age estimate would assign to this individual an age of 1 (i.e., 1 winter survived), with a range of 1–2 winters survived.

A.8 References

Arnold, T. W. (2010). “Uninformative Parameters and Model Selection Using Akaike’s Information Criterion”. *The Journal of Wildlife Management* 74.6, pp. 1175–1178. DOI: `10.2193/2009-367`.

Burnham, K. P. and D. R. Anderson (2002). *Model Selection and Multimodel Inference: A Practical Information-Theoretic Approach (2nd ed)*. 2nd ed. Springer-Verlag New York, pp. XXVI, 488.

Claris International Inc. (2015). *FileMaker Pro Advanced*. Santa Clara, CA. URL: `https://www.claris.com/filemaker/pro/`.

CWA Methods Team (2016). *Definition and Procedure for the Determination of the Method Detection Limit, Revision 2 (EPA 821-R-16-006)*. Tech. rep. Washington, D.C.: Environmental Protection Agency, p. 8. URL: `https://www.epa.gov/cwa-methods`.

Durston, D. J. and R. W. El-Sabaawi (2017). “Bony traits and genetics drive intraspecific variation in vertebrate elemental composition”. *Functional Ecology* 31.11, pp. 2128–2137. DOI: `10.1111/1365-2435.12919`.

Elser, J. J. et al. (2000). “Nutritional constraints in terrestrial and freshwater food webs”. *Nature* 408.6812, pp. 578–580. DOI: `10.1038/35046058`.

Feldhamer, G. A., B. C. Thompson, and J. A. Chapman (2003). *Wild mammals of North America: biology, management, and conservation*. JHU Press.

González, A. L. et al. (2011). “Exploring patterns and mechanisms of interspecific and intraspecific variation in body elemental composition of desert consumers”. *Oikos* 120.8, pp. 1247–1255. DOI: `10.1111/j.1600-0706.2010.19151.x`.

Iason, G. R. (1988). “Age determination of mountain hares (*Lepus timidus*): a rapid method and when to use it”. *Journal of Applied Ecology* 25 (2), pp. 389–395. DOI: `10.2307/2403831`.

Labocha, M. K., H. Schutz, and J. P. Hayes (2014). “Which body condition index is best?” *Oikos* 123.1, pp. 111–119. DOI: `10.1111/j.1600-0706.2013.00755.x`.

Leroux, S. J. (2019). “On the prevalence of uninformative parameters in statistical models applying model selection in applied ecology”. *PLoS One* 14 (2), pp. 1–12. DOI: `10.1371/journal.pone.0206711`.

McIntyre, P. B. and A. S. Flecker (2010). “Ecological Stoichiometry as an Integrative Framework in Stream Fish Ecology”. *American Fisheries Society Symposium* 73, pp. 539–558.

Meija, J. et al. (2016). *Atomic weights of the elements 2013 (IUPAC Technical Report)*. DOI: `10.1515/pac-2015-0305`.

Naimi, B. et al. (2014). “Where is positional uncertainty a problem for species distribution modelling?” *Ecography* 37.2, pp. 191–203. DOI: `10.1111/j.1600-0587.2013.00205.x`.

Peig, J. and A. J. Green (2009). “New perspectives for estimating body condition from mass/length data: The scaled mass index as an alternative method”. *Oikos* 118.12, pp. 1883–1891. DOI: `10.1111/j.1600-0706.2009.17643.x`.

— (2010). “The paradigm of body condition: A critical reappraisal of current methods based on mass and length”. *Functional Ecology* 24.6, pp. 1323–1332. DOI: `10.1111/j.1365-2435.2010.01751.x`.

El-Sabaawi, R. W., T. J. Kohler, et al. (2012). “Environmental and organismal predictors of intraspecific variation in the stoichiometry of a neotropical freshwater fish”. *PLoS One* 7.3, e32713. DOI: `10.1371/journal.pone.0032713`.

El-Sabaawi, R. W., J. Travis, et al. (2014). “Intraspecific variability modulates interspecific variability in animal organismal stoichiometry”. *Ecology and Evolution* 4.9, pp. 1505–1515. DOI: `10.1002/ece3.981`.

Scott, W. B. and E. J. Crossman (1973). “Freshwater Fishes of Canada.” *Bulletin of Fisheries Research Board of Canada* 184, pp. 1–966.

Shaw, C. N., P. J. Wilson, and B. N. White (2003). “A Reliable Molecular Method of Gender Determination for Mammals”. *Journal of Mammalogy* 84.1, pp. 123–128. DOI: `10.1644/1545-1542(2003)084<0123:ARMMOG>2.0.CO;2`.

Stevenson, R. D. and W. A. Woods (2006). “Condition indices for conservation: New uses for evolving tools”. *Integrative and Comparative Biology* 46.6, pp. 1169–1190. DOI: `10.1093/icb/icl052`.

Warton, D. I. et al. (2012). “smatr 3 – an R package for estimation and inference about allometric lines”. *Methods in Ecology and Evolution* 3.2, pp. 257–259. DOI: `10.1111/j.2041-210X.2011.00153.x`.

Yalcin, S. and S. J. Leroux (2018). “An empirical test of the relative and combined effects of land-cover and climate change on local colonization and extinction”. *Global Change Biology* 24.8, pp. 3849–3861. DOI: `10.1111/gcb.14169`.

APPENDIX B

Supplementary Information for Chapter 3: Forage stoichiometry predicts the home range size of a small terrestrial herbivore.

B.1 Introduction

This appendix contains supplementary information on the study species, area, and methods used in investigating the influence of forage elemental composition on the home range size of snowshoe hares (*Lepus americanus*) in the boreal forest of the island of Newfoundland, Canada. Appendix B.2 provides additional details on the ecology of the snowshoe hare, a keystone herbivore species in the boreal ecosystem. Appendix B.3 describes the rationale and techniques used in establishing our snowshoe hares live trapping grids. Appendix B.4 describes the groups of covariates included in our Stoichiometric Distribution Models, whereas Appendix B.5 and Appendix B.6 provide details on our live trapping and triangulation protocols, respectively. We provide details on home range size estimation in Appendix B.7, describing our handling of pseudoreplicates in Appendix B.7.1 and our rationale for not including sampling year in our models of hare home range size in Appendix B.7.2. Appendix B.8 details the methods we used to review the literature on elemental and macromolecular definitions of food quality. In Appendix B.9, we provide supplementary tables, including model selection summary tables for the analyses ran on home range size estimated at the 75% and 90% UD isopleths, as well as a model selection summary table for the Stoichiometric Distribution Models. In Appendix B.9.1, we present full AICc model selection tables for our analyses of the relationship between home range size and forage ecological stoichiometry. Finally, in Appendix B.10, we provide visual supporting materials, including a map of our study area, the layout of our live trapping grids, and maps showing the degree of overlap among home range estimates from consecutive sampling years for four snowshoe hares.

We refer the interested reader to the companion R notebook "Supporting Code" for an in-depth description of the R workflow and code used to perform UD home range size estimation, overlap analyses, stoichiometric data extraction, and model fitting, as well as additional visual supporting materials including Utilization Distribution maps and an interactive map of our study area.

B.2 Study species

The snowshoe hare (*L. americanus*) is a keystone herbivore in the boreal forest and has been extensively studied for the role its characteristic boom-bust population cycle plays in the boreal forest's ecosystem dynamic (Krebs, Boonstra, and Boutin 2018). Snowshoe hare populations cycle regularly in their abundance, with an 8–11 years periodicity that was already evident to 19^{th} century fur trappers (Feldhamer, Thompson, and Chapman 2003; Krebs, Boonstra, and Boutin 2018). Active year-round, snowshoe hares (*L. americanus*) seasonally forage on different plant species (see Dodds 1960, for an extensive list) and face consistently high predation risk from a diverse group of both land-based and airborne predators (Krebs, Boonstra, and Boutin 2018). Among these predators, the lynx (*Lynx canadensis*) is the most well-known, as its own population dynamics closely follow that of the snowshoe hare (Krebs, Boonstra, and Boutin 2018). Furthermore, snowshoe hares have low fat tissue accumulation, ≤5% of their body weight on average, and vary their diet seasonally (Feldhamer, Thompson, and Chapman 2003). They face high reproductive investment, with up to four litters per year and 6–8 leverets per litter (Feldhamer, Thompson, and Chapman 2003). Thus, access to good quality resources is paramount for their survival throughout the winter and to support their reproductive costs in spring and summer (Murray 2002). Finally, in south-eastern portions of their range—like the island of Newfoundland—their distribution is patchier and more discontinuous compared to core areas, like the Yukon (Thornton et al. 2013; Krebs, Boonstra, and Boutin 2018). As well, recent evidence points to their population cycle being less regular and shorter in Newfoundland than in the core areas of their range, like the Yukon (e.g., 8–9 years; Reynolds et al. 2017). In turn, this makes hares likely more sensitive to differences in resource quality and its variation over the landscape (Thornton et al. 2013).

B.3 Grid establishment

We selected forest stands to house live trapping grid using data from the Forest Resource Inventory compiled by the Provincial Government of Newfoundland and Parks Canada. We selected two forest stands inside the border of Terra Nova National Park, and two forest stands outside the protected area (Figure B.1). We selected forest stands based on snowshoe hare habitat preferences and along a stand age chronosequence, with age groups 20–40, 41–60, 61–80, 81–100 years old. To reduce error in deploying the traps, we drew each grid's trap lines layout in ArcGIS (v. 10.4, ESRI, Redlands, CA) and then used digital, geo-referenced maps showing the location of each trap to deploy them. Upon deployment, we further confirmed trap location by taking averaged waypoints with a GPS unit (GPSMAP 64s, Garmin Ltd., Olathe, KS).

B.4 Stoichiometric Distribution Models data and covariates

We collected plant samples to build our Stoichiometric Distribution Models from three preferred summer forage species of snowshoe hares: red maple (*Acer rubrum*), white birch (*Betula papyrifera*), and lowbush blueberry (*Vaccinium angustifolium*). We collected foliar material samples for each plant species in and around our snowshoe hare trapping grids. Inside each grid, we collected plant foliar samples for stoichiometric analyses to assess their C:N:P content. Around each grid, we collected plant foliar samples to calculated biomass (see main text for further details). Table B.4 provides a breakdown of the number of foliar samples collected for each plant species in each study site for the stoichiometric analyses (see Figure B.7 for a visual breakdown).

We built our Stoichiometric Distribution Models using a set of spatially explicit covariates grouped in four classes: land cover, productivity, biotic, and abiotic (Heckford et al. 2021). We considered three land cover types—coniferous, deciduous, and mixed wood—derived from the

Commission for Environmental Cooperation Land Cover publicly available dataset. We quantified productivity using the Enhanced Vegetation Index (EVI) as a proxy, because the Normalized Difference Vegetation Index saturates easily in the wet conditions of the boreal forest. Our biotic covariate included stand height, age, and canopy closure as categorical variables, each derived from the Forest Resource Inventory compiled by the Provincial Government of Newfoundland and Labrador and the Federal Government of Canada. Stand height in our analyses comprised 6.6–9.5 m (class 3), 9.6–12.5 m (class 4), and 12.6–15.5 m (class 5). Stand age included 41–60 (class 3), 61–80 (class 4), and 81–100 (class 5) years old. Crown density included 51–75% (class 2), 25–50% (class 3), and 10–25% (class 4) canopy closure. Finally we included elevation, aspect, and slope in our abiotic covariate, each derived from a Canadian Digital Elevation Model (see Heckford et al. 2021, for more details on spatial covariates in our StDMs).

Each of these covariates groups can influence plant species of interest (SOI) spatial stoichiometry, either individually or together with one, two, or all other groups. Accordingly, we fit a set of 16 different Generalized Linear Models, including all possible additive combinations of our four covariate groups and a null model (for full results see Heckford et al. 2021).

B.5 Live trapping

Live trapping sessions lasted 3–4 days, with a pattern of one night of trapping, followed by one night of no trapping, followed by 1–2 additional trapping nights. In 2016 and 2017, we also used an optional pre-baiting night—i.e., baiting with the trap door jammed open—to allow individuals to familiarize themselves with the traps. Live-trapping nights depended on weather conditions: as snowshoe hares rely on movement to thermoregulate, due to their low body fat reserve (Feldhamer, Thompson, and Chapman 2003), trapping in cold or wet nights may jeopardize their survival. Hence, whenever weather forecasts would call for night temperatures below 5 °C or for intense precipitation, e.g., rain or snow, we would suspend live trapping.

Before handling begun, we transferred trapped individuals from the trap to a burlap sack of known weight (∼200 g). We inserted the door-end of the trap in the burlap sack, then opened the door and waited for the hare to walk in the sack. Once the hare was in the sack, we weighted (g) the whole sack. We then eartagged the individual and fitted it with a radio-collar before proceeding to collect data on sex, age, left hind foot length (mm), percent white fur estimated visually, and tick load. After releasing the individual, we calculated net wet body weight of the trapped hare by subtracting the weight of the empty burlap sack from the weight of the burlap sack with the hare in it. We further weighted the burlap sack between handling different individuals, to account for increased weight due to the sack getting soaked in rain and/or morning dew.

During our initial trapping season of 2016–2017, we had low capture rates and most of the individuals trapped and fitted with radiocollars where on the live trapping grid located in the 20–40 years old forest stand (cfr., "hare study area" in the main text). Because of this, we decided to focus our trapping efforts on this grid and trapped in both spring and fall for the subsequent three years.

B.6 Triangulation and data processing

Triangulation happened daily from May to September in 2017, 2018, and 2019. Our daily triangulation timeframe changed slightly from year to year, to accommodate changes in workforce available and fieldwork logistics: we relocated hares between 0600–2100 in 2017, 0630–2200 in 2018, and 0500–2100 in 2019. We attempted to triangulate all active collars present on the grid every day, randomizing the order and time at which we attempted to locate each collar. In summer 2017, a single operator (MR) performed all triangulations, whereas in summers 2018 and 2019 two to three operators collected azimuths simultaneously from different locations: this greatly reduced the time necessary to triangulate all individuals and improved precision of triangulations. We estimated triangulation error for two of our operators using the `razimuth` R package (Gerber et al. 2018). In 2017, our sole observer had a mean (±SD) error of 151 (±90.3) m, whereas in 2018 an additional observer had a mean error of 269 (±372.2) m.

In R, we used package `razimuth` (Gerber et al. 2018) to estimate the location of each snowshoe hare for each set of azimuths collected daily during the sampling season. `razimuth` fits an

Azimuthal Telemetry Model (ATM) to telemetry data using a Markov Chain Monte Carlo process. The ATM estimates both the location of the transmitter, in our case a radio-collar, and an error ellipse encircling it, which represents the uncertainty around the transmitter location (Gerber et al. 2018). These error ellipses can then be used to inform home range estimation using the `ctmm` package (Fleming and Calabrese 2017; Fleming, Noonan, et al. 2019). To estimate the location of a transmitter, the ATM requires an estimate of the maximum distance between the transmitter and the receiver. Our live trapping grid was a square of 500 m per side (see above, Appendix B.3). While standing on the highest point of the grid, our observers could barely hear the signal of a collar on the opposite side of the grid—a challenge likely due to the dense, young vegetation of the grid and significant presence of water on it. Based on these observations, we conservatively estimated the maximum distance between transmitter and receiver to be 750 m. We assessed the ATM fit to our triangulation data by visually checking the values of parameter κ, which captures the uncertainty in the azimuthal data (Gerber et al. 2018). We checked both the variation in the values of κ and their running mean, as described in Gerber et al. (2018). The Supporting Code document, available through our online repository, contains the complete workflow to perform these triangulations—from data preparation to output.

B.7 Home Range Estimation

We used an Autocorrelated Kernel Density Estimator corrected for small sample size (henceforth, AKDEc) method to estimate home range area in hectares (ha) of our snowshoe hares, as this method is more reliable and accurate than more traditional approaches even with low relocation sample size (Fleming and Calabrese 2017; Fleming, Noonan, et al. 2019).

We first visually checked each individual's telemetry relocation dataset for outliers, i.e., relocations too far from the median latitude and longitude of an individual's dataset, and removed them using function `outlie` in R package `ctmm` (Fleming and Calabrese 2020). Following guidelines in Fleming and Calabrese (2017), we visually assessed space use patterns for each individual in our dataset containing both relocations and error ellipses using variograms. We then used function `ctmm.guess` in the same package to fit a continuous time movement model (Fleming and Calabrese 2017) based on the variogram's shape and extract the estimated model parameters for each individual. Then, using the function `ctmm.select`, we fit hypothetical movement models with the initial estimates from `ctmm.guess` for each individual using a perturbative hybrid residual maximum likelihood method (pHREML; Fleming, Noonan, et al. 2019). We evaluated model fit using summary tables for each model, AICc, and variogram fit. Finally, we selected the top-ranking movement model for each individual and used it to calculate the Utilization Distribution (UD) for each individual in our dataset. We calculated the UD using function `akde` from the same package. From the UDs, we then estimated the area (ha) of the 50%, 75%, and 90% UD slices. We used the contours of these estimates to extract plant SOI stoichiometric data from our StDMs predictive surfaces as described in the main text.

Below we describe how we addressed the few pseudoreplication issues that arose in our sample. The Supporting Code document available through the online repository contains code and outputs for this entire R workflow.

B.7.1 Accounting for pseudoreplication

For four snowshoe hares in our sample, we had telemetry data for two consecutive sampling years: three individuals were collared in the 2018 sampling season and were followed again in the 2019 sampling season, and one individual was collared in the 2017 and was followed again in the 2018 sampling seasons. We used the Bhattacharyya's affinity index (Fieberg and Kochanny 2005) to estimate overlap in the utilization distribution of these four individuals between consecutive years (Winner et al. 2018). Results from this analysis highlight a high degree of overlap, likely an indication of strong site-fidelity across years (Table B.3 and Figures B.3 to B.6). Armed with this knowledge, we addressed this issue in two ways: we decided to use only one year of sampling for each of these four individuals, and we used only the year with the most relocations for each individual.

B.7.2 Testing for sampling year-related effects

Evidence in the literature suggests that year of sampling—that is, the year during which relocations are collected—can play a role in determining home range size (Börger et al. 2006). Because of this, we ran preliminary analyses on our data using a model that included only the variable "sampling year", including only the year with most locations for the four individuals with year replicates (see section Appendix B.7.1). We found no evidence of a relationship between sampling year and home range size (see the Supporting Code document for code and model output). Alternative methods of considering the four individuals with year replicates, e.g., randomization, selecting the year closest to plant SOI sampling, yielded qualitatively similar results. Based on these results, we decided to not include the variable sampling year in our analyses.

B.7.3 Nighttime relocations and home range size estimates

Snowshoe hares are nocturnally active but we did not collect nighttime relocations, due to labour and logistical limitations (see above, Appendix B.6). However, we do not expect this to influence our estimates of the location and size of our snowshoe hares' home ranges, for several reason. First, while snowshoe hare may move within their home range during night hours, we would expect this to more likely influence patterns of use of different portions of the home range rather than where or how large it is. Indeed, the results from our home range overlap analysis for the four snowshoe hare for which we had two consecutive years of telemetry data appear to confirm this expectation (Table B.3). In particular, Figures B.3 to B.6 show minimal variation in the location of the home ranges with respect to the live-trapping grid or other features—natural or otherwise—of the landscape. Finally, our home range size estimates are consistent with those of the only other study we could find on snowshoe hare home range size in Newfoundland (Barta, Keith, and Fitzgerald 1989). Together, we take these elements as evidence that we did capture summer home range size of our sample of snowshoe hare across multiple years.

B.8 Food Quality: elements and macromolecules

The majority of studies investigating the influence of food quality on consumer home range size use nutritional measures of food such as macromolecules: carbohydrates, protein, cellulose, etc. We propose a parsimonious definition of food quality that considers the basic elemental content of food: its content of carbon (C), nitrogen (N), and phosphorus (P) among others (Kaspari and Powers 2016). The strength of an elemental approach and the ability to compare our elemental approach to other, more common approaches depends on how well the elemental content of food relates to the nutritional content of food. Consequently, we performed a literature review. We collated data from two recent reviews on the topic of leporid and cervid food choice by Felton et al. (2018) and Champagne et al. (2020) to investigate the relationship between elemental content and nutritional content of food. The datasets used in both these reviews are publicly available online and we extracted data from them to perform our analyses. Our data extraction proceeded in two steps. First, we identified potential studies from Felton et al. (2018) and Champagne et al. (2020) that measured elemental or nutritional content of food (n = 101). Second, we selected, reviewed, and extracted data from papers identified in the first step that measured both elemental and nutritional content. In some cases, we used data extraction software to collect data from graphs or figures (PlotDigitizer v 2.6.8; Huwaldt 2014). Our review revealed that N was the most common element measured in food along with six classes of structural and non-structural macromolecules in plants: Neutral Detergent Fiber, Acid Detergent Fiber, Cellulose, Hemicellulose, Lignin, and Total Non-Structural Carbohydrates (Figure B.9).

From the Felton et al. (2018) and Champagne et al. (2020) datasets, we identified 40 studies that measured both N content and at least one of the six nutritional indicators listed above. In case of multiple entries for the same plant species, e.g., data recorded at different times of the year or for different phenotypes, we recorded each entry as a separate record for that species to capture intra-specific variability. We further recorded the type of herbivore involved in the study, the type of plants—e.g., broadleaved, coniferous, legumes—, the type of study, and whether protein content had been estimated from N content using a conversion factor (Mariotti, Tomé, and Mirand 2008). There was substantial overlap in the datasets from the Felton et al. (2018) and Champagne et al. (2020) meta-analyses.

Once we completed data extraction, we used the statistical language R (v. 4.0.1; R Core Team 2020) to visually examine the data. First, as units of measurements for macromolecules content varied across studies, we subset our dataset to include only data reported as % dry matter/mass or % dry weight of N or the nutritional macromolecules measured. Our final dataset thus included data from n = 14 studies. We then proceeded to fit linear regression models to these data for each of the six groups of macromolecules of interest and N (listed above). We present and interpret results from these analyses in Figure B.9.

B.9 Additional Tables

Here we provide additional tables from our analyses of the influence of forage elemental composition on home range size of snowshoe hare. Table B.1 and Table B.2 show top ranking models for the analyses ran on home range size estimates at 75% and 90% AKDEc isopleths, respectively. Table B.3 provides details on the degree of overlap between home range estimates for the four individuals for which we had two years of telemetry data. Table B.4 provides a breakdown of the number of foliar material samples collected for each plant species of interest, in each study site. Table B.5 present summary statistics and coefficient estimates for the Stoichiometric Distribution Models we used to predict forage species stoichiometry over our study area. In Tables B.6 to B.10, we show the full AICc model selection tables for home range size calculated at the 50% UD, for each stoichiometric ratio. Likewise, in Tables B.11 to B.15 we present the full AICc model selection tables for home range size at the 75% UD. Finally, in Tables B.16 to B.20 we show full AICc model selection tables for home range size at 90% UD.

Table B.1: Top ranking GLMs describing relationship between home range area at the 75% AKDEc isopleth and resource stoichiometry, after removing uninformative parameters (see Table 2 in the main text for a list of variables included in each model and appendix B.9.1 for full AICc tables). For each plant SOI and stoichiometric ratio pair, we report the top model, any model above the intercept, and the intercept. For coefficients, we report values estimates and 95% Confidence Intervals. Mean and coefficient of variation (CV) refer to the metrics calculated for the relevant stoichiometric ratio within the home range core area (see main text for details). Column headers: k, number of parameters in the model; LL, log-likelihood.

				Coefficients		
k	ΔAICc	LL	R^2	Intercept	Mean	CV
Lowbush blueberry C:N top models						
4	0.00	−70.99	0.66	−449.17 (−685.52– −212.83)	9.50 (4.49–14.52)	8.16 (5.59–10.73)
3	10.65	−77.65	0.47	−1.64 (−5.06–1.78)		7.59 (4.47–10.71)
3	25.70	−85.17	0.12	−352.62 (−721.30–16.09)	7.63 (−0.21–15.47)	
2	27.20	−87.16	0.00	6.10 (4.42–7.78)		
Lowbush blueberry N:P top models						
3	0.00	−85.46	0.11	18.94 (−46.93–9.05)	0.86 (−0.10–1.82)	
2	0.93	−87.16	0.00	6.10 (4.42–7.78)		
Lowbush blueberry C:P top models						
3	0.00	−85.13	0.13	−17.93 (−42.36–6.51)	0.02 (−0.00–0.04)	
2	1.60	−87.16	0.00	6.10 (4.42–7.78)		
Red maple N:P top models						
3	0.00	−85.88	0.08	2.36 (−2.74–7.46)		1.04 (−0.31–2.39)
2	0.10	−87.16	0.00	6.10 (4.42–7.78)		
Red maple C:N top models						
3	0.00	−85.39	0.11	2.48 (−1.80–6.75)		0.37 (−0.03–0.76)
2	1.06	−87.16	0.00	6.10 (4.42–7.78)		

Table B.2: Top ranking GLMs describing relationship between home range area at the 90% AKDEc isopleth and resource stoichiometry, after removing uninformative parameters. All specification as in Table B.1.

				Coefficients		
k	ΔAICc	LL	R^2	Intercept	Mean	CV
Lowbush blueberry C:N top models						
4	0.00	−85.50	0.66	−895.04 (−1313.68– −476.39)	18.94 (10.04–27.84)	13.95 (9.19–18.71)
3	13.35	−93.51	0.43	−4.21 (−11.00–2.58)		13.52 (7.43–19.61)
3	22.82	−98.25	0.21	−827.72 (−1454.51– −200.92)	17.82 (4.49–31.15)	
2	27.46	−101.81	0.00	10.11 (7.37–12.84)		
Lowbush blueberry N:P top models						
3	0.00	−100.37	0.09	−29.08 (−77.07–18.91)	1.35 (−0.30–2.99)	
2	0.39	−101.81	0.00	10.11 (7.37–12.84)		
Lowbush blueberry C:P top models						
3	0.00	−100.16	0.10	−27.14 (−69.62–15.33)	0.03 (−0.00–0.06)	
2	0.81	−101.81	0.00	10.11 (7.37–12.84)		
Red maple N:P top models						
2	0.00	−101.81	0.00	10.11 (7.37–12.84)		
Red maple C:N top models						
3	0.00	−100.56	0.08	4.09 (−4.27–12.44)		0.59 (−0.19–1.37)
2	0.02	−101.81	0.00	10.11 (7.37–12.84)		

Table B.3: Quantification of home range core area overlap for the four individuals with more than one year of telemetry sampling (see Appendix B.7.1), as calculated with the Bhattacharyya affinity index (Fieberg and Kochanny 2005; Winner et al. 2018). Note that we calculated the overlap for the whole Utilization Distribution (UD) of each individual between consecutive years of telemetry sampling. Figures B.3 to B.6 provide a visual representation of the overlap among these yearly home ranges.

UD1	UD2	Bhattacharyya Index
A1425		
2018	2018	1.00
2019	2018	0.84
2018	2019	0.84
2019	2019	1.00
A1698		
2018	2018	1.00
2019	2018	0.26
2018	2019	0.26
2019	2019	1.00
A3719		
2017	2017	1.00
2018	2017	0.91
2017	2018	0.91
2018	2018	1.00
A3769		
2018	2018	1.00
2019	2018	0.84
2018	2019	0.84
2019	2019	1.00

Table B.4: Breakdown of foliar samples collected per plant species of interest (SOI), per study site. Study sites are listed by forest stand age, from youngest to oldest. For each plant SOI, we provide a breakdown of how many samples were collected for stoichiometric analyses and for local biomass extimation, respectively.

Sample	Bloomfield	Unicorn	Terra Nova North	Dunphy's Pond
Red maple				
Stoichiometry	2	30	19	40
Biomass	10	14	13	20
White birch				
Stoichiometry	11	25	15	20
Biomass	9	13	12	16
Lowbush blueberry				
Stoichiometry	39	36	41	44
Biomass	14	10	10	16

Table B.5: Summary model selection table for the Stoichiometric Distribution Models used to predict foliar C:N, C:P, N:P values over the study area. We report the top-ranked models within 2ΔAICc of the highest ranked one. For each model, we report coefficient estimates and 95% Confidence Intervals. Column headers: k, number of parameters, LL, log-likelihood, Age Class 3 (41–60 years old), Age Class 4 (61–80 y.o.), Age Class 5 (81–100 y.o.), Height Class 3 (6.6 m to 9.5 m), Height Class 4 (9.6 m to 12.5 m), Height Class 5 (12.6 m to 15.5 m), Crown Density 2 (51–75%), Crown Density 3 (26–50%), Crown Density 4 (10–25%). Adapted from Heckford et al. (2021).

				Coefficients															
k	ΔAICc	LL	R^2	Intercept	Land Cover		Productivity	Biotic									Abiotic		
					Deciduous	Mixed wood		Age Class 3	Age Class 4	Age Class 5	Height Class 3	Height Class 4	Height Class 5	Crown Density 2	Crown Density 3	Crown Density 4	Aspect	Slope	Elevation
Lowbush blueberry C:N ratio models																			
3	0.00	−539.51	0.09	48.81 (47.71–49.91)			−2.21 (−3.31– −1.11)												
5	0.79	−537.79	0.11	48.14 (45.35–50.93)	5.87 (−0.62–12.38)	0.60 (−2.67–3.86)	−2.45 (−3.79– −1.11)												
Lowbush blueberry C:P ratio models																			
11	0.00	−1189.78	0.33	1236.66 (871.64–1601.45)				600.19 (347.73–852.65)	438.81 (82.57–795.06)	585.00 (305.37–864.64)	18.98 (−224.77–262.73)	118.38 (−170.51–407.27)	−6.08 (−335.39–323.23)	−48.19 (−384.27–287.89)	49.93 (−265.13–365.00)	204.86 (−224.67–634.39)			
12	0.03	−1188.63	0.34	1188.23 (819.07–1557.39)			69.94 (−23.29–163.18)	653.17 (391.96–914.39)	578.27 (177.66–978.87)	652.94 (360.03–945.85)	18.95 (−223.87–261.76)	84.36 (−206.97–375.69)	−90.02 (−436.61–256.58)	−33.56 (−368.91–301.79)	45.40 (−268.51–359.31)	190.11 (−238.21–618.44)			
Lowbush blueberry N:P ratio models																			
15	0.00	−541.26	0.41	29.35 (22.46–36.24)			2.44 (0.70–4.19)	11.99 (5.63–18.35)	7.76 (−0.20–15.73)	11.98 (6.45–17.51)	−1.98 (−6.35–2.39)	1.17 (−3.99–6.32)	−2.31 (−8.54–3.92)	−2.84 (−8.86–3.19)	−1.46 (−7.02–4.10)	−0.13 (−7.71–7.44)	−1.33 (−3.00–0.34)	0.05 (−1.59–1.69)	−1.72 (−3.36– −0.08)
12	0.04	−544.89	0.39	27.62 (21.02–34.23)			3.05 (1.38–4.72)	13.24 (8.57–17.91)	10.93 (3.76–18.10)	13.45 (8.21–18.69)	−1.26 (−5.61–3.08)	1.20 (−4.02–6.41)	−2.89 (−9.09–3.31)	−2.39 (−8.39–3.61)	−1.84 (−7.46–3.77)	0.06 (−7.60–7.73)			
17	0.94	−539.24	0.43	31.58 (23.67–39.50)	−7.48 (−15.25–0.29)	−3.46 (−8.47–1.56)	2.63 (0.89–4.37)	11.98 (5.58–18.37)	6.42 (−2.25–15.10)	12.28 (6.64–17.91)	−2.28 (−6.65–2.09)	0.62 (−4.55–5.79)	−2.30 (−8.50–3.89)	−1.37 (−7.56–4.81)	−0.06 (−5.83–5.71)	0.48 (−7.10–8.06)	−1.30 (−2.96–0.36)	0.26 (−1.42–1.94)	−1.74 (−3.38– −0.11)
14	1.44	−543.2	0.4	29.27 (21.88–36.66)	−7.02 (−14.86–0.83)	−3.00 (−7.92–1.91)	3.26 (1.58–4.94)	13.57 (8.89–18.25)	10.27 (2.64–17.90)	14.00 (8.69–19.32)	−1.61 (−5.96–2.74)	0.64 (−4.59–5.88)	−2.85 (−9.03–3.33)	−0.95 (−7.16–5.27)	−0.58 (−6.41–5.26)	0.62 (−7.07–8.31)			
Red maple C:N ratio models																			
13	0.00	−267.39	0.39	23.77 (16.69–30.85)	7.80 (2.01–13.59)	3.02 (−1.36–7.40)		12.05 (4.81–19.29)	16.38 (8.79–23.97)	13.51 (7.45–19.58)	−4.60 (−11.19–1.98)	−7.48 (−12.45– −2.50)	−11.94 (−16.77– −7.10)	4.10 (−0.20–8.40)	6.04 (1.28–10.79)	6.98 (1.19–12.77)			
Red maple N:P ratio models																			
6	0.00	−324.45	0.17	29.44 (27.63–31.25)			2.37 (0.52–4.21)										−1.87 (−4.07–0.33)	−2.52 (−4.72– −0.33)	−3.67 (−5.84– −1.50)

B.9.1 Model Selection Tables

B.9.1.1 Model selection for home range area calculated at 50% UD

Table B.6: Full AICc table for the model set fit to home range size at the 50% UD (core area) using stoichiometric data from red maple C:N, sorted in ascending order of ΔAICc. Uninformative parameters (*sensu* Leroux 2019) include the mean C:N ratio values and body weight. Column headers: k, number of parameters in the model, LL, log-likelihood. Colons indicate interaction terms, asterisks identify uninformative parameters.

Models	k	AICc	ΔAICc	LL	R^2
Home Range size ∼ C:N CV	3	138.07	0.00	−65.57	0.11
Home Range size ∼ C:N CV + Weight*	4	138.31	0.24	−64.36	0.18
Intercept	2	138.93	0.86	−67.25	0.00
Home Range size ∼ Mean C:N* + C:N CV	4	140.56	2.49	−65.48	0.11
Home Range size ∼ Mean C:N* + Weight*	4	141.01	2.93	−65.70	0.10
Home Range size ∼ Mean C:N*	3	141.08	3.01	−67.08	0.01
Home Range size ∼ Mean C:N* + C:N CV + Weight*	5	141.17	3.10	−64.34	0.18
Home Range size ∼ Mean C:N* + CV C:N + Mean:CV	5	143.45	5.38	−65.48	0.11
Home Range size ∼ Mean C:N* + C:N CV + Mean:CV + Weight*	6	144.26	6.19	−64.31	0.18

Table B.7: Full AICc table for the model set fit to home range size at the 50% UD (core area) using stoichiometric data from red maple N:P, sorted in ascending order of ΔAICc. Uninformative parameters (*sensu* Leroux 2019) include the mean N:P ratio values and body weight. Column headers: k, number of parameters in the model, LL, log-likelihood. Colons indicate interaction terms, asterisks identify uninformative parameters.

Models	k	AICc	ΔAICc	LL	R^2
Home Range size ∼ N:P CV	3	137.06	0.00	−65.07	0.14
Home Range size ∼ N:P CV + Weight*	4	137.89	0.83	−64.15	0.19
Home Range size ∼ Mean N:P* + N:P CV + Mean:CV	5	138.78	1.72	−63.14	0.24
Intercept	2	138.93	1.87	−67.25	0.00
Home Range size ∼ Mean N:P* + N:P CV	4	139.10	2.04	−64.75	0.15
Home Range size ∼ Mean N:P* + N:P CV + Mean:CV + Weight*	6	139.78	2.72	−62.06	0.29
Home Range size ∼ Mean N:P* + N:P CV + Weight*	5	140.02	2.96	−63.76	0.21
Home Range size ∼ Mean N:P* + Weight*	4	141.04	3.98	−65.72	0.10
Home Range size ∼ Mean N:P*	3	141.16	4.10	−67.12	0.01

Table B.8: Full AICc table for the model set fit to home range size at the 50% UD (core area) using stoichiometric data from lowbush blueberry C:N, sorted in ascending order of ΔAICc. Uninformative parameters (*sensu* Leroux 2019) include body weight and the interaction of C:N ratio mean and CV. Column headers: k, number of parameters in the model, LL, log-likelihood. Colons indicate interaction terms, asterisks identify uninformative parameters.

Models	k	AICc	ΔAICc	LL	R^2
Home Range size ∼ Mean C:N + C:N CV	4	108.47	0.00	−49.43	0.70
Home Range size ∼ Mean C:N + C:N CV + Weight*	5	109.68	1.22	−48.59	0.71
Home Range size ∼ Mean C:N + C:N CV + Mean:CV*	5	110.19	1.72	−48.84	0.71
Home Range size ∼ Mean C:N + C:N CV + Mean:CV* + Weight*	6	111.86	3.39	−48.11	0.72
Home Range size ∼ C:N CV	3	123.33	14.87	−58.21	0.45
Home Range size ∼ C:N CV + Weight*	4	125.25	16.78	−57.83	0.47
Home Range size ∼ Mean C:N + Weight*	4	136.20	27.73	−63.30	0.23
Home Range size ∼ Mean C:N	3	137.66	29.19	−65.37	0.12
Intercept	2	138.93	30.47	−67.25	0.00

Table B.9: Full AICc table for the model set fit to home range size at the 50% UD (core area) using stoichiometric data from lowbush blueberry C:P, sorted in ascending order of ΔAICc. Body weight and the coefficient of variation are uninformative parameters (*sensu* Leroux 2019). Column headers: k, number of parameters in the model, LL, log-likelihood. Colons indicate interaction terms, asterisks identify uninformative parameters.

Models	k	AICc	ΔAICc	LL	R^2
Home Range size ∼ Mean C:P	3	138.20	0.00	−65.64	0.10
Home Range size ∼ Mean C:P + Weight*	4	138.24	0.04	−64.32	0.18
Intercept	2	138.93	0.73	−67.25	0.00
Home Range size ∼ Mean C:P + C:P CV* + Weight*	5	140.44	2.24	−63.97	0.20
Home Range size ∼ Mean C:P + C:P CV*	4	140.50	2.29	−65.45	0.11
Home Range size ∼ C:P CV*	3	140.61	2.40	−66.84	0.03
Home Range size ∼ C:P CV* + Weight*	4	140.65	2.45	−65.53	0.11
Home Range size ∼ Mean C:P + C:P CV* + Mean:CV	5	141.41	3.21	−64.45	0.17
Home Range size ∼ Mean C:P + C:P CV* + Mean:CV + Weight*	6	142.15	3.95	−63.25	0.23

Table B.10: Full AICc table for the model set fit to home range size at the 50% UD (core area) using stoichiometric data from lowbush blueberry N:P, sorted in ascending order of ΔAICc. Column headers: k, number of parameters in the model, LL, log-likelihood. Colons indicate interaction terms.

Models	k	AICc	ΔAICc	LL	R^2
Home Range size ∼ Mean N:P	3	138.91	0.00	−65.99	0.08
Intercept	2	138.93	0.03	−67.25	0.00
Home Range size ∼ Mean N:P + Weight	4	138.95	0.04	−64.68	0.16
Home Range size ∼ N:P CV	3	140.22	1.31	−66.65	0.04
Home Range size ∼ N:P CV + Weight	4	140.43	1.53	−65.42	0.12
Home Range size ∼ Mean N:P + N:P CV + Weight	5	141.48	2.57	−64.49	0.17
Home Range size ∼ Mean N:P + N:P CV	4	141.50	2.59	−65.95	0.08
Home Range size ∼ Mean N:P + N:P CV + Mean:CV	5	143.87	4.96	−65.68	0.10
Home Range size ∼ Mean N:P + N:P CV + Mean:Cv + Weight	6	144.46	5.55	−64.41	0.17

B.9.1.2 Model selection for home range area calculated at 75% UD

Table B.11: Full AICc table for the model set fit to home range size at the 75% UD using stoichiometric data from red maple C:N, sorted in ascending order of ΔAICc. Uninformative parameters (*sensu* Leroux 2019) including body weight and the mean C:N ratio. Column headers: k, number of parameters in the model, LL, log-likelihood. Colons indicate interaction terms, asterisks identify uninformative parameters.

Models	k	AICc	ΔAICc	LL	R^2
Home Range size ∼ C:N CV	3	177.71	0.00	−85.39	0.11
Home Range size ∼ C:N CV + Weight*	4	178.37	0.66	−84.38	0.17
Intercept	2	178.77	1.06	−87.16	0.00
Home Range size ∼ Mean C:N* + C:N CV	4	180.38	2.67	−85.39	0.11
Home Range size ∼ Mean C:N*	3	181.13	3.42	−87.10	0.00
Home Range size ∼ Mean C:N* + Weight*	4	181.24	3.53	−85.82	0.09
Home Range size ∼ Mean C:N* + C:N CV + Weight*	5	181.27	3.56	−84.38	0.17
Home Range size ∼ Mean C:N* + C:N CV + Mean:CV	5	182.96	5.26	−85.23	0.12
Home Range size ∼ Mean C:N* + C:N CV + Mean:CV + Weight*	6	184.22	6.51	−84.28	0.18

Table B.12: Full AICc table for the model set fit to home range size at the 75% UD using stoichiometric data from red maple N:P, sorted in ascending order of ΔAICc. Body weight and mean N:P ratio are uninformative parameters (*sensu* Leroux 2019). Column headers: k, number of parameters in the model, LL, log-likelihood. Colons indicate interaction terms, asterisks identify uninformative parameters.

Models	k	AICc	ΔAICc	LL	R^2
Home Range size ∼ N:P CV	3	178.67	0.00	−85.88	0.08
Intercept	2	178.77	0.10	−87.16	0.00
Home Range size ∼ N:P CV + Weight*	4	179.41	0.74	−84.91	0.14
Home Range size ∼ Mean N:P* + N:P CV	4	180.79	2.12	−85.60	0.10
Home Range size ∼ Mean N:P*	3	181.25	2.58	−87.16	0.00
Home Range size ∼ Mean N:P* + Weight*	4	181.26	2.58	−85.83	0.09
Home Range size ∼ Mean N:P* + N:P CV + Weight*	5	181.55	2.88	−84.53	0.16
Home Range size ∼ Mean N:P* + N:P CV + Mean:CV	5	182.73	4.05	−85.11	0.13
Home Range size ∼ Mean N:P* + N:P CV + Mean:CV + Weight*	6	183.36	4.68	−83.85	0.20

Table B.13: Full AICc table for the model set fit to home range size at the 75% UD using stoichiometric data from lowbush blueberry C:N, sorted in ascending order of ΔAICc. Uninformative parameters (*sensu* Leroux 2019) include body weight and the interaction of C:N ratio mean and CV. Column headers: k, number of parameters in the model, LL, log-likelihood. Colons indicate interaction terms, asterisks identify uninformative parameters.

Models	k	AICc	ΔAICc	LL	R^2
Home Range size ∼ Mean C:N + C:N CV	4	151.57	0.00	−70.99	0.66
Home Range size ∼ Mean C:N + C:N CV + Weight*	5	153.21	1.64	−70.36	0.67
Home Range size ∼ Mean C:N + C:N CV + Mean:CV*	5	154.25	2.67	−70.87	0.66
Home Range size ∼ Mean C:N + C:N CV + Mean:CV* + Weight*	6	156.35	4.77	−70.35	0.67
Home Range size ∼ C:N CV	3	162.22	10.65	−77.65	0.47
Home Range size ∼ C:N CV + Weight*	4	163.68	12.11	−77.04	0.49
Home Range size ∼ Mean C:N + Weight*	4	177.20	25.62	−83.80	0.20
Home Range size ∼ Mean C:N	3	177.27	25.70	−85.17	0.12
Intercept	2	178.77	27.20	−87.16	0.00

Table B.14: Full AICc table for the model set fit to home range size at the 75% UD using stoichiometric data from lowbush blueberry C:P, sorted in ascending order of ΔAICc. Body weight and C:P ratio CV are uninformative parameters (*sensu* Leroux 2019). Column headers: k, number of parameters in the model, LL, log-likelihood. Colons indicate interaction terms, asterisks identify uninformative parameters.

Models	k	AICc	ΔAICc	LL	R^2
Home Range size ∼ Mean C:P	3	177.18	0.00	−85.13	0.13
Home Range size ∼ Mean C:P + C:P CV*	4	177.79	0.61	−84.09	0.19
Home Range size ∼ Mean C:P + Weight*	4	178.12	0.95	−84.26	0.18
Home Range size ∼ Mean C:P + C:P CV* + Weight*	5	178.70	1.53	−83.10	0.24
Intercept	2	178.77	1.60	−87.16	0.00
Home Range size ∼ Mean C:P + C:P CV* + Mean:CV	5	180.39	3.22	−83.95	0.19
Home Range size ∼ C:P CV*	3	180.94	3.76	−87.01	0.01
Home Range size ∼ C:P CV* + Weight*	4	181.21	4.04	−85.81	0.09
Home Range size ∼ Mean C:P + C:P CV* + Mean:CV + Weight*	6	181.59	4.42	−82.97	0.24

Table B.15: Full AICc table for the model set fit to home range size at the 75% UD using stoichiometric data from lowbush blueberry N:P, sorted in ascending order of ΔAICc. Body weight and the CV of N:P ratio are uninformative parameters (*sensu* Leroux 2019). Column headers: k, number of parameters in the model, LL, log-likelihood. Colons indicate interaction terms, asterisks mark uninformative parameters.

Models	k	AICc	ΔAICc	LL	R^2
Home Range size ∼ Mean N:P	3	177.84	0.00	−85.46	0.11
Intercept	2	178.77	0.93	−87.16	0.00
Home Range size ∼ Mean N:P + Weight*	4	178.81	0.97	−84.60	0.16
Home Range size ∼ Mean N:P + N:P CV*	4	178.93	1.09	−84.66	0.15
Home Range size ∼ Mean N:P + N:P CV* + Weight*	5	179.74	1.90	−83.62	0.21
Home Range size ∼ N:P CV*	3	180.59	2.75	−86.84	0.02
Home Range size ∼ N:P CV* + Weight*	4	181.07	3.22	−85.73	0.09
Home Range size ∼ Mean N:P + N:P CV* + Mean:CV	5	181.83	3.98	−84.66	0.15
Home Range size ∼ Mean N:P + N:P CV* + Mean:CV + Weight*	6	182.89	5.05	−83.62	0.21

B.9.1.3 Model selection for home range area calculated at 90% UD

Table B.16: Full AICc table for the model set fit to home range size at the 90% UD using stoichiometric data from red maple C:N, sorted in ascending order of ΔAICc. Column headers: k, number of parameters in the model, LL, log-likelihood. Colons indicate interaction terms.

Models	k	AICc	ΔAICc	LL	R^2
Home Range size ∼ C:N CV	3	208.04	0.00	−100.56	0.08
Intercept	2	208.06	0.02	−101.81	0.00
Home Range size ∼ C:N CV + Weight	4	208.96	0.92	−99.68	0.13
Home Range size ∼ Mean C:N	3	210.34	2.30	−101.71	0.01
Home Range size ∼ Mean C:N + C:N CV	4	210.72	2.68	−100.56	0.08
Home Range size ∼ Mean C:N + Weight	4	210.80	2.76	−100.60	0.08
Home Range size ∼ Mean C:N + C:N CV + Weight	5	211.86	3.82	−99.68	0.13
Home Range size ∼ Mean C:N + C:N CV + Mean:CV	5	213.44	5.40	−100.47	0.09
Home Range size ∼ Mean C:N + C:N CV + Mean:CV + Weight	6	214.96	6.92	−99.65	0.13

Table B.17: Full AICc table for the model set fit to home range size at the 90% UD using stoichiometric data from red maple N:P, sorted in ascending order of ΔAICc. Column headers: k, number of parameters in the model, LL, log-likelihood. Colons indicate interaction terms.

Models	k	AICc	ΔAICc	LL	R^2
Intercept	2	208.06	0.00	−101.81	0.00
Home Range size ∼ N:P CV	3	208.92	0.86	−101.00	0.05
Home Range size ∼ N:P CV + Weight	4	209.75	1.69	−100.07	0.11
Home Range size ∼ Mean N:P	3	210.44	2.38	−101.76	0.00
Home Range size ∼ Mean N:P + Weight	4	210.67	2.61	−100.53	0.08
Home Range size ∼ Mean N:P + N:P CV	4	210.85	2.80	−100.63	0.08
Home Range size ∼ Mean N:P + N:P CV + Weight	5	211.63	3.57	−99.56	0.14
Home Range size ∼ Mean N:P + N:P CV + Mean:CV	5	213.75	5.70	−100.63	0.08
Home Range size ∼ Mean N:P + N:P CV + Mean:CV + Weight	6	214.78	6.72	−99.56	0.14

Table B.18: Full AICc table for the model set fit to home range size at the 90% UD using stoichiometric data from lowbush blueberry C:N, sorted in ascending order of ΔAICc. Uninformative parameters (*sensu* Leroux 2019) include body weight and the interaction of C:N ratio mean and CV. Column headers: k, number of parameters in the model, LL, log-likelihood. Colons indicate interaction terms, asterisks identify uninformative parameters.

Models	k	AICc	ΔAICc	LL	R^2
Home Range size ∼ Mean C:N + C:N CV	4	180.60	0.00	−85.50	0.66
Home Range size ∼ Mean C:N + C:N CV + Weight*	5	183.06	2.46	−85.28	0.69
Home Range size ∼ Mean C:N + C:N CV + Mean:CV*	5	183.26	2.66	−85.38	0.67
Home Range size ∼ Mean C:N + C:N CV + Mean:CV* + Weight*	6	186.15	5.55	−85.25	0.67
Home Range size ∼ C:N CV	3	193.95	13.35	−93.51	0.43
Home Range size ∼ C:N CV + Weight*	4	195.38	14.78	−92.89	0.45
Home Range size ∼ Mean C:N	3	203.42	22.82	−98.25	0.21
Home Range size ∼ Mean C:N + Weight*	4	204.57	23.97	−97.48	0.25
Intercept	2	208.06	27.46	−101.81	0.00

Table B.19: Full AICc table for the model set fit to home range size at the 90% UD using stoichiometric data from lowbush blueberry C:P, sorted in ascending order of ΔAICc. Body weight and C:P ratio CV are uninformative parameters (*sensu* Leroux 2019). Column headers: k, number of parameters in the model, LL, log-likelihood. Colons indicate interaction terms, asterisks identify uninformative parameters.

Models	k	AICc	ΔAICc	LL	R^2
Home Range size ∼ Mean C:P	3	207.25	0.00	−100.16	0.10
Home Range size ∼ Mean C:P + C:P CV*	4	207.58	0.33	−98.99	0.17
Intercept	2	208.06	0.81	−101.81	0.00
Home Range size ∼ Mean C:P + Weight*	4	208.55	1.30	−99.47	0.14
Home Range size ∼ Mean C:P + C:P CV* + Weight	5	208.92	1.67	−98.21	0.21
Home Range size ∼ C:P CV*	3	210.41	3.16	−101.74	0.00
Home Range size ∼ Mean C:P + C:P CV* + Mean:CV	5	210.48	3.22	−98.99	0.17
Home Range size ∼ C:P CV* + Weight*	4	210.94	3.69	−100.67	0.07
Home Range size ∼ Mean C:P + C:P CV* + Mean:CV + Weight*	6	212.06	4.81	−98.20	0.21

Table B.20: Full AICc table for the model set fit to home range size at the 90% UD using stoichiometric data from lowbush blueberry N:P, sorted in ascending order of ΔAICc. Column headers: k, number of parameters in the model, LL, log-likelihood. Colons indicate interaction terms.

Models	k	AICc	ΔAICc	LL	R^2
Home Range size ∼ Mean N:P	3	207.67	0.00	−100.37	0.09
Intercept	2	208.06	0.39	−101.81	0.00
Home Range size ∼ Mean N:P + N:P CV	4	208.69	1.02	−99.54	0.14
Home Range size ∼ Mean N:P + Weight	4	209.01	1.34	−99.70	0.13
Home Range size ∼ Mean N:P + N:P CV + Weight	5	210.04	2.37	−98.77	0.18
Home Range size ∼ N:P CV	3	210.13	2.46	−101.60	0.01
Home Range size ∼ N:P CV + Weight	4	210.85	3.18	−100.63	0.08
Home Range size ∼ Mean N:P + N:P CV + Mean:CV	5	211.47	3.80	−99.48	0.14
Home Range size ∼ Mean N:P + N:P CV + Mean:CV + Weight	6	213.14	5.47	−98.74	0.19

B.10 Additional Figures

Here we provide supporting visual materials for our field protocols, analyses, and results. Figure B.1 shows the location of our study area. For an interactive study area map, please see the Supporting Code document. Figure B.2 provides a visualization of the grid layout. Figures B.3 to B.6 show the overlap in the 50%, 75%, and 90% AKDEc isopleths of the four individuals for which we had multiple sampling years. Figure B.7 provides a breakdown of the plant foliar samples collected in each study site, by plant species of interest and intended purpose (i.e., stoichiometric analyses or local plant biomass estimation). Figure B.8 shows a comparison of the C, N, P content of red maple and lowbush blueberry in our hare study area. In Figure B.9, we inspect the relationship between six classes of macromolecules and nitrogen content across 23 species of broadleaved and coniferous plants.

Figure B.1: Map of study area. Each dot represents a sampling area. The pink dot represent the hare study area, where both plant sampling and snowshoe hare triangulation took place. The green dots show the location of the three areas where we only performed plant sampling. In clockwise direction, starting from the pink dot, forest stad ages are 20–40 years old, 81–100 y.o., 41–60 y.o., and 61–80 y.o. The gray-shaded area with black outline is Terra Nova National Park. Inset (a) shows the relative position of the island of Newfoundland to the rest of Canada, with the pink dot showing the location of our study area on the island of Newfoundland. Inset (b) shows the location of the study area on the island of Newfoundland in pink, with the border of Terra Nova National Park in black.

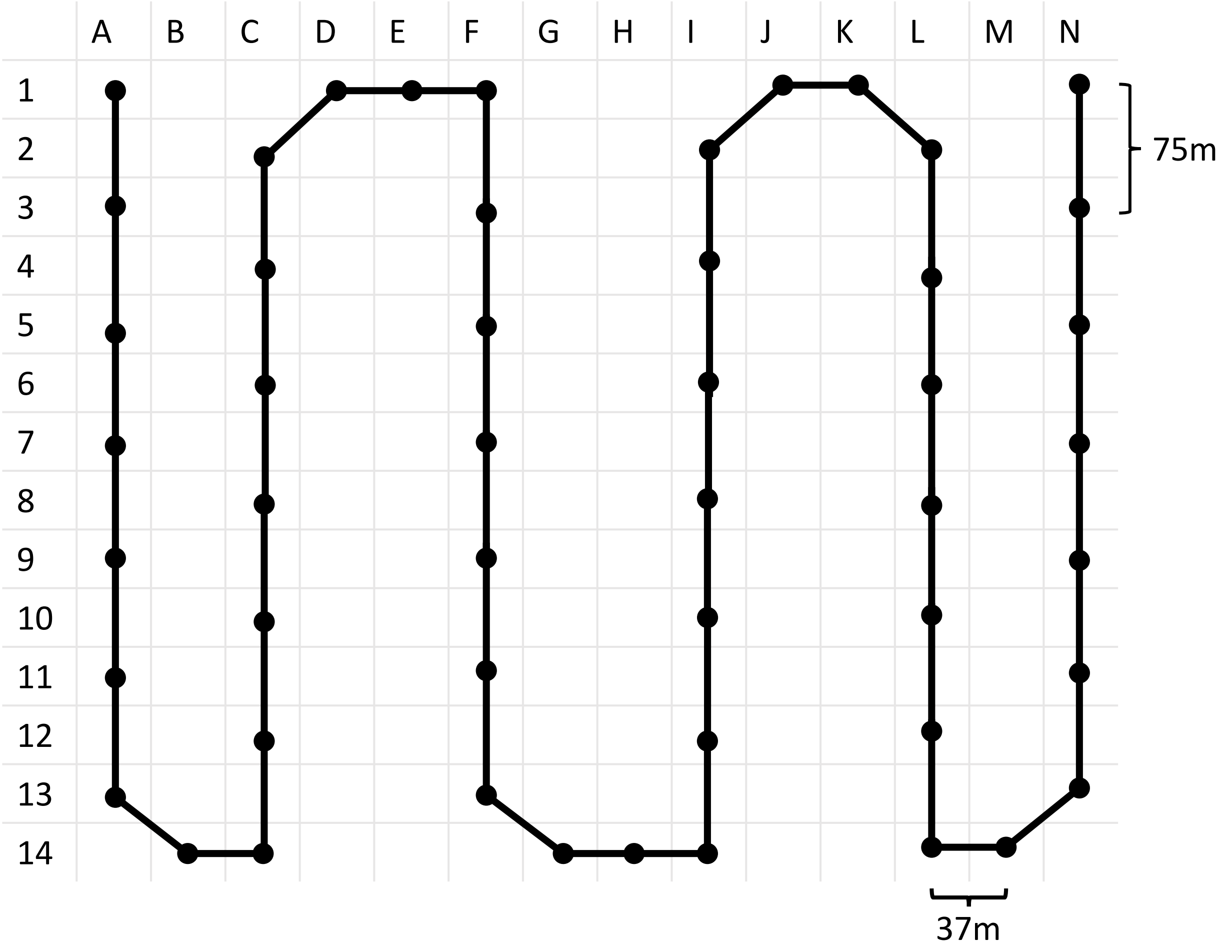

Figure B.2: Layout of a snowshoe hare trapping grid. The grid consists of 14 rows and 14 columns (fine gray lines). At each intersection we placed a trap (full circles), alternating odd and even rows on adjacent lines. Traps on a line were 75 m apart, the only exceptions being traps placed on turns for which the distance was necessarily shorter.

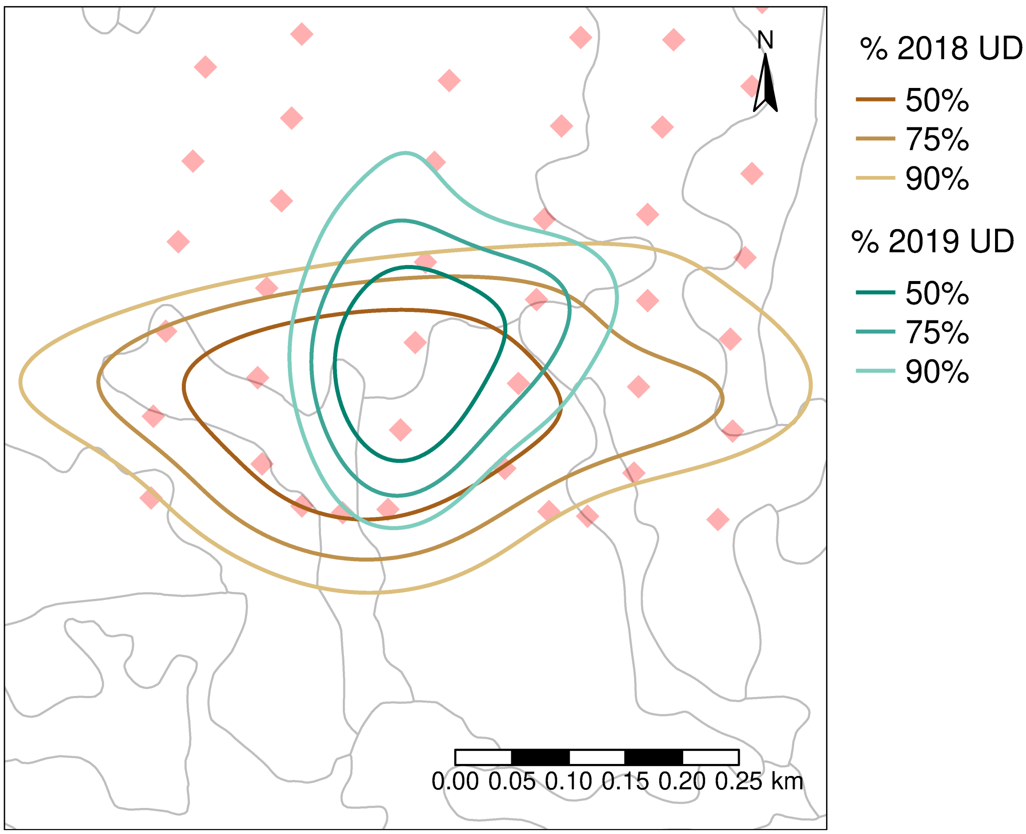

Figure B.3: Map showing the high degree of overlap between 2018 and 2019 kernel Utilization Distribution estimates for snowshoe hare A1425. For both years, the map shows the 50%, 75%, and 90% isopleth contours. Light red diamonds show traps locations on the trapping grid. Grey lines enclose Forest Resource Inventory-classified polygons.

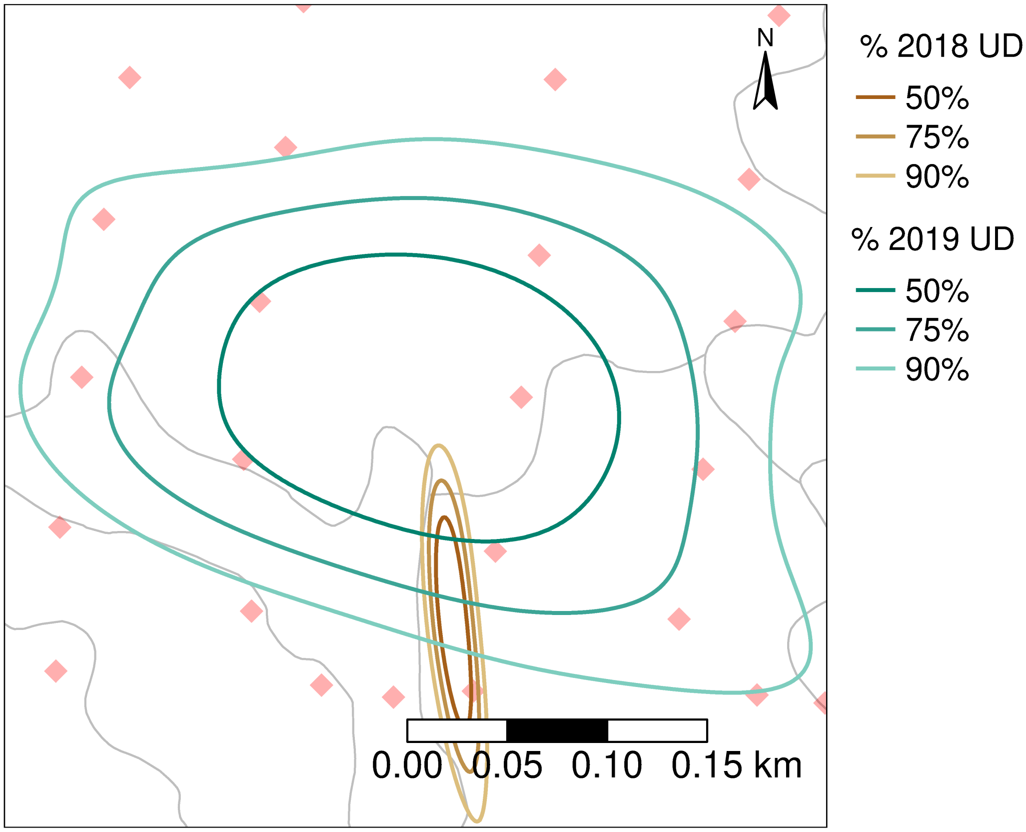

Figure B.4: Map showing the overlap between 2018 and 2019 kernel Utilization Distribution estimates for snowshoe hare A1698. For both years, the map shows the 50%, 75%, and 90% isopleth contours. All specifications as in Figure B.3.

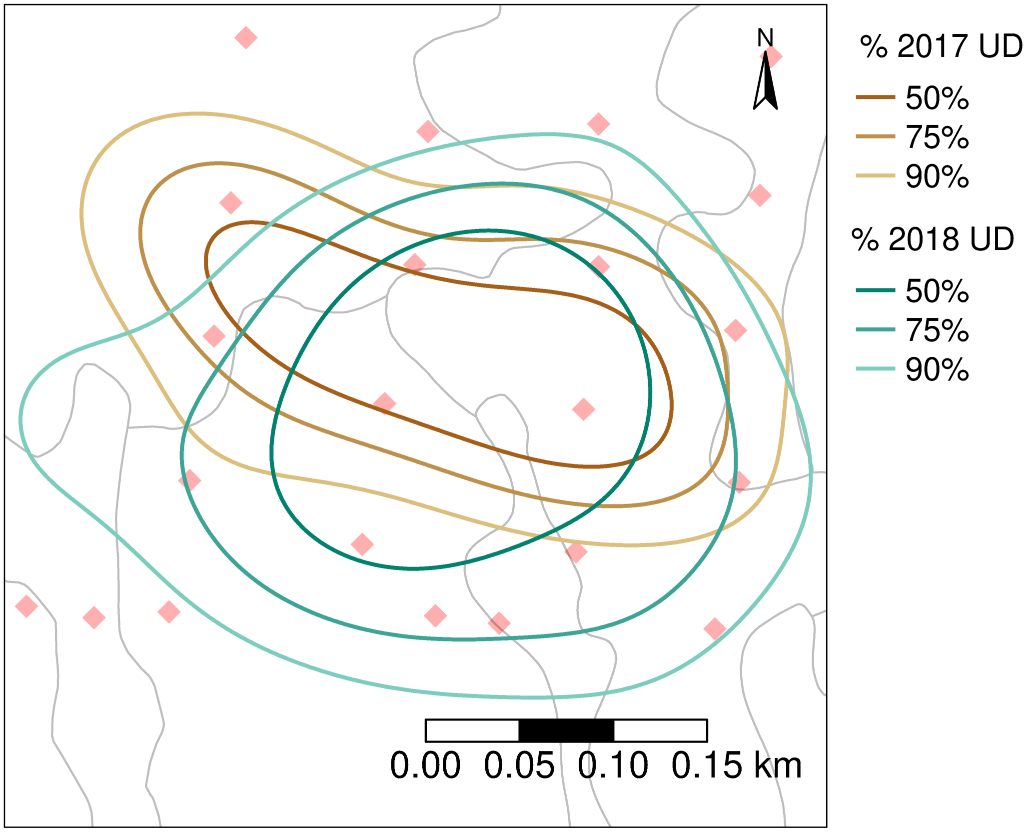

Figure B.5: Map showing the high degree of overlap between 2017 and 2018 kernel Utilization Distribution estimates for snowshoe hare A3719. For both years, the map shows the 50%, 75%, and 90% isopleth contours. Note that we do not show the AKDEc for 2019 as this individual died halfway through the sampling season, when not enough relocations had been collected to produce an estimate of its UD. All specifications as in Figure B.3.

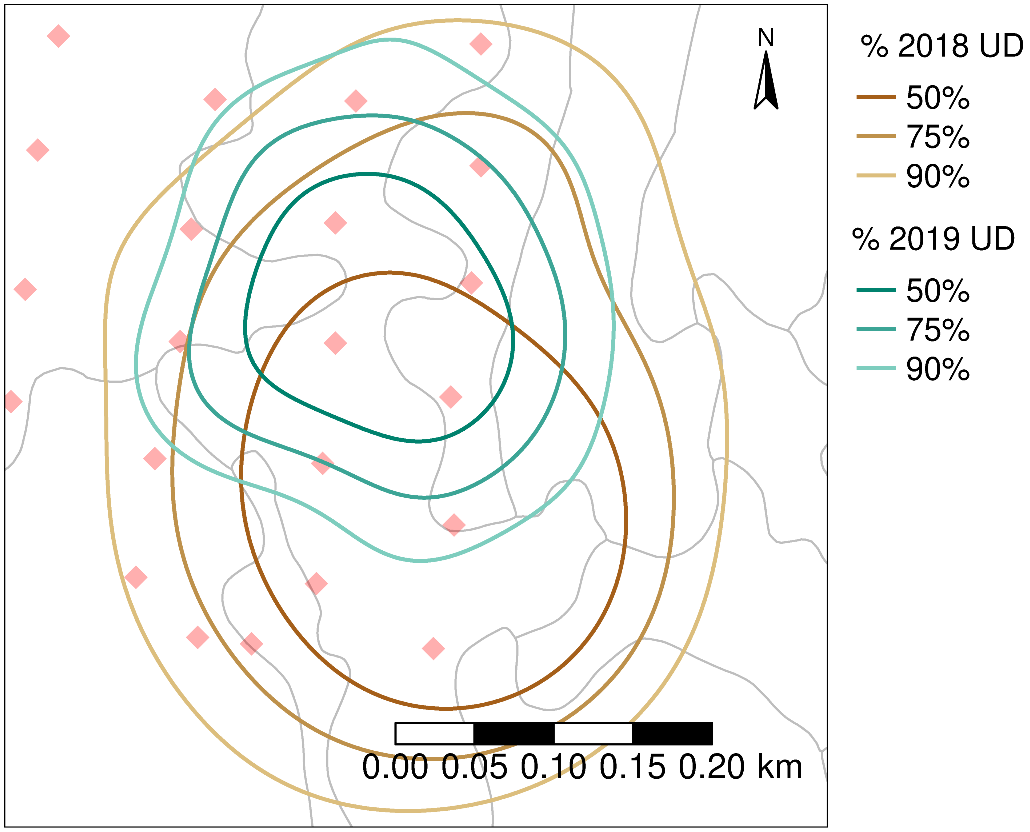

Figure B.6: Map showing the high degree of overlap between 2018 and 2019 kernel Utilization Distribution estimates for snowshoe hare A3769. For both years, the map shows the 50%, 75%, and 90% isopleth contours. All specifications as in Figure B.3.

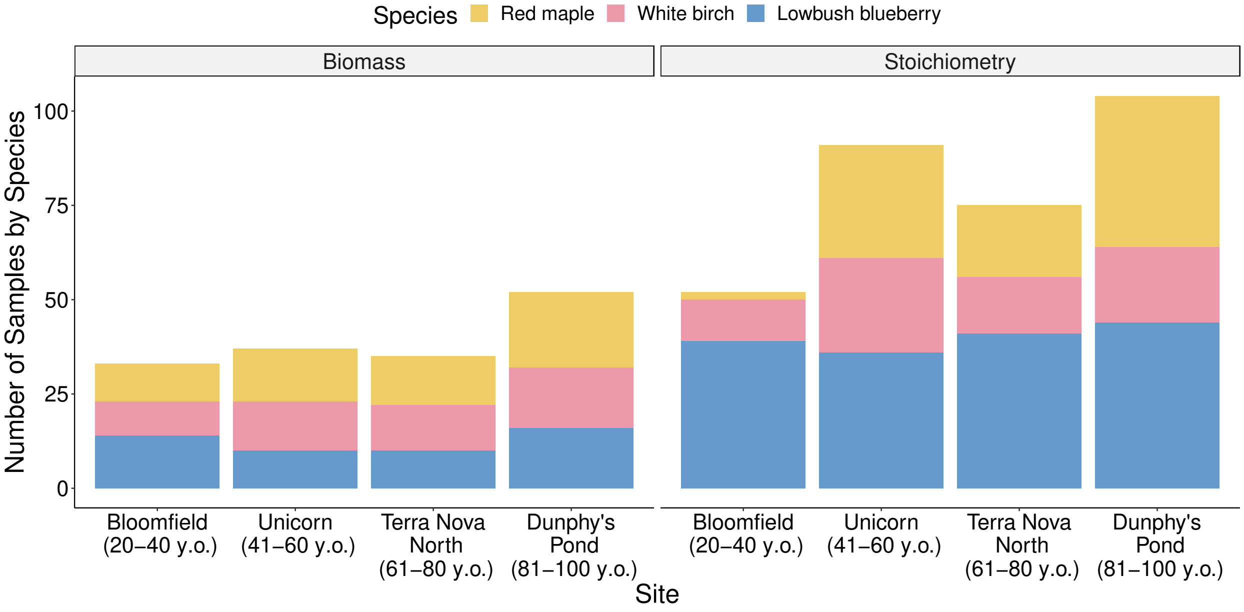

Figure B.7: Breakdown of the number of samples collected for each plant species of interest in each study site. Samples are identified as either "Stoichiometry" when intended for stoichiometric analyses, or as "Biomass" when intended for local plant species biomass estimation.

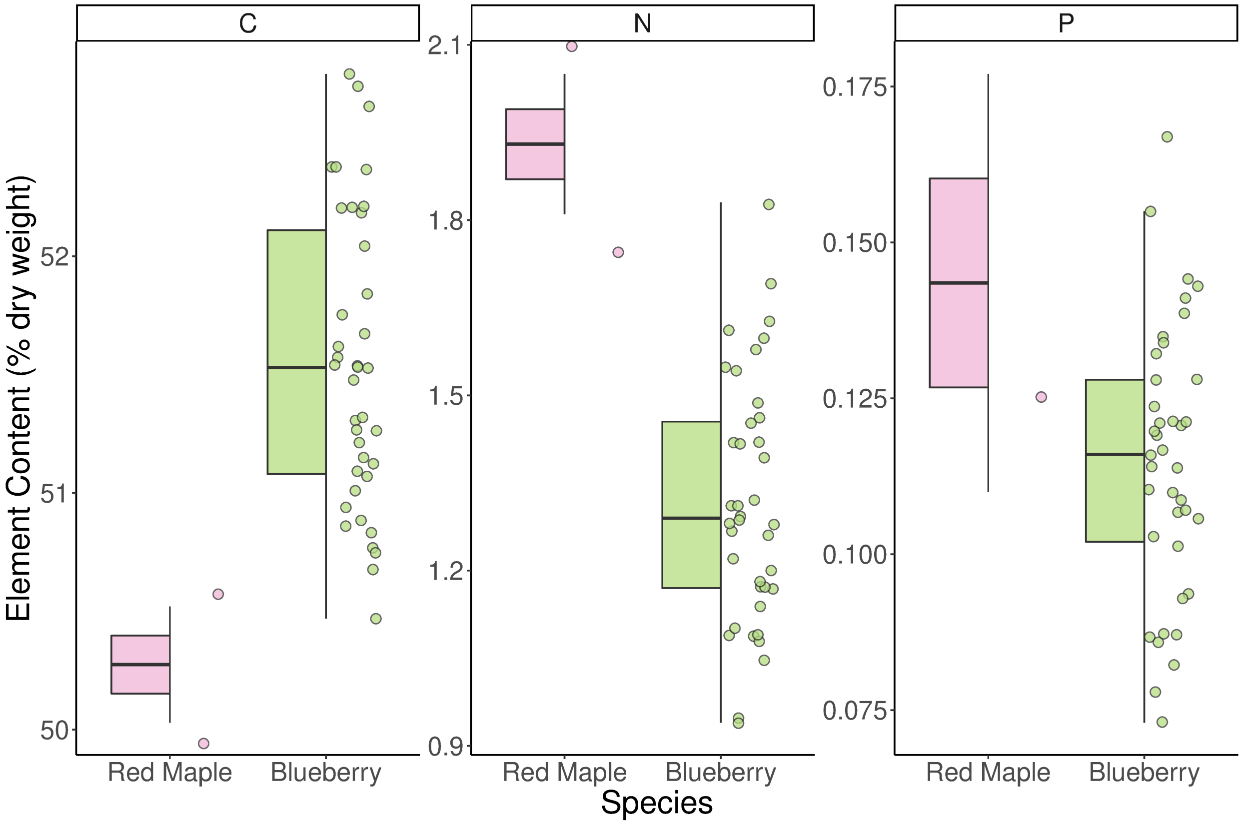

Figure B.8: Comparison of the elemental content of C, N, and P in red maple and lowbush blueberry in our hare study area. While red maple appears to have higher amounts of both N and P, the rarity of this plant on the grid makes lowbush blueberry a much more profitable forage species for snowshoe hares.

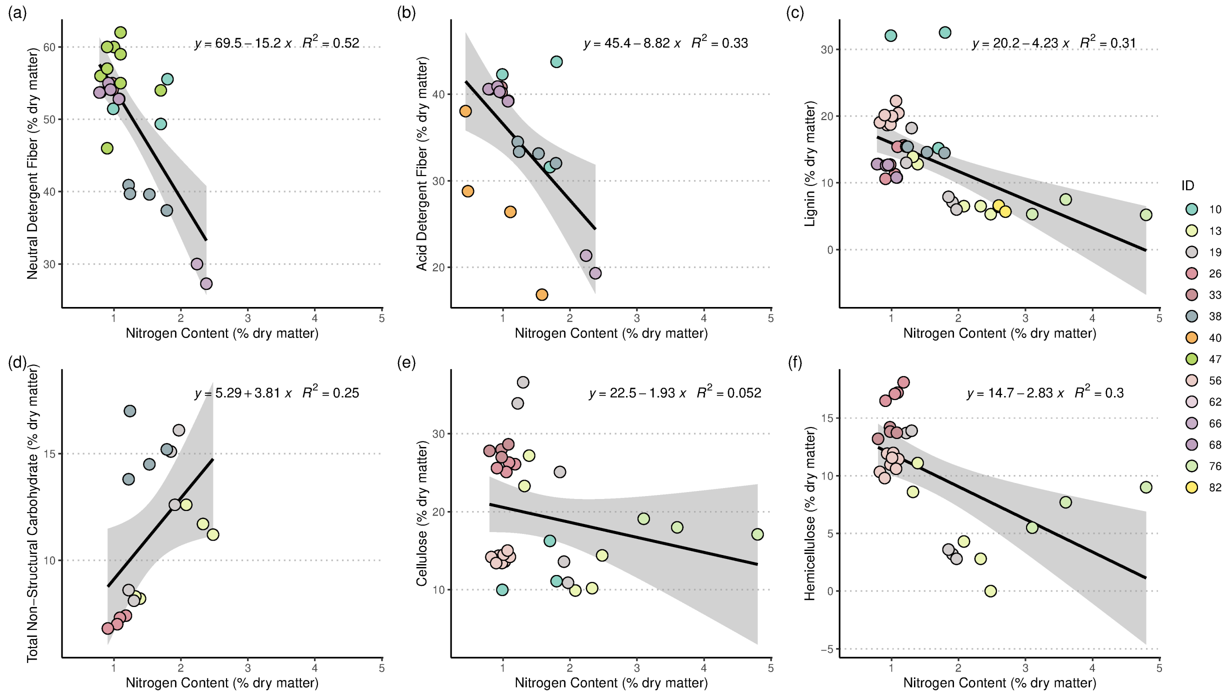

Figure B.9: Structural macromolecules can make up a significant portion of a plant's biomass and thus influence its uptake by consumers. Here, we use data collected from n = 14 published studies across 23 plant species to investigate the relationship between Nitrogen (N) and six C-based structural and non-structural compounds: (a) Neutral Detergent Fiber, (b) Acid Detergent Fiber, (c) Lignin, (d) Total Non-Structural Carbohydrates, (e) Cellulose, and (f) Hemicellulose. We sourced the studies from the datasets used in two recently published reviews: Felton et al. (2018) on the nutritional drivers underlying food selection in cervids and Champagne et al. (2020) on the role of phytochemicals in plant resistance to leporid and cervid herbivory. Except for Total Non-Structural Carbohydrates, structural macromolecules content decreases as N content increases—pointing towards a potentially higher nutritional value of plants containing high amounts of N for consumers. Solid black lines are linear regressions, and the light grey shaded area around them represent 95% Confidence Intervals. Data are grouped by study ID, see the online repository for the complete dataset, analyses code, and full references.

B.11 References

Barta, R. M., L. B. Keith, and S. M. Fitzgerald (1989). “Demography of sympatric arctic and snowshoe hare populations: an experimental assessment of interspecific competition”. *Canadian Journal of Zoology* 67.11, pp. 2762–2775. DOI: `10.1139/z89-392`.

Börger, L. et al. (2006). “Effects of sampling regime on the mean and variance of home range size estimates”. *Journal of Animal Ecology* 75 (6), pp. 1393–1405. DOI: `10.1111/j.1365-2656.2006.01164.x`.

Champagne, E. et al. (2020). “Phytochemicals Involved in Plant Resistance to Leporids and Cervids: a Systematic Review”. *Journal of Chemical Ecology* 46 (1), pp. 84–98. DOI: `10.1007/s10886-019-01130-z`.

Dodds, D. G. (1960). “Food Competition and Range Relationships of Moose and Snowshoe hare in Newfoundland”. *The Journal of Wildlife Management* 24 (1), pp. 52–60. DOI: `10.2307/3797356`.

Feldhamer, G. A., B. C. Thompson, and J. A. Chapman (2003). *Wild mammals of North America: biology, management, and conservation*. JHU Press.

Felton, A. M. et al. (2018). “The complexity of interacting nutritional drivers behind food selection, a review of northern cervids”. *Ecosphere* 9 (5). DOI: `10.1002/ecs2.2230`.

Fieberg, J. and C. O. Kochanny (2005). “QUANTIFYING HOME-RANGE OVERLAP:THE IMPORTANCE OF THE UTILIZATION DISTRIBUTION”. *The Journal of Wildlife Management* 69.4, pp. 1346–1359. DOI: `10.2193/0022-541X(2005)69[1346:QHOTIO]2.0.CO;2`.

Fleming, C. H. and J. M. Calabrese (2017). “A new kernel density estimator for accurate home-range and species-range area estimation”. *Methods in Ecology and Evolution* 8 (5), pp. 571–579. DOI: `10.1111/2041-210X.12673`.

— (2020). *ctmm: Continuous-Time Movement Modeling*. v. 0.5.10. URL: `https://cran.r-project.org/package=ctmm`.

Fleming, C. H., M. J. Noonan, et al. (2019). “Overcoming the challenge of small effective sample sizes in home-range estimation”. *Methods in Ecology and Evolution* 10 (10), pp. 1679–1689. DOI: `10.1111/2041-210X.13270`.

Gerber, B. D. et al. (2018). “Accounting for location uncertainty in azimuthal telemetry data improves ecological inference”. *Movement Ecology* 6 (1), pp. 1–14. DOI: `10.1186/s40462-018-0129-1`.

Heckford, T. R. et al. (2021). “Does where you live influence what you are made of? Spatial correlates of chemical traits across commonly occurring boreal plants”. *Landscape Ecology*. DOI: `10.1007/s10980-021-01334-3`.

Huwaldt, J. A. (2014). *Plot Digitizer*. http://plotdigitizer.sourceforge.net. URL: `http://plotdigitizer.sourceforge.net`.

Kaspari, M. and J. S. Powers (2016). “Biogeochemistry and Geographical Ecology: Embracing All Twenty-Five Elements Required to Build Organisms”. *The American Naturalist* 188 (S1), S62–S73. DOI: `10.1086/687576`.

Krebs, C. J., R. Boonstra, and S. Boutin (2018). “Using experimentation to understand the 10-year snowshoe hare cycle in the boreal forest of North America”. *Journal of Animal Ecology* 87.1. Ed. by K. Wilson, pp. 87–100. DOI: `10.1111/1365-2656.12720`. eprint: `0608246v3`.

Leroux, S. J. (2019). “On the prevalence of uninformative parameters in statistical models applying model selection in applied ecology”. *PLoS One* 14 (2), pp. 1–12. DOI: `10.1371/journal.pone.0206711`.

Mariotti, F., D. Tomé, and P. P. Mirand (2008). “Converting Nitrogen into Protein—Beyond 6.25 and Jones’ Factors”. *Critical Reviews in Food Science and Nutrition* 48.2, pp. 177–184. DOI: `10.1080/10408390701279749`.

Murray, D. L. (2002). “Differential body condition and vulnerability to predation in snowshoe hares”. *Journal of Animal Ecology* 71 (4), pp. 614–625. DOI: `10.1046/j.1365-2656.2002.00632.x`.

R Core Team (2020). *R: A Language and Environment for Statistical Computing*. R Foundation for Statistical Computing. Vienna, Austria. URL: `https://www.R-project.org/`.

Reynolds, J. J. et al. (2017). “Does prey density predict characteristics of primiparity in a solitary and specialized predator, the Canada lynx (*Lynx canadensis*)?” *Canadian Journal of Zoology* 95.10, pp. 779–785. DOI: `10.1139/cjz-2016-0269`.

Thornton, D. H. et al. (2013). “Habitat quality and population density drive occupancy dynamics of snowshoe hare in variegated landscapes”. *Ecography* 36.5, pp. 610–621. DOI: `10.1111/j.1600-0587.2012.07737.x`.

Winner, K. et al. (2018). “Statistical inference for home range overlap”. *Methods in Ecology and Evolution* 9.7. Ed. by K. Scales, pp. 1679–1691. DOI: `10.1111/2041-210X.13027`.

APPENDIX C

Supplementary Information for Chapter 4: Animal-vectored nutrient flow along different resource gradients influences the nature of local and meta-ecosystem functioning.

C.1 Introduction

Here we provide additional details on our model's equilibria and on our results. In Appendix Appendix C.2, we report all model equilibria—both feasible and unfeasible. In Appendix Appendix C.3, we show raw data results for the model analyses when we vary both environmental nutrient availability conditions and primary producers recycling rates. Stability analyses for the model can be found in the Supporting Code document, available through our online repository at: https://doi.org/10.6084/m9.figshare.16479933.

C.2 Model Equilibria

Here we report the feasible and un-feasible equilibria of our model (see text, eq. 4.1). As described above (Section 4.2.2.1), we first solve equation eq. 4.1g to find the quasi-equilibrium Q^* (eq. 4.2). We then substitute eq. 4.2 in equation eq. 4.1f and solve for C_2^*. Through subsequent rounds of substitution, we solve for all other state variables. Finally, we substitute the solution for C_1^* into eq. 4.2, to get the solution for Q^*.

Feasible equilibria:

$$N_1^* = \frac{(d_1 - d_1 e_1 + g)h_1 + a_1 e_1 I_1)}{a_1 e_1 l + (d_1 - d_1 e_1 + g)u_1} \tag{C.1a}$$

$$P_1^* = \frac{d_1 + g}{a_1 e_1} \tag{C.1b}$$

$$C_1^* = \frac{e_1(-h_1 l + I_1 u_1)}{a_1 e_1 l + (d_1 - d_1 e_1 + g)u_1} \tag{C.1c}$$

$$N_2^* = \frac{-a_1e_1(d_2(-1+e_2)h_2-a_2e_2I_2)lA+d_2(-1+e_2)(d_1(-1+e_1)-g)h_2Au_1+a_2(e_2(d_1+g)I_2Au_1-e_1(d_1e_2I_2Au_1+gm(h_1l-I_1u_1)))}{AB(a_2e_2l-d_2(-1+e_2)u2)} \tag{C.1d}$$

$$P_2^* = \frac{l(-d_2(d_1(-1+e_1)-g)h_2Au_1+a_2e_1gm(-h_1l+I_1u_1))+d_2(d_1e_1I_2Au_1-(d_1+g)I_2Au_1+e_1gm(h_1l-I_1u_1))u_2+a_1d_2e_1lA(h_2l-I_2u_2)}{a_2e_2h_2lAB-a_2(a_1e_1e_2I_2lA+e_2(d_1+g)I_2Au_1-e_1(d_1e_2I_2Au_1+gm(h_1l-I_1u_1)))u_2} \tag{C.1e}$$

$$C_2^* = \frac{\frac{e_1gm(-h_1l+I_1u_1)u_2}{AB+e_2(-h_2l+I_2u_2)}}{a_2e_2l-d_2(-1+e_2)u_2} \tag{C.1f}$$

$$Q^* = \frac{e_1g(-h_1l+I_1u_1)}{AB} \tag{C.1g}$$

Where,

$$A = (c+m)$$

$$B = (a_1e_1l+(d_1-d_1e_1+g)u_1)$$

Other, unfeasible equilibria:

Case 1:

$$N_1^* = \frac{I_1}{l} \tag{C.2a}$$

$$P_1^* = 0 \tag{C.2b}$$

$$C_1^* = 0 \tag{C.2c}$$

$$N_2^* = \frac{I_2}{l} \tag{C.2d}$$

$$P_2^* = 0 \tag{C.2e}$$

$$C_2^* = 0 \tag{C.2f}$$

Case 2:

$$N_1^* = \frac{(d_1-d_1e_1+g)h_1+a_1e_1I_1}{a_1e_1l+(d_1-d_1e_1+g)u_1} \tag{C.3a}$$

$$P_1^* = \frac{d_1 + g}{a_1 e_1} \tag{C.3b}$$

$$C_1^* = \frac{e_1(-h_1 l + I_1 u_1)}{a_1 e_1 l + (d_1 - d_1 e_1 + g)u_1} \tag{C.3c}$$

$$N_2^* = \frac{a_1 e_1 I_2 l(c + m) + (d_1 + g)I_2(c + m)u_1 - e_1(d_1 I_2(c + m)u_1 + gm(h_1 l - I_1 u_1))}{l(c + m)(a_1 e_1 l + (d_1 - d_1 e_1 + g)u_1)} \tag{C.3d}$$

$$P_2^* = 0 \tag{C.3e}$$

$$C_2^* = \frac{e_1 gm(-h_1 l + I_1 u_1)}{d_2(c + m)(a_1 e_1 l + (d_1 - d_1 e_1 + g)u_1)} \tag{C.3f}$$

Case 3:

$$N_1^* = \frac{I_1}{l} \tag{C.4a}$$

$$P_1^* = 0 \tag{C.4b}$$

$$C_1^* = 0 \tag{C.4c}$$

$$N_2^* = \frac{d_2 h_2 - d_2 e_2 h_2 + a_2 e_2 I_2}{a_2 e_2 l + d_2 u_2 - d_2 e_2 u_2} \tag{C.4d}$$

$$P_2^* = \frac{d_2}{a_2 e_2} \tag{C.4e}$$

$$C_2^* = \frac{e_2(-h_2 l + I_2 u_2)}{a_2 e_2 l - d_2(-1 + e_2)u_2} \tag{C.4f}$$

C.3 Additional Figures

Here, we present additional figures that provide more detail into our model's result. In Figure C.1, we report the untransformed values for the results shown in Figure 4.3. Figures C.2 and C.3 report the untransformed values for the results presented in Figure 4.4 and Figure 4.5, respectively. Finally, in Figures C.4 to C.9, we report the results obtained from running 10 000 iterations of our model.

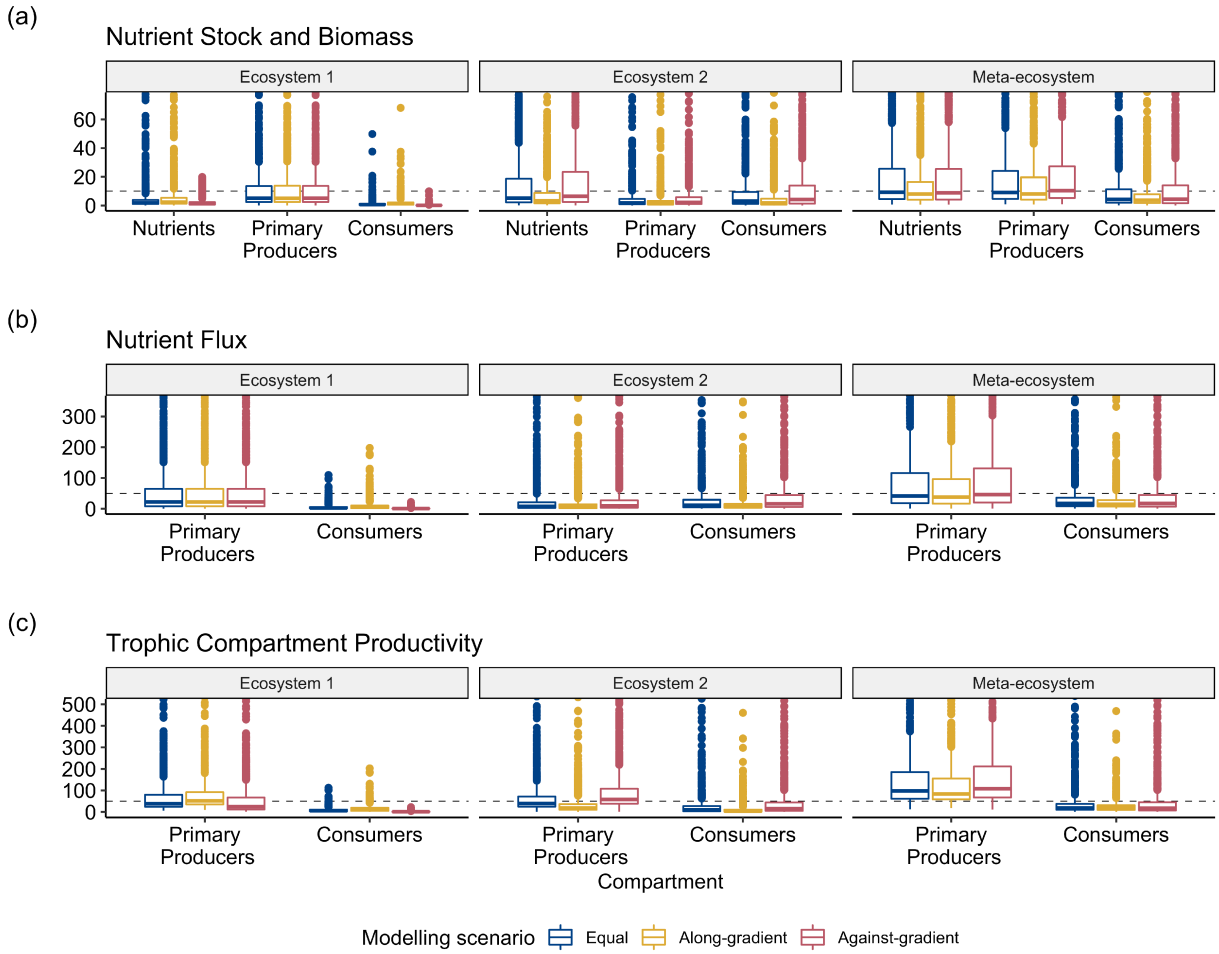

Figure C.1: Comparison of (a) nutrient stock and biomass, (b) nutrient flux, and (c) trophic compartment productivity untransformed values, when consumers move in a heterogeneous meta-ecosystem. Consumer movement happens from ecosystem 1 to ecosystem 2. At the meta-ecosystem scale, function values are generally higher for the against-gradient movement scenario (red) than for either the gradient-neutral (blue) or along-gradient (yellow) scenarios. Increased stock, nutrient flux, and productivity are likely a consequence of the spatial trophic cascade established by consumers moving from a less to a more nutrient-rich ecosystem (compare left and central panels in (a)). Conversely, the lower functions values observed for the along-gradient scenario (yellow) likely arise from the source-sink dynamics linking the local ecosystems. Blue boxplots show function values for the case of consumer movement in a homogeneous landscape, i.e., gradient-neutral movement. For each ecosystem function, thick lines inside the boxes represent median values, the upper and lower hinges correspond to the first (25%) and third (75%) quartiles, and upper and lower whiskers extend from the respective hinge to the largest and smaller value no further than 1.5×interquartile range. Note the different scales of the y-axis. The dashed line represents a reference value to help interpreting the relative magnitudes of the function values plotted; it intercepts the y-axis at $y = 10$ for panel (a) and at $y = 50$ for panel (b) and panel (c).

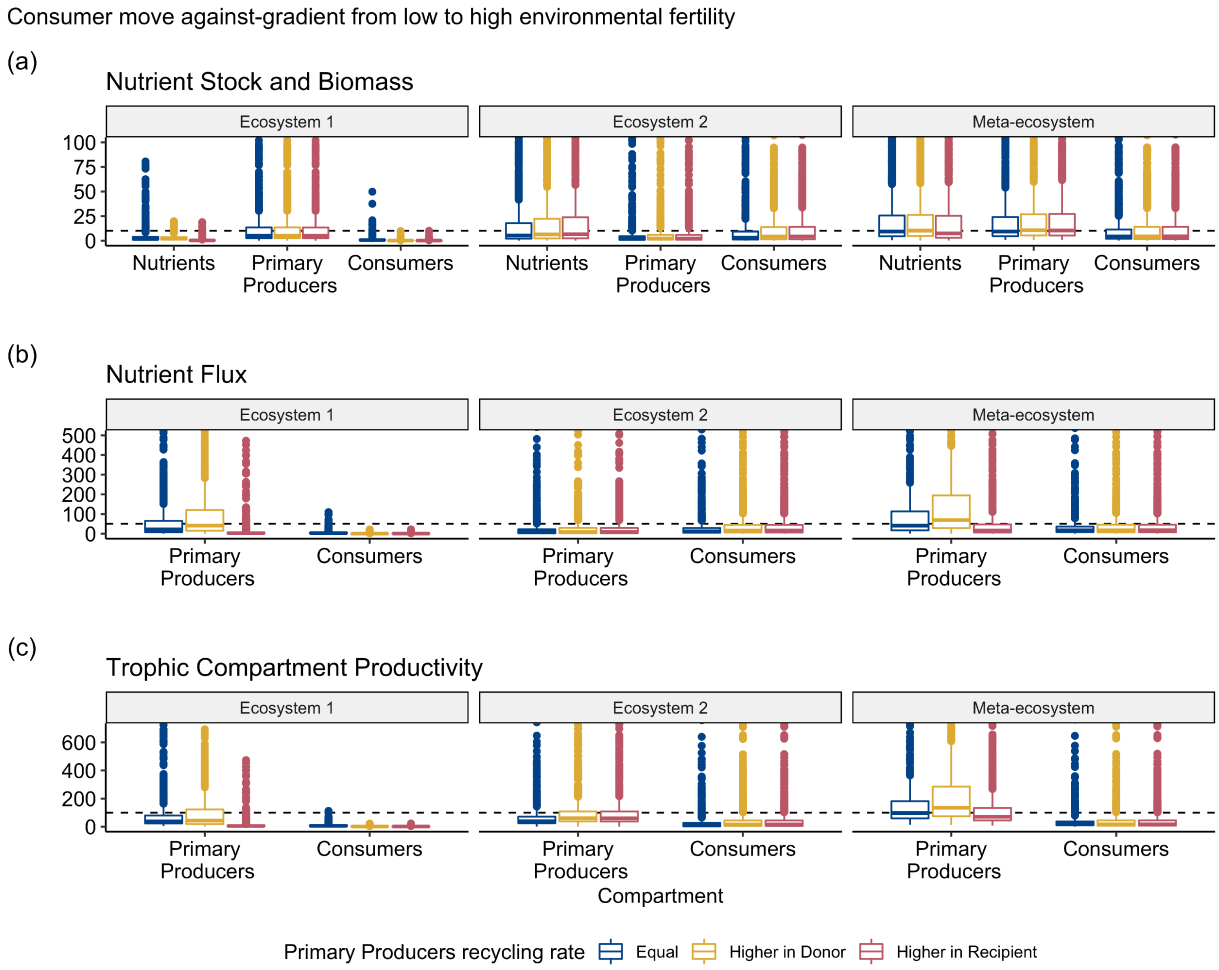

Figure C.2: Untransformed data for (a) nutrient stock and biomass, (b) nutrient flux, and (c) trophic compartment productivity, when consumers move against nutrient availability gradient over an autotroph recyclability gradient. When consumers move along the gradient of autotroph recyclability (yellow boxplots), the release of foraging pressure on primary producers in ecosystem 1 leads to higher nutrient flux and productivity for autotrophs (panels (b), (c)). Interestingly, the increase in nutrient flux does not lead to a nutrient stock increase in ecosystem 1 (panel (a)). Conversely, the input of nutrients into ecosystem 2 deriving from consumer movement brings the stock here to values larger than the equal recycling rates case (panel (a), compare yellow and blue). The release is large enough to influence ecosystem functioning at regional extents. When consumers move to an ecosystem that is more fertile and contains more easily recyclable autotrophs (red), ecosystem 1 sees a stark reduction in nutrient flux and primary productivity. These reduce nutrient stock accumulation (panel (a)). At the meta-ecosystem scale, ecosystem 1 drives a reduction in primary producers nutrient flux and primary productivity, but not in biomass and nutrient stock accumulation. The dashed line represents a reference value to help interpreting the relative magnitudes of the function values plotted; it intercepts the y-axis at $y = 10$ for panel (a) and at $y = 50$ for panel (b), and at $y = 100$ for panel (c). All specifications as in Figure C.1.

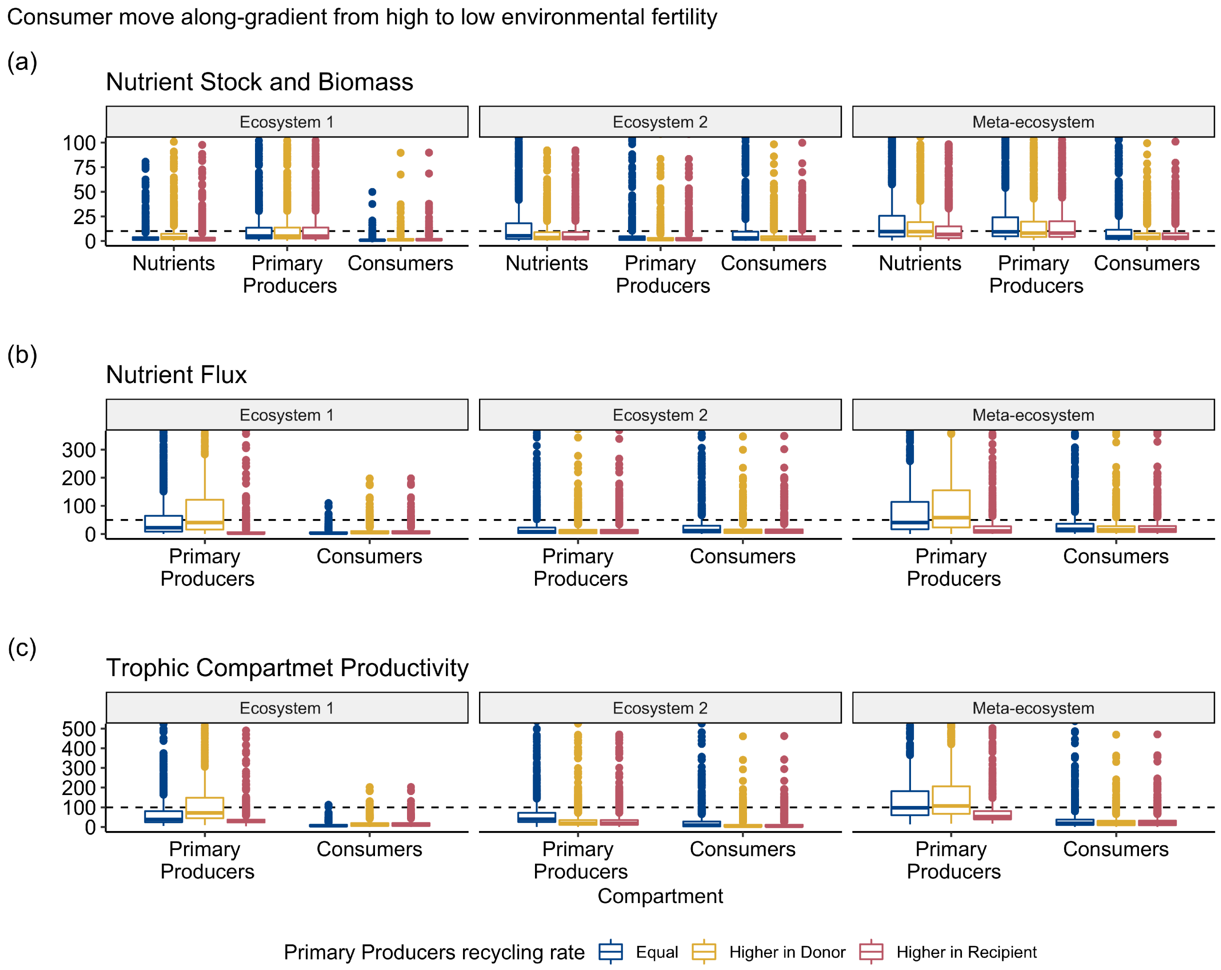

Figure C.3: Untransformed data for (a) nutrient stock and biomass, (b) nutrient flux, and (c) trophic compartment productivity, when consumers move along nutrient availability gradient over an autotroph recyclability gradient. Higher autotroph recyclability in ecosystem 1 (yellow boxplots) leads to primary productivity and nutrient flux that are higher than both the other two scenarios investigated. In turn, we observe a higher nutrient retention in ecosystem 1 (yellow boxplots in panel (a)), while in ecosystem 2 we observe a reduction of nutrients stock compared to the equal recycling rates scenario (compare blue and yellow boxplots). The enhanced ecosystem functions for primary producers scale up to the regional scale, with primary producers nutrient flux and productivity being higher at meta-ecosystem scale when autotrophs are more easily recyclable in ecosystem 1 (yellow boxplots, right-most column). When autotrophs are more easily recyclable in the recipient ecosystem, ecosystem functions of primary producers in ecosystem 1 are reduced compared to the two other cases (compare red boxplots with blue and yellow ones, panel (b), (c)). This reduction in autotrophs productivity and nutrient flux in the donor ecosystem influences the whole meta-ecosystem (red boxplots, right-most column). The dashed line represents a reference value to help interpreting the relative magnitudes of the function values plotted; it intercepts the y-axis at $y = 10$ for panel (a) and at $y = 50$ for panel (b), and at $y = 100$ for panel (c). All specifications as in Figure C.1.

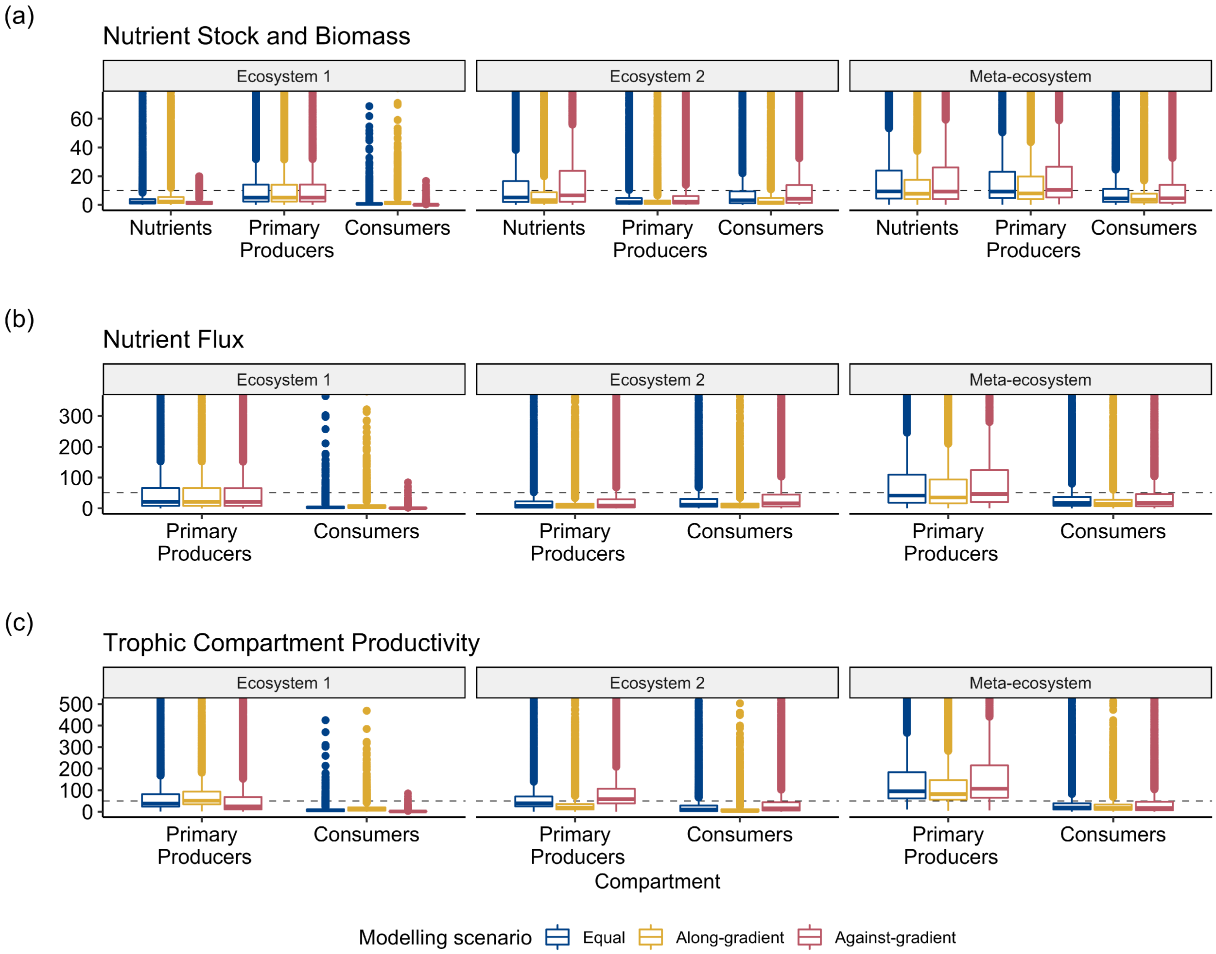

Figure C.4: Comparison of (a) nutrient stock and biomass, (b) nutrient flux, and (c) trophic compartment productivity untransformed values for 10 000 iterations of our model. Consumer movement happens from ecosystem 1 to ecosystem 2. The results do not change qualitatively from those reported in Figure C.1. For each ecosystem function, thick lines inside the boxes represent median values, the upper and lower hinges correspond to the first (25%) and third (75%) quartiles, and upper and lower whiskers extend from the respective hinge to the largest and smaller value no further than 1.5×interquartile range. Note the different scales of the y-axis. The dashed line represents a reference value to help interpreting the relative magnitudes of the function values plotted; it intercepts the y-axis at $y = 10$ for panel (a) and at $y = 50$ for panel (b) and panel (c).

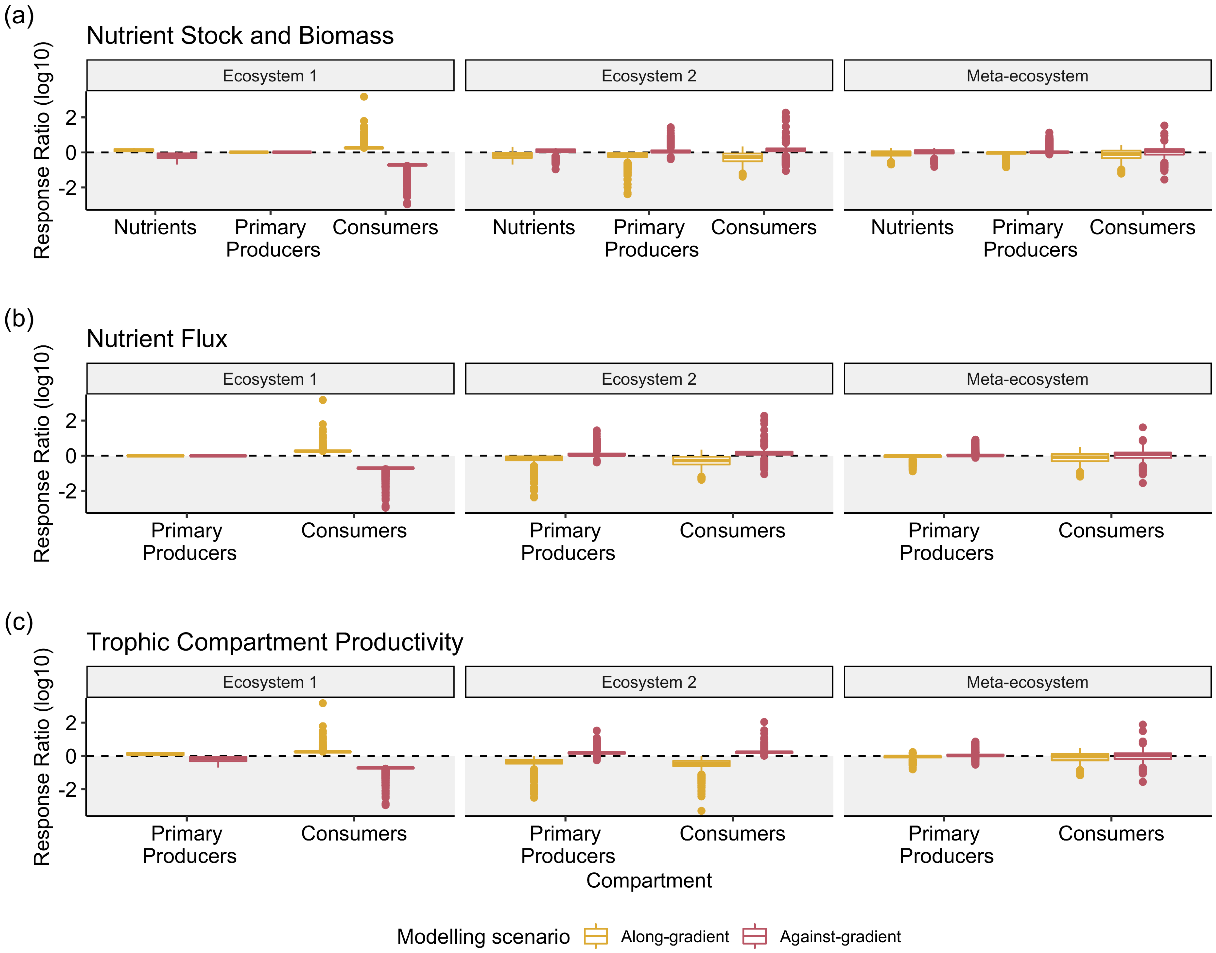

Figure C.5: Comparison of log_{10} response ratio values for 10 000 iterations of our model. (a) Nutrient stock and biomass, (b) nutrient flux, and (c) trophic compartment productivity. Consumer movement happens from ecosystem 1 to ecosystem 2. Our results do not qualitatively change when increasing the number of iterations of the model (compare with Figure 4.3). All other specifications as in Figure C.1

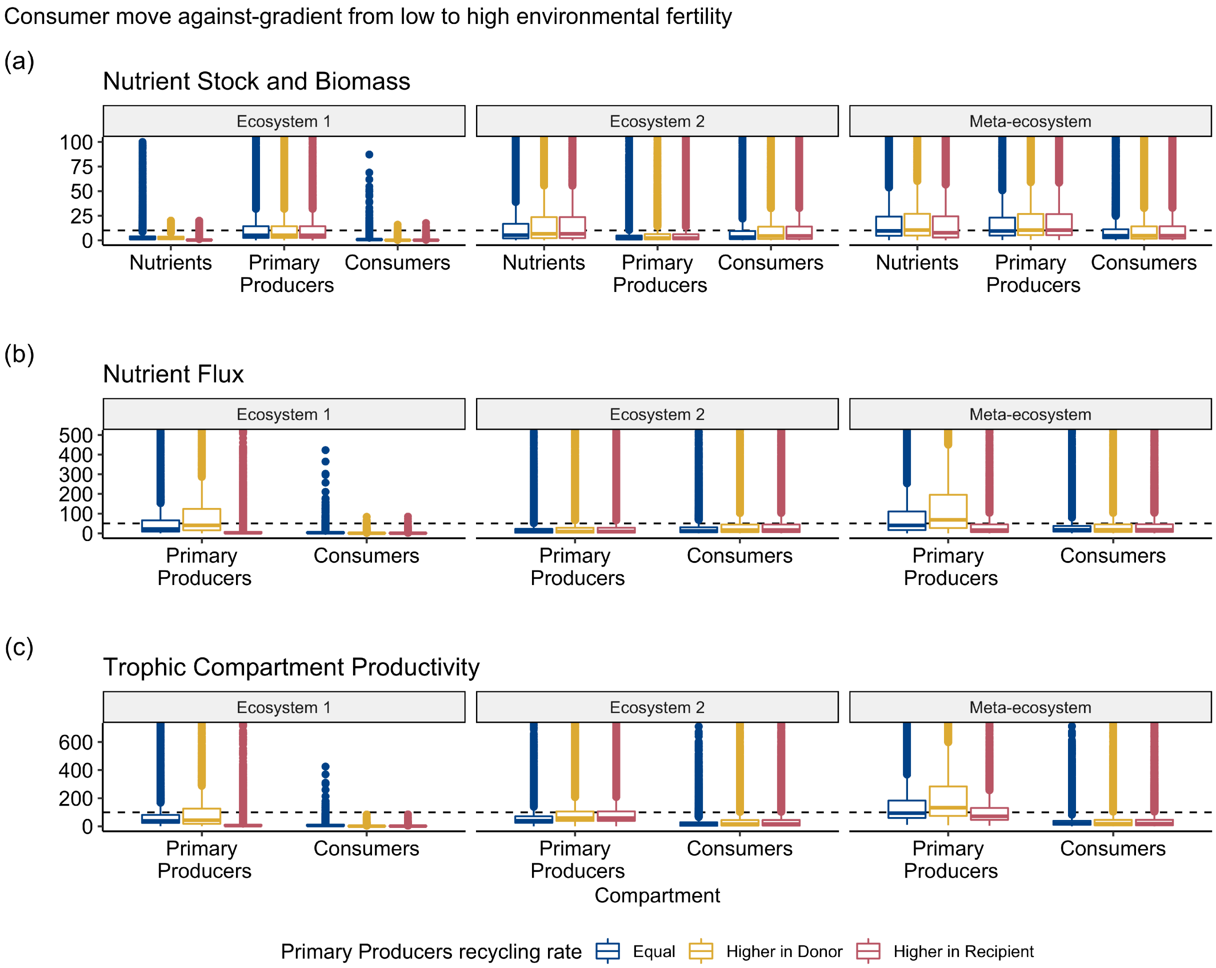

Figure C.6: Untransformed values for (a) nutrient stock and biomass, (b) nutrient flux, and (c) trophic compartment productivity, when we ran 10 000 iterations of our model. Consumers here move against nutrient availability gradient over an autotroph recyclability gradient. Our results do not qualitatively change, showing similar influences of consumer movement in local and meta-ecosystem as those shown in Figure C.2. The dashed line represents a reference value to help interpreting the relative magnitudes of the function values plotted; it intercepts the y-axis at $y = 10$ for panel (a) and at $y = 50$ for panel (b), and at $y = 100$ for panel (c). All specifications as in Figure C.1.

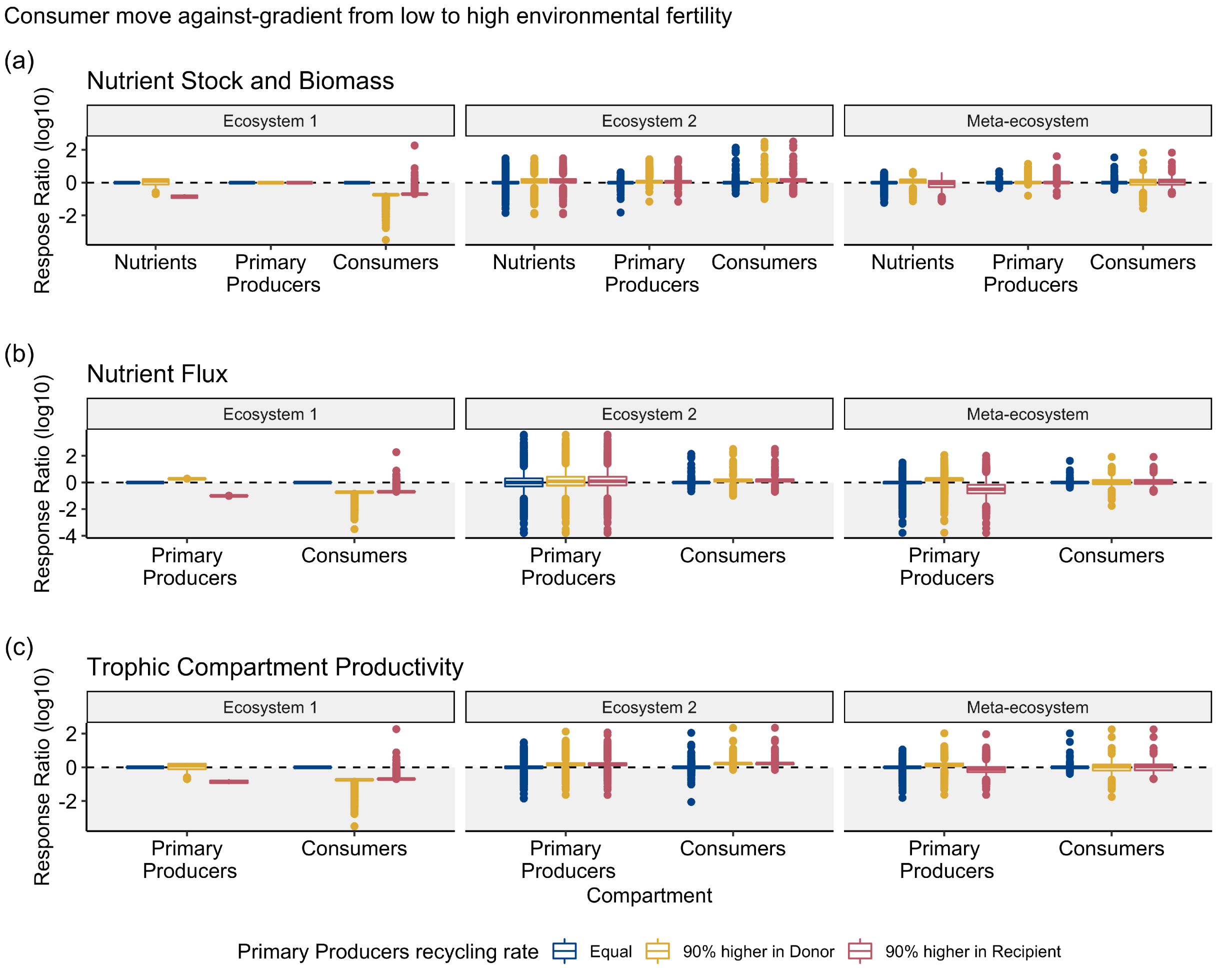

Figure C.7: Comparison of log_{10} response ratio values for (a) nutrient stock and biomass, (b) nutrient flux, and (c) trophic compartment productivity, when we ran 10 000 iterations of our model. Consumers here move against nutrient availability gradient over an autotroph recyclability gradient. Our results show a qualitatively comparable influence of consumer movement on functions and processes in local and meta-ecosystem as those shown in Figure 4.4. All specifications as in Figure C.1.

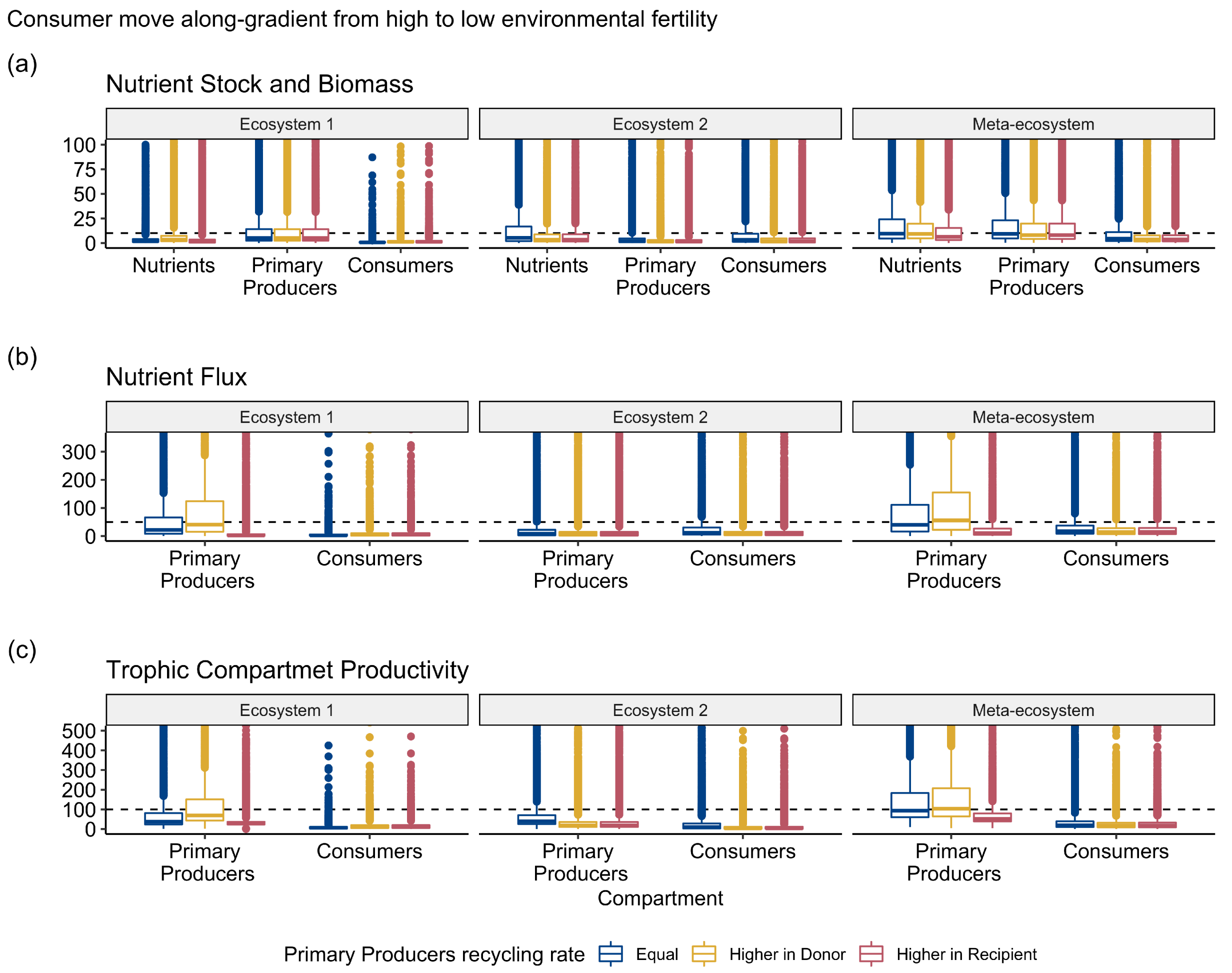

Figure C.8: Untransformed values for (a) nutrient stock and biomass, (b) nutrient flux, and (c) trophic compartment productivity, when we ran 10 000 iterations of our model. Consumers move along nutrient availability gradient over an autotroph recyclability gradient. Our results are robust to this increase in the number of model iterations, showing equivalent patterns to those presented in Figure C.3. The dashed line represents a reference value to help interpreting the relative magnitudes of the function values plotted; it intercepts the y-axis at $y = 10$ for panel (a) and at $y = 50$ for panel (b), and at $y = 100$ for panel (c). All specifications as in Figure C.1.

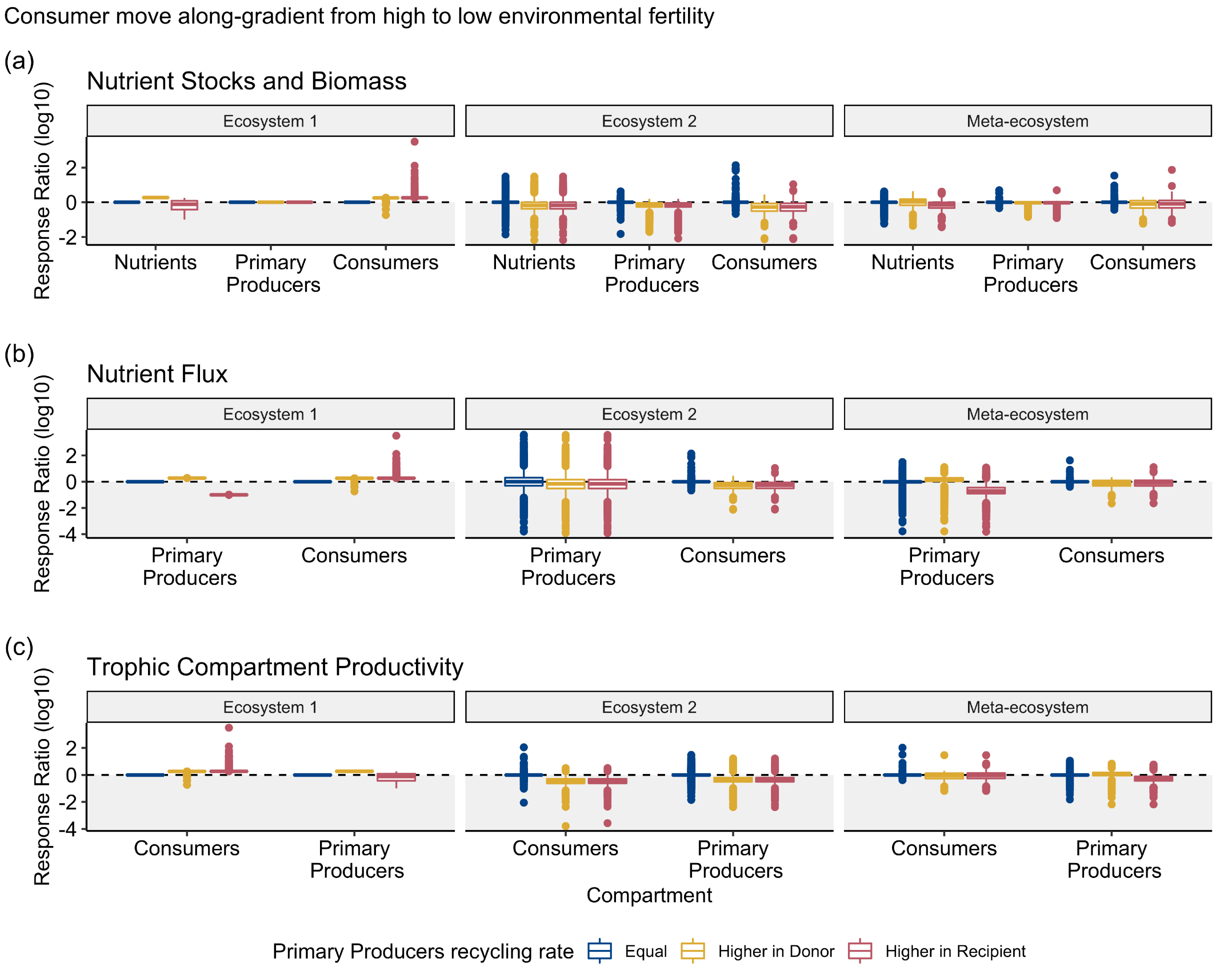

Figure C.9: Comparison of log_{10} response ratio values for (a) nutrient stock and biomass, (b) nutrient flux, and (c) trophic compartment productivity, when we ran 10 000 iterations of our model. Consumers move along nutrient availability gradient over an autotroph recyclability gradient. Our results are robust to the increase in the number of iterations, remaining qualitatively similar to those shown in Figure 4.5. All specifications as in Figure C.1.

APPENDIX D

Abstracts of collaborative papers

D.1 Introduction

Here, I provide abstracts for the collaborative papers listed in Section 1.6.1. For ease of reference, papers are organized in the same three groups used in Section 1.6.1.

D.2 As part of the Terrestrial Ecology Research Group

D.2.1 Abstract for Balluffi-Fry, Leroux, Wiersma, Heckford, et al. (2020)

Herbivores consider the variation of forage qualities (nutritional content and digestibility) as well as quantities (biomass) when foraging. Such selection patterns may change based on the scale of foraging, particularly in the case of ungulates that forage at many scales. To test selection for quality and quantity in free-ranging herbivores across scales, however, we must first develop landscape-wide quantitative estimates of both forage quantity and quality. Stoichiometric distribution models (StDMs) bring opportunity to address this because they predict the elemental measures and stoichiometry of resources at landscape extents. Here, we use StDMs to predict elemental measures of understory white birch quality (% nitrogen) and quantity (g carbon m^{-2}) across two boreal landscapes. We analyzed global positioning system (GPS) collared moose ($n = 14$) selection for forage quantity and quality at the landscape, home range, and patch extents using both individual and pooled resource selection analyses. We predicted that as the scale of resource selection decreased from the landscape to the patch, selection for white birch quantity would decrease and selection for quality would increase. Counter to our prediction, pooled-models showed selection for our estimates of quantity and quality to be neutral with low explanatory power and no scalar trends. At the individual-level, however, we found evidence for quality and quantity trade-offs, most notably at the home-range scale where resource selection models explain the largest amount of variation in selection. Furthermore, individuals did not follow the same trade-off tactic, with some preferring forage quantity over quality and vice versa. Such individual trade-offs show that moose may be flexible in attaining a limiting nutrient. Our findings suggest that herbivores may respond to forage elemental compositions and quantities, giving tools like StDMs merit toward animal ecology applications. The integration of StDMs and animal movement data represents a promising avenue for progress in the field of zoogeochemistry.

D.2.2 Abstract for Balluffi-Fry, Leroux, Wiersma, Richmond, et al. (2021)

Intraspecific feeding choices account for a large portion of herbivore foraging in many ecosystems. Plant resource quality is heterogeneously distributed, affected by nutrient availability and growing conditions. Herbivores navigate landscapes, making feeding decisions according to food qualities, but also energetic and nutritional demands. We test three non-exclusive foraging hypotheses using the snowshoe hare (*Lepus americanus*): 1) herbivores feeding choices and body conditions respond to intraspecific plant quality variation, 2) feeding responses are mitigated when energetic demands are high, and 3) feeding responses are inflated when nutritional demands are high. We measured black spruce (*Picea mariana*) nitrogen, phosphorus, and terpene compositions, as indicators of quality, within a snowshoe hare trapping grid and found plant growing conditions to explain spruce quality variation ($R^2 < 0.36$). We then offered two qualities of spruce (H1) from the trapping grid to hares in cafeteria-style experiments and measured their feeding and body condition responses ($n = 75$). We proxied energetic demands (H2) with ambient temperature and coat insulation (% white coat) and nutritional demands (H3) with the spruce quality (nitrogen and phosphorus content) in home ranges. Hares that preferred higher-quality spruce lost less weight during experiments ($p = 0.018$). The results supported our energetic predictions: hares in colder temperatures and with less insulative coats (lower % white) consumed more spruce and were less selective towards high-quality spruce. Collectively, we found variation in plant growing conditions within herbivore home ranges substantial enough to affect herbivore body conditions, but any plant-herbivore interactions are also mediated by animal energetic states.

D.2.3 Abstract for Richmond, Leroux, et al. (2021)

Aims Intraspecific variation in plant traits has important consequences for individual fitness and herbivore foraging. For plants, trait variability across spatial dimensions is well documented. However, temporal dimensions of trait variability are less well known, and may be influenced by seasonal differences in growing degree days (GDD), temperature and precipitation. Here, we aim to quantify intraspecific temporal variation in traits and the underlying drivers for four commonly occurring boreal plant species.

Methods We sampled the elemental and stoichiometric traits (%C, %N, %P, C:N, C:P, N:P) of four common browse species' foliage across 2 years. Using a two-step approach, we first fitted generalized linear models (GzLM, $n = 24$) to the species' elemental and stoichiometric traits, and tested if they varied across years. When we observed evidence for temporal variability, we fitted a second set of GzLMs ($n = 8$) with temperature, productivity and moisture as explanatory variables.

Important Findings We found no evidence of temporal variation for most of the elemental and stoichiometric traits of our four boreal plants, with two exceptions. Year was an important predictor for percent carbon across all four species ($R^2 = 0.47$–0.67) and for multiple elemental and stoichiometric traits in balsam fir (5⁄8, $R^2 = 0.29$–0.67). Thus, variation in percent carbon was related to inter-annual differences, more so than nitrogen and phosphorus, which are limiting nutrients in the boreal forest. These results also indicate that year may explain more variation in conifers' stoichiometry than for deciduous plants due to life history differences. GDD was the most frequently occurring variable in the second round of models (8⁄8 times, $R^2 = 0.21$–0.41), suggesting that temperature is an important driver of temporal variation in these traits.

D.2.4 Abstract for Richmond, Balluffi-Fry, et al. (2021)

Herbivores making space use decisions must consider the trade-off between perceived predation risk and forage quality. Herbivores, specifically snowshoe hares (*Lepus americanus*), must constantly navigate landscapes that vary in predation risk and food quality, providing researchers with the opportunity to explore the factors that govern their foraging decisions. Herein, we tested predictions that intersect the Risk Allocation Hypothesis (RAH) and Optimal Foraging Theory (OFT) in a spatially explicit ecological stoichiometry framework to assess the trade-off between predation risk and forage quality. We used individual and population estimates of snowshoe hare ($n = 29$) space use derived from biotelemetry across three summers. We evaluated resource forage quality for lowbush blueberry (*Vaccinium angustifolium*), a common and readily available forage species within our system, using carbon:nitrogen and carbon:phosphorus ratios. We used habitat complexity to proxy perceived predation risk. We analyzed how forage quality of blueberry, perceived predation risk, and their interaction impact the intensity of herbivore space use. We used generalised mixed effects models, structured to enable us to make inferences at the population and individual home range level. We did not find support for RAH and OFT. However, variation in the individual-level reactions norms in our models showed that individual hares have unique responses to forage quality and perceived predation risk. Our finding of individual-level responses indicates that there is fine-scale decision making by hares, although we did not identify the mechanism. Our approach illustrates spatially explicit empirical support for individual behavioural responses to the food quality-predation risk trade-off.

D.2.5 Abstract for Heckford et al. (2021)

Context Spatially explicit correlates of foliar elemental, stoichiometric, and phytochemical (ESP) traits represent links to landscape patterns of resource quality.

Objectives We investigate spatial correlates for multiple foliar ESP traits at the species level and across species at the trait level for five boreal forest understory plants.

Methods On the island of Newfoundland, Canada, we collected plot-level foliar material from four chronosequenced forest grids. We integrate plot-level response variables of foliar elemental (C, N, P, percent and quantity), stoichiometric (C:N, C:P, N:P), and phytochemical (terpenoids) traits, with spatial predictors available for the whole landscape to test multiple competing hypotheses. These hypotheses include the effects of land cover (e.g., coniferous, deciduous, mixedwood), productivity (e.g., enhanced vegetation index), biotic (e.g., stand age/height, canopy closure) and abiotic (e.g., elevation, aspect, slope) factors.

Results Spatial correlates of foliar ESP traits were generally species specific. However, at the trait level, some species shared spatial predictors, notably for foliar percent carbon, C:P, N:P, sesquiterpene traits. Here we highlight that foliar C, C:P, and sesquiterpene traits between different species were explained by abiotic spatial correlates alone. Similarly, foliar terpenoid traits between different species were related to a combination of abiotic and biotic factors (mean $R^2 = 0.26$).

Conclusions Spatial-trait relationships mainly occur at the species level, with some commonalities at the trait level. By linking plot-level foliar ESP traits to spatial predictors, we can map plant chemical composition patterns that influence landscape-scale ecosystem processes and thus inform sustainable landscape management.

D.2.6 Abstract for Heckford et al. (*in revision*)

1. Life history and leaf economic strategies relate Intraspecific Trait Variability (ITV) of foliar C, N, and P to differing environmental conditions. Foliar C, N, and P traits may vary across community (conspecific, heterospecific) and geographic gradients where differences in community structure, temperature, and precipitation may influence elemental homeostatic-physiological processes. Foliar elements are intrinsically coupled and collective shifts in intraspecific trait variability can be represented along niches axes defined by foliar C, N, and P.

2. Using foliar C, N, and P traits of balsam fir (*Abies balsamea*) and white birch (*Betula papyrifera*), species with different life history and leaf economic strategies, we compare con-

specific and heterospecific niche similarity and volume in terms of ITV at the regional and local spatial extent. At the local extent, we compare within and between two biogeographic separated populations. We test the predictions that balsam fir and white birch will exhibit heterospecific niche responses that reflect their elemental homeostatic constraints and that northerly populations have higher foliar N, and P content.

3. We found no evidence to support our prediction for balsam fir at regional and local extents; however, ITV increased for heterospecific niches ranging from 0–35.49 %. At the regional and local extent, we found no evidence to support our white birch niche predictions, although significant differences between conspecific and heterospecific niches were detected. Comparing conspecific and heterospecific niches between northern and southern populations yielded significant differences, on average northerly niches had higher N (fir: conspecific = 0.176 % and heterospecific = 0.15 %; birch: conspecific = 1.26 % and heterospecific = 1.214 %) and P foliar content (fir: conspecific = 0.046 % and heterospecific = 0.053 %; birch: conspecific = 0.146 % and heterospecific = 0.141 %).
4. Our results suggest balsam fir exhibits a rigorous, yet geographically specific elemental homeostasis. Although white birch is also geographically specific, it may exhibit greater plasticity given our mixed findings between populations in terms of community structure. Understanding how foliar elemental traits vary across spatial scales can be useful to predict ecosystem processes that influence nutrient and trophic dynamics at multiple scales.

D.3 As visiting scholar at the Yale University School of the Environment

D.3.1 Abstract for Ellis-Soto et al. (2021)

1. Energy, nutrients and organisms move over landscapes, connecting ecosystems across space and time. Meta-ecosystem theory investigates the emerging properties of local ecosystems coupled spatially by these movements of organisms and matter, by explicitly tracking exchanges of multiple substances across ecosystem borders. To date, meta-ecosystem re-

search has focused mostly on abiotic flows—neglecting biotic nutrient flows. However, recent work has indicated animals act as spatial nutrient vectors when they transport nutrients across landscapes in the form of excreta, egesta and their own bodies.

2. Partly due to its high level of abstraction, there are few empirical tests of meta-ecosystem theory. Furthermore, while animals may be viewed as important mediators of ecosystem functions, better integration of tools is needed to develop predictive insights of their relative roles and impacts on diverse ecosystems. We present a methodological roadmap that explains how to do such integration by discussing how to combine insights from movement, foraging and ecosystem ecology to develop a coherent understanding of animal-vectored nutrient transport on meta-ecosystems processes.

3. We discuss how the slate of newly developed technologies and methods—tracking devices, mechanistic movement models, diet reconstruction techniques and remote sensing—that when integrated have the potential to advance the quantification of animal-vectored nutrient flows and increase the predictive power of meta-ecosystem theory.

4. We demonstrate that by integrating novel and established tools of animal ecology, ecosystem ecology and remote sensing, we can begin to identify and quantify animal-mediated nutrient translocation by large animals. We also provide conceptual examples that show how our proposed integration of methodologies can help investigate ecosystem impacts of large animal movement. We conclude by describing practical advancements to understanding cross-ecosystem contributions of animals on the move.

5. Understanding the mechanisms by which animals shape ecosystem dynamics is important for ongoing conservation, rewilding and restoration initiatives around the world, and for developing more accurate models of ecosystem nutrient budgets. Our roadmap will enable ecologists to better qualify and quantify animal-mediated nutrient translocation for animals on the move.

D.4 From other collaborations

D.4.1 Abstract for Little et al. (*in review*)

Fluxes of matter, energy, and information over space and time contribute to ecosystems' functioning. The meta-ecosystem framework addresses the dynamics of ecosystems linked by these fluxes, however, to date, meta-ecosystem research focused solely on fluxes of energy and matter, neglecting information. This is problematic due to organisms' varied responses to information, which influence local ecosystem dynamics and can alter spatial flows of energy and matter. Furthermore, information itself can move between ecosystems. Therefore, information should contribute to meta-ecosystem dynamics, such as stability and productivity. Specific sub-disciplines of ecology currently consider different types of information (e.g., social and cultural information, natural and artificial light or sound, body condition, genotype, and phenotype). Yet neither the spatiotemporal distribution of information nor its perception are currently accounted for in general ecological theories. Here, we provide a roadmap to synthesize information and meta-ecosystem ecology. We begin by defining information in a meta-ecological context. We then review and identify challenges to be addressed in developing information meta-ecology. Finally, we present new hypotheses for how information could impact dynamics across scales of spatio-temporal and biological organization.

D.5 References

Balluffi-Fry, J., S. J. Leroux, Y. F. Wiersma, T. R. Heckford, et al. (2020). “Quantity-quality trade-offs revealed using a multiscale test of herbivore resource selection on elemental landscapes”. *Ecology and Evolution* 10.24, pp. 13847–13859. DOI: `10.1002/ece3.6975`.

Balluffi-Fry, J., S. J. Leroux, Y. F. Wiersma, I. C. Richmond, et al. (2021). “Integrating plant stoichiometry and feeding experiments: state-dependent forage choice and its implications on body mass”. *Oecologia*. DOI: `10.1007/s00442-021-05069-5`.

Ellis-Soto, D. et al. (2021). “A methodological roadmap to quantify animal-vectored spatial ecosystem subsidies”. *Journal of Animal Ecology* 90.7, pp. 1605–1622. DOI: `10.1111/1365-2656.13538`.

Heckford, T. R. et al. (2021). “Does where you live influence what you are made of? Spatial correlates of chemical traits across commonly occurring boreal plants”. *Landscape Ecology*. DOI: `10.1007/s10980-021-01334-3`.

— (*in revision*). “Foliar elemental niche responses of balsam fir (*Abies balsamea*) and white birch (*Betula papyrifera*) to differing community types across geographic scales.” *Functional Ecology*. manuscript id: FE-2020-00432.

Little, C. J. et al. (*in review*). “Filling the Information Gap in Meta-Ecosystem Ecology”. *Oikos*. manuscript id: OIK-08892.R1. EcoEvoRxiv preprint. DOI: `10.32942/osf.io/hc83u`.

Richmond, I. C., J. Balluffi-Fry, et al. (2021). “Individual snowshoe hares manage risk differently: Integrating stoichiometric distribution models and foraging ecology.” *Journal of Mammalogy*. Accepted, manuscript id: JMAMM–2021–026.R2.

Richmond, I. C., S. J. Leroux, et al. (2021). “Temporal variation and its drivers in the elemental traits of four boreal plant species”. *Journal of Plant Ecology* 14.3, pp. 398–413. DOI: `10.1093/jpe/rtaa103`.